NEW EPOXY COMPOSITES WITH ENHANCED THERMAL CONDUCTIVITY KEEPING ELECTRICAL INSULATION.

Isaac Isarn Garcia

ADVERTIMENT. L'accés als continguts d'aquesta tesi doctoral i la seva utilització ha de respectar els drets de la persona autora. Pot ser utilitzada per a consulta o estudi personal, així com en activitats o materials d'investigació i docència en els termes establerts a l'art. 32 del Text Refós de la Llei de Propietat Intel·lectual (RDL 1/1996). Per altres utilitzacions es requereix l'autorització prèvia i expressa de la persona autora. En qualsevol cas, en la utilització dels seus continguts caldrà indicar de forma clara el nom i cognoms de la persona autora i el títol de la tesi doctoral. No s'autoritza la seva reproducció o altres formes d'explotació efectuades amb finalitats de lucre ni la seva comunicació pública des d'un lloc aliè al servei TDX. Tampoc s'autoritza la presentació del seu contingut en una finestra o marc aliè a TDX (framing). Aquesta reserva de drets afecta tant als continguts de la tesi com als seus resums i índexs.

ADVERTENCIA. El acceso a los contenidos de esta tesis doctoral y su utilización debe respetar los derechos de la persona autora. Puede ser utilizada para consulta o estudio personal, así como en actividades o materiales de investigación y docencia en los términos establecidos en el art. 32 del Texto Refundido de la Ley de Propiedad Intelectual (RDL 1/1996). Para otros usos se requiere la autorización previa y expresa de la persona autora. En cualquier caso, en la utilización de sus contenidos se deberá indicar de forma clara el nombre y apellidos de la persona autora y el título de la tesis doctoral. No se autoriza su reproducción u otras formas de explotación efectuadas con fines lucrativos ni su comunicación pública desde un sitio ajeno al servicio TDR. Tampoco se autoriza la presentación de su contenido en una ventana o marco ajeno a TDR (framing). Esta reserva de derechos afecta tanto al contenido de la tesis como a sus resúmenes e índices.

WARNING. Access to the contents of this doctoral thesis and its use must respect the rights of the author. It can be used for reference or private study, as well as research and learning activities or materials in the terms established by the 32nd article of the Spanish Consolidated Copyright Act (RDL 1/1996). Express and previous authorization of the author is required for any other uses. In any case, when using its content, full name of the author and title of the thesis must be clearly indicated. Reproduction or other forms of for profit use or public communication from outside TDX service is not allowed. Presentation of its content in a window or frame external to TDX (framing) is not authorized either. These rights affect both the content of the thesis and its abstracts and indexes.

UNIVERSITAT
ROVIRA i VIRGILI

New epoxy composites with enhanced thermal conductivity keeping electrical insulation

ISAAC ISARN GARCIA

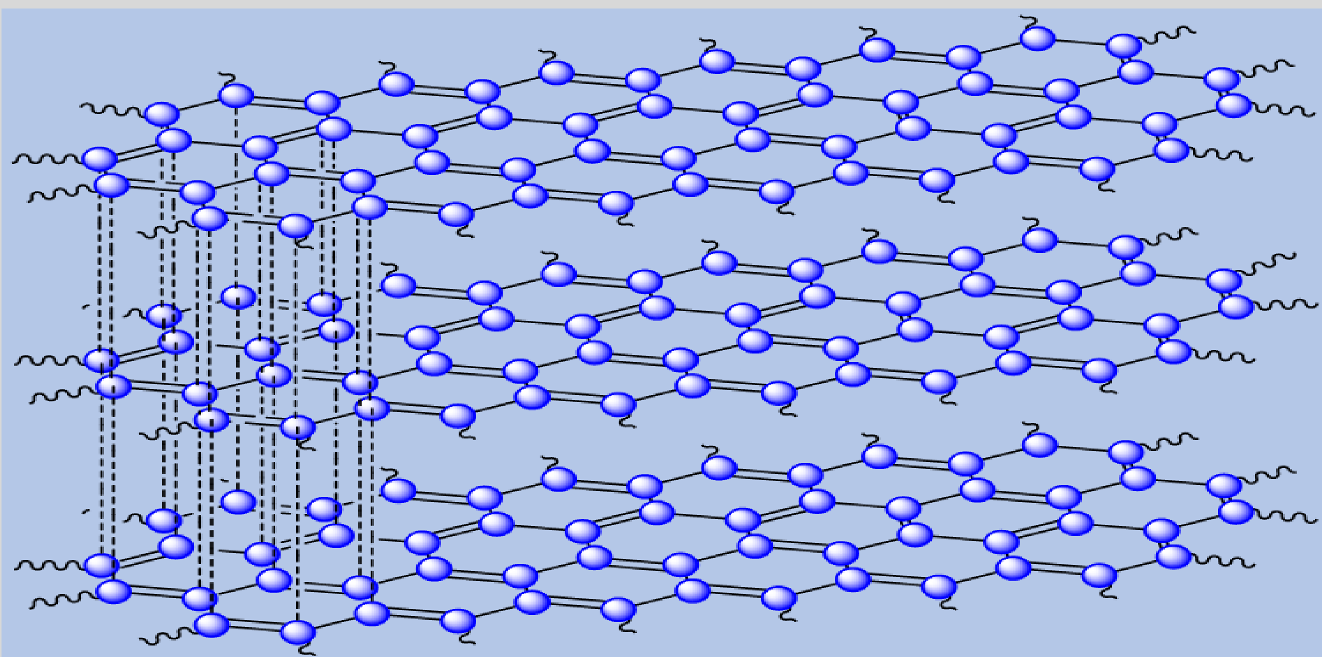

DOCTORAL THESIS
2019

Isaac Isarn Garcia

NEW EPOXY COMPOSITES WITH ENHANCED THERMAL CONDUCTIVITY KEEPING ELECTRICAL INSULATION

DOCTORAL THESIS

Supervised by:

Prof. Francesc Ferrando Piera and Prof. Àngels Serra i Albet

Department of Mechanical Engineering

UNIVERSITAT
ROVIRA i VIRGILI

Tarragona, Spain (2019)

UNIVERSITAT
ROVIRA i VIRGILI

Department of Mechanical Engineering
Campus Sescelades
Av. Països Catalans, 26
43007 Tarragona, Spain

Professor Francesc Ferrando Piera of the Department of Mechanical Engineering and Professor Àngels Serra i Albet of the Department of Analytical and Organic Chemistry, both at the Universitat Rovira i Virgili,

Certify that the present study, entitled,

"New epoxy composites with enhanced thermal conductivity keeping electrical insulation"

presented by Isaac Isarn Garcia for the award of the degree of Doctor, has been carried out under our supervision and meets the requirements to qualify for the European Mention.

Tarragona, July 2nd, 2019

Prof. Francesc Ferrando Piera

Prof. Àngels Serra i Albet

Doctoral Thesis Supervisors

Agraïments

Fa poc més de tres anys que vaig arribar a Tarragona per començar una tesi. Era una ciutat que no havia visitat mai, però que des del principi em va encantar i acollir. És una ciutat amb una llarga història, i el caràcter de la seva gent és molt afable. És el que podríem dir un poble gran, en el sentit que és molt fàcil trobar-se gent coneguda pel carrer, ja que com en tots els pobles, tothom es coneix. A més, he tingut la sort que la Vanesa va vindre a viure amb mi tot i seguir treballant a Barcelona. Gràcies a ella toco de peus a terra i enseguida em fa baixar si començo a enlairar-me.

Primer de tot voldria donar les gràcies als meus directors de tesi, en Francesc i l'Àngels. Gràcies per la seva confiança en mi, per haver-me deixat complir el meu anhel de realitzar una tesi doctoral. Des del principi es van convertir en els meu pares "científics".

El que primer recordo del laboratori quan vaig arribar va ser un bon grup d'amics que treballaven plegats. Liderats per la Cristina (que en pocs dies ja es convertirà en una madrassa), el grup el conformaven la Dailyn, en David, l'Alberto, en Rubén, i durant els primers mesos, en Xavi que era a Alemanya. A ell el vaig conèixer per Skype. La Cristina va ser la primera que em va ajudar a aclimatar-me. Va ser la primera en marxar, però de tant en tant encara ens veiem. En Xavi va ser el segon en acabar el doctorat, però va aconseguir feina al ICIQ, i fins fa poc ens veiem cada setmana per anar a peu a la EOI. Perquè ara és a França continuant amb la seva carrera. Amb l'Alberto i en Rubén són amb els que més coses vaig compartir. Anàvem a nedar i fins i tot, vam poder coincidir un cap de setmana a Holanda, aprofitant el post doc d'Alberto a Eindhoven, una cosa per feina d'en Rubén i la meva estada a Bèlgica. Tot i ser doctors avui dia encara segueixen en el laboratori 330 la Dailyn i en David. Sort en tenim d'ells! Són els "jefes" del laboratori i gràcies a ells tot funciona genial. Pel març de 2016 també corrien pel laboratori el rialler Blai fent el màster i una petitona Yvoone, amb una empenta, positivisme i ganes de treballar admirables, que havia vingut d'estada per uns mesos. Pel laboratori també corria sovint en Krys, un noi que sempre es prestava a ajudar.

Pocs mesos després van arribar dos italians, en Michele i en Francesco. Feien uns mesos d'investigació per el seu màster. Al segon em va tocar ensenyar-li tot el que havia après jo fins llavors! Ara ja m'ha superat. Però aquests dos només van ser l'inici d'una tropa incomptable d'italians que van venir després (tots ells ja havien fet el màster abans d'això) a fer el doctorat: Gianmarco, Mario, Rita, Mimo, Claudio... i molts més que només he conegut de passada però que omplen la ciutat amb una gran comunitat d'italians. Amb ells tot ha sigut molt més divertit. I com no, recordar a Ulpiano, el noi mexicà que sempre se'l recordarà per la seva simpatia i la salutació cada dia a tothom quan arribava i quan marxava.

També vull recordar a tota la gent que vaig conèixer durant els meus quatre mesos a Mons, començant per la Leïla. Es nota que és una experta en investigació. Merci al matrimoni Marius i Oltea que hem van ajudar quan necessitava qualsevol cosa. I a en Jevgenij, Julien, Luic, Bertrand i Jérôme per passar estones explicant-me coses.

Després vull agrair a tota aquella gent que m'ha ajudat perquè la meva investigació acabés a bon port. Com sempre, gràcies a la dedicació, experiència i saviesa dels meus directors. Infinites gràcies li tinc que donar a en Xavier Ramis que posava experiments després que jo tingués que marxar per poder tornar amb bus des de Barcelona. A en Xavi petit, que amb la seva clarividència, en poques paraules et solucionava els teus dubtes. A en Lluís per les hores invertides en obtenir els resultat elèctrics que tant importants són. També vull recordar a la Mariana i les seves companyes de microscòpia les estones passades recollint imatges de les meves mostres. A en Josep del taller mecànic on tantes hores de ensenyaments m'ha donat. I a en Francesc de raigs X per la seva disponibilitat a l'hora de fer els difractogrames. He d'agrair l'ajut que em va donar en Miguel Ángel Acebo en els càlculs matemàtics on jo no hi arribava , així com a en Diego i en Marc pel temps que van dedicar.

Vull agrair especialment a en John la seva disposició a deixar-nos fer servir l'aparell de conductivitat tèrmica sempre que el necessitàvem. I per compartir les nostres inquietuds al voltant d'aquesta propietat tan difícil de fer augmentar. També agrair a la Frida, a la Yolanda i al Sasan l'acompanyament que m'han fet sempre que he anat a Terrassa.

També tinc que donar les gràcies a Aismalibar del Grup Benmayor per haver-nos facilitat els diferents tipus de partícules inorgàniques per poder dur a terme l'estudi. Així com a Materia Nova per haver-me donat les partícules de base carboni.

En el últims temps al laboratori amb qui més he compartit hores de feina han sigut en Francesco i en Claudio. Junt amb la Valentina, en Francesc, l'Anna Maria, en Federico, Alirezaa, i la Michelle. I amb la Cristina Urbina, a la qual he intentat ensenyar a treballar en mgs i ella a mi a tenir més paciència. Ha estat un bon últim any.

Isaac

"Every morning when I wake,

Dear Lord, a little prayer I make.

O please to keep Thy lovely eye

On all poor creatures born to die."

Dylan Thomas

UNIVERSITAT ROVIRA I VIRGILI
NEW EPOXY COMPOSITES WITH ENHANCED THERMAL CONDUCTIVITY KEEPING ELECTRICAL INSULATION.
Isaac Isarn Garcia

Table of contents

A. Abstract……………………………………………………………………………………………I

B. List of abbreviations…………………………………………………………………………… V

C. List of publications……………………………………………………………………………XI

D. Meeting contributions and stages…………………………………………………………… XIII

Chapter 1. Introduction and objectives……………………………………………………… 1

1.1. Overview of polymeric materials……………………………………………… 3
1.2. Thermosets……………………………………………………………………………8
1.3. Epoxy thermosets……………………………………………………………………14
1.4. Heat conduction through materials……………………………………………20
1.4.1. Thermal conductivity in crystalline structures………………………… 22
1.4.2. Thermal conductivity and their composites……………………………… 24
1.5. Epoxy composites with high thermal conductive fillers……………………… 27
1.6. Scope and objectives………………………………………………………………… 33

Chapter 2. Experimental part…………………………………………………………………43

2.1. Materials………………………………………………………………………………45
2.2. Experimental techniques……………………………………………………………45
2.2.1. Differential Scanning Calorimetry (DSC)…………………………………46
2.2.2. Rheology……………………………………………………………………… 48
2.2.3. Dynamo-Mechanical Thermal Analysis (DMTA)……………………………49
2.2.4. Thermal Mechanical Analysis (TMA)…………………………………… 50
2.2.5. Thermo-Gravimetric Analysis (TGA)………………………………………51
2.2.6. Microindentation Knoop hardness and impact test………………………52
2.2.7. Environmental Scanning Electron Microscopy (ESEM) and X-ray diffraction……………………………………………………………………… 54
2.2.8. Electrical measurements……………………………………………………56
2.2.9. Thermal conductivity measurements………………………………………57

Chapter 3. New BN-epoxy composites obtained by thermal latent cationic curing with enhanced thermal conductivity…………………………………………………………61

Chapter 4. New epoxy composite thermosets with enhanced thermal conductivity and high T_g obtained by cationic polymerization…………………………………………… 91

Chapter 5. Thermoconductive thermosetting composites based on boron nitride fillers and thiol-epoxy matrices……………………………………………………………111

Chapter 6. Thermal conductive composites prepared by addition of several ceramic fillers to thermally cationic curing cycloaliphatic epoxy resins……………………………… 135

Chapter 7. Study on the cooperative effect of boron nitride and carbon nanotubes in the improvement of the thermal conductivity of epoxy composites……………………………………………………………………………………………………… 155

Chapter 8. Enhancement of thermal conductivity in epoxy coatings through the combined addition of expanded graphite and boron nitride fillers……………………….. 183

Chapter 9. General conclusions…………………………………………………………………………….207

A. Abstract

The tendency in electronics to produce smaller and lighter devices with higher power output causes the need to improve some properties that existent materials do not meet. Reducing the size of these devices while increasing their work speed results in an increase in the frequency of electrons circulating in a specific area. As it is known, the circulation of electrons emits heat by Joule effect, which must be removed to maintain the operating temperature. This is directly related to efficiency, useful lifetime and prevention of premature equipment failures.

In this doctoral thesis we delve into the field of high thermal conductive and electrically insulating epoxy thermosets. The next generation of packaging materials are expected to possess high thermal dissipation characteristics in addition to low thermal expansion coefficient (CTE). To remove the accumulated heat generated by high performance electronic devices is crucial for proper operation and would contribute to the improvement of their capabilities. Moreover, the enhancement of these properties may fulfill the demands in other spreading out industries as power, thermal energy storage, electrical, light emitting diodes (LEDs), sensors, aerospace, automotive or naval engineering among others.

Epoxy resins are a kind of thermosets extensively used to coat and encapsulate elements of electronic devices such as laptops, smartphones, digital cameras, televisions, and all types of modern appliances. Epoxies are used for their excellent properties such as exceptional adhesion ability to a huge range of different surfaces, the good protection capacity against moisture and physical and chemical aggressive environments, notable temperature resistance, electrical insulative character to avoid short circuits in electronic devices and their easy processability and relative low cost. However, as is common in polymers, epoxy-based thermosets lack good thermal conductivity (in the range of 0.2 W/m·K). The most economic and simple technique to face this issue is still today through the addition of high thermal conductive fillers.

Two different epoxy resins have been used as the starting material. One based on a diglycidyl derivative (DGEBA) and the other on a cycloaliphatic epoxy (ECC). During the research, we have developed the optimization of two different latent cationic epoxy systems, which leads to the homopolymerization of the epoxy resins used. The initiator selected in both cases was a commercial benzylanilinium salt. In the case of ECC monomer, it was required the addition of little amounts of triethanolamine (TEA) to confer the latency to the formulation. In order to facilitate the curing of the DGEBA resin, a little proportion of glycerol was added favoring the activated monomer (AM) mechanism. Alternatively, a tetrafunctional thiol hardener (PETMP) was used to cure ECC by a polycondensation mechanism using 4-(*N,N*-dimethylamino)pyridine (DMAP) as the base acting as the catalyst.

The fillers added into the matrix in this work can be divided in two groups: ceramic fillers and carbon-based materials. Among the ceramic particles used, stands out the hexagonal form of boron nitride (BN). This material gathers a set of properties that make it ideal to be used as a filler to meet the objectives. BN provides high thermal conductivity, low dielectric constant and high electrical resistivity, low CTE and density, high mechanical strength and chemical and thermal stability. Different sizes and shapes of this filler were tested. Other ceramics were also essayed, such as alumina (Al_2O_3), aluminium nitride (AlN) and silicon carbide (SiC). Among carbon-based materials, carbon nanotubes (CNTs) and expanded graphite (EG) were used. Carbon nanotubes are the most studied nanomaterials to date, motivated by the intrinsic high thermal conductivity as well as the mechanical behavior they present. Expanded graphite has received much attention in recent years in the field of composites for its properties, emphasizing its low cost and extremely low density. Due to the electrical conductivity of the carbonaceous materials, their proportion in the composite had to be limited and they were mixed with BN to maintain the electrical insulation of the composites, improving the thermal conductivity.

Differential scanning calorimetric (DSC) analyzes were performed to optimize the curing of the epoxy formulations and determine the influence of the filler addition during the reaction. The rheological tests allowed to determine the gel point of DGEBA formulations and the influence of a variable proportion of added BN. Also, this technique provides information of the viscoelastic properties of the formulations before curing. These studies allowed us to determine the percolation threshold concentration.

Once cured, the thermosets were characterized by many different techniques. The thermogravimetric analysis (TGA) determined the stability of the composites against temperature. The dynamic mechanical thermal analysis (DMTA) evaluated the dependence of the mechanical characteristics with temperature. Knoop microindentations were performed to evaluate the hardness of the materials. The composites were inspected by environmental scanning electron microscopy (ESEM) to observe the fracture surfaces and the final dispersion of the particles in the matrix. Thermo mechanical analysis (TMA) allowed to determine the thermal expansion coefficient of the materials obtained. Some materials were examined by X-ray diffraction to know the purity of the fillers and their crystalline structure.

DGEBA thermosets were evaluated both in their adhesion to metallic surfaces by tensile lap-shear strength of bonded assemblies' and in their resistance to fracture by impact test. Moreover, their dielectric breakdown strength was determined. In addition, the electrical resistivities of the materials with BN and carbon particles were determined, to discern their possible use as electrical insulating materials. More importantly, the thermal conductivity of all the performed materials were determined by the transient hot bridge (THB) method.

In general, the fillers act as reinforcement inside the epoxy matrix and improve the mechanical behavior of the materials. The CTE is gradually reduced with the addition of fillers. Up to a certain concentration of particles, the toughness of epoxy resins is improved. Slight differences in thermal stability were found between the neat and composite materials, only differentiated by the less proportion of matrix that could be degraded.

Low proportions of carbon materials are enough to cause a decrease of several orders of magnitude in the electrical resistivity of the thermosets. Nevertheless, the combination with BN particles leads to the possibility to use EG and CNT at higher concentration since BN acts as a barrier for the transmission of the electrons. The materials with the best performances in the proposed objectives were those of homopolymerized ECC with the combined addition of 70 wt. % of BN platelets and 2.5 and 5 wt. % of EG. The values of thermal conductivity improved by more than 1600 % in reference to the neat epoxy and were 2.08 and 2.22 W/m·K, respectively. These materials also kept sufficient electrical insulation, in the range of 10^{10} and 10^{6} Ω·m, respectively.

A. List of abbreviations

°C	Celsius degree
1-MI	1-Methyl imidazole
3D	Three dimensional
A	Electrode area
AC	Alternating current circuit
ACE	Activated chain end mechanism
AM	Activated monomer mechanism
A_p	Area of indentation in mm^2
b	Width of sample
CNT	Carbon nanotube
C_p	Heat capacity or Indenter constant
CTE	Thermal expansion coefficient
CVD	Chemical vapor deposition
d	Distance between crystalline planes
DC	Direct current circuit
DGEBA	Diglycidyl ether of bisphenol A
dH/dt	Heat rate
DMAP	4-(N,N-dimethylamine)pyridine
DMTA	Dynamic-mechanical thermal analysis
DNA	Deoxyribonucleic acid
DSC	Differential scanning calorimetry
dT/dt	Heating rate
dT/dx	Rate of temperature change in one direction
dx/dt	Curing rate
E	Activation energy / Energy loss of pendulum with the sample / Experimental breakdown strength / Young Modulus

E^*	Complex modulus
E'	Elastic storage modulus
E''	Viscous loss modulus
E_0	Energy loss of pendulum without the sample / Scale parameter
E_a	Activation energy
ECC	3,4-epoxy cyclohexylmethyl 3,4-epoxy cyclohexane carboxylate
ee	Epoxy equivalent
EEW	Molecular weight per epoxy equivalent
E_f	Elastic modulus of the filler
EG	Expanded graphite
EHP	Electrical heated plates
E_m	Elastic modulus of the matrix
Eq.	Equation
ESEM	Environmental scanning electron microscopy
ETW	Molecular weight per thiol equivalent
f	Volume fraction
FWHM	Full width at half maximum
g	Gram
G'	Elastic shear modulus
G''	Viscous shear modulus
Gly	Glycerol
GNP	Graphite nanoplatelets
GO	Graphene oxide
i	Number of results sorted in ascending order
ICDD	International center of diffraction data
IS	Impact strength
IUPAC	International Union of Pure and Applied Chemistry

J	Heat flux per unit area / Joule
K	Kelvin degree
k	Kinetic constant / Thermal conductivity
k_e	Thermal conductivity contribution due to the movement of electrons
KHN	Knoop microindentation hardness
k_L	Thermal conductivity contribution due to the movement of phonons
l	Length of indentation in mm / Phonon mean free path / Sample thickness
L	Load applied / Sample thickness / Support span
L_0	Initial sample length
LED	Light emitting diodes
LVR	Linear viscoelastic region
m	Gradient of the slope / Meters
min	Minutes
MWCNT	Multiwalled carbon nanotube
n	Number of samples / Variable number
o-CNT	Oxidized carbon nanotube
P	Cumulative probability
PC	Polycarbonate
PCB	Printed circuit boards
PE	Polyethylene
PET	Polyethylene terephthalate
PETMP	Pentaerythritol tetrakis (3-mercaptopropionate)
phr	Parts per hundred of resin
PMC	Polymer-matrix composite
PMMA	Poly(methyl methacrylate)
PP	Polypropylene

PS	Polystyrene
PU	Polyurethane
PVC	Polyvinylchloride
R	Electrical resistance / Gas constant
ROP	Ring-opening polymerization
S	Cross-section of the sample
s	Seconds
SAOS	Small amplitude oscillatory shear
SSA	Specific surface area
SWCNT	Single walled carbon nanotube
$T_{\tan\delta}$	Temperature of maximum of the tan δ peak
T	Temperature
t	Time / Thickness of sample
$T_{2\%}$	Temperature of decomposition for a 2% weight loss
$T_{5\%}$	Temperature of decomposition for a 5% weight loss
T_c	Curing temperature
TC	Thermal conductivity
TCA	Thermally conductive adhesive
TEA	Triethanolamine
TES	Thermal energy storage materials
T_g	Glass transition temperature
TGA	Thermogravimetric analysis
t_{gel}	Gel time
TIM	Thermal interface material
TMA	Thermomechanical analysis
T_{max}	Maximum temperature
T_{peak}	Temperature of the peak

T_{room}	Room temperature
U-process	Umklapp process
UV	Ultra violet
V	Volume
vol. %	Volume percentage
W	Watts
wt. %	Weight percentage
x	Degree of curing
X_{gel}	Gel conversion degree
XRD	X-ray diffraction
α	Thermal diffusivity
β	Critical exponent / Shape parameter
Δh	Enthalpy of the curing proces
ΔH	Heat difference
Δh_g	Heat released of gelled samples
Δh_T	Heat of complete conversion
η	Viscosity
η^*	Complex viscosity
Θ	Angular diffraction angle
κ	Thermal conductivity
λ	Thermal conductivity / Wavelength of X-ray beam
v	Average of phonon velocity
ρ	Density / Electrical resistivity
σ	Electrical conductivity
τ	Apparent lap-shear strength
ω	Angular frequency

C. List of publications

1. Isarn I, Massagués L, Ramis X, Serra À, Ferrando F. **New BN-epoxy composites obtained by thermal latent cationic curing with enhanced thermal conductivity.** Composites: Part A 2017; 103: 35-47.
   IF: 4.514 (2017), Q1 (4/26) in Materials Science, Composites.

2. Isarn I, Gamardella F, Massagués L, Fernàndez-Francos X, Serra À, Ferrando F. **New epoxy composite thermosets with enhanced termal conductivity and high Tg obtained by cationic homopolymerization.** Polym Comp 2018; 39: 1760-1769.
   IF: 2.268 (2018), Q2 (10/25) in Materials Science, Composites.

3. Isarn I, Ramis X, Ferrando F, Serra À. **Thermoconductive thermosetting composites based on boron nitride fillers and thiol-epoxy matrices.** Polymers 2018; 10: 277-292.
   IF: 3.164 (2018), Q1 (17/87) in Polymer Science.

4. Isarn I, Gamardella F, Fernàndez-Francos X, Serra À, Ferrando F. **Enhancement of thermal conductivity by the addition of several conductive fillers to thermal cationic curing of cycloaliphatic epoxy resins.** Polymers 2019; 11: 138-151.
   IF: 3.164 (2018), Q1 (17/87) in Polymer Science.

5. Isarn I, Bonnaud L, Massagués L, Serra À, Ferrando F. **Enhancement of thermal conductivity in epoxy coatings through the combined addition of expanded graphite and boron nitride fillers.** Prog Org Coat 2019; 133: 299-308.
   IF: 3.420 (2018), D1 (2/20) in Materials Science, Coatings&Films.

6. Isarn I, Bonnaud L, Massagués L, Serra À, Ferrando F. **Study on the cooperative effect of boron nitride and carbon nanotubes in the improvement of the thermal conductivity of epoxy composites.** Submitted to Polym Comp.
   IF: 2.268 (2018), Q2 (10/25) in Materials Science, Composites.

D. Meeting contributions and stages

Research stay from February 1st, 2018 to May 31st, 2018 in:

Site: Laboratory of Polymeric and Composite Materials, Center of Innovation and Research in Materials and Polymers (CIRMAP), Materia Nova Research Center & University of Mons, 23 Place du Parc, B-7000, Mons, Belgium.
Under supervision of PhD Leïla Bonnaud, project leader.
Task: Preparation and characterization of thermoset composites filled with boron nitride, expanded graphite and carbon nanotubes.

Oral and poster contributions

- **APME 2017**, Advanced Polymers via Macromolecular Engineering, Ghent, Belgium, 2017 (May 21-25). Poster.
  Title: "New BN-epoxy composites obtained by thermal latent cationic curing with enhanced thermal conductivity".
  Authors: *I. Isarn, L. Massagués, X. Ramis, À. Serra, F. Ferrando.*
- **JIP 2017**, Jóvenes Investigadores en Polímeros, Salou, Spain, 2017 (June 5-8). Oral.
  Title: "New epoxy composites thermosets with enhanced thermal conductivity obtained by latent cationic homopolymerization".
  Authors: *I. Isarn, F. Gamardella, X. Fernández-Francos, F. Ferrando, À. Serra.*
- **CIBEM 2017**, Congreso Iberoamericano de Ingeniería Mecánica, Lisboa, Portugal, 2017 (October 23-26). Oral.
  Title: "Nuevos materiales compuestos epoxídicos con conductividad térmica mejorada por adición de nitruro de boro".
  Authors: *I. Isarn, À. Serra, F. Ferrando.*
- **CNIM 2018**, Congreso Nacional de Ingeniería Mecánica, Madrid, Spain, 2018 (September 19-21). Poster.
  Title: "Mejora de la conductividad térmica de resinas epoxídicas".
  Authors: *I. Isarn, F. Gamardella, À. Serra, F. Ferrando.*
- **GEP 2018**, Reunión del Grupo Especializado en Polímeros, Huelva, Spain, 2018 (September 24-27). Poster.
  Title: "Enhancement of thermal conductivity by addition of several conductive fillers in thermally cured cycloaliphatic epoxy thermosets".
  Authors: *I. Isarn, F. Gamardella, X. Fernández-Francos, À. Serra, F. Ferrando.*
- **HYMA 2019**, 6th International Conference on Multifunctional, Hybrid and Nanomaterials, Sitges, Spain, 2019 (March 11-15). Poster.
  Title: "Enhancement of thermal conductivity in epoxy composites through the addition of expanded graphite and boron nitride fillers".
  Authors: *I. Isarn, L. Bonnaud, L. Massagués, À. Serra, F. Ferrando.*

Chapter 1. Introduction and objectives

1.1. Overview of polymer materials
1.2. Thermosets
1.3. Epoxy thermosets
1.4. Heat conduction through materials
1.5. Epoxy composites
1.6 Scope and objectives

UNIVERSITAT ROVIRA I VIRGILI
NEW EPOXY COMPOSITES WITH ENHANCED THERMAL CONDUCTIVITY KEEPING ELECTRICAL INSULATION.
Isaac Isarn Garcia

1.1. Overview of polymeric materials

From the point of view of materials science, a material is any substance that is useful to humanity. Highlighting the group of solid materials, they were traditionally classified as metals, ceramics, polymers and a combination of them to form composites. The ability to produce and handle materials reaches such importance that labelled the progress of the early civilizations (Stone Age, Bronze Age, Iron Age).[1] The development of technologies has caused a transformation in the way that science has studied and produced new materials. From the conception of having a material with given characteristics; what can be used for? To the need for a material with specific properties; how to create it? The key idea for this change is the understanding of the materials paradigm, which can be represented as a tetrahedron with the vertices: structure, properties, processing and performance; with characterization in the centre (**Figure 1.1**).[1] Knowing the structure-property correlation leads scientists to understand the principles for modulating new materials through different manufacturing processes with the needed performances and improvements.

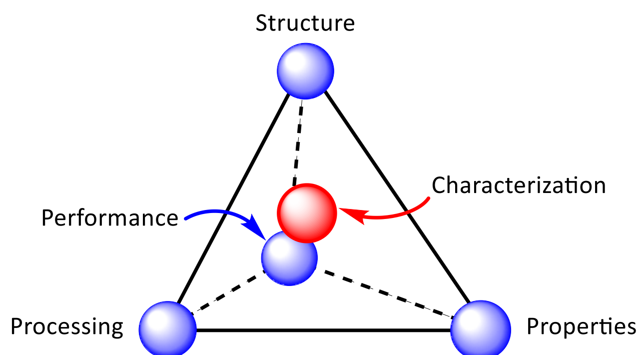

Figure 1.1. Materials paradigm represented in form of tetrahedron.

Much of the knowledge about materials has been developed during the last 200 years, when technology has experienced a spreading advancement. This has allowed to create thousands of new materials with the desired characteristics to make lives easier and more comfortably. One of the material types that has contributed the most to the well-being of society, coinciding with its "discovery" with the great technological development, has been polymers, including familiar plastic and rubber materials. Although the great industrial development of polymeric materials occurred since the mid-twentieth century, they have been used for many years. Strictly speaking, polymers have been used since the dawn of man, considering that materials such as wood, animal skins or vegetal fibres are being used since ancient times. Moreover, the indigenous cultures of Mesoamerica have used rubbers for centuries, from which the natural latex tree *Hevea brasiliensis* comes from.[2]

A polymer is a material with large molecules made of many smaller repeating units of the same kind. By definition "poly" indicates a several number of repetitive parts ("mer") or molecules, which are usually called monomers and refers to single blocks. Within this group we can find diverse types of macromolecules such as DNA or plastics. The common word plastic comes from the Greek verb *plassein*, meaning "to mold or shape" in terms of deformability, and this is thanks to their structure of flexible chains of carbon atoms or the small molecules bonded in a repeating pattern.[3] Polymers are mainly characterized to be organic materials based on hydrogen and carbon atoms, connected to each other to form chains or more complex structures, commonly including other non-metallic atoms such as S, N, O, Si, etc.

Polymers can be classified from different perspectives according to several characteristics. A general classification of polymers can be represented as follows:

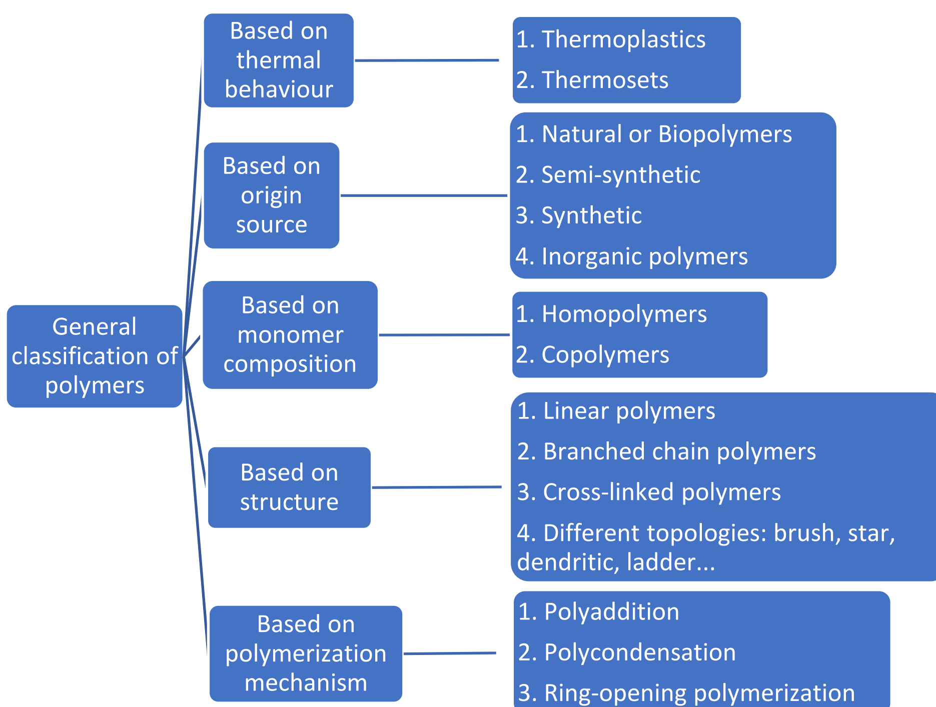

Figure 1.2. General classification of polymer materials.

There are two main categories of polymer materials based on their thermal behaviour. An accepted general way to distinguish thermoplastics from thermosets is examining their behaviour when exposed to heat. Thermoplastics, whether amorphous or semi-crystalline, when heated, their chains move freely, and fluidity increases. On the contrary, the thermosets remain in solid state thanks to their strong covalent bonds, which when destroyed at high temperatures, they are degraded into gases and ashes without flowing.[4] Hence the difficulty of recycling thermoset polymers once processed.

The processing of thermosets and thermoplastics are also differentiated. While thermoplastics must be heated at a certain temperature to flow and solidifies on cooling on the desired mould shape, thermosets are irreversibly formed by curing the appropriate formulations directly on the desired mould or surface. The curing requires a curing agent and it is induced by heat or suitable radiation. Thermoplastic materials, with weak interactions or secondary forces (Van der Waals or dipole-dipole hydrogen bonding) between their chains, can be deformed elongating by the action of external forces. On the other hand, thermosets can create an insoluble 3D polymer network that can be considered to have an infinite molecular weight, with strong bonds that can poorly withstand deformation. There are also thermosets having a linear structure, but their rigid chain leads to these polymers to be insoluble and infusible like if they were 3D structures.

Mechanically, we can add another class of polymers according to their stress-strain behaviour when a force is applied: brittle, plastic and elastomeric. The brittle ones, according to their crosslinked structures, are related to thermosets. They possess high Young's modulus, but they are fragile and can break without plastic deformation. Plastic polymer materials, showing both elastic and plastic behaviour, are associated to thermoplastics. In the viscoelastic materials, part of the deformation suffered is recovered (elastic part) and the other is not (viscous). Polymers with long elastic deformation, able to reach hundreds of strain percentages, are known as elastomers (being vulcanized rubber the most illustrative example), and they are included in the thermosets group. The elasticity they possess is derived from the ability to reconfigure the arrangement of their chains to distribute an applied force, reversibly when the stress is removed.

Based on their source we can distinguish separate kinds of polymer materials. Those derived from plants and animals are named natural or biopolymers and used without suffering any chemical process. In this group we can find materials such as wool, silk, leather, natural rubber and others formed by polynucleotides, polypeptides, polysaccharides, lignin, etc. DNA, of crucial importance in biology, and cellulose, from which wood and paper are manufactured, stand out among this type of polymers. If they are subjected to a chemical process they are converted into semi-synthetic polymers, as in the case of the vulcanized rubber, nitrocellulose and cellulose acetate.

Many of the polymers that are used today are synthetic, considering that they can be produced economically on a large scale from the corresponding monomers, and their properties can be managed to obtain products that improve natural polymers characteristics. They can be obtained from a great variety of monomers following different synthetic procedures and therefore a huge variety of materials can be produced. Among synthetic polymers we can consider: nylon, Neoprene, Teflon, polystyrene (PS), polyethylene (PE), polyvinylchloride (PVC), polypropylene (PP),

polyethylene terephthalate (PET), polyurethanes (PU), epoxy resins and melamine, phenol and urea formaldehydes, as examples.

A singular case of polymers are the so-called inorganic polymers, since their principal backbone chain are not constituted by carbon atoms. Silicones, also known as polysiloxanes, and polyphosphazenes and polysulphides belongs to this class. Lubricants, coatings and sealants are the most typical uses of that silicones, as well as in biomedicine and cosmetics.

The incorporation of monomers into the polymeric structure leads to the formation of repetitive units. As introduced above, the classification of the polymers can also be based on the presence of one or more repeating units in the polymeric structure. If there is a single kind of structure, they are known as homopolymers, whereas if they are made up of at least two different repeating units, they are termed copolymers. PE, PVC, PP, PS, phenol-formaldehyde or polycarbonate (PC) are some standard examples of homopolymers, and the nature of monomers mainly determine the final properties of materials. However, when more than one monomer in various quantities are polymerized, an infinite variety of polymers can be synthesized. Depending on the disposition of the repeating units we can differentiate copolymer types as: statistical or random, alternating or regular, block or graft copolymers.[5]

Large differences in the physical characteristics of polymers depends on the topological structure they present. Linear polymers are those formed for long single chains. The tetrahedral geometry of carbon atoms can lead to the formation of non-straight chains and for this reason linear polymers have always been imagined as a mass of spaghetti. Some common linear polymers are high density PE, PVC, PS, nylon and poly(methyl methacrylate) (PMMA).

Branched polymers may be synthesized in which ramifications have grown in the main chain. The length and the ratio of branches to linear segments change the materials behaviour. The chain packing efficiency is reduced by the formation of branches, lowering the polymer density compared to linear structures.[1] Low density PE, with short branches in its primary chain is an example of branched polymer. A perfectly symmetrical branched macromolecule, resembling a family tree with spherical and three-dimensional morphology is denominated *dendrimer*.[5]

Another important structure that polymers can have is the crosslinked or three-dimensional network. Crosslinked polymers are those whose chains are covalently bonded among them at various positions and extended through the whole material to form a bulk polymer. The degree of crosslinking determines the polymer behaviour and can be calculated according to Flory's Network Theory.[6] In rubbers this covalent bonding is called vulcanization. Most thermosets are formed by repetitive units covalently bonded forming a 3D network.

There are other different topologies, named also architectures, such as brushes, stars, ladders, hyperbranched, etc., which can be engineered for advanced applications (**Figure 1.3**).

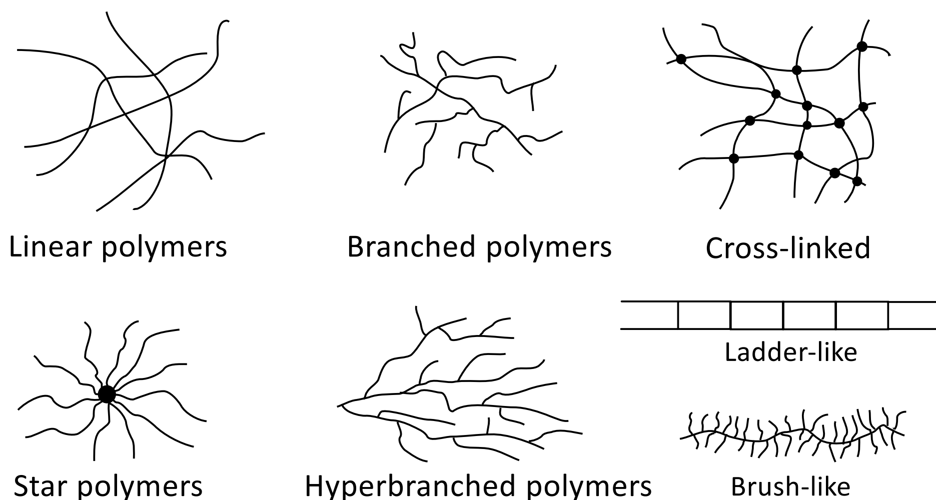

Figure 1.3. Some topologies that polymers can adopt.

The polymerization process is carried out basically by three different mechanisms: polyaddition, polycondensation and ring-opening polymerization. One of the classifications of polymers are based on these mechanisms. PE, PP and PVC are obtained by polyaddition, which occurs by adding monomers to a growing polymer chain, usually in three steps: initiation, propagation and termination. Polyaddition requires an initiator to start the first step and to form an active specie. Then, the reaction propagates enlarging the polymer chain, by adding the monomer molecules, one by one, to this active point. Finally, when all the monomers have been incorporated or the active chain end has been deactivated, the termination step occurs. High molecular weight polymers are formed even at low conversion degrees.

The second polymerization mechanism is polycondensation, also named step-growth polymerization. The monomers usually have two functional groups of different characteristics able to react by typical organic synthetic reactions. These reactions are produced step by step, and in some cases little molecules such as water are evolved. High molecular weights are not reached until the conversion is practically complete. Functional groups disappear rapidly on reacting and therefore polymerization rate goes down. Polyamides, polyacetals, nylons and polyesters are examples of polymers performed by this mechanism.

The last important type of mechanism is the ring-opening polymerization (ROP), which is a form of chain-growth polymerization as the polyaddition. ROP can proceed via radical, anionic or cationic polymerization. The distinctive characteristic of these mechanism falls in the presence of rings in the starting monomers, opened by the

reaction of the groups forming new bonds. Some cyclic monomer groups are listed as: epoxide, oxetane, aziridine, lactone, lactide or oxazoline for example.

Other possible classifications, not included in **Figure 1.2**, could be based on the molecular weight, the crystallinity degree and structural isomerism or tacticity they presented, as well as their application field.

Polymer characteristics such as chemical structure, crystallinity degree, molecular weight, topology or regularity notably influence on properties such as viscosity, thermal behaviour, mechanical resistance and applicability. For this reason, polymers can be considered among the most versatile materials, with a non-stop development of new polymers for a growing number of applications. From the discovery of the Bakelite in 1907 the civilization starts The Age of Polymers.

1.2. Thermosets

The first polymer synthesized made of chemically crosslinked chains was a phenol-formaldehyde resin. It was called Bakelite and was the first thermoset, discovered by Baekeland.[7] Since then, a large variety of different thermoset families have been developed, among them the most typical examples, with the largest amount of production, are the urea-formaldehyde resins, unsaturated polyesters and epoxy resins. Other typical thermosets families are alkyds, vinyl esters or allyl resins among others.

Globally, thermosets represent less than 20% of world polymer production. Despite this, the quantities produced per year are quantified in millions of tons and it is estimated that the global market will reach several tens of billion dollars.[8] The large consumption of these materials is due to their specific properties that make them irreplaceable for the superior mechanical and thermal behaviour and chemical protection capability. From a very general point of view, polymers are considered "soft" materials and have a higher elastic and plastic deformation capacity compared to ceramic and metallic materials. In contrast, thermosets, as mentioned above, are characterized by forming a covalent network that makes them “rigid”, within the rigid that polymers can be.

The preparation of crosslinked thermosets, also called curing, usually starts from liquids or dense resins which are polymerized in the presence of curing agents. The formulations used to prepare thermosets can be composed of several ingredients, being a mixture of monomers or comonomers the essence, but also containing curing agents, additives and in some cases catalysts.

Conventional thermosets, after curing, cannot be reshaped in contrast with thermoplastics. They withstand high temperatures before degrading, and they possess high stability against chemical attacks and a high structural integrity. These characteristics are used in applications that require thermal stability and resistance to

aggressive environments such as coatings and paints, or objects that require a stable form and durable materials such as polymeric recipients, construction equipment panels and components, etc., all this being able to be made in complex shapes.

One of the most important parameters in the polymer chemistry is the monomer's functionality, which determine the final topology of the polymer. According to IUPAC, the term functionality is defined as the number of bonds that a given monomer can form with others. The functionality of a monomer depends both on the number of reactive functional groups in the structure, and on the curing mechanism selected. In some cases, a functional group can form an only new bond in the polymerization, but changing the type of mechanism, the same functional group can act as a bifunctional, because it forms two new bonds. To obtain 3D networks at least, each monomer must have a functionality higher than two. The addition of bifunctional monomers to the formulation reduces the crosslinking density of the thermoset and increases the flexibility of the network. These types of monomers are named reactive diluents.

Non-crystalline or amorphous polymers are characterized to present a "glass transition temperature" (T_g), such a discontinuity in the heat capacity. It is a crucial physical parameter for polymer manufacturing, processing and use. Inherent in polymer materials even they are semi-crystalline, T_g is a physical change of the properties at a certain temperature range. Below T_g, a polymer has hard properties (vitreous or glassy state), while above T_g, there is a sudden decrease in the mechanical properties (rubber state). The glass transition may be modified by adjusting the degree of branching or crosslinking or by the addition of plasticizers.[9] The stiffness, heat capacity or thermal expansion coefficient are some of the properties affected by this transition. Rubbers are so named because their T_g is below ambient temperature. Microscopically implies the cooperative movement of the polymeric chains sliding to each other when they are subjected to a force.

One of the more important physical transitions during the crosslinking of thermosets is the "gelation" whatever the polymerization procedure is produced, even though the transition primarily depends on the type of reaction. Also known as gel point, this phenomenon occurs during the branching and creation of the covalent bonds among the monomers and is characterized to transform the liquid resin into a crosslinked gel, while the viscosity of the system is increasing. At a particular conversion degree (X_{gel}), the viscosity system rises to infinite, and from that moment, the material starts to become a solid and no longer can be reshaped. It must be noticed that gelation is an irreversible process. Hence it is importance to know this transition in industrial production processes. From the molecular viewpoint, the insoluble gel is produced when a network that interconnect all the species present in the blend is formed, even though not all the functional groups have already been reacted. The gelation process is, in general, a phenomenon that does not affect the rate of curing, so it must be analysed

by techniques sensitive to changes in viscoelastic properties, such as rheology or thermomechanical analysis, or by solubility tests.

The other important transition that can take place during the curing of thermosets is the “vitrification”. Vitrification may occur when the conversion of the monomers reaches a point such as the material changes from behaving as a liquid or gel (if the conversion is greater than the X_{gel}) to a glass. The vitrification is highly influenced by the temperature at which the curing is carried out, since if it is far lower than the T_g the mobility of the molecules is restricted, and the reaction rate becomes controlled by diffusion. At that point, the only way to complete the polymerization is by heating to a temperature close to or higher than T_g. It is a reversible process, unlike gelation. It must be mentioned that the T_g of the system increases as the functional groups react. Hence the importance of choosing the curing temperature well, in which the differential scanning calorimetry (DSC) can be very useful.

As discussed in the previous section, thermoset polymers are generally mechanically stronger than thermoplastics due to their 3D crosslinked network. In addition, they better suit applications at high temperature up to their decomposition, keeping shape and most of their characteristics. However, a wide range of properties exists, which can be obtained from the proper combination of monomers, catalyst, curing agents, curing schedule and additives used. The higher the crosslinking density the higher the resistance when exposed to heat or chemical attacks. In the same way, the mechanical strength and hardness improve with the crosslinking degree, at expenses of brittleness. Some fibbers or fillers are also commonly added to the formulation, which can respond both to obtain the desired final properties and to reduce the production cost. We can refer to them as reinforced polymers or composites, and practically all thermosets used for structural applications are within this group.

Thermosets can be divided in different types, according to the monomers used, curing agents and the chemistry implied. A brief comment will be exposed on each of the most common ones. Epoxy resins will be extensively reviewed in the next section.

Phenolic or phenol formaldehyde resins, the first commercialized synthetic resins as Bakelite, are obtained by the reaction of phenol with formaldehyde. Many molded products as billiard balls, various sorts of boards, laboratory countertops, coatings and wood adhesives are among its most important applications that resins offer at low cost and good compatibility with substrates. Phenolic resins are also found in myriad industrial products and laminates. An important subgroup of phenolic resins is the Novolac (name appointed by Baekeland), composed by a stoichiometric deficiency of formaldehyde (see **Scheme 1.1**). A second monomer must be used to complete the phenol polymerization (usually methylphenols) using acid-catalysis and needs a hardener to be crosslinked. The uses of Novolac include high temperature resistance resins, tire tackifiers, binders with glass and mineral fibers to produce thermal and acoustic insulators and as curing agent for epoxy resins.[10]

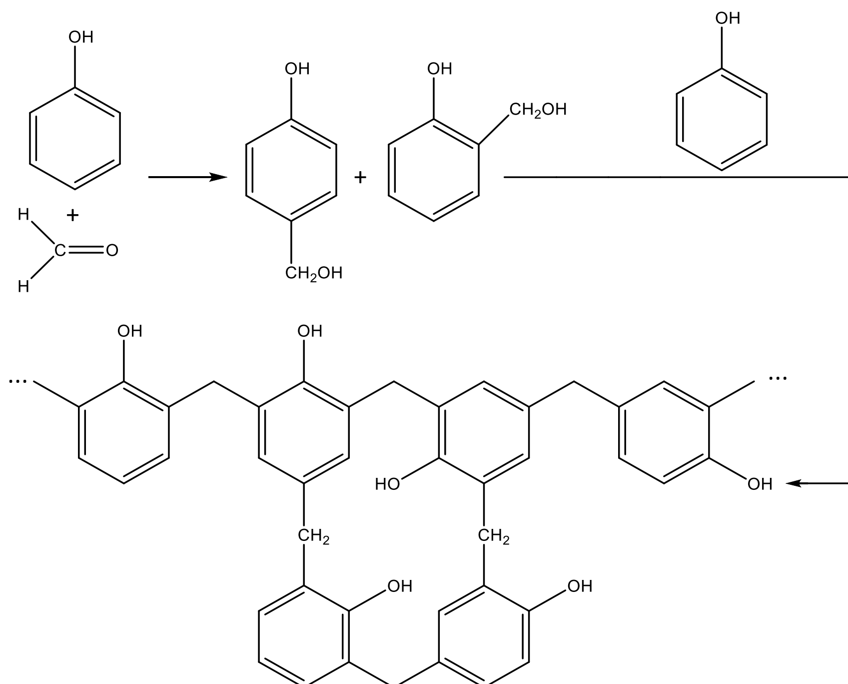

Scheme 1.1. Preparation of phenol-formaldehyde resins.

Urea-formaldehyde thermosets are primarily used as a binder for plywood and particle or fiberboards. The idealized structure of the resin is depicted in **Scheme 1.2**. The good adhesion to wood is due the high concentration of polar groups and the reaction between hydroxyl groups of the resin and cellulose to form ketal moieties. Related amino and melamine formaldehydes are used in paper for improving tear strength, in molding electrical devices, jar caps, kitchen surfaces, cooking tools, etc. They possess a good compatibility with pigments and dyes and are ease of printing for an attractive appearance.[11]

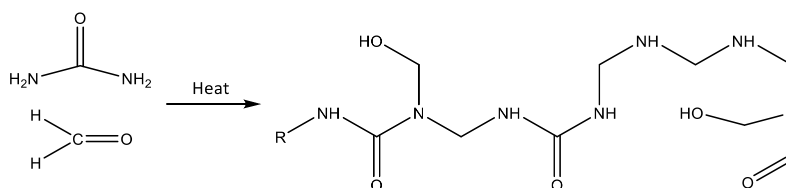

Scheme 1.2. Preparation of urea-formaldehyde resins.

Polyurethanes (PUs) are made by condensation of bi- or trifunctional isocyanates with polyols (see **Scheme 1.3**). They require the use of a catalyst. The variety of applications of PUs is huge by varying the isocyanate, polyol or additives. Aromatic polyurethanes discolor when exposed to light while aliphatic isocyanates have a better color stability. High resistance to moisture and long-time durable, in general, temperature limits their applications in the range of 100-150 °C because the reaction

between isocyanates and alcohols is reversible at higher temperatures. The most extended use of PUs (approximately three-quarters) is in form of foams, ranging from flexible to rigid, giving products with good insulating characteristics at considerably low density. For that reason, is extensively utilized to fill gaps as insulator in construction and furniture. Other foam uses include seat cushions in vehicles and upholstered furniture, cleaning sponges, in sculptures and decorates and plant substrates. Uses of non-foam urethanes include: varnishes, wheels, skateboards, adhesives such as glue for bookbinders, and for encapsulating electronic components.

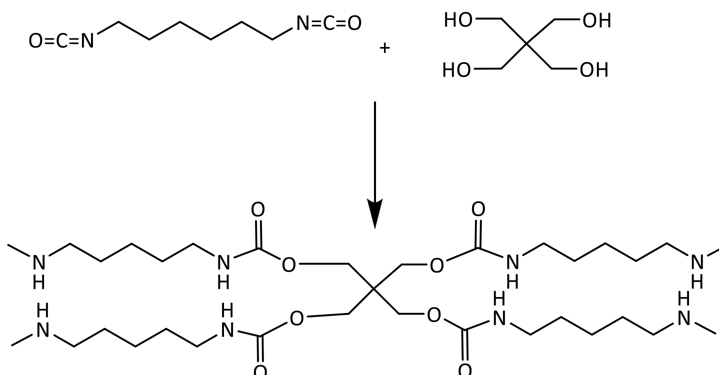

Scheme 1.3. Example of the preparation of polyurethanes.

Cyanate thermosets are considerably expensive which limits their extensive use. High temperature resistant, cyanates can be continuously used in ranges from -200 °C to 250 °C for long service times, appreciated in aerospace composites.[12] Their monomers are typically solid crystals at T_{room} and they are usually cured at high temperatures, forming triazine, a stable aromatic group with no carbon-hydrogen bonds. They are usually tightly crosslinked and brittleness appears as one of its few disadvantages along with its price. That is why cyanates are often used in combination with other monomers such as epoxides and bismaleimides to achieve more convenient properties. The resistance to fatigue and radiation makes them very useful for structural elements for satellites and aircrafts fuselages as well as structural elements for dielectric and electromagnetic devices. **Scheme 1.4** depicts the formation of a network from cyanate ester monomers.

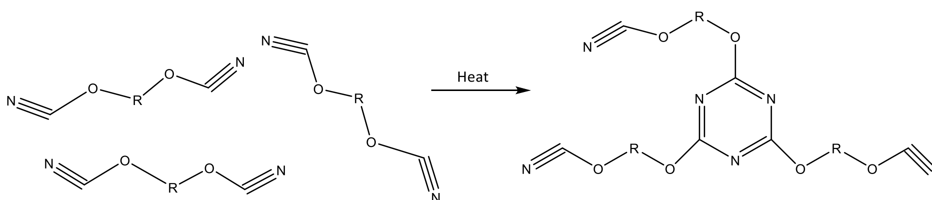

Scheme 1.4. Crosslinking of cyanate esters.

From the esterification of an epoxy resin, typically formulated with styrene, are composed vinyl esters resins (see **Scheme 1.5**). The polymerization process of that resins is initiated by radicals, induced by UV radiation of by peroxides. The low viscosity of these formulations makes them highly adequate to produce polymer composites, even though the volatility of styrene is a drawback to be considered and operators must be suitable protected. The economic value and mechanical strength of this resin are between polyesters and epoxy resins. The chemical resistance to marine and gases environments is quite good to be used as naval coatings and the manufacture of vessels and tanks for the chemical industry.

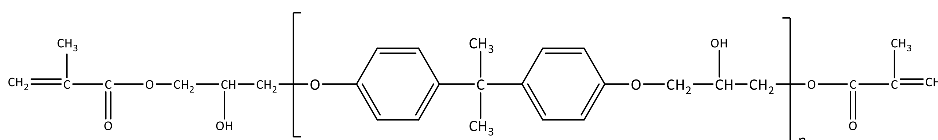

Scheme 1.5. Example of a vinyl ester resin.

Alkyd resins are derived from polyesters modified with components such as fatty acids, which confers a tendency to form flexible coatings (see **Scheme 1.6**). Extensively used in paints, they can also be casted in moulds. The crosslinking reaction undergoes in the presence oxygen and no heating is required. Alkyds are one of the most inexpensive thermosets. The low durability in outdoors surfaces and the presence of organic solvents have been decreasing their use, although is still consumed for low performance industrial coatings and for interior paints.

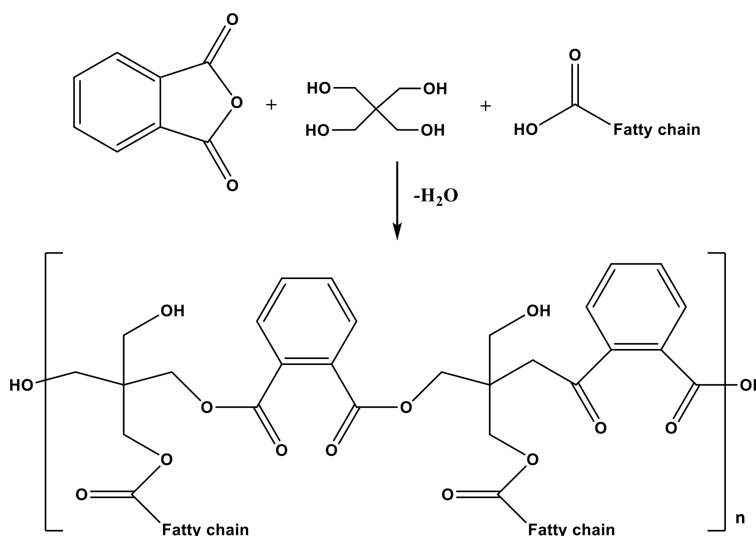

Scheme 1.6. Synthesis of an alkyd resin.

Unsaturated polyesters are produced by condensation of polyols with saturated or unsaturated anhydrides or dibasic acids (see **Scheme 1.7**). The unsaturation of this type of polyesters provides the subsequent crosslinking in an exotherm reaction. One of

the most extensively used thermosets due to their low cost, adequate environmental resistance, light weight, rigidity, electrical resistance and good wetting to glass fibres contribute to having a wide range of properties, can withstand temperatures about 80 °C. By the other hand produces toxic fumes, is not proper for bonding many substrates and their bonding is manifested weaker than epoxy resins. Among its applications stand out: ship's hull, pipelines, vehicles parts, storage tanks, building components and laminated panels.

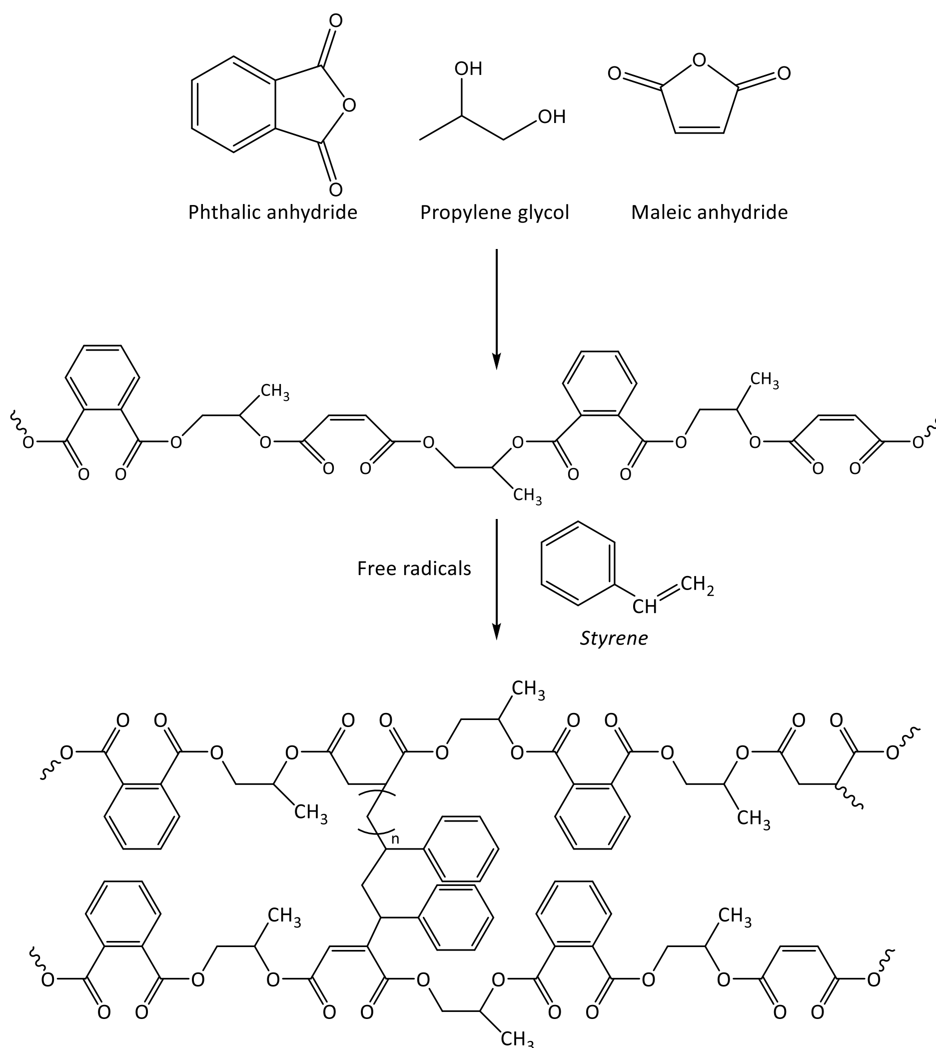

Scheme 1.7. Synthesis and crosslinking of an unsaturated polyester.

1.3. Epoxy thermosets

In this work we will delve in the field of epoxy thermosets, one of the most consumed. In fact, approximately 70% of thermosetting polymer market is spent in

epoxies when polyurethanes (some of them may be thermoplastics) are not considered.[13] From them, nearly the 80% of the epoxy market production are applied in coatings and electronics.[14] The term "epoxy" designates a functional group that the monomers or resins contain. Also known as oxirane ring, is a three-member group characterized by an oxygen atom bonded to two carbon atoms to form a cycle as shown in **Scheme 1.8**:

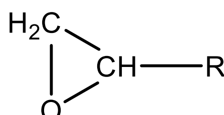

Scheme 1.8. Epoxy or oxirane ring functional group.

Since the functionality is defined as the number of arms a functional group can form in the reaction, and this, as discussed above, depends on the curing system, the creation of a crosslinked network needs at least the presence of two or more epoxy groups per molecule. That means that each molecule has a functionality of two or higher and in consequence, the global functionality of the system to reach a network structure is a minimum of four. In some cases, when an increased crosslinking density is aimed, higher functionalities are required. Commonly speaking, epoxy resins are referred both to uncured and cured epoxy polymers, although all the reactive groups may have been reacted during the polymerization. In fact, the polymers that have been produced by the reaction of these oxirane monomers are known as epoxy thermosets, although they no longer contain those functional groups in their structure. One of the most commercialized epoxy resins since 1940 is the well-known diglycidyl ether of bisphenol A (DGEBA), a resin based on the reaction of bisphenol A with epichlorohydrin in strong basic conditions. P. Castan and S. O. Greenlee share the recognition of being the first to synthesize this resin (**Scheme 1.9**) in 1936.[15]

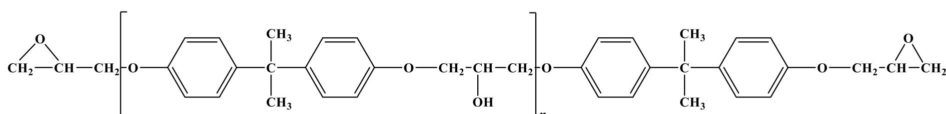

Scheme 1.9. Structure of DGEBA resins.

The molecular weight of the epoxy precursors, and hence their viscosity, can be controlled by the number of repeating units that it can contain. This *n* (present in the scheme 1.9.) can be adjusted by the stoichiometric ratio of the reagents used, giving rise to liquid resins with low *n*, or waxy or solid prepolymers for high numbers of repeating units, what would also affect the end properties of the material. However, the most affecting variable is the change of the non-epoxy part of the molecule, which may contain aliphatic, cycloaliphatic or aromatic structure, as well as the functionality of the molecule. Other important epoxy monomer for their low viscosity before the curing is the 3,4-epoxy cyclohexylmethyl 3,4-epoxy cyclohexane carboxylate (ECC). Cycloaliphatic epoxy compounds are less reactive with usual amine hardeners and they preferable

react in cationic conditions by ring-opening polymerization mechanism. The chemical structure of this monomer is depicted in the following scheme:

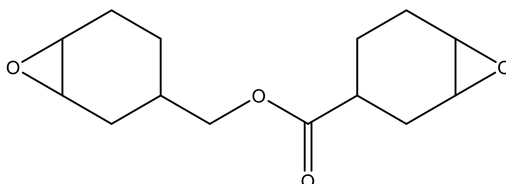

Scheme 1.10. Chemical structure of ECC monomer.

On the other hand, the properties of the final materials are affected by the type of curing agent (also known as hardener) used, that defines the curing kinetics and mechanism. Epoxies cannot be polymerized by chain growth mechanism, but they are polymerized by polycondensation and ring-opening.

The polycondensation process, which requires a second substance with active functional groups able to react with epoxides, proceeds via step by step succession of elementary reactions between reactive sites creating new covalent bonds. In this type of reaction epoxide group acts with a functionality of one, and therefore a minimum of two epoxy groups in the resins per molecule are needed to form the networked structure. They can be cured with a large number of hardeners or curing agents, among them: amines, acids, anhydrides, phenols, dihydrazides and thiols.[16,17] The most used hardener is the group of amines. They need a functionality equal or higher than three, and therefore primary diamines are commonly used. These curing agents are usually added in stoichiometric amounts to the formulation to reach the maximum crosslinking degree. However, in some cases, off-stoichiometric proportions are used to decrease crosslinking density that can improve mechanical characteristics, such as toughness. The polycondensation of epoxies with primary amines is depicted in **Scheme 1.11**:

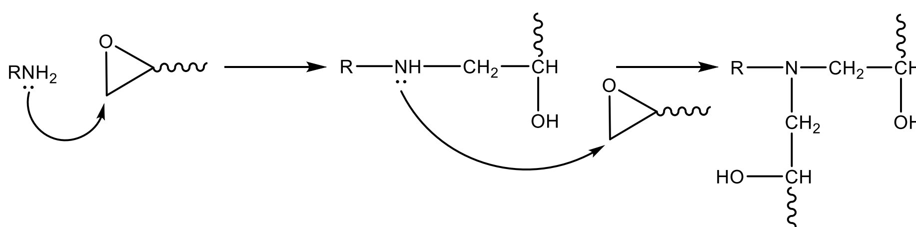

Scheme 1.11. Reaction mechanism between epoxides and primary amines.

Epoxy resins can be homopolymerized either by anionic and cationic reactions (ring-opening polymerization), using a nucleophilic or electrophilic initiator taking advantage of the highly polar oxygen-carbon bonds and the strain of oxiranic cycle. Catalytic amounts of these initiators promote the homopolymerization of epoxides, i.e. the formation of a polymer from a single type of monomer. In this case the functionality of an epoxy group is two and therefore a diepoxide is needed to create a network. This reaction, as the polyaddition, presents three main steps: initiation, propagation and

termination.[18] Depending on the propagation mechanism, as mentioned in the previous section, there are two main types of reactions: anionic and cationic. Radical mechanism is not working for epoxy polymerizations.

Anionic polymerizations take place with initiators with elevated nucleophilicity. Lewis bases such as tertiary amines as 4-(N,N-dimethylamine)pyridine (DMAP) or 1-methyl imidazole (1-MI) are the most extended anionic initiators used in epoxy curing.[19] The ring opening of the epoxy ring is produced by the nucleophilic attack of the nitrogen atom forming an alkoxide in the initiation step. The presence of species which can coordinate with the epoxy groups, as hydroxyl groups, promotes the initiation accelerating the reaction. In the propagation step is the alkoxide which propagates the polymerization opening the remaining epoxides and forming at the end the crosslinked network constituted by polyether structures.[20,21]

Brönsted and Lewis acids are used to initiate the ring opening polymerization via cationic mechanism. The most extended acid used is the BF_3/amine complex.[22] $TiCl_4$, $AlCl_3$, $ZnCl_2$, BCl_3, $SiCl_4$, $FeCl_3$, $MgCl_2$ or $SbCl_5$ are other acids used for the cationic polymerization of epoxides. Last decades lanthanide and rare earth metal triflates have demonstrated to be also good cationic initiators.[23] Interestingly, our research group studied some earth rare triflates that exhibit certain advantages to conventional initiators, since they are tolerant to water, stable under ambient conditions and relatively soluble in organic solvents.[24-27]

Kubisa and Penczek described the existence of two different propagation mechanism that coexist in cationic polymerization of epoxides.[28] They are activated chain end (ACE) and active monomer (AM) mechanisms, depicted in **Scheme 1.12**.

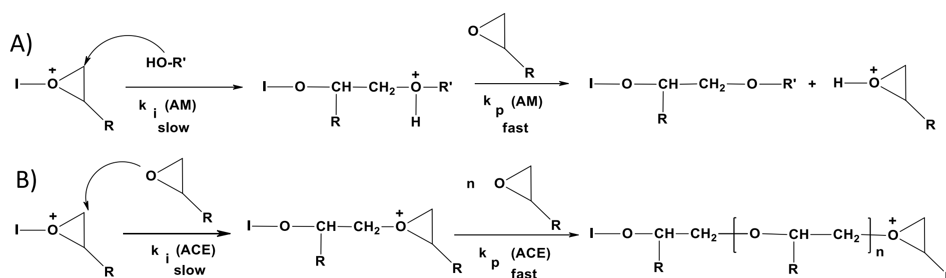

Scheme 1.12. Activated monomer mechanism (A) and active chain end mechanism (B).

Both mechanisms start with the coordination of the initiator in the oxygen of the epoxide to promote the ring opening. ACE mechanism consists in the reaction between an activated epoxide and another. On that way, the activated epoxide is always linked at the end of the growing chain. On the contrary, AM mechanism requires a hydroxyl group to first open an activated epoxide. Then, there is an intermolecular interchange of protons with an epoxide that becomes now activated. Thus, AM mechanism is favoured in the presence of hydroxyl groups and is not rare the appearance of two

overlapped exothermic peaks in DSC scans.[29] On that way is always the monomer the activated epoxide.

Depending on the hardener or initiator used, epoxy monomers can react even at ambient conditions or require an external stimulus such as heat or UV radiation.[30] The irradiation is the more convenient from the point of view of the energy savings but present some disadvantages such as it is limited to cure thin samples and with simple geometries. The use of thermal curing reagents is the easiest in technological applications.

Cured epoxy materials possess a large number of properties that make them valuable in front of other types of thermosets. Even long polymer chains with epoxy groups at the ends can be used to form thermoplastic materials. But not only their properties, but also their ease ability to vary them, are what make epoxy resins widely used in everyday products, as well as in engineering applications. Also, the absence of volatile matter on curing is a point in favour for the extensive use of this type of material. For example, a given epoxy monomer can be produced with a T_g that can vary from values lower than T_{room} to values higher than 200°C depending on the hardener selected. This makes them usable when working conditions require relatively high temperatures. The crosslinking structure with covalent bonds has a lot of influence. Not only to maintain their mechanical properties at high temperature, but also to offer a good stiffness to maintain their shape and be unreactive to chemical attacks. This is what makes them durable and resistant to the pass of time and to aggressive environmental agents.

Another property that makes them widely used is their ability to strongly adhere to many different substrates during the curing process. Epoxy resins are commonly used in protection coatings because of their good adherence and the fact that they are one of the less brittle thermosets. Epoxies, as adhesive, can bond by three mechanisms: mechanically, if the coated surface is rough; by proximity, because the resin does not leave free space making their separation difficult; and ionically, the strongest of the three, forming ionic bonds with the substrate.

Automotive and naval industries select epoxy coatings as a first protection layer in many hull components. Another feature that makes them convenient is their high insulation power, both electrical and thermal, which is given in part by their amorphous structure. That is why they are desired as insulative material in the electric industry and electronics, to avoid short circuiting and protect electrical and electronic packaging from dust and humidity. During last decades aerospace and aeronautics are using epoxy resins to replace heavy materials in order to save weight of aircraft, taking advantage of their high temperature resistance and high strength-weight ratio compared to other kind of polymers.

However, not all are benefits. Epoxy resins also have some drawback that must be considered. The first drawback is found during the thermal curing (partially avoided in UV irradiated systems at room temperature). This is the thermal and chemical shrinkage, which leads to the reduction of the material's volume during the polymerization. All types of curing reactions are accompanied by a reduction of the bonding distance, producing shrinkage, although epoxy resins are one of the thermosets with less volume reduction during curing. Shrinkage is particularly critical when these thermosets are used as coatings, because it produces debonding, the creation of micropores, microcracks and an accumulation of internal stresses that play against the adhesion of the coating and its durability.[31] In addition, the difference in the thermal expansion coefficient (CTE) that exists with the substrate is another issue that produces the failure of the coating. The miss-match in CTEs between the epoxy coating and the substrate can produce similar problems.

The thermal shrinkage can be reduced with changes in the temperature schedule of the curing, helping to the better relaxation of the network. This can be carried out by reducing the initial curing temperature or decreasing the temperature increases in a multistep program, as well as decreasing the cooling rate once the process has been completed.

The chemical shrinkage can be reduced by many ways. One can be the addition of different types of fillers, including inorganic or polymeric particles, but this can reduce the T_g and toughness of the final material, reduce the transparency and increase the viscosity of the uncured mixture, worsen the processability. Another option is the use of the so-called expanding monomers, with no volume's reduction or even a small expansion during the polymerization, as can be cyclic orthoesters or orthocarbonates.[32,33] In the last years, the incorporation of hyperbranched polymers as modifiers reducing the shrinkage without affecting other properties of the resin have been also applied.[34]

Another drawback which appears during curing is the high heat evolved for the opening of the oxirane ring, limiting the production of large pieces.

Once cured, epoxy resins are characterized, in terms of structural applications, to be brittle and notch sensitive. This leads to a fragile rupture with low energy absorbed during breakage, which results in low toughness. The processes performed to reduce brittleness are based on increasing the flexibility of the network, decreasing the crosslinking density or adding rubbery particles, which usually leads to a lowering of the T_g.[35] The addition of hyperbranched polymers have been proposed to enhanced toughness without affecting T_g and viscosity of the formulation.[36]

As told before, thanks to their relative low cost, light weight and corrosive resistance, thermosets have been actively studied to replace metallic components in some industries such as automotive, aeronautics, electronics or heat exchangers.[10] To

carry out this, one of the simplest and most effective ways has been the addition of fibbers and fillers of all kinds taking advantage of their adhesion capacity and dimension stability. The materials in which fibbers or fillers are dispersed in a polymeric matrix are known as composites. A composite is defined as a material that consist at least of two constituents. The major ingredient is commonly called matrix, being the other constituent the filler. The use of fillers will be extensively reviewed in **section 1.5**. The aim of adding fillers is to enhance some properties of epoxy resins thanks to the properties that reinforcements possess. When two different materials are mixed, there is a stablished equation to predict the upper limit of the elastic modulus of the composite materials (**Eq. 1.1**):[1]

$$E = fE_f + (1 - f)E_m \qquad \textbf{(Eq. 1.1)}$$

where E is the elastic modulus, f is the volume fraction of the filler and E_f and E_m are the filler and matrix property values. Nevertheless, this guiding principle is not fulfilled for all the properties. For example, the thermal conductivity in composites does not follow such type of relationship.

1.4. Heat conduction through materials

The theory of heat conduction represents an exceptionally complex statistical problem. Therefore, in this section we try to clarify the most general trends.

Heat refers to the energy absorbed (endothermic) or evolved (exothermic) during a reaction or a change of state of the material (solidification, sublimation, condensation, boiling, etc.). This consideration is used in thermodynamics to refer to the energy transferred to or from a system. It is stated that three different mechanisms to transfer the heat exist: conduction, convection and radiation.

Heat convection involves a transfer of heat due to the movement of matter within a medium. This mechanism will not be considered, since in most solid materials the movement of matter is restricted.

Radiation is referred to the transmission of energy in form of waves or particles through the space or a medium. The importance of the radiation is exemplified by the energy capture from the sun or by the production of electromagnetic waves or radiation of particles, to measure or quantify some kinds of phenomena. The thermal radiation that affects a body can be reflected, transmitted or partially absorbed. This absorption is transformed quantitatively into heat. However, the thermal radiation that materials can produce at temperatures near the room temperature is negligible.

The most important mechanism inside the materials is the conduction. The conduction is the transfer of heat by microscopic collisions and vibrations of particles and movement of electrons. Spontaneously, this energy transfer goes from a high to a low temperature region, in accordance with the 2nd law of thermodynamics. The

property that characterizes this ability in materials is the thermal conductivity (TC), and for a steady state heat flow, the conduction rate can be expressed by a Fourier's equation[37]:

$$J = -k\frac{dT}{dx} \qquad \textbf{(Eq. 1.2)}$$

where J is the heat flux per unit area (W/m^2), k is the thermal conductivity (W/m·K) and dT/dx is the rate of temperature change in one direction (K/m). TC is commonly denoted as well by Greek letters λ or κ.

To clearly understand the TC, firstly must be defined what the heat is. Any atom, even subjected to temperatures close to 0 K, has an internal energy (or thermal energy), what is explained as a constant vibration at very high frequencies and relatively small amplitudes. In a three dimensional solid the vibrations of each atom are partially coupled by their atomic bonds and thus, the vibration is coordinated across the material in the form of elastic waves. When the material is heated or receive energy, this is partially absorbed by the material depending on the heat capacity (C_p) and other factors. It should be taken into account, that not all the energy can be transformed into heat because the energy is quantized, and a single quantum of vibrational energy is called "phonon". A phonon is a collective excitation of atoms in condensed matter that represents an excited state of the vibrational modes of interparticle elastic structures. This excited state is observed as an increase of the temperature of the material and atomically, can be represented as an increase of atom vibrations or phonon waves in the structure (**Figure 1.4**). The propagation of these phonon waves through the material occurs at the speed of sound, and according to quantum mechanics, phonons have a dual particle-wave character.

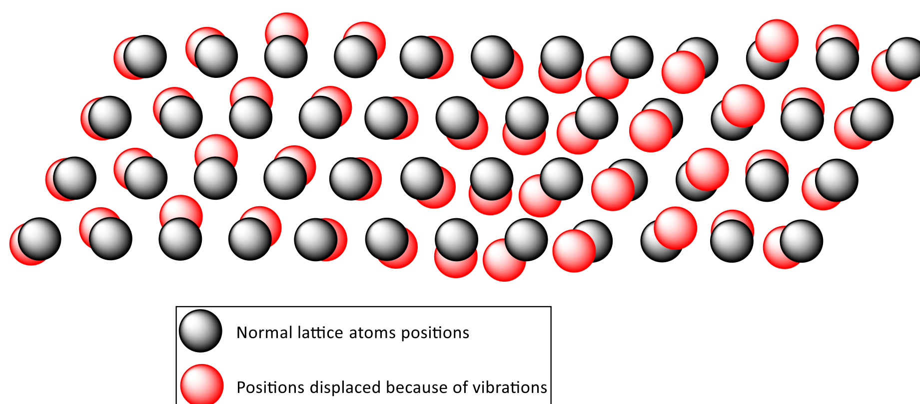

Figure 1.4. Representation of the atomic vibration of ordered structured material.

TC not only propagates through the elastic movement of phonons, but the energy can also be transferred by the movement and collisions of electrons or by the combination of both. Other types of excitations (electromagnetic waves, spin waves, etc.) have a minimum effect on the heat transport, especially at room temperature.[38]

Normally, k is written as the sum of all possible contributions, being lattice waves (k_L) and electrical carriers (k_e) the most important ones. Free electrons can absorb energy in form of kinetic energy. Then, the electrons can migrate to the adjacent atoms transferring their energy mainly by collisions. It must be said that the electron thermal conductivity is as fast as electron velocity inside the material, and their contribution increases with the free electron concentration in the matter.[1] Apart from that, many other parameters affect the thermal conduction through the materials. The mentioned nature, as the crystalline structure has a lot of influence, as the presence of defects as dislocations or grain boundaries greatly suppress the transmission of heat. The size of material and proportions of defects are important parameters, since the thinner the material, the less time it takes for the heat to pass. The temperature dependence also influences drastically the TC from one material to another. The following subsections will serve as a simple comprehensive description of the widespread thermal conduction mechanisms, all in the range of room temperature.

1.4.1. Thermal conductivity in crystalline structures

Geometric atomic disposition and bonding among the constituents of the materials produce a fundamental influence on their properties. An ordered and a dense packing of atoms and the strong chemical bonds between them lead to a rapid transfer of energy to the neighbouring atoms through the vibrations of phonons and electrons as depicted in **Figure 1.5**.

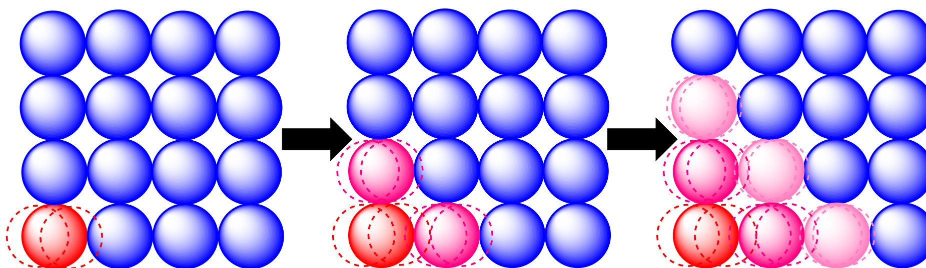

Figure 1.5. Representation of heat conduction in an ordered crystalline structure.

Materials with good electrical conductivities, like most of metals, also present a good thermal conductivity. As mentioned above, the higher the free electron density, the higher the thermal conduction for the flow of electrons and then, the faster the propagation of heat. Copper, for example, is a good thermal conductor (about 400 W/m·K at room temperature) and just 1-2% of the heat flux is attributable to phonons.[39] Gold, silver or aluminium present a similar behaviour. Because free electrons carry both heat and charge, there is a close relation between the electronic thermal conductivity contribution (k_e) and the electrical conductivity (σ) in this type of pure metals. In this case the electrons are considered to interact by three different processes: scattering on static defects, electron-phonon interaction and interaction with other electrons.

At temperatures close to room temperature is when phonons more effectively hinder the flow of heat (more than the electric charge).[38] In fact, phonons are the dominant scatterer of electrons for pure and high-quality metals, with inelastic collisions among them. Other metals or semiconductors present a different behaviour, as transition metals and certain alloys, in which the electronic term is less dominant, and the phonon contribution (k_L) must be considered. The reduction in the electronic contribution in these metals is produced by the minor density of free electrons and by several types of defects. Inhomogeneities which affect the crystalline structure can scatter electrons (also phonons) reducing the TC of materials. Alloy atoms, vacancies, dislocations, phase changes, dopants or isotope variations are some of these defects. Being a single crystal or a polycrystalline material, the last one introducing grain boundaries, also change the conductivity.[40]

Differentiated from metals, TC governed by lattice waves is dominant for all the other types of materials, if not the only mechanism. In these cases, the thermal conductivity of an isotropic three-dimensional material is primarily conducted by the acoustic phonons, and can be theoretically estimated by the Debye approximation:

$$k = \frac{1}{3} C_P v l \qquad \textbf{(Eq. 1.3)}$$

where C_p is the heat capacity of the material, v is the average phonon velocity, and l is the phonon mean free path, the distance a phonon travel before being scattered. In pure crystalline materials, the dominant phonon scattering mechanism are the boundary scattering and the phonon-phonon Umklapp processes (U-process).

The boundary scattering, also known as Kapitza resistance, is the measure of an interface thermal resistance to the thermal flow. In each interface, phonon and electrons can be scattered due to the different vibrational properties between the two sides of the grain/phase, the orientation of the crystals, and so on.

The Umklapp process is an anharmonic interaction between phonons which scatter them limiting the thermal conductivity in crystalline materials (can also control the scattering behaviour in amorphous materials). For low defect crystals, U-process increases with temperature, while for an insulating material, the dependence is inverted (1/T).

All the above-mentioned defects or impurities lower the phonon mean free path by adding additional scattering centres. The presence of defects in the crystals can dramatically reduce the TC of tabulated values for a single crystal. For example, the room temperature *k* of pure AlN along the *c-axis* can be as high as 320 W/m·K, while the grain boundaries can reduce it for a polycrystalline AlN to about 40 W/m·K.[41] Despite this, it must be said that some additives or doping microparticles (in the case of AlN they can be lanthanide oxides) can increase the thermal conductivity, depending in the crystalline distortion they produce.[42,43] In general terms, the more crystalline a material

is and the greater its atomic density in the unit cell and, of course, the fewer imperfections, the greater its thermal conductivity. This is especially true for high insulative materials, while some electrically semiconductors can vary notably the TC if the k_e contribution is considerable.

The type of structure can also lead to a different behaviour. In the group of perfect ceramic crystals, we can find materials as diamond (cubic structure) with an extremely high TC (about 2000 W/m·K). In the same way, as other properties do, a laminar arrangement (hexagonal structure), such as graphite, with the same composition of diamond, presents a great difference according to the direction in which the material is analysed, i.e. anisotropy. In this case, through the plane where the hexagons of the carbons are formed, the conductivity is high (not as high as in diamond), while through the layers, bonded by secondary forces, the TC decreases considerably.

The importance of the crystalline structure is such that large differences can be observed in a crystalline and amorphous material despite having the same composition. For example, crystalline SiO_2 can have a conductivity of 10 W/m·K, while its amorphous state falls an order of magnitude in its value.[44] In semicrystalline materials the amorphous part, with a disordered packaging, act as point defects leading to a high phonon scattering processes.

In recent years the growth in the research of nanostructured materials have been considerable, such as in the case of graphene and carbon nanotubes (CNT). Theory predicts extraordinarily large values of k for isolated nanotubes, over 6000 W/m·K,[45] with k_e and k_L contributions. The conduction of electrons in a 1D system as CNT occurs ballistically,[46] but as noticed above, Kapitza resistance drastically falls down the TC when they are added in a composite in which the quantity of interfaces becomes large.

Recent calculations have predicted an unusual high thermal conductivity for cubic boron arsenide (BAs).[47,48] Even surpassing the conductivity of the diamond, this surprising result comes partly from the combination of acoustic phonon dispersions, a large frequency gap between the branches of the acoustic and optical phonons and the weak phonon-isotope dispersion. The uncommon vibrational properties of BAs provoke a weak phonon scattering resulting in an anomalously large phonon mean free path. However, it has been demonstrated the necessity to fabricate large single crystals with few defects to observe the predicted ultrahigh k for BAs,[49] since it is very sensitive to phonon scattering from crystal boundaries and defects. The results suggest that not only reducing the defect and boundary scatterings but also to better understand and control the electron scattering of phonons is required to achieve the predicted values.[50]

1.4.2. Thermal conductivity in polymers and their composites

Lattice thermal conduction is the dominant mechanism in most of the non-metallic materials. In the case of polymer materials there are few free electrons and

therefore k_e is negligible,[51] and in most cases the TC is in the range of 0.1 to 0.5 W/m·K, insufficient for heat conduction applications.[52] Enhance the TC of polymers can be considered unnatural, since they are insulators, but it is a crucial issue in applications that requires new performances with specific properties. However, what is considered a defect, in some cases may be a virtue. In contrast to the will of increasing the thermal conductivity of polymers, we find the production of construction materials to reduce it. Nearly the half fraction of the world's energy consumption is spent in buildings, and large part is destined to heating and cooling, what involves the burning of fossil fuels. Improving the thermal insulation of greenhouses providing good thermal resistance, using nanoporous foams for example, can increase the energy efficiency of habitats by reducing the emission of gases and diminishing the temperature inflation in few degrees.[53]

For most polymers, both C_p and v are the same in bulk than in individual chains (see Eq. 1.3). Henry et al. found that the thermal conductivity of a single extended chain of polyethylene (PE) could be as high as 350 W/m·K (chain length < 100 nm).[54] What differs in a single chain from a bulk material is the phonon mean free path (l), larger in an ordered arrangement of atoms covalently bonded than in atoms associated with secondary forces.[55] The amorphous structure they behave is considered as a scattering defect, what gives rise to the most known insulating materials. When atom distances are higher than in a crystalline structure and when the layout does not follow any pattern, the coupling of the phonon waves are highly restricted. Then, the ability of atoms to transfer their thermal energy to the neighbouring particles is primarily conducted by the vibrations, atom by atom, not as a wave (see **Figure 1.6**).[56]

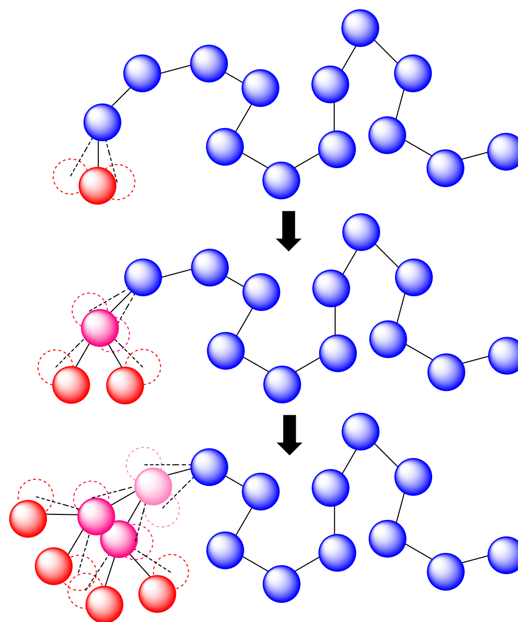

Figure 1.6. Representation of heat conduction in amorphous polymer materials.

Thermoplastics can be semi-crystalline, and they use to have higher TC than the purely amorphous polymers. Exceptionally, polypropylene (PP), even with high crystallinity, has a very low TC due to the relatively high free volume in its structure, what causes long bonding distances. In the same way, amorphous thermosets have a low thermal conductivity of about 0.2 W/m·K.[52] Despite this, there are some liquid crystalline thermosets, with long rigid chains that can form an ordered structure, reaching a TC of about 5-fold of neat resin, but highly increasing the production cost.[57] Thus, the most used and economic way to enhance the TC of polymeric materials is by the use of fillers.

Filled polymers has been used almost since the appearance of the first commercial products. Fibbers or common ceramics were added to improve their mechanical properties and to reduce costs. Nowadays, fillers are added for many different purposes. For polymer composites the heat transport is largely determined by the way in which filler particles transfer the heat. For purely phonon heat transfer mechanism, the TC is lower than those having phonon and electron conductivity. So metallic and carbon fillers usually possess better TC than ceramic materials, but they have to be avoided or limited in electrically insulating applications.

Besides the intrinsic TC of fillers and matrices, there are some affecting factors in the thermal properties of composites. The main primary factor is the *filler loading level*. The general trend, obviously, is that TC increases with the increasing proportion of particles or fibbers. The increase of *k* in front of the filler loading is not often linear,[58] and very high filler level must be achieved to see an abrupt enhancement. At a certain filler loading an interconnected network of particles is formed, which are the pathways to transport the phonons. This concentration is known as percolation threshold and can be described as the point at which a property experiments a drastic change on increasing the filler concentration. However, this filler ratio may depend on the measured property. It should be noted that the use of a high filler loading is not always preferred, since can lead to a high viscosity increase, which ruins the processability and makes the final materials too fragile. According to that, low filler loadings with smooth surfaces are favoured, yet they could be less efficient in increasing the TC.

The *filler shape* is another important parameter that must be considered. The aim to increase the TC at the minimum filler loading leads to the use of high aspect ratio fillers, as platelet like fillers with one or two dimensional components larger than the others. Fibbers, rods, wires or tubes are expected to significantly improve the TC compared with other shape fillers, constructing long heat conductive pathways along the longitudinal direction at low filler loadings.[59] They often guide to anisotropic thermally conductivity with much higher TC in the planar direction than in the perpendicular one. Examples of this type of filler can be the hexagonal form of boron nitride (h-BN), or graphene and graphite (all with the same hexagonal crystalline

structure).[60] Other high aspect fillers can be CNTs or other nanosized fillers, but then other problems appear for the improvement of conductivity.

Nanometric fillers usually form aggregates due to the small size and high Van der Waals forces.[61] In addition, there is a high Kapitza resistance for the large increase in the number of interfaces that phonons must pass. This is related with a different filler factor that should be taken into account, the size of filler. Large particles lead to lower filler-polymer interface areas compared to the smaller ones at the same filler loading. That leads to a lower interfacial thermal resistance and, as consequence, a higher TC. This is clearly shown by the comparison between nano and micro-sized particles,[62] indicating a high influence of the interfacial thermal resistance. However, behaviour differences from experimental results with the use of nanoparticles are found.[63] As we have seen, the particle size is not the only influencing parameter, apart that nanosized particles can exhibit differences from their micro-sized forms.

Other influencing parameters can be list as: *combination of different fillers, use of combined different sized particles, orientation of fillers, compression moulding or surface treatments* among other procedures.

The combined use of different types of fillers can help to enhance the TC at the same level with a lower filler loading, thus, reducing the viscosity and improving the processability.[64] With different sized particles, the packing density can be increased and consequently, the TC.[65,66] Non-spherical particles can be oriented when heat is desired to be removed in one direction of the composite.[67] The use of pressure before or during the curing avoid the appearance of voids at high filler loadings, which are important thermal conductive defects.[68] The surface treatments or functionalization of the particles are carried on, reducing the interfacial thermal resistance of filler-matrix, one of the most important limiting parameters.[69] The dispersion state of fillers also influences the conductivity of the composites. If they form aggregates embedded in the matrix the insulative character of the polymer can significantly reduce the phonon heat transfer.[70] On the other hand, the formation of filler structured pathways can substantially improve the TC.[71] All these methods aim to improve the TC with the minimum filler load and maintain the good processability of the polymers.

1.5. Epoxy composites with high thermal conductive fillers

Epoxy resins are versatile and adaptable to a wide range of applications. In addition to the use of different hardeners, initiators or curing procedures to change crosslinking densities, what can greatly change the final properties of the materials are the fillers that can be added. The addition of fibbers, particles or fillers to an epoxy matrix form the epoxy composites. The combined material exhibits better characteristics (or preferred) than each component individually without compromising, or even enhance, the weakness of either. In this type of composites, the filler must be

added before the curing process, as can be assumed with the aforementioned properties that epoxy polymers have.

The most common fillers used at the beginning of epoxy composites were fibbers and glasses or traditional ceramics. The principal aim was to increase the mechanical strength of the epoxies to be used as structural materials. While nowadays the enhancement of mechanical properties are still of interest, other desired properties have grown in attention. The use of epoxy resins as adhesives, coatings or encapsulating material to a variety of different electronic components is due to the high thermal stability, electric insulative conduction, moisture resistance and low cost they offer among other needed characteristics. Nevertheless, their intrinsic low thermal conductivity and high CTE become disadvantages with the miniaturization and the larger heat production emitted by electronic devices.

The low thermal conductivity of epoxy resins, usually in the range of 0.2 W/m·K, is far below the usual conductivities of ceramics (tens of W/m·K) and metals (hundreds of W/m·K). This is a critical issue in the electronic industry since it is known that electron circulation in materials produces heat by Joule's effect, and epoxy resins are used to coat some electronic components. As the Moore's law predicted five decades ago and has been met until today, the number of transistors in a dense integrated circuit doubles every two years.[72] This continuous trend of development in electronic miniaturization that works in higher frequencies and speed causes that more heat must be removed from devices to maintain their working temperature. This is directly related to ensure the efficiency, the live time operating and to prevent premature failures or damage of equipment.[73] It must be taking into account that coatings in integrated circuit boards are thinner than 120 microns, which limits the size of the fillers.

Enhance TC and reduce CTE would contribute to the improvement of device capabilities; inasmuch dielectric thin films have important applications in microelectronics and may serve as electrical insulators or coatings for thermal interface materials (TIMs). Moreover, the improvement of these properties may answer the demands in other spreading out industries as power, thermal energy storage, electrical, light emitting diodes (LEDs), sensors, aerospace, automotive or naval engineering among others.[74,75]

To achieve these purposes, while maintaining electrical insulation, the addition of metallic fillers must be avoided, despite being one of the best candidates for increasing thermal conductivity. In addition, this type of fillers can experience oxidation, so their useful life time can be reduced. Several types of fillers have been tried to overcome these defects. Among them we can classify them in two different groups: high thermally conductive ceramic fillers and carbon-based materials.

In the first group ceramics as aluminium nitride (AlN), aluminium oxide (Al_2O_3), hexagonal boron nitride (h-BN), silicon carbide (SiC) can be cited, among others. In the

second, fillers as graphite, carbon black, graphene, carbon nanotubes (CNTs) and so on. Despite finding better enhancements of TC in the second group, most of them lack in electric insulation character. However, they are mainly used to substitute tin/lead soldering as electrically conductive adhesives for environmental preferences.[14] Some of the most important fillers employed to enhance the thermal conductivity are listed below.

Al_2O_3, also called alumina, appears in the group of oxides as one of the most common fillers used in epoxy composites due to its low price and relatively high TC (about 30-40 W/m·K).[52] The most general form is α- Al_2O_3, which is crystalline and stable. It is used as abrasive and coating protection and paints due to its hardness, it is an important component of many glass formulations and is naturally used in sun's lotions or creams for UV body protection. A thermal conductivity of 4.3 W/m·K in an epoxy composite at 60 vol. % of 10 µm alumina particles has been reported.[76]

Another oxide is silicon dioxide (SiO_2) or silica. Extensively used as packaging materials for electronic devices, epoxy composites containing 55 to 75 vol. % of silica lacks in good TC.[77] As commented before, the TC of polycrystalline sample is in the range of 1-2 W/m·K, and at a given level of loading, silica composites show lowest conductivities compared with other fillers.[78]

Zinc oxide (ZnO) is a semiconductor widely used as additive in the rubber industry, used to improve the thermal conductivity of tires. When cars are rolling, heat is produced by friction and it is crucial to dissipate it. However, ZnO also exhibits a high dielectric constant which limits their use for electronic packaging applications.[79] With moderate intrinsic TC (about 60 W/m·K), ZnO epoxy composite has reported to reach 1.6 W/m·K at 50 wt. % fraction.[80] However, the authors used a functionalization of the filler giving rise to a TC of 4.38 at the same loading, but they did not report any electrical characterization.

Beryllium oxide (BeO) has a high thermal conductivity in the range of 300 W/m·K. It is also corrosion resistant and exhibits excellent electrical insulating properties. However, the high toxicity (produces berylliosis) and the high cost make BeO powders unattractive for commercial use.[52]

As non-oxide ceramic fillers are found some materials. SiC is another semiconductor with good TC. As single crystal can reach conductivities as high as 360 to 490 W/m·K depending on the chemical structure,[81] but in polycrystalline form the value is reduced to about 85 W/m·K.[52] With an extremely high hardness is widely used as abrasive. Hwang and co-workers fabricated epoxy-based composite with 3.85 W/m·K with 70 wt. % of SiC loading fraction.[82]

AlN has gained much interest due to its high TC (120-220 W/m·K), low CTE and high electrical resistivity. Thus, there are a large number of research works on high thermal conductive polymer-AlN composites for electronic packaging application,

finding conductivities usually in the range of 1 to 5 W/m·K.[83] One of the best results reported is a conductivity of 11.0 W/m·K for an epoxy composite with 60 vol. % of this filler.[84]

BN has emerged as one of the best candidates for high thermal conductivity composites and electrical insulating applications. It is a synthetic material with high similarities with carbon, since present a cubic form as diamond, and hexagonal structure as graphite. Also, BN nanotubes and nanosheets can be produced. Known as white graphite, BN provides the best combination of properties in terms of high thermal conductivity, low dielectric constant, high electrical resistivity and low thermal expansion coefficient. Besides all, BN also presents low density (2.2 g/cm^3), high mechanical strength, high aspect ratio and chemical and thermal stability. The cubic form is the hardest material know only below diamond.[85] The hexagonal form (h-BN) is the most stable with a layered structure, and the TC can vary from 2 to 390 W/m·K depending on the direction measured and its purity.[86] Last developments estimate the TC of a single layer of h-BN of 751 W/m·K.[87] Until the late 1990s lower values of TC of this material were expected.[88] Since then, optimizations of h-BN production processes reduce cost and increase purity[89] and, as consequence, enhance the thermal conductivity. Besides a huge range of different TCs of BN composites, stands out the best result reported till date of 32.5 W/m·K by Ishida et al. in polybenzoxazine matrix, although they needed the extremely high loading of 88 wt. %.[90] Usual conductivities of epoxy-BN composite ranges from 0.5 to 10 W/m·K.[91]

The group of carbon-based materials are one of the most popular additives due to the high TC, stable chemical nature, abundance and low density.[92] Despite its high production cost, diamond is included in this group and the most appropriate to use for its high electrical resistance. The rest of carbon-based materials are more prone to the flow of electrons which convert them as inappropriate for electrical insulating composites. Diamond presents the highest conductivity (about 2000 W/m·K) from all the natural materials known due to the strong covalent bonding, cubic structure and low phonon scattering. Zhang et al. reported a TC of 4.1 with a 68 vol. % in filler-based epoxy composites.[93] However, no substantial improvements in TC of composites were found compared with other economical fillers.

Natural graphite is a carbon allotrope and relative abundant mineral that can be classified according to its crystalline sizes and the carbon purity. The hexagonal structure of graphite confers anisotropy in mechanical and physical properties. Containing free electrons, is a good conductor both of electricity and heat. Since the mid-1950s is known that high perfect crystals of graphite can reach values of about 500 W/m·K for the in-plane direction at room temperature.[94,95] Synthetic graphite can also be produced from many carbon resources. However, achieve the crystallinity of natural graphite are costly and thus, the same level of TC. A conductivity of 5.8 W/m·K was reported in an epoxy composite with 20 wt. % of chemically functionalized graphite.[96]

Due to the superior crystallinity of natural graphite, it can be intercalated.[97] Expanded graphite (EG) comes from the intercalation of liquids such as strong acids followed by a thermal shock to evaporate them. This method produces low density and large surface area materials. The bulk material presents a conductivity of about 70 W/m·K.[98] The material can be subjected to varying levels of compression, resulting in a wide range of properties. Celzard et al. found a logarithmic relationship between the measured TC and the density, reaching conductivities as high as 250 W/m·K.[99] Reported results determine that compressed EG is the most economical filler to enhance the thermal conductivity of thermal energy storage (TES) materials.[98] Wang et al. reached a conductivity of an epoxy composite of 1 W/m·K with just 4.5 wt. % of EG.[100]

Graphite nanoplatelets (GNP) and graphene are only distinguished by the number of bonded hexagonal graphite sheets. Theoretical estimations indicate TC values in the range of 3000-6000 W/m·K, but experimental measurements vary comparatively widely from 600 to 5000 W/m·K.[101] Graphene oxide, introducing hydroxyl and acid groups to the structure, can prevent the electrical conductivity to some extent. In most cases, the results achieved for GNPs are slightly better than for EG and the percolation threshold is achieved at lower loading level.[98] Epoxy nanocomposites with a TC of about 1.7 W/m·K are published with 30 wt. % of GNP.[102] Guo et al. reached a value of 2.67 with just 25 wt. % of graphene.[103]

CNTs are characterized by a high aspect ratio, excellent mechanical properties, remarkable thermal and electric conductivities, low density and good corrosion resistance against oxidative environments.[104] A wide variety of TCs are reported for CNT, ranging from 1100 to 7000 W/m·K due to the difficulty in characterizing the true nanotube thickness.[101] CNT is the most studied nanomaterial as additive mainly due to its earlier discovery by Iijima.[105] The performance in their properties depends on a variety of factors such as tube chirality, length, diameter, aggregation, functionalization and edge effects, and it is demonstrated a significant difference between the electronic and thermal transport ability.[106] Results lower than expected are obtained because of the high phonon scattering and the enhancement factors in TES materials reported did not exceed 3.5 at loadings of 5 wt. %.[98] In fact, CNT/epoxy composites are currently used for the mechanical improvement they show and not in high thermally conduction applications.[14]

There is a huge amount of literature related to the topic to enhance the TC of epoxy matrices. Some general trends can be extracted according to the influencing parameters mentioned in the previous section, although only few studies will be mentioned.

Most of the studies display a progressive enhancement of TC with the filler loading but lacking in abrupt enhancement of the property even at very high filler loading. Burger et al. use graphite particles in epoxy matrix reaching approximately 1.75 W/m·K at about 23 wt. %, observing a linear trend of the TC with particle loading without

any outstanding value.[56] However, some other authors observed sharp changes at a given concentration. Zhou et al. observed a percolation threshold of micro SiC/epoxy composites near to 55 wt. %.[107]

The use of nanofillers rends more controversial results. Evseeva et al. observed a decrease in the TC when CNTs loading overpass the 3 wt. %,[108] which highlight the importance of the scattering interface resistance and the formation of aggregates. Moisala et al. observed lower TC than neat epoxy with the use of single walled CNTs.[109] In a different way, other authors reported enhancements with the use of CNTs as Biercuk[105] and Yu.[110] Surface modification of carbon fillers are commonly performed to decrease the Kapitza resistance and the aggregate formation, by covalent and non-covalent functionalization. Experimental findings indicated that the interfacial thermal resistance arises from a poor mechanical or chemical adherence at interfaces and CTE mismatch.[111] In the case of ceramic fillers without functionalization, Wattanakul et al. obtained a thermal conductivity of 1.97 W/m·K with 28 vol. % of BN fillers.[112] Lee et al required 57 vol. % of AlN in epoxy matrix to reach 3.4 W/m·K.[113] On the contrary, Xu et al. considered necessary the surface treatment of AlN, resulting in a TC of 11.0 W/m·K by the addition of 60 vol. %, and 10.3 W/m·K with 57 vol. % of treated BN.[114] But the use of so high filler loading led to worse the mechanical properties.

The application of pressure is helpful to evade the appearance of voids, but only from a certain % of filler, when the viscosity is high enough.[56] Another general trend that can be found in the literature is referred to the filler size. Heat is quickly diffuse through crystalline fillers, whereas it is considerably slowed down by the polymer. In micro sized particles, as larger the filler, higher the thermal conductivity.[115] It should be commented that the crystallinity and impurity proportion must be similar in the different sized particles to observe this behaviour. From that, it can be inferred that nanoparticles are not the best option to enhance the TC. However, the aspect ratios of fillers play a very important role. Mortazavi et al. demonstrated that higher aspect ratios are a better choice to increase the TC.[116] The use of graphene or other 2D materials, with high aspect ratios, leads to composites with very high TC, but distant of the range of some metals (typically in the order of 70-300 W/m·K), what is the goal to be reached.[117] Anyway, an ultra-high TC of 12.4 W/m·K was reached by Shtein et al. using approximately 24 vol. % of graphene nanoplatelets.[118] To achieve this, they needed the application of pressure to avoid gaps in the material and verified how the size, thickness, aspect ratio and, most importantly, the amount of defects and impurities, affect the TC in an extraordinary way. This kind of particles can be aligned or oriented giving anisotropic thermal conduction.

In summary, many efforts have been spent on fabricating thermal conductive electrically insulating epoxy composites. In general, nitrides as AlN and BN provide better TC enhancement in comparison with oxides, despite increasing the costs. In the last decades carbon-based materials gained importance due their intrinsic high thermal conductivity. Despite the progresses done in the field, materials still cannot meet the

requirements of industry, both in properties and economically. It is believed that the advance of nanomaterials and nanotechnology can conclude the requirements of highly powered electronic devices in near future.[119]

1.6. Scope and objectives

As explained along this introductory section, epoxy resins are a useful material for many industrial applications. The crosslinking density of their structure leads to excellent properties. The combination of high strength and stiffness, the excellent corrosion and electrical resistance, the adhesion ability to a huge range of different surfaces make them ideal candidates to be used as adhesives, coatings and some structural components. Nevertheless, other properties they possess can limit their use in specific fields. The low thermal conductivity they present can compromise the thermal management in electronic devices which, every time, produces more and more heat due to the increase in their working capacities and speeds. In this doctoral thesis, the increase in the thermal conductivity of epoxy resins by the addition of adequate fillers is the main objective, and highly related, the reduction of the CTE.

Including some other purposes, specific objectives are outlined as follows:

- To optimize a novel cationic thermal curing system for a DGEBA epoxy.
- To increase the thermal conductivity of the DGEBA thermosets obtained by the use of the previously developed curing system by adding h-BN particles.
- To optimize the previously developed curing system for ECC epoxies.
- To increase the thermal conductivity of the ECC thermosets by adding h-BN particles.
- To improve thermal conductivities of epoxy/thiol matrices with the addition of h-BN to the formulation.
- To enhance the mechanical and thermal characteristics of ECC composites by using different ceramic fillers (AlN, Al_2O_3, SiC)
- To investigate the cooperative effect of carbon-based fillers (expanded graphite and carbon nanotubes) and h-BN in the improvement of the thermal conductivity of ECC composites keeping electrical insulation.

References

[1] Callister WD, Rethwisch DG. Materials science and engineering: an introduction. 8th edition. Versailles, KY: Wiley, 2010.

[2] Tully J. The devil's milk: a social history of rubber. New York: Monthly Review Press, 2011.

[3] Freinkel S. Plastic: a toxic love story. 6th edition. Boston: Houghton Mifflin Harcourt, 2011.

[4] Pascault J-P, Williams RJJ. Overview of thermosets: Present and future. Chapter 1. In: Guo Q, editor. Thermosets: structure, properties and applications. 2nd edition. Amsterdam: Elsevier, 2018.

[5] Koltzenburg S, Maskos M, Nuyken O. Polymer chemistry. Berlin: Springer-Verlag, 2017.

[6] Flory PJ. Principles of polymer chemistry. New York: Cornell University Press, 1953.

[7] Baekeland LH. The synthesis, constitution, and uses of bakelite. Ind Eng Chem 1909; 1: 149-161.

[8] Market Research Store. Accessed on June 14th of 2019. Available online: www.marketresearchstore.com/news/global-thermosets-market-232

[9] Brandrup J, Immergut EH, Grulke EA. Polymer Handbook. Abe A, Bloch DR, editors. 4th edition. New York: John Wiley and Sons, 1999.

[10] Mullins MJ, Liu D, Sue H-J. Mechanical properties of thermosets. Chapter 2. In: Guo Q, editor. Thermosets: structure, properties and applications. 2nd edition. Amsterdam: Elsevier, 2018.

[11] Diem H, Matthias G, Wagner RA. Amino Resins. In: Ullmann's Encyclopedia of industrial chemistry. Berlin: Wiley-VCH Verlag GmbH & Co., 2012.

[12] Biron M. Thermosets and composites: Technical information for plastic users. Oxford: Elsevier Advanced Technology, 2003.

[13] Auvergne R, Caillol S, David G, Boutevin B, Pascault JP. Biobased thermosetting epoxy: present and future. Chem Rev 2014; 114: 1082-1115.

[14] Kausar A, Rafique I, Muhammad B. Review of applications of polymer/carbon nanotubes and epoxy/CNT composites. Polym. Plast. Technol. Eng. 2016; 55: 1167-1191.

[15] Castan P. Verfahren zur Herstellung eines Hartbaren Kunstharzes. Switzerland Patent Nº: CH 211, 116, 1940.

[16] Petrie EM. Epoxy adhesive formulations. New York: McGraw-Hill, 2006.

[17] Vidil T, Tournilhac F, Musso S, Robisson A, Leibler L. Control of reactions and networks structures of epoxy thermosets. Prog Polym Sci 2016; 62: 126-179.

[18] Brunelle DJ. Ring-opening polymerization: Mechanism, catalysts, structure and utility. Munich: Hanser Publishers, 1993.

[19] May C. Epoxy resins: Chemistry and technology. New York: Marcel Dekker, 1988.

[20] Fernández-Francos X, Cook W D, Serra A, Ramis X, Liang GG, Salla, JM. Crosslinking of mixtures of DGEBA with 1,6-dioxaspiro[4,4] nonan-2,7-dione initiated by tertiary

amines. Part IV. Effect of hydroxyl groups on initiation and curing kinetics. Polymer 2010; 51: 26-34.

[21] Rozenberg BA. Epoxy resins and composites II. Dušek K, editor. Berlin: Springer, 1986, vol. 75.

[22] Ghaemy M, Khandani MH. Kinetics of curing reaction of DGEBA with BF-amine complexes using isothermal DSC technique. Eur Polym J 1998; 34: 477-486.

[23] Delfrey KN. Rare Earths: Research and Applications. New York: Nova Science Publishers, 2008.

[24] Castel, P, Galià M, Serra A, Salla JM, Ramis X. Study of lanthanide triflates as new curing initiators for DGEBA. Polymer 2000; 41: 8465-8474.

[25] Mas C, Serra A, Mantecón A, Salla JM, Ramis X. Study of Lanthanide Triflates as New Curing Initiators for Cycloaliphatic Epoxy Resins. Macromol Chem Phys 2001; 202: 2554-2564.

[26] García SJ, Ramis X, Serra A, Suay J. Addition effect of erbium (III) trifluoromethanesulfonate in the homopolymerization kinetics of a DGEBA resin Termochim Acta 2006; 441: 45-52.

[27] García SJ, Ramis X, Serra A, Suay J. Cationic crosslinking of solid DGEBA resins with ytterbium(III) trifluoromethanesulfonate as initiator. J Therm Anal Calorim 2006; 83: 429-438.

[28] Kubisa P, Penczek S. Cationic activated monomer polymerization of heterocyclic monomers. Prog Polym Sci 1999; 24: 1409-1437.

[29] Matejka L, Chabanne P, Tighzert L, Pascault JP. Cationic polymerization of diglycidyl ether of bisphenol A. J Polym Sci Part A Polym Chem 1994; 32: 1447-1458.

[30] Sangermano M. UV-Cured nanostructured epoxy coatings. In: Epoxy Polymers. Pascault JP, Williams RJJ, editors. Weinheim: Wiley-VHC, 2010.

[31] Expanding monomers. Synthesis, characterization and applications. Sadhir RK, Luck MR, editors. Boca Raton: CRC Press, 1992.

[32] Mas C, Ramis X, Salla JM, Mantecón A, Serra A. Copolymerization of diglycidyl ether of bisphenol A with γ-butyrolactone catalysed by ytterbium triflate: Shrinkage during curing. J Polym Sci Part A: Polym Chem 2003; 41: 2794-2808.

[33] Fernández-Francos X, Salla JM, Cadenato A, Morancho JM, Serra A, Mantecón A, Ramis X. New thermosets obtained by cationic copolymerization of DGEBA with γ-caprolactone with improvement in the shrinkage. II. Time-temperature-transformation (TTT) cure diagram. J Appl Polym Sc 2009; 111: 2822-2929.

[34] Fernández-Francos X, Salla JM, Cadenato A, Morancho JM, Serra A, Mantecón A, Ramis R. A new strategy for controlling shrinkage of DGEBA resins cured by cationic copolymerization with hydroxil-terminated hyperbranched polymers and ytterbium triflate as initiator. J Appl Polym Sci 2009; 111: 2822-2829.

[35] Bagheri R, Marouf BT, Pearson RA. Rubber-toughened epoxies: A critical review. J Polym Rev 2009; 49: 201-225.
[36] Flores M, Fernández-Francos X, Ferrando F, Ramis X, Serra A. Efficient impact resistance improvement of epoxide/anhydride thermosets by adding hyperbranched polyesters partially modified with undecenoyl chains. Polymer 2012; 53: 5232-5241.
[37] Tong XC. Advanced materials for thermal management of electronic packaging. New York: Springer, 2011.
[38] Tritt TM. Thermal conductivity - theory, properties & applications. New York: Plenum Publishers; 2004.
[39] Balandin AA. Thermal properties of graphene and nanostructured carbon materials. Nat Mater 2011; 10: 569-581.
[40] Toberer ES, Baranowski LL, Dames C. Advances in thermal conductivity. Annu Rev Mater Res 2012; 42: 179–209.
[41] Watari K, Kawamoto M, Ishizaki K. Sintering chemical reactions to increase thermal conductivity of aluminium nitride. J Mater Sci 1991; 26: 4727-4732.
[42] Jackson TB, Virkar AV, More KL, Dinwiddie RB, Cutler Jr, Cutler RA. High-thermal conductivity aluminium nitride ceramics: the effect of thermodynamic, kinetic, and microstructural factors. J Am Ceram Soc 1997; 80: 1421-1435.
[43] Xu X, Zhuang H, Li W, Xu S, Zhang B, Fu X. Improving thermal conductivity of Sm_2O_3-doped AlN ceramics by changing sintering conditions. Mat Sci Eng A 2003; 342: 104-108.
[44] Cahill DG, Pohl RO. Lattice vibrations and heat transport in crystals and glasses. Ann Rev Phys Chem 1988; 39: 93-121.
[45] Berber S, Kwon Y-K, Tomanek D. Unusually high thermal conductivity of carbon nanotubes. Phys Rev Lett 2000; 84: 4613.
[46] Dresselhaus MS, Lin Y-M, Rabin O, Black MR, Dresselhaus G. Nanowires. In: Bhushan B, editor. Handbook of Nanotechnology. Heidelberg: Springer-Verlag; 2004.
[47] Lindsay L, Broido DA, Reinecke TL. First-principles determination of ultrahigh thermal conductivity of boron arsenide: A competitor for diamond? Phys Rev Lett 2013; 111: 025901.
[48] Jain A, McGaughey JH. Thermal conducticity of compound semiconductors: Interplay of mass density and acoustic-optical phonon frequency gap. J Appl Phys 2014; 116: 073503.
[49] Broido DA, Lindsay L, Reinecke TL. *Ab initio* study of the unusual thermal transport properties of boron arsenide and related materials. Phys Rev B 2013; 88: 214303.
[50] Kim J, Evans DA, Sellan DP, Williams OM, Ou E, Cowley AH, Shi L. Thermal and thermoelectric transport measurements of an individual boron arsenide microstructure. Appl Phys Lett 2016; 108: 201905.

[51] Lee JH, Koh CY, Singer JP, Jeon SJ, Maldovan M, Stein O, Thomas EL. 25th anniversary article: ordered polymer structures for the engineering of photons and phonons. Adv Mater 2014; 26: 532-569.
[52] Huang XY, Jiang PK, Tanaka T. A review of dielectric polymer composites with high thermal conductivity. IEEE Electr Insul Mag 2011; 27: 8-16.
[53] Heifferon KV, Long TE. Advanced polymers for reduced energy consumption in architecture. Macromol. Rapid Commun, 2018; 40(3): 1800597.
[54] Henry A, Chen G. High thermal conductivity of single polyethylene chains using molecular dynamics simulations. Phys Rev Lett 2008; 101: 235502/1–235502.
[55] Yorifuji D, Ando S. Molecular structure dependence of out-of-plane thermal diffusivities in polyimide films: a key parameter for estimating thermal conductivity of polymers. Macromolecules 2010; 43: 7583-7593.
[56] Burger N, Laachachi A, Ferriol M, Lutz M, Toniazzo V, Ruch D. Review of thermal conductivity in composites: Mechanism, parameters and theory. Prog Polym Sci 2016; 61: 1-28.
[57] Yang Y. Thermal conductivity. In: Mark JE, editor. Physical properties of polymers handbook. New York: Springer-Verlag; 2007.
[58] Bigg DM. Electrical properties of metal-filled polymer composites. In: Bhattacharya SK, editor. Metal-filled polymers. New York: Marcel Dekker; 1986.
[59] Tao Y, Yang ZG, Lu XL, Tao GL, Xia YP, Wu HP. Influence of filler morphology on percolation threshold of isotropical conductive adhesives (ICA). Sci China Technol Sci 2012; 55: 28-33.
[60] Guerra V, Wan C, McNally T. Thermal conductivity of 2D nano-structured boron nitride (BN) and its composites with polymers
[61] Mallakpour S, Khadem E. Progress in polymer science recent development in the synthesis of polymer nanocomposites based on nano-alumina Prog Polym Sci 2015; 51: 74–93.
[62] Li TL, Hsu SLC. Enhanced thermal conductivity of polyimide films via a hybrid of micro- and nano-sized boron nitride. J Phys Chem B 2010; 114: 6825–6829.
[63] Fu JF, Shi LY, Zhang DS, Zhong QD, Chen Y. Effect of nanoparticles on the performance of thermally conductive epoxy adhesives. Polym Eng Sci 2010; 50: 1809-1819.
[64] Yuan FY, Zhang HB, Li XF, Li XZ, Yu ZZ. Synergistic effect of boron nitride flakes and tetrapod-shaped ZnO whiskers on the thermal conductivity of electrically insulating phenol formaldehyde composites. Composites A 2013; 53: 137-144.
[65] Kanuparthi S, Subbarayan G, Siegmund T, Sammakia B. The effect of polydispersivity on the thermal conductivity of particulate thermal interface materials. IEEE Trans Compon Packag Technol 2009; 32: 424-434.

[66] Kemaloglu S, Ozkoc G, Aytac A. Properties of thermally conductive micro and nano size boron nitride reinforced silicon rubber composites. Thermochimica Acta 2010; 499: 40-47.
[67] Kim K, Kim J. Vertical filler alignment of boron nitride/epoxy com-posite for thermal conductivity enhancement via external magneticfield. Int J Therm Sci 2016; 100: 29-36.
[68] Yu SZ, Hing P, Hu X. Thermal conductivity of polystyrene-aluminumnitride composite. Composites A 2002; 33: 289-292.
[69] Xu YS, Chung DDL. Increasing the thermal conductivity of boron nitride and aluminium nitride particle epoxy-matrix composites by particle surface treatments. Compos Interfaces 2000; 7: 243-256.
[70] Song YS, Youn JR. Influence of dispersion states of carbon nanotubes on physical properties of epoxy nanocomposites. Carbon 2005; 43: 1378-1385.
[71] Yao Y, Sun J, Zeng X, Sun R, Xu J-B, Wong C-P. Construction of 3D Skeleton for Polymer Composites Achieving a High Thermal Conductivity. Small 2018; 14: 1704044.
[72] Moore G. Chapter 7: Moore’s low at 40. In Brock DC, editor. Understanding Moore’s law: Four decades of innovation. Philadelphia, PA, Chemical Heritage Foundation, 2006.
[73] Hong J, Park DW, Shim SE. A review on thermal conductivity of polymer composites using carbon-based fillers: Carbon nanotubes and carbon fibers. Carbon Lett 2010; 11: 347-356.
[74] Sanjuán AM, Reglero JA, Garcia FC, Garcia JM. Recent developments in sensing devices based on polymeric systems. React Funct Polym 2018; 133: 103-125.
[75] Lau AKT, Hui D. The revolutionary creation of new advanced materials-carbon nanotube composites. Compos Part B: Engineer 2002; 33: 263-277.
[76] Kozako M, Okazaki Y, Hikita M, Tanaka T. Preparation and evaluation of epoxy composite insulating materials toward high thermal conductivity. 10th IEEE International Conference on Solid Dielectrics 2010: 1-4.
[77] Procter P, Solc J. Improved thermal-conductivity in microelectronic encapsulants. IEEE Trans Compon Hybrids Manuf Technol 1991; 14: 708-713.
[78] Lee WS, Yu J. Comparative study of thermally conductive fillers in underfill for the electronic components. Diamond Relat Mater 2005; 14: 1647-1653.
[79] Varlow BR, Robertson J, Donnelly KP. Nonlinear fillers in electrical insulating materials. IET Sci Meas Tech 2007; 1, 96-102.
[80] Guo L, Zhang Z, Kang R, Chan Y, Hou X, Wu Y, Wang M, Wang B, Cui J, Jiang N, Lin C-T, Yu J. Enhanced thermal conductivity of epoxy composites filled with tetrapod-shaped ZnO. RSC Adv 2018; 8: 12337.
[81] Yu G, Levinshtein ME, Rumyantsev SL, in Properties of advanced semiconductor materials: GaN, AlN, SiC, BN, SiC, SiGe. Levinshtein ME, Rumyantsev SL, Shur MS, editors. New York: John Wiley & Sons Inc, 2001, 93-148.

[82] Hwang Y, Kim J, Cho W. Thermal conductivity of thermally conductive ceramic composites and silicon carbide/epoxy composites through wetting process. Polymer-Korea 2014; 38: 782-786.

[83] Huang X, Iizuka T, Jiang P, Ohki Y, Tanaka T. Role of interface on the thermal conductivity of highly filled dielectric epoxy/AlN composites. J Phys Chem C 2012; 116: 13629-13639

[84] Xu Y, Chung D, Mroz C. Thermally conducting aluminum nitride polymer-matrix composites. Compos A: Appl Sci Manuf 2001; 32: 1749-1757

[85] Pan Z, Sun H, Zhang Y, Chen C. Harder than diamond: Superior indentation strength of wurtzite BN and Lonsdaleite. Phys Rev Lett 2009; 102: 055503.

[86] Alam MT, Bresnehan MS, Robinson JA, Haque MA. Thermal conductivity of ultra-thin chemical vapor deposited hexagonal boron nitride films. Appl Phys Lett 2014; 104: 13113-13118.

[87] Cai Q, Scullion D, Gan W, Falin A, Zhang S, Watanabe K, Taniguchi T, Chen Y, Santos EJG, Li LH. High thermal conductivity of high-quality monolayer boron nitride and its thermal expansion. Sci Adv 2019; 5: eaav0129.

[88] Levinshtein ME, Rumyantsev SL, Shur MS. Properties of advanced semiconductor materials: GaN, AlN, SiC, BN, SiC, SiGe. New York: John Wiley & Sons Inc, 2001.

[89] Engler M, Lesniak C, Damasch R, Ruisinger B, Eichler J. Hexagonal boron nitride (hBN) applications from metallurgy to cosmetics. Ger Ceram Soc 2007; 84: 49-53.

[90] Ishida H, Rimdusit S. Very high thermal conductivity obtained by boron nitride-filled polybenzoxazine. Thermochim Acta 1998; 320: 177-186.

[91] Tanaka T, Kozako M, Okamoto K. Towards high thermal conductivity nano micro epoxy composites with sufficient endurance voltage. J Inter Counc Elect Eng 2012; 2: 90-98.

[92] Wang CY, Feng LL, Li W, Zheng J, Tian WH, Li XG. Shape-stabilized phase change materials based on polyethylene glycol/porous carbon composite: the influence of the pore structure of the carbon materials. Sol Energy Mater Sol Cells 2012; 105: 21-26.

[93] Zhang YX, Hu XY, Zhao JH, Sheng K, Cannon WR, Wang XH, Fursin L. Rheology and thermal conductivity of diamond powder filled liquid epoxy encapsulants for electronic packaging. IEEE Trans Compon Packag Technol 2009; 32: 716-723.

[94] Berman R. The thermal conductivity of some polycrystalline solids at low temperatures. Proc Phys Soc Sect A 1952; 65: 1029-1040.

[95] Smith AW. Low-temperature thermal conductivity of a Canadian natural graphite. Phys Rev 1954; 95: 1095-1096.

[96] Ganguli S, Roy AK, Anderson DP. Improved thermal conductivity for chemically functionalized exfoliated graphite/epoxy composites. Carbon 2008; 46: 806-817.

[97] Van Heerden X, Badenhorst H. The influence of three different intercalation techniques on the microstructure of exfoliated graphite. Carbon 2015; 88: 173-184.

[98] Badenhorst H. A review of the application of carbon materials in solar thermal energy storage. Sol Energy 2019, https://doi.org/10.1016/j.solener.2018.01.062 In press.
[99] Celzard A, Mareche JF, Furdin G. Modelling of exfoliated graphite. Prog Mater Sci 2005; 50: 93-179.
[100] Wang Z, Qi R, Wang J, Qi S. Thermal conductivity improvement of epoxy composite filled with expanded graphite. Ceram Inter 2015; 41: 13541-13546.
[101] Balandin AA. Thermal properties of graphene and nanostructured carbon materials. Nat Mater 2011; 10: 569-581.
[102] Gu J, Yang X, Lv Z, Li N, Liang C, Zhang Q. Functionalized graphite nanoplatelets/epoxy resin nanocomposite with high thermal conductivity. Inter J Heat and Mass Transfer 2016; 92: 15-22.
[103] Guo W, Chen G. Fabrication of graphene/epoxy resin composites with much enhanced thermal conductivity via ball milling technique. J Appl Polym Sci 2014; 131: 40565.
[104] Cha J, Jun GH, Park JK, Kim JC, Ryu HJ, Hong SH. Improvement of modulus, strength and fracture toughness of CNT/Epoxy nanocomposites through the functionalization of carbon nanotubes. Composites Part B 2017; 129: 169-179.
[105] Biercuk MJ, Llaguno MC, Radosavljevic M, Hyun JK, Johnson AT, Fischer JE. Carbon nanotube composites for thermal management. Appl. Phys. Lett. 2002; 80: 2767-2769.
[106] Han Z, Fina A. Thermal conductivity of carbon nanotubes and their polymer nanocomposites: a review. Prog. Polym. Sci. 2011; 36: 914-944.
[107] Zhou T, Wang X, Liu X, Xiong D. Improved thermal conductivity of epoxy composites using a hybrid multi-walled carbon nanotube/micro-SiC filler. Carbon 2010; 48: 1171-1176.
[108] Evseeva LE, Tanaeva SA. Thermal conductivity of micro- and nano-structural epoxy composites at low temperatures. Mech Compos Mater 2008; 44: 117-126
[109] Moisala A, Li Q, Kinloch I, Windle A. Thermal and electrical conductivity of single- and multi-walled carbon nanotube-epoxy composites. Compos Sci Technol 2006; 66: 1285-1288.
[110] Yu A, Ramesh P, Sun X, Bekyarova E, Itkis ME, Haddon RC. Enhanced thermal conductivity in a hybrid graphite nanoplatelet-carbon nanotube filler for epoxy composites. Adv Mater 2008; 20: 4740-4744.
[111] Singh AK, Panda BP, Mohanty S, Kumar S, Gupta NK, Gupta MK. Recent developments on epoxy based thermally conductive adhesives (TCA): a review. Polym Technol Eng 2018; 57: 903–934.
[112] Wattanakul K, Manuspiya H, Yanumet N. Thermal conductivity and mechanical properties of BN-filled epoxy composite: effects of filler content, mixing conditions, and BN agglomerate size. J Compos Mater 2011; 45: 1967-1980.

[113] Lee ES, Lee SM, Shanefieldz DJ, Cannon WR. Enhanced thermal conductivity of polymer matrix composite via high solids loading of aluminum nitride in epoxy resin. J Am Ceram Soc 2008; 91: 1169-1174.

[114] Xu Y, Chung D. Increasing the thermal conductivity of boron nitride and aluminium nitride particle epoxy-matrix composites by particle surface treatments. Compos Interfaces 2000; 7: 243-256.

[115] Zhou W, Yu D, An Q. A novel polymeric coating with high thermal conductivity. Polym Plast Technol 2009; 48: 1230-1238.

[116] Mortazavi B, Baniassadi M, Bardon J, Ahzi S. Modeling of two-phase random composite materials by finite element, Mori-Tanaka and strong contrast methods. Composites B 2013; 45: 1117-1125.

[117] Mu M, Wan C, McNally T. Thermal conductivity of 2D nano-structured graphitic materials and their composites with epoxy resins. 2D Mater. 2017; 4: 042001.

[118] Shtein M, Nadiv R, Buzaglo M, Kahil K, Regev O. Thermally conductive graphene-polymer composites: size, percolation, and synergy effects. Chem Mater 2015; 27: 2100-2106.

[119] Wang Z, Zhi C. Chapter 11. Thermally conductive electrically insulating polymer nanocomposites. In: Huang X, Zhi C, editors. Polymer nanocomposites: electrical and thermal properties. New York: Elsevier, 2016.

UNIVERSITAT ROVIRA I VIRGILI
NEW EPOXY COMPOSITES WITH ENHANCED THERMAL CONDUCTIVITY KEEPING ELECTRICAL INSULATION.
Isaac Isarn Garcia

Chapter 2. Experimental part

2.1. Materials
2.2. Experimental techniques

2.1. Materials

All the products used in this thesis are commercially available and are detailed in the following list:

- Diglycidyl ether of bisphenol A (DGEBA) from Huntsman International LLC., Araldite GY 240 with a molecular weight per epoxy equivalent (EEW) of 182 g/eq.
- Cycloaliphatic epoxy resin 3,4-epoxy cyclohexylmethyl 3,4-epoxy cyclohexane carboxylate (ECC) with an EEW=126.15 g. ERL-421D was supplied by Dow Chemical Company for some studies and for others was provided by Sigma Aldrich.
- Pentaerythritol tetrakis (3-mercaptopropionate) (PETMP), with an EEW=122.165 g/thiol eq, was purchased by Sigma Aldrich.
- 4-(*N,N*-dimethylamino)pyridine (DMAP) was provided by Fluka Analytical.
- N-(4-methoxybenzyl)-N,N-dimethylanilinium hexafluoroantimonate, from King Industries Inc. is commercialized as CXC1612.
- Propylene carbonate was provided by Sigma Aldrich.
- Triethanolamine (TEA) was supplied by Sigma Aldrich.
- Glycerol was purchased by Sigma Aldrich.
- BN platelets, TPC 006, were purchased from ESK Ceramics GmbH, with a particle size of 6µm.
- BN platelets, PCTP30, were purchased from Saint-Gobain, with an average size of 30µm.
- BN platelets of 180 µm of length average, PCTP30D, were supplied by Saint Gobain.
- BN agglomerates, PCTL5MHF, were provided by Saint Gobain, with an average size of 80 µm.
- Aluminium oxide (Al_2O_3) was purchased from Showa Denko, with a size in the range of 1-5 µm.
- Aluminium Nitride (AlN) was provided by Sigma Aldrich.
- Silicon Carbide (SiC) was provided from Shengli Abrasives.
- Expanded graphite (EG), BNB90, was provided by Songhan Plastic Technology Co. Ltd., with an average size of 85 µm and specific surface area (SSA) of 28.4 m^2/g.
- Multiwalled CNTs (NC7000) were provided by Nanocyl SA, with 9.5 nm and 1.5 µm of diameter and length averages, respectively, and SSA in the range of 250-300 m^2/g.

2.2. Experimental techniques

Virtually, all important properties of solid materials may be grouped into six different categories: mechanical, electrical, thermal, magnetic, optical, and deteriorative. For each there is a characteristic type of stimulus capable of provoking

different responses.[1] In this section, each of the analysis techniques used will be explained. We will make a brief explanation of the fundamentals, the main applications of interest for the study and, finally, the treatment of the obtained results.

2.2.1.Differential Scanning Calorimetry (DSC)

Differential scanning calorimetry (DSC) is the most popular thermal analysis technique. It is a technique in which the heat flow rate difference between a substance and a reference is measured as a function of temperature, while the sample is subjected to a controlled temperature program. Among the applications of DSC must be mentioned the easy and fast determination of the glass transition temperature the heat capacity jump at the glass transition, melting and crystallization temperatures, heat of fusion, heat of reactions, very fast purity determination, fast heat capacity measurements, characterization of thermosets, and measurements of liquid crystal transitions.[2]

Different DSC devices were used according to availability. Small amount of sample, between 2-10 mg, are enough for the use of technique. The sample was placed in closed aluminium pans with a pierced lid to avoid overpressure if gases evaporate with the increase of temperature. An empty aluminium pan is placed as a reference to determine the changes in the heat evolved or absorbed during the experiment. **Figure 2.1** shows the last device used.

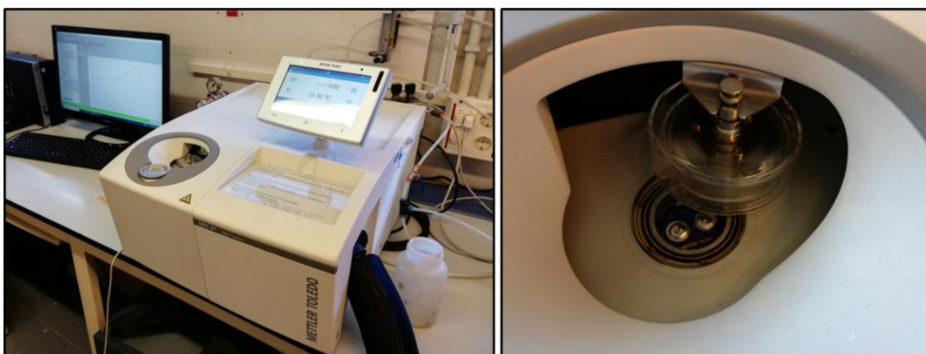

Figure 2.1. DSC-3+ device from Mettler Toledo and its furnace of sample and reference pans.

The determination of the curing kinetics, highly related with the degree of conversion, and the glass transition temperature are the most valuable data that can be extracted by DSC. Cure kinetics is the mathematical relationship between time, temperature, and conversion. In a kinetic study using DSC the heat released during the reaction is assumed to be proportional to the conversion degree, a first order transition.[2] Additionally, the curing rate (*dx/dt*) is directly related to this released heat (*dH/dt*). When the reaction is completed, the integral related to the signal obtained yields the total released heat ΔH_{total}. Reaction rate and conversion degree can be calculated with the following expressions:

$$\frac{dx}{dt} = \frac{dH/_{dt}}{\Delta H_{tot}} = \frac{dh/_{dt}}{\Delta h_{tot}} \qquad \textbf{(Eq. 2.1)}$$

$$x = \frac{\Delta H_t}{\Delta H_{tot}} = \frac{\Delta h_t}{\Delta h_{tot}} \qquad \textbf{(Eq. 2.2)}$$

where *dh/dt* and Δh_{tot} are the heat releasing rate and the total heat released normalized in respect to the sample size, ΔH_t is the heat released up to a time *t*, and Δh_t is the heat released normalized in respect to the sample size. It can be expressed in J/g or in kJ/ee. Finally, *x* is the degree of curing, and can also be expressed as *α*.

The kinetics of a system can be studied in either isothermal or dynamic conditions. The dynamic experiments were preferred since they present some advantages when compared with isothermal experiments, being the most important fact using isothermal conditions the losing of information at the beginning of the curing process and, in another hand, the curing is not always completed.[2]

The reaction rate is usually expressed as *dx/dt = k f(x)* being *k* the kinetic constant and *f(x)* a function depending on the conversion. The kinetic constant, *k*, usually follows the Arrhenius expression:

$$k = Ae^{\frac{-E}{RT}} \qquad \textbf{(Eq. 2.3)}$$

where *A* is the pre-exponential factor, *E* the activation energy, *R* the gas constant and *T* the absolute temperature.

In general, a kinetic process is well characterized if one knows *E*, *A* and *f(x)*, the so-called kinetic triplet. Although strictly speaking this methodology should only be valid for one-step processes it can also be applied in systems where more than one chemical (or physical) process coexists. There are two main approaches in the kinetic analysis, isoconversional methods and model-fitting methods. In the present thesis only isoconversional kinetic analysis has been used.

The isoconversional methodology assumes that the reaction function *f(x)* is independent of the heating rate.[3] On that way, the kinetics of a process only depends on the degree of conversion at a certain time. It also requires the performance of series of experiments to determine the apparent activation energy. Those experiments can be, for example, dynamic DSC curing at different heating rates.

A second order transition, such as the glass transition, can be measured through the step variation of the heat capacity associated to the structural reorganization of the network. T_g is usually reported as the temperature at the half height of the heat capacity change. Can also be taken as the inflexion point, which is slightly different and corresponds to the peak on the derivative of the heat flow or heat capacity against temperature.

As usual, DSC experiments in dynamic conditions at 10 °C/min were performed to the cured materials. With the help of software analysis, the T_gs can be easy determined.

2.2.2. Rheology

Rheology is the science of deformation and flow of materials. In fact, all materials can flow, given enough time. In very short processing times, the polymer may behave as a solid, while in long processing times the material may behave as a fluid. This dual nature (fluid-solid) is referred to as viscoelastic behaviour.[4]

Viscosity is one of the most important flow properties to be measured by rheology and is the resistance to flow. Strictly speaking, it is the resistance to shearing and it can be defined as the ratio of the imposed shear stress and the shear rate. In this way, rheological measurements are based on monitoring the tension generated in the sample as a response to the application of an oscillatory shear force.[4]

In this way, rheological measurements are based on monitoring the tension generated in the sample as a response to the application of an oscillatory shear force. The viscoelasticity of a given polymer reflects in the difference in the applied and measured angle δ. By rheology it was possible to study the gel time, the conversion at the gel point, as well as determining the viscosity and viscoelastic properties such as elastic shear modulus (G') and viscous shear modulus (G'') of uncured formulations. Likewise, the complex viscosity (η^*) is determined in multi-frequency experiments at a certain temperature and amplitude. This amplitude must be comprised within the range of linear viscoelasticity.

Rheological results of filled formulations can be used to calculate the rheological percolation threshold. At a given frequency, theory predicts a power law relation:

$$G' \propto (V - V_c)^{\beta} \qquad \textbf{(Eq. 2.4)}$$

where G' is the storage modulus, V is the volume or mass fraction of BN composites, V_c is the volume or mass fraction at rheological percolation and β is the critical exponent. This relation is often valid only on a very narrow concentration region.[5]

Rheological measurements were carried out in the parallel plates (25 mm) mode with an AR G2 rheometer (TA Instruments, **Figure 2.2**), equipped with a Peltier system for controlling the temperature. Curable formulations are placed between two aluminium plates with a distance between plates (gap) of approximately in the range of 500-1000 µm (must be identical to compare different mixtures).

The curing of thermosets is a complex process of network growing, weight distribution and branching in which two well-known phenomena take place, the gelation and the vitrification of the network. The gelation is defined as the time in which the chains form a unique path, hence, the molar mass becomes infinite. It is a giant macromolecule consisting of covalently bonded repeating units forming during the polymerization process. This giant molecule that percolates throughout the sample is called a gel.[6] From an applicative point of view, it is defined as the time in which the material cannot be processed anymore. The gelation leads to a drastic change in the

physical response: the viscosity tends to infinite and the material response becomes more elastic than viscous. The vitrification takes place when the material behaves as a glassy network and the glass transition temperature is close or higher to the curing temperature (T_c). This phenomenon happens when the T_g of the thermoset is too high, thus, two polymerization steps are usually performed: an initial pre-cure at $T_c < T_g$ and a final post-cure at $T_c > T_g$. During the pre-cure, the T_g approaches T_c resulting in the vitrification phenomenon that is overcome after the post-cure, enabling the completion of the polymerization.[6]

Figure 2.2. AR G2 rheometer from TA instruments equipped with a Peltier temperature controller system.

The gel time is determined in isothermal experiments where the oscillation amplitude changes to adjust to the changes in the material. The point at which *tan δ* is independent of the frequency is defined as the gel point.[7] By stopping the experiment at that point and performing a DSC scan to determine the remaining heat it is possible to determine the conversion at gelation (x_{gel}) following the next expression:

$$x_{gel} = 1 - \frac{\Delta h_g}{\Delta h_T} \quad \textbf{(Eq. 2.5)}$$

where Δh_g is the heat released up of gelled samples, obtained by integration of the calorimetric signal, and Δh_T is the heat associated with the complete conversion of all reactive groups.

2.2.3. Dynamo-Mechanical Thermal Analysis (DMTA)

Dynamic-mechanical thermal analysis (DMTA) stablish relationships between the viscous and elastic response of a polymer depending on the deformation time. Generally, in DMTA analysis a sinusoidal pulse is applied to the sample and its response is measured. The analysis involves imposing a small cyclic strain on a sample and measuring stress response, or equivalently, imposing a cyclic stress on a sample and measuring the resultant strain response. DMTA is used both to study molecules relaxation processes in polymers and to determine inherent mechanical or flow properties as a function of time and temperature.[8] In other words, DMTA studies the

viscoelastic nature of a material by applying an oscillatory stress with a fixed frequency to the sample and monitoring its response at different temperatures. Likewise, the complex modulus (E^*) and the loss factor ($tan\ \delta$) can be calculated. The modulus contains real and imaginary contributions ($E^*=E'+i\cdot E''$). The real part, E', is the elastic response measure of the material, whereas imaginary part, E'', is the viscous response. The maximum obtained on $tan\ \delta$ curve is, in most cases accepted as the T_g of a material, although it changes with the frequency used in the experiment. The shape of the peak is a measure of the heterogeneity of the process: the broader and the smaller, the more heterogeneous. To quantify the heterogeneity, the width at half-height (FWHM) and the value of the peak are used.

In this investigation, DMTA experiments were carried out at using a DMA Q800 (TA Instruments, **Figure 2.3**) equipped with 3-point-bending clamp geometry, at oscillatory mode. The oscillation frequency was fixed to 1 Hz and the oscillation strain to 0.1%. A heating rate of 3 °C/min was imposed.

Young Modulus (E) also can be calculated by DMTA. Using 3-point bending clamp the Young modulus in a non-destructive flexural test at room temperature can be obtained. The modulus of elasticity (MPa) is calculated using the slope of the load deflection curve in accordance with:

$$E = \frac{L^3 m}{4bt^3} \qquad \textbf{(Eq. 2.6)}$$

where L is the support span (mm), b and t are the width and the thickness of test sample (mm) and m is the gradient of the slope (N/mm).

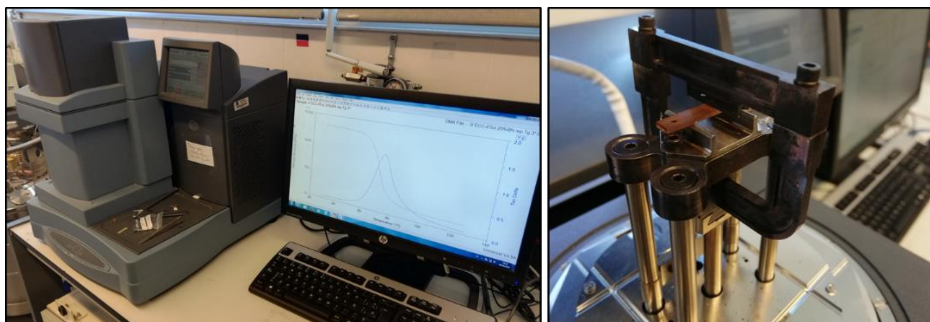

Figure 2.3. DMTA equipment and 3-point bending clamb.

2.2.4.Thermal Mechanical Analysis (TMA)

Polymeric materials suffer dimensional changes, contraction or expansion, during the formation of the network or when are subject to heating/cooling processes. Thermomechanical analysis (TMA) measures changes in sample length or volume as a function of temperature or time under load at atmospheric pressure. The most important TMA measurements include determination of the coefficient of linear thermal expansion (CTE) and the glass transition temperature, T_g. However, several

other measurements can be made by applying special modes and various attachments. These include stress relaxation, creep tensile properties of films and fibbers, flexural properties and volume dilatometry.[9]

For our studies, a Mettler TMA/SDTA840 (**Figure 2.4**), were used to evaluate the thermal expansion coefficient (CTE) of cured samples in static force mode. Cured samples were supported by the clamp and a silica disc to distribute the force uniformly and heated at 5 K/min from 35 °C to needed rubber state temperature. A minimum force of 0.01 N was applied to avoid results distortion. The coefficients of thermal expansion (CTEs) in the glassy state of the material were calculated as follows:

$$CTE = \frac{1}{L_0} \cdot \frac{dL}{dT} = \frac{1}{L_0} \cdot \frac{dL/dt}{dT/dt} \qquad \textbf{(Eq. 2.7)}$$

where L is the thickness of sample, L_0 the initial length, t the time, T the temperature and dT/dt the heating rate.

Figure 2.4. Image of TMA device and the probe which subject the sample inside the furnace.

2.2.5. Thermo-Gravimetric Analysis (TGA)

Thermogravimetric analysis (TGA) is a technique where the mass of a polymer is measured as a function of temperature or time while the sample is subjected to a controlled temperature program in a controlled atmosphere.[10] The heart of the TGA is the thermobalance, which is capable of measuring the sample mass as a function of temperature and time while a purge gas flowing through the balance creates an atmosphere that can be inert, oxidizing or reducing. The moisture content of the purge gas can vary from dry to saturated.[11] TGA can be used to evaluate the thermal stability of a material. In a desired temperature range, if a species is thermally stable, there will

be no observed mass change. Negligible mass loss corresponds to little or no slope in the TGA trace. TGA also gives the upper use temperature of a material. Beyond this temperature the material will begin to degrade.

A thermobalance (**Figure 2.5**) was used to analyze the thermal degradation of cured samples. The degradation was carried out in dynamic conditions, at 10 °C/min under nitrogen or air, from 30 to 600 or 800 °C depending on the experiment selected. The most important parameters extracted from the analysis of such curves are the initial degradation temperature, the temperature of the maximum degradation rate and the char yield.

Figure 2.5. Thermobalance Mettler TGA2 and a detailed image of the oven and balance.

2.2.6. Microindentation Knoop hardness and impact test

A microindentation test hardness is a mechanical hardness test used particularly for very brittle materials where only a small indentation may be made for testing purposes. Here, a pyramidal diamond point is pressed into the polished surface of the test material with a known force for a specified time. Thereby, the length of the long diagonal produced by the indentation of a rhomboidal tip can be related with the hardness of the material. Moreover, the length is directly related to the hardness of the material, so the shorter the diagonal the hardest the material.

Following the ASTM D1474-13 standard procedure and using a Wilson Wolpert (MicroKnoop 401MAV) the microhardness measurements were carried out (**Figure 2.6**).

For each material at least 10 measurements were made with a confidence level of 95%. The Knoop microhardness (KHN) was calculated following:

$$KHN = \frac{L}{A_p} = \frac{L}{l^2 C_p} \qquad \textbf{(Eq. 2.8)}$$

where L is the load applied by the indenter (0.010 Kg), A_p is the area of indentation in mm^2 and C_p the indenter constant ($7.028 \cdot 10^{-2}$) relating l^2 (length of indentation) with A_p.

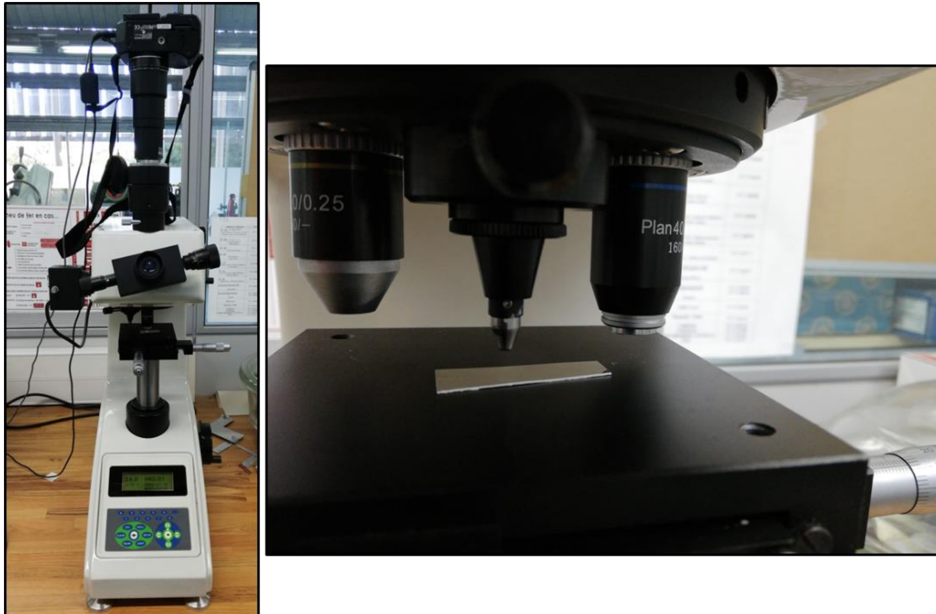

Figure 2.6. Microindentation tester used for the determination of the Knoop hardness of the prepared thermosets.

Impact tests are designed to measure the resistance to failure of a material to a suddenly applied force such as collision, falling object or instantaneous blow. The test measures the impact energy, or the energy absorbed prior to fracture. The Izod test has become the standard testing procedure for comparing the impact resistances of plastics. The Izod test is most commonly used to evaluate the relative toughness or impact resistance of materials. The Izod test involves striking a test piece mounted at the end of a pendulum. The striker swings downwards impacting the test piece at the bottom of its swing.[12]

Zwick 5110 impact tester to perform impact test at room temperature was used (**Figure 2.7**). Impact test were carried out according to ASTM D4508-10 where prismatic rectangular specimens were used. Adjustable pendulum at different kinetic energy was used. The impact strength (*IS*) was calculated from the energy absorbed by the sample upon fracture as:

$$IS = \frac{E-E_0}{S} \qquad \textbf{(Eq. 2.9)}$$

where E and E_0 are the energy loss of the pendulum with and without sample respectively, and S is the cross-section of the samples. The fracture area of impact samples was observed with ESEM (environmental scanning electron microscopy) Quanta 600.

Figure 2.7. Zwick 5110 impact tester used to determine the impact energy absorbed.

2.2.7. Environmental Scanning Electron Microscopy (ESEM) and X-ray diffraction

Electron microscopy is a technique based on the irradiation of an electron beam on the surface of a test specimen. The main signals which are generated by the interaction of the primary electrons of the electron beam and the specimen´s bulk are secondary electrons and backscattered electrons and furthermore X-rays. The electrons interact with the atoms that make up the sample producing signals that contain information about the sample's surface. Thanks to a scanner of the emitted beam of electrons it is possible to observe the topography of the surface and obtain an image that we can see through a display.[13]

A SEM microscope was used, a FEI Quanta 600 Environmental Scanning Electron Microscope (ESEM) equipped with an X-Ray analyser (**Figure 2.8**). The low vacuum mode used by this technique allows collecting micrographs at 10–20 kV and make not necessary to coat the samples despite analyse high electron insulation materials. The analysis has allowed us to obtain detailed images of the internal structure of our cured material, in order to analyse the shape of the break after the impact tests or fragile rupture after subject the sample under liquid nitrogen, and the dispersion of the fillers added.

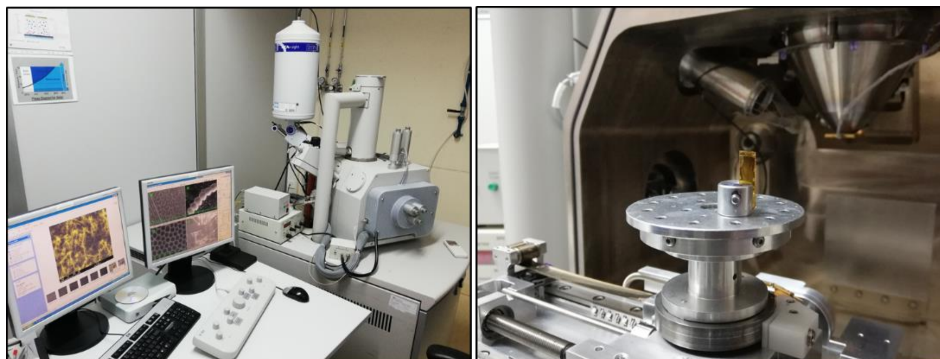

Figure 2.8. ESEM microscope used to analyse fillers and cured samples.

X-ray diffraction is used to analyse the atomic arrangement of the materials. An X-ray beam with a wavelength (λ) comparable to the atomic dimensions hits the sample and the scattered intensity is detected. The principle is behind the Bragg's law (**Eq. 2.10**). According to this law, X-rays are reflected in-phase from the crystalline planes making possible to determine the distance between planes (*d)* and the angle between the incident beam and the scattering plane (Θ).[14]

$$2 \cdot d \cdot sin\theta = n \cdot \lambda \qquad \textbf{(Eq. 2.10)}$$

Measurements of X-ray diffraction (XRD) were performed with a Siemens D5000 diffractometer (Bragg-Brentano parafocusing geometry and vertical Θ-Θ goniometer) fitted with a curved graphite diffracted beam monochromator, using incident and diffracted beam Soller slits, a 0.06° receiving slit and scintillation counter as detector. The angular 2Θ diffraction range was between 5 and 70°. The data were collected with an angular step of 0.05° at 3 s per step and sample rotation. $Cu_{k\alpha}$ radiation was obtained from a copper X-ray tube operated at 40 kV and 30 mA.

Figure 2.9. Diffractometer Siemens D5000 used in this thesis.

2.2.8. Electrical measurements

Electrical conductivity (S/m), or its converse, electrical resistivity (Ω·m), is a fundamental property of a material that quantifies how easily conducts or resists the flow of electric current. Although conductors are required to transmit this form of energy, insulating materials as thermosets are needed to prevent their loss during the transport. Thermosets, very important in electrical engineering, in modern times have become a decisive material in the world of electronics.

There are many methods to determine the electrical resistivity (*ρ*) of a material, but the technique may vary depending upon the type of material, magnitude of resistance, shape and thickness. The most common method is to apply a voltage (V) to a material by electrodes and measure the electrical resistance (Ω) it offers. Following the next expression, it can be easily calculated:

$$\rho = R\frac{A}{l} \qquad \textbf{(Eq. 2.11)}$$

where *R* is the electrical resistance measured by the device, *A* the electrode area and *l* the sample thickness. Electrical resistance of materials was tested using different multimeters at room temperature based on ASTM D257-14 standard depending on the resistance of the materials: 34,410 A 6½ Digit from Agilent Technologies, a Megohmmeter Resistomat 24,508 and a Metrel MI 2077 TeraOhm 5 kV.

Figure 2.10. The multimeters from Agilent Technologies and Resistomat and a detailed view of the montage to measure the electrical resistance of samples between two electrodes.

Other important property can be measured in electrical insulators is the dielectric breakdown. This is the point at which the applied voltage is to high that the insulator permits current to flow, often associated with the failure of the material. Dielectric breakdown strength was measured using a Lamsa TD-51 alternating current dielectric strength tester, with a voltage supplied of 6.6 kV, 50 Hz transformer, according to ASTM D 149-09. Tests were made at room temperature with point/plane electrodes. The rate of voltage rising speed was 1 kV/s until breakdown. A minimum of 16 values were recorded for each specimen, discarding which one's flash over occur. Considering tabulated dielectric strength of epoxy resins (19.7 kV/ mm) and BN (37.4 kV/mm)[15] and maximum voltage of tester, films of about 100–150 mm were prepared, by curing the composition between two Norton FEP Fluoropolymer films. Thickness measurements

were made by a micrometer with rounded tips with a precision of ±0.001 mm. Different results were obtained for each specimen and the data obtained may be represented by statistical distribution. Two-parameter Weibull distribution are used to obtain failure prediction response and reliability of the materials because of its advantages such as high accuracy of results even with few determinations and a confinable method to estimate useful life of materials. Distribution is written as:

$$P = 1 - exp\left[(-E/E_0)^{\beta}\right] \qquad \textbf{(Eq. 2.12)}$$

where *P* is the cumulative probability of electrical failure, *E* is the experimental breakdown strength, E_0 is the scale parameter, the characteristic breakdown strength at a cumulative failure probability of 63.2%, which is frequently used to compare different samples, and *β* is the shape parameter, inversely proportional to deviation of data. For failure probability, IEEE 930-2004 standard recommends a good, simple approximation:[16]

$$P_i = \frac{i-0.44}{n+0.25} \cdot 100\% \qquad \textbf{(Eq. 2.13)}$$

where *i* is the i-th result when values of *E* are sorted in ascending order, and *n* the number of samples.

2.2.9.Thermal conductivity measurements

The measurement techniques of thermal conductivity can be divided into two groups. They are steady state methods and transient methods. Steady state methods are applied when the system has achieved stability, while the transient methods are used during the process of heating up or cooling down a material. The transient methods are generally used to measure thermal diffusivity by recording temperature as function of time following a transient or periodic heat added at the sample surface. Thermal diffusivity can be calculated from the specimen thickness and the time required for the temperature rise to reach a percentage of its maximum value. Thermal conductivity (*k*) can be calculated through:

$$k = \alpha C_p \rho \qquad \textbf{(Eq. 2.14)}$$

where *k* is the thermal conductivity, *α* is the thermal diffusivity, *ρ* is the density, C_p is the specific heat. The transient methods are much faster than steady state methods. Typical measurement duration of one hour for a steady state measurement is reduced to a few minutes or to a subsecond interval for a transient method. However, transient methods usually have lower accuracy and require more complicated data analysis. The method employed is a transient pulse heating technique used for thermal conductivity and thermal diffusivity measurements. This technique uses a thin, plane, electrically insulated resistive element, usually in a spiral pattern, as both the temperature sensor and the heat source. Heating element is placed between two test samples of the same material. By recording the increase in resistance as a function of time while heating with

an electrical current pulse, the thermal conductivity can be deduced from one single transient recording

Thermal conductivity was measured using the Transient Hot Bridge method by a THB 100 device from Linseis Messgeräte GmbH. A HTP G 9161 sensor was used with a 3x3 mm^2 of area calibrated with poly (methyl methacrylate) (PMMA), borosilicate crown glass, marble, Ti-Al alloy and titanium. Two equal polished rectangular samples were placed in each one of the faces of the sensor. Due to the small size of sensor, side effects can be neglected. A measuring time of 100 s applying a current of 10 mA to each sample. Five measures were done for each material.

Figure 2.11. Thermal conductivity device from Linseis Messgaräte GmbH and the assembly to place the sensor in the middle of two equal polished samples.

References

[1] Callister WD, Rethwisch DG. Materials science and engineering: an introduction. 8th edition. Versailles, KY: Wiley, 2010.
[2] A. Turi. Thermal Characterization of Polymeric Materials. 2nd edition. San Diego: Academic Press; 1997.
[3] Vyazovkin S, Wight CA. Model-free and model-fitting approaches to kinetic analysis of isothermal and nonisothermal data. Thermochim Acta 1999; 340-341: 53-68.
[4] Malkin AY, Isayev AI. Rheology: Concepts, Methods & Applications. Toronto: ChemTec; 2006.
[5] Kamal MR, Mutel A. Rheological properties of suspensions in Newtonian and non Newtonian fluids. J Polym Eng 1985; 5: 293-382.
[6] Pascault JP, Sautereau H, Verdu J, Williams RJJ. Thermosetting polymers. New York: Marcel Dekker Inc.; 2002.
[7] Pascault JP, Sautereau H, Verdu J, Williams RJJ. Rheological and dielectric monitoring of network formation in thermosetting polymers. New York: Marcel Dekker Inc.; 2002.
[8] Chartoff RP, Menczel JD, Dillman SH. Thermal Analysis of Polymers. Chapter 5. Hoboken: John Wiley&Sons; 2008.
[9] Bair HE, Akinay AE, Menczel JD, Prime RB, Jaffe M. Thermal Analysis of Polymers. Chapter 4. Hoboken: John Wiley&Sons; 2008.
[10] Earnest CM. Compositional Analysis by Thermogravimetry. Philadelphia: ASTM; 1988.
[11] Prime RB, Bair HE, Vyazovkin S, Gallagher PK, Riga A. Thermal Analysis of Polymers. Chapter 3. Hoboken: John Wiley&Sons; 2008.
[12] Brown R. Handbook of Polymer Testing - Short-Term Mechanical Tests. London: Rapra Technology; 2002.
[13] Goldstein J, Newbury DE, Joy DC, Lyman CE, Echlin P, Lifshin E, Sawyer L, Michael JR. Scanning Electron Microscopy and X-ray Microanalysis. New York: Springer; 2007.
[14] Roe R-J. X-ray Diffraction by Polymers. New York: John Wiley&Sons; 2015.
[15] Shugg WT. Handbook of electrical and electronic insulating materials. New York: Van Nostrand Reinhold; 1986.
[16] Ross R. Graphical methods for plotting and evaluating Weibull distribution data. Proc IEEE 1994; 1: 250-253.

Chapter 3

New BN-epoxy composites obtained by thermal latent cationic curing with enhanced thermal conductivity

UNIVERSITAT ROVIRA I VIRGILI
NEW EPOXY COMPOSITES WITH ENHANCED THERMAL CONDUCTIVITY KEEPING ELECTRICAL INSULATION.
Isaac Isarn Garcia

Composites: Part A ***2017****, 103, 35-47*

New BN-epoxy composites obtained by thermal latent cationic curing with enhanced thermal conductivity

Isaac Isarn[a], Lluís Massagués[b], Xavier Ramis[c], Àngels Serra[d], Francesc Ferrando[a]

a. Department of Mechanical Engineering, Universitat Rovira i Virgili, C/Av. Països Catalans, 26, 43007 Tarragona, Spain.
b. Department of Electronic, Electric and Automatic Engineering, Universitat Rovira i Virgili, C/Av. Països Catalans, 26, 43007 Tarragona, Spain.
c. Thermodynamics Laboratory, ETSEIB, Universitat Politècnica de Catalunya. C/Av. Diagonal 647, 08028 Barcelona, Spain.
d. Department of Analytical and Organic Chemistry, Universitat Rovira i Virgili, C/ Marcel·lí Domingo s/n, 43007 Tarragona, Spain.

Abstract

A series of boron nitride (BN) composites, with different BN content, were prepared and characterized by cationic curing of DGEBA/BN formulations. As cationic initiator a commercial benzylanilinium salt was used. This cationic system shows good latent characteristics that were not lost on adding the filler. The performance of the catalytic system was optimized by varying the amount of initiator and adding little proportions of glycerol. The kinetics of the curing process was evaluated by calorimetric measurements. The addition of BN allowed increasing thermal conductivity without loss of mechanical properties like Young modulus, impact resistance, adhesion and other thermal characteristics like Tg or thermal stability. In addition, dielectric properties were improved with the increment of filler.

Keywords

Polymer-matrix composites (PMCs), thermosetting resin, layered structures, mechanical properties.

1. Introduction

The continuous trend of doing more with less is the tendency in our technological world and definitely it will continue in the future. This is especially true in the electronic miniaturization and the increasing power output of electrical equipment. Efficient thermal management is imperative for these applications, since the improvement in the heat elimination of such devices is directly related to their improved efficiency, lengthening of half-life time operating and the prevention of premature failures or damage of equipment. The electron circulation in materials produces heat by Joule effect and this heat must be removed from devices in order to maintain their work temperature. The electronic packing materials must disperse the heat produced to

lower temperature, but also must possess low dielectric constant and low dielectric loss to avoid the signal distortion, which in turn provides better equipment performance.[1,2,3] It is know, that the reliability of an electronic device is exponentially related to the operating temperature of the junction. Therefore, a small difference in the operating temperature (10–15 °C) can result in a twofold reduction in the lifespan of the device.[4] Thus, thermal dissipation is a challenging problem and the development of new highly thermally conductive but electrically insulating materials is of capital interest to address this challenge.[5,6]

Epoxy resins have been recognized as versatile materials with good properties extensively used in the fields of electric and electronic industries as encapsulants, packaging or coatings, in printed circuit boards, integrated circuit chips and a huge range of electronic devices, electrical and communication equipment and lighting appliances.[7-10] Apart from brittleness, due to their high cross-linking density, one of the drawbacks of these materials is the very low thermal conductivity that exhibit (~0.2 W/m·K), which is mainly attributed to phonon scattering.[2,8,11,12] Some liquid crystalline epoxy thermosets, with ordered structure, can promote the movement of phonons, giving rise to thermal conductivity until 1 W/m·K, but the cost to fabricated them increase considerably.[3]

Much more convenient from the technological and economical point of view is the introduction of conductive fillers as an effective method to solve thermal conductivity drawbacks of epoxy resins.[11,13,14] Metallic particles or carbon materials, like carbon nanotubes (CNT), graphene and graphite, could be attractive fillers due to their high thermal conductivity, but they can make materials electrically conductive. Thus, they are useless to encapsulate electronic devices although they are important in aerospace and aeronautics technologies, where high-performance composites replace metallic materials in some applications to save weight.[4,15-17] Also metallic fillers have several disadvantages including high density and they are susceptible to oxidation.[18] For this reason, only selected fillers with high thermal conductivity and acceptable dielectric breakdown strength, such as some inorganic materials, can be used in order to maintain electrical insulation of composites.[3,19]

Among common inorganic particles, boron nitride (BN) provides the best combination of properties in terms of high thermal conductivity, low dielectric constant, high electrical resistivity and low coefficient of thermal expansion (CTE). Besides all this, BN also presents low density (2.2 g/cm^3), high mechanical strength, high aspect ratio and chemical and thermal stability. BN can be synthesized in hexagonal and cubic forms. In particular hexagonal-BN, known as “white graphite”, is a platelet-shaped synthetic ceramic, with a crystal structure similar to graphite (hexagonal layer crystals) except for the stacking of layers, its layered lattice structure give BN good lubricating properties.[6,11,13,20] The hexagonal BN layers are bonded by weak van der Waals forces, which enable the layers to slide easily against each other. These are the reasons for

which BN has been selected in the present study to prepare new materials with enhanced thermal conductivity from epoxy matrices.

Most of the studies performed in epoxy BN composites are based in epoxy-amine or epoxy-anhydride matrices.[14] However, the curing by homopolymerization of epoxides carries several advantages and broadens the field of applications of this type of materials. Homopolymerization of epoxies can be done by cationic or anionic initiators, in both thermal and photoirradiation conditions.[21,22] Although the use of thermal latent cationic initiators for epoxy curing has not been much studied, it has superior advantages, especially in advanced processing technologies. Under environmental conditions the previously prepared formulations are stable and, only show activity by external stimulation on reaching high temperatures and once initiated they present high curing rates.[21,23-27] In this way, an effective control of initiation and curing process by heating leads to desirable advantages in handling and storage stability and makes these curing systems very advantageous in terms of energy saving and eco-friendly processing compared with conventional curing agents like polyfunctional amines or organic anhydrides. It should be emphasized that heating is easier than photoirradiation for practical use since homogeneous heating of reaction mixtures can be easily attained. Moreover, homogeneous photoirradiation has a higher difficulty since the irradiation area depends on the irradiation source. Thick samples are difficult to completely cure and shadowed areas remain unaltered. [28]

In the present work, an optimization of a latent cationic epoxy system to prepare BN composite materials with enhanced thermal conductivity has been carried out from the point of view of the kinetics. As the base resin, we used diglycidyl ether of Bisphenol A (DGEBA) and a commercially available quaternary ammonium-antimonium hexafluoride salt as initiator. This benzylanilinium salt was previously developed by Endo et al.[29] and has shown a good compatibility on adding several proportions of BN as filler. The kinetic studies of the curing have been performed by differential scanning calorimetry and the processability has been determined by rheological measurements. The BN-composites obtained have been characterized by thermogravimetric and thermomechanical analysis and mechanical characteristics like adhesion, hardness and impact resistance have been evaluated and compared to the unfilled material. The thermal conductivity and other parameters like thermal expansion coefficient, dielectric breakdown strength or electric resistivity have also been determined.

2. Experimental

2.1. Materials

DGEBA from Huntsman International LLC., Araldite GY 240 (EEW=182 g/eq.) was dried at 80°C under vacuum for 6h before use. Initiator CXC1612, from King Industries Inc., USA, was solubilised in propylene carbonate at 50 wt %. Propylene carbonate, distilled before use, was provided by Sigma-Aldrich Co. Ltd. Glycerol, supplied by Sigma-

Aldrich Co. Ltd., was used as received. BN was purchased by ESK Ceramics GmbH, TPC 006, with a particle size of ~6µm.

2.2. Sample preparation

All the samples were prepared by weight, by adding varying initiator and glycerol proportions from 1 to 4 and from 0 to 8 phr (parts per hundred of resin) respectively to the DGEBA resin. For composite samples, the required amount of BN was added in wt. % to the previous formulation. The samples were mechanically stirred until homogeneous mixture and degassed under vacuum to prevent the appearance of bubbles during curing process. Finally, the samples were poured onto aluminium moulds and cured at 120°C for 1h, followed by a post-curing at 150°C for another 1h.

2.3. Characterization techniques

A differential scanning calorimeter (DSC) Mettler DSC-821e calibrated using an indium standard (heat flow calibration) and an indium-lead-zinc standard (temperature calibration) was used to analyse epoxy system. Samples of approximately 5-10 mg were tested in aluminium pans with a pierced lid in a nitrogen atmosphere with a gas flow of 100 mL/min. The dynamic studies were performed in a temperature range of 30-250°C with a heating rate of 10 K/min. Enthalpy (Δh) of samples was calculated by integration of the calorimetric signal. The glass transition temperature (T_g) of cured samples was determined in a second scan as the temperature of the half-way point of the jump in the heat capacity when the material changed from glassy to the rubbery state under nitrogen atmosphere. The error is estimated to be approximately ±1°C.

The curing kinetics was analyzed by means of isoconversional integral and Coats-Redfern[30] procedures applied to non-isothermal DSC experiments at heating rates of 5, 10, 15 and 20 ºC/min. Details of the kinetic methodology are given in previous studies.[31]

The thermal stability of cured samples was studied by thermogravimetric analysis (TGA), using a Metler TGA/SDTA 851e thermobalance. Experiments were performed under inert atmosphere (N_2 at 100 mL/min.). Pieces of cured samples of 10-15 mg were degraded between 30 and 600°C at a heating rate of 10 K/min. Also experiments in oxidant atmosphere were performed (synthetic air at 100 mL/min) to measure stability of the composite and BN residues in the samples, at the same heating rate between 30 and 800°C.

Dynamic mechanical thermal analyses (DMTA) were carried out with a TA Instruments DMA Q800 analyzer. The samples were cured isothermally in an aluminium mould a 120°C for 1h and a post-curing of 150°C for another 1h. Prismatic rectangular samples (15 x 7.3 x 2.4 mm^3) were analyzed by 3-point bending at a heating rate of 3 K/min from 35 to 195°C, the temperature at which rubbery state was observed, using a frequency of 1 Hz and oscillation of 0.1% of sample deformation. The Young modulus (E) was determined at 35°C by means of a force ramp at a constant rate, 1 N/min, never

exceeding 0.25% of deformation to make sure that only elasticity was evaluated, linear zone of stress-strain graph. The slope between 0.1% and 0.2% of deformation was taken. E was calculated using the slope of the load deflection curve in accordance with the following equation:

$$E = \frac{L^3 m}{4bt^3} \qquad (1)$$

where E is the elastic modulus of epoxy sample (MPa), L is the support span (mm), b and t are the width and the thickness of test sample (mm) and m is the gradient of the slope (N/mm).

Thermomechanical analyses (TMA) were carried out on a Mettler TMA40 thermomechanical analyzer. Cured samples (9 x 9 x 2.2 mm^3) were supported by the clamp and one silica disc to distribute uniformly the force and heated at 5°C/min from 35 up to 200°C by application of a force of 0.01N, a minimum force to not distort the results. Two heating were performed, the first one to erase the thermal history and the second one to determine the thermal expansion coefficients (CTEs), below and above the T_g, calculated as follows:

$$CTE = \frac{1}{L_0} \cdot \frac{dL}{dT} = \frac{1}{L_0} \cdot \frac{dL/dt}{dT/dt} \qquad (2)$$

where L is the thickness of sample, L_0 the initial length, t the time, T the temperature and dT/dt the heating rate.

Impact test was performed at room temperature by means of a Zwick 5110 impact tester according to ASTM D 4508-10 using rectangular samples (25x12x2.3 mm^3), cured in the same way of the other techniques. The pendulum employed had a kinetic energy of 0.56 J. For each material a minimum of 7 determinations were made with a confidence level of 95%. The impact strength (*IS*) was calculated from the energy absorbed by the sample upon fracture as:

$$IS = \frac{E - E_0}{S} \qquad (3)$$

where E and E_0 are the energy loss of the pendulum with and without sample respectively, and S is the cross-section of the samples. The fracture area of impact samples was observed with ESEM (environmental scanning electron microscopy) Quanta 600.

Microindentation Knoop hardness was measured with a Wilson Wolpert 401 MAV device following ASTM D1474-13. For each material a minimum of 20 determinations were made with a confidence level of 95%. The Knoop microindentation hardness (KHN) was calculated from the following equation:

$$KHN = \frac{L}{A_P} = \frac{L}{l^2 C_P} \qquad (4)$$

where L is the load applied to the indenter (0.025 Kg), A_P is the projected area of indentation in mm^2, C_P is the indenter constant (7.028 x 10^{-2}) relating l^2 to A_P.

Rheometric measurements were carried out in parallel aluminium plates (geometry of 25 mm Ø) mode with a TA AR G2 rheometer, equipped with electrical heated plates (EHP). Viscosity (η) and complex viscosity ($\eta*$) of the pre-cured mixtures were recorded as function of shear rate (s^{-1}) and angular frequency ω (rad/s), respectively. In the case of $\eta*$ with a constant deformation in the range of linear viscoelasticity for each mixture, obtained from constant shear elastic modulus (G') in a strain sweep experiment at 1 Hz, always at 35°C. The curing was monitored at 90°C in order to determine the gel point and the conversion at gelation. Gel time was taken as the point where tan δ is independent of frequency.[32] The conversion at the gelation (x_{gel}) was determined by stopping the rheology experiment at gelation taking a sample and quenched in liquid nitrogen, and performing a subsequent dynamic DSC scan at 10 K/min of the gelled sample. The degree of conversion in the gelation point was calculated as follows:

$$x_{gel} = 1 - \frac{\Delta h_g}{\Delta h_T} \qquad (5)$$

where Δh_g is the heat released up of gelled samples, obtained by integration of the calorimetric signal, and Δh_T is the heat associated with the complete conversion of all reactive groups.

Adhesion test of the different mixtures on rectangular steel plates were done by tensile lap-shear strength of bonded assemblies' method by Houndsfield H10KS universal test machine with a 10kN load cell, following ASTM D 1002-10. At least, eight samples were tested for each mixture. The plate measures were 100 mm x 25 mm in plane and 1.5 mm in thickness. The overlap regions, 12.5 mm (± 0.25 mm) x 25 mm, were gently abraded with emery paper (320 grade) in two directions in 45 degrees to optimize the adhesion of the plates. The resin was cured in the oven for 3h at 170°C, followed by a post curing of 3h at 200°C. The apparent lap-shear strength (τ) was calculated following:

$$\tau = \frac{P}{A} \qquad (6)$$

where P the maximum load until fracture and A the overlapping area.

Thermal conductivities were measured by a Transient Hot Bridge THB 100 from Linseis Messgeräte GmbH. The sensor was a HTP G 9161 with a 3 x 3 mm^2 of area. Two equal polished rectangular samples (15x12x2.2 mm^3) were placed in each one of the faces of the sensor. Due to the small size of sensor, side effect can be neglected. A measuring time of 100 s with a current of 10 mA was applied to each of the five measures done for different formulation.

Composites: Part A ***2017**, 103, 35-47*

Dielectric breakdown strength was measured using a Lamsa TD-51 alternating current dielectric strength tester, with a voltage supplied of 6.6 kV, 50 Hz transformer, according to ASTM D 149-09. Tests were made at room temperature with point/plane electrodes. The rate of voltage rising speed was 1 kV/s until breakdown. A minimum of 16 values were recorded for each specimen, discarding which ones flash over occur. Taking into account tabulated dielectric strength of epoxy resins (19.7 kV/mm) and BN (37.4 kV/mm)[33] and maximum voltage of tester, films of about 100-150 µm were prepared, by curing the composition between two Norton FEP Fluoropolymer films. Thickness measurements were made by a micrometer with rounded tips with a precision of ± 0.001 mm. Different results were obtained for each specimen and the data obtained may be represented by statistical distribution. Two-parameter Weibull distribution are used to obtain failure prediction response and reliability of the materials because of its advantages such as high accuracy of results even with few determinations and a confinable method to estimate useful life of materials. Distribution is written as:[34]

$$P = 1 - exp\left[(-E/E_0)^{\beta}\right] \qquad (7)$$

where *P* is the cumulative probability of electrical failure, *E* is the experimental breakdown strength, E_0 is the scale parameter, the characteristic breakdown strength at a cumulative failure probability of 63.2%, which is frequently used to compare different samples, and β is the shape parameter, inversely proportional to deviation of data. For failure probability, IEEE 930-2004 standard recommends a good, simple approximation:[35]

$$P_i = \frac{i-0.44}{n+0.25} \cdot 100\% \qquad (8)$$

where *i* is the i-th result when values of E are sorted in ascending order, and *n* the number of samples.

Volume resistivity of samples was measured on a Metrel MI 2077 TeraOhm 5 kV insulation tester at room temperature. Pieces of 2.2 x 12 x 17 mm^3 were essayed between stainless steel circular electrodes with an area of 19.655 mm^2 placed on both faces of samples. The applied voltage to the thermosetting composites were 5 kV for 1 min. Electrical resistivity (ρ) of uniform cross sectional materials can be determined by:

$$\rho = R\frac{A}{l} \qquad (9)$$

where *R* is the resistance measured by the apparatus, *A* and *l* the area and the thickness of sample.

3. Results and discussion

3.1. Optimization of the curing process of the neat and BN modified formulations

Initiators are important in curing processes since they have a catalytic effect and decrease the activation energies, accelerating the process. In cationic systems, not only

the cation plays a role, but also the anion can increase the reactivity of the system if it has a low nucleophilicity, minimizing or preventing the reaction of the cationic growing chain with the anionic species.

The cationic homopolymerization of epoxides initiated by benzylanilinium salts was firstly developed by Endo's group.[23,24,29] The catalyst N-(p-methoxybenzyl)-N,N-dimethylanilinium hexafluoroantimonate has been selected for the present study and is commercialized as CXC 1612. The structure of this compound was determined by NMR spectroscopy and the spectra and the thermal behaviour fit well with the data reported.[23,24] It was also demonstrated by the same authors, that on heating, benzyl cations are released, which are the true catalytic species that initiate the attack to the oxiranic oxygen. As anion, hexafluoroantimoniate compensate the positive charge and has a very low nucleophilicity, which is required to avoid termination of epoxy homopolymerization.

Cationic epoxide homopolymerization follows two different mechanisms, known as AM (activated monomer) and ACE (active chain end). Both mechanisms are depicted in **Scheme 1**. AM mechanism is favoured in the presence of OH groups.[36,37]

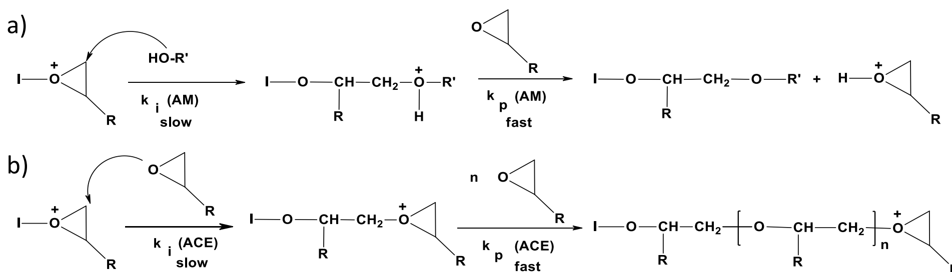

Scheme 1. Activated monomer mechanism (a) and active chain end mechanism (b).

Both processes compete and in some cases they were detected by calorimetric scans.[38,39] The proportion of hydroxyl groups can influence the global propagation rate. In addition to the initiation and chain growing, inter and intramolecular transfer processes can occur besides to termination reactions. This is due to the fact that this epoxide ring-opening mechanism follows a chain-wise polymerization pattern. Therefore, the kinetics of the cationic curing should be studied from the process as a whole. As the first step of the work, the optimization of the composition of the neat formulation (without BN) was performed be means of DSC studies (kinetics of curing) and other techniques like DMTA and TGA, to reach the most adequate characteristics of the final material. First, we studied the evolution of the curing process by varying the proportion of initiator (from 1 to 4 phr) by means of calorimetric studies. **Figure 1A** shows the DSC curves corresponding to this process.

We can see in the figure that the curing process starts at slightly lower temperatures with the increasing proportion of initiator, although the difference is

Composites: Part A ***2017***, *103, 35-47*

scarce from 3 to 4 phr of catalyst. However, a little difference in the shape of the curves is noticeable on varying the proportion of initiator. The highest peak at lower temperature has a complex shape that can be attributed to the coexistence of AM and ACE mechanisms that occurs overlapped giving rise to a certain splitting in the exotherm. As the process AM is faster,[40] it is assumed that the first peak is due to this mechanism.[21,37,38] Also, a shoulder after the maximum can be observed, decreasing when the proportion of initiator increases. These shoulders are sometimes due to phenomenological issues like vitrification or to thermal epoxy homolymerization. **Table 1** shows the most important data extracted from the calorimetric analysis.

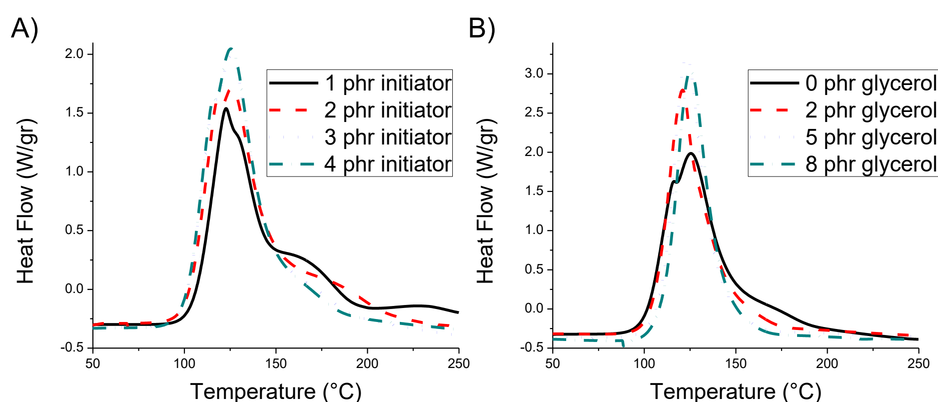

Figure 1. DSC curves showing the effect of the different proportions of initiator (A) and adding different proportions of glycerol (B) in the curing process.

Table 1. Calorimetric data of formulations of DGEBA with several proportions of initiator and glycerol.

Initiator (phr)	**Glycerol** (phr)	T_{max}[a] (°C)	**Δh**[b] (J/g)	**Δh**[b] (kJ/ee)	**Tg**[c] (°C)
1	0	122	381	71	121
2	0	125	502	95	152
3	0	124	531	102	135
4	0	125	523	103	131
3	2	120	504	99	129
3	5	122	481	97	122
3	8	124	483	100	120

[a] Temperature of the maximum of the curing exotherm.
[b] Enthalpy of the curing process by gram of mixture or by epoxy equivalent.
[c] Glass transition temperature determined by DSC in a second scan after a dynamic curing.

One of the most important calorimetric parameters is the heat evolved during the curing process, which can be expressed by gram or by epoxy equivalent. If we look to the heat released by epoxy equivalent we can evaluate if the curing has been completed. It is reported that the enthalpy evolved by epoxy equivalent in a complete curing is about 100 kJ/ee,[41] and in principle, the maximum heat evolved the higher crosslinking degree reached. From the values of the table we can go to the conclusion that 3 phr of initiator is the best proportion to reach the curing with a quite good T_g

value and a simple shape of the curve without any shoulder at high temperature that usually leads to increase unnecessarily the curing time or temperature.

As we have introduced above, AM mechanism is favoured by the presence of hydroxyl groups and this mechanism is faster than ACE.[38] In order to facilitate the curing, we added small proportions of glycerol, which is a trifunctional alcohol that does not produce any reduction of the crosslinking density, as occurs in compounds with an only hydroxyl group.

As we can see in **Figure 1B**, the addition of a little amount of glycerol leads to a simplification of the curve, which turns unimodal. It is also noticeable than the temperature of the maximum of the peak is maintained but the curing rate is increased according to a higher contribution of the AM mechanism on adding hydroxyl groups.[42] Also, the shoulder at higher temperature tends to disappear. Table 1 shows the most significant data extracted from DSC curves.

The addition of glycerol to the reactive mixture does not affect negatively the evolution of the curing or the enthalpy released but it can influence the network structure and therefore thermomechanical and thermostability should be evaluated. By looking to the values in the table, we can see that there is a difference in the glass transition temperature reached in the cured material. The higher the proportion of glycerol in the formulation the lower the Tg. This can be explained by the contribution of two different factors: the flexible structure of the glycerol and that AM mechanism, which leads to chain transfer processes, which limits the growing of the chain, reducing the crosslinking degree. The stability to high temperature of these materials was evaluated by thermogravimetry. **Table 2** collects the most representative data extracted by TGA.

Table 2. Thermogravimetric and thermomechanical data on varying the glycerol proportion in DGEBA formulations with 3 phr of initiator.

Glycerol (phr)	$T_{2\%}$[a] (°C)	T_{max}[b] (°C)	**Char yield**[c] (%)	**Young's modulus**[d] (GPa)	$T_{\tan\delta}$[e] (°C)	**E'**[f] (MPa)
0	306	432	14.1	2.0	147	50
2	310	433	13.4	2.3	138	44
5	300	432	11.2	2.4	122	25
8	154	432	9.2	-[g]	-[g]	-[g]

[a] Temperature of decomposition in TGA calculated for a 2% of weight loss.
[b] Temperature of the maximum decomposition rate determined by TGA in N_2 at 10°C/min.
[c] Char residue at 600°C.
[d] Young's modulus determined by DMTA at 35°C by the three point bending mode
[e] Temperature of maximum of the tan δ at 1 Hz.
[f] Relaxed modulus determined at the $T_{\tan\delta}$ + 40°C (in the rubber state).
[g] Not determined.

Composites: Part A ***2017***, *103, 35-47*

As can be seen in the table, the sample with 8 phr of glycerol presents an initial weight loss at low temperature and a lower char yield that could be attributed to the fact that not all the glycerol molecules have been chemically incorporated to the network. In fact, exudation phenomena was observed in samples containing 8 phr of glycerol during storage, which confirms that some proportion of glycerol remained unreacted in the cured material. According to that, this formulation has not been further tested.

Then, DMTA analyses were carried out. The increase of glycerol proportion provides an enhancement of Young modulus. The increase is higher on adding little proportions of glycerol (2 phr) and then a minor effect is observed on adding 5 phr. However, temperature of the α relaxation and modulus in the rubbery state decrease, especially when 5 phr of glycerol was in the formulation. By taking into consideration all these data and the reactivity observed by DSC we selected as the most adequate formulation for the base material, the one constituted by 3 phr of cationic initiator and 2 phr of glycerol as additive of DGEBA resin that meets the best compromise. It should be commented that this formulation keeps its latent characteristics, since the storage at room temperature for three months leads only to a slight decrease of a 1% in the heat evolved during curing.

Once selected the base epoxy formulation, different proportions of BN were added with the aim to enhance thermoconductivity and the effect in several characteristics in the final thermosets. The proportion of BN in these DGEBA formulations is limited to the 20% in weight, since higher amounts of this filler rends too high viscosity to the formulation and big difficulties to reach homogeneous mixtures, without use of solvents. The different formulations prepared were analysed by calorimetry to investigate their reactivity on curing and the calorimetric curves are represented in **Figure 2**.

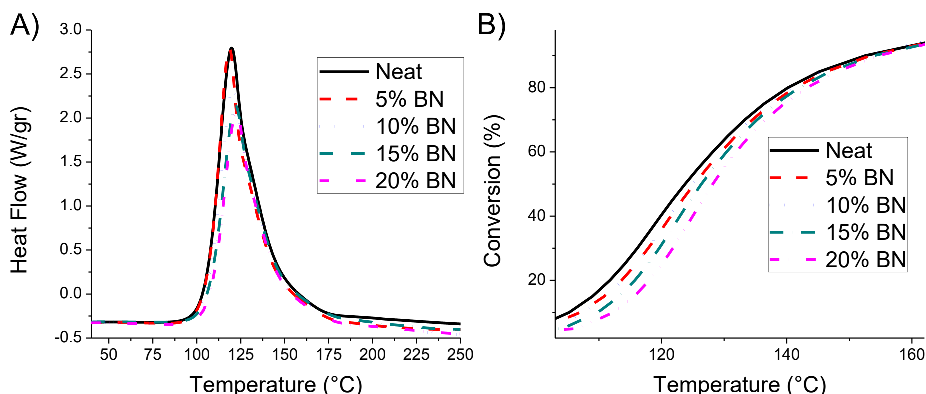

Figure 2. (A) DSC curves showing the effect of the addition of different proportions of BN to the neat formulation and (B) plot of conversion against temperature at 10 °C/min.

In the figure we can observe a slight shift of the exotherms at higher temperatures on increasing the proportion of filler in the formulation and also a decrease in the height of these curves, both indicating a reduction in the reactivity. The fact that the shape of the curves is similar and all formulations begin the curing at the same temperature confirms that the latency is kept unaltered. It is worth noting, that in the plots of conversion against temperature the bigger differences in reactivity appear at low temperatures and are proportional to the amount of BN in the formulation. From these results, it can be stated that BN does not participate in the homopolymerization mechanism due to its inert character and does not affect the active cationic species. However, the reduction expected by the dilution of epoxide groups or the hindrance produced by the BN particles have been detected. It should be noted that in BN sheets, the basal plane is molecularly smooth and has no surface functional groups available for chemical bonding or interaction. Only the edge planes of the BN platelets do have functional groups such as hydroxyl groups (-OH) and amino groups ($-NH_2$).[43] OH groups, although scarce, could participate in the AM mechanism producing not only a little effect on the kinetics, but also helping to form some covalent bonds between the BN particles and the epoxy matrix.[44] Amino groups can also help to increase the BN-epoxy interactions. The most representative data extracted from the calorimetric study are collected in **Table 3**.

Table 3. Calorimetric data on varying the BN proportion in DGEBA formulation with 3 phr of initiator and 2 phr of glycerol

% BN	T_{max} [a] (°C)	Δh [b] (J/g)	Δh [b] (kJ/ee)	T_g [c] (°C)	E_a [d] (kJ/mol)	ln A [e] (min^{-1})	$k_{120°}$ [f] (min^{-1})
0	120	504	99	129	127.1	38.4	0.65
5	119	469	97	129	144.0	43.6	0.61
10	121	459	100	129	135.7	40.9	0.56
15	122	420	97	130	122.3	36.7	0.47
20	123	394	97	130	121.1	36.2	0.42

[a] Temperature of the maximum of the curing exotherm.
[b] Enthalpy of the curing process by gram of mixture or by epoxy equivalent.
[c] Glass transition temperature determined by DSC in a second scan after a dynamic curing.
[d] Activation energy at 0.5 of conversion evaluated by isoconversional non-isothermal integral procedure KAS.
[e] Values of pre-exponential factor at 0.5 of conversion for second order (n=2) kinetic model with $g(\alpha)=-1+(1-\alpha)^{-1}$.
[f] Rate constant at 0.5 of conversion determined by using Arrhenius equation.

The data do not show any significant difference in the heat evolved by epoxy equivalent, which indicates that the curing is completed even in formulations with high proportions of BN. However, the heat evolved by gram of mixture is decreasing, because of the lower proportions of epoxide on increasing the filler percentage. The differences in the T_g are not relevant, which seems to support that the type of network formed

remains unaltered and that the balance between AM and ACE mechanism does not change by the addition of BN to the formulation.

By KAS isoconversional kinetic analysis, it was observed that the activation energy barely changes with the conversion (results do not show). This result confirms that the kinetic reaction mechanism is constant during curing and suggests that the kinetic model can be determined by Coats Redfern procedure. Using this methodology it was determined that all formulations follow a second order kinetic model with $n = 2$, as it is expected for cationic epoxy homopolymerization. Table 3 shows, as an example, the kinetic parameters for all formulations at conversion of 0.5. Activation energies and pre-exponential factor varies in a non-regular trend on increasing the proportion of BN in the formulation. In many reaction processes the variations in activation energy do not actually reflect kinetic changes, due to the compensation effect between the activation energy and the pre-exponential factor.[45] The value of the rate constant is a better reflection of the actual kinetic changes, since it includes both the effect of the activation energy and the pre-exponential factor. It can be observed as the rate constant is reduced on increasing BN content (Table 3), according to the retarding effect exerted of BN and in agreement with the calorimetric data (Fig. 2B). This behaviour can be attributed to the increased viscosity of the formulation and to the dilution effect of BN.

3.2. Rheological study of the BN formulations

Rheological analysis can provide insights into the evolution of the structure of BN networks, interactions between BN and polymer chains, and the dispersion of BN sheets in the matrix. This type of mixtures have complex rheological properties and depend on many factors such as particle size, particle shape, volume fraction of filler and the applied shear rate. In the same way the interactions particle-particle and particle-matrix play an important role.[46,47] Accurate measurements of viscosity are absolutely necessary for understanding these interactions, control and optimize process conditions and product performance and computer simulations.[48] Thus, the formulations with different amounts of BN were investigated by this technique.

The first point to consider is the Newtonian behaviour of the unfilled resin (**Figure 3**). The experimental data exhibited some usual properties of suspensions of particles in Newtonian fluids: unbounded viscosities at low shear rates (yield stress), strain dependent properties and shear thinning.[47] These effects are the results of the changes in the structure generated by particle interactions causing redistribution of particles and their orientations. The flow study showed that with the increasing of BN particles, as found by Han and Lem with different fillers,[49] the viscosity is raised more than two orders of magnitude and the degree of shear thinning at low shear rates was highly increased, as it is shown in **Figure 3**.

This effect is accompanied with a Newtonian asymptote at high shear rates. This observation is in accordance with previous results in the field of layered silicate-polymer

systems.[50] This rheological behaviour is determined by the balance of hydrodynamic force, that tend to align the major axis with the flow, and rotary Brownian motion (non-hydrodynamic forces) that tends to randomize the orientation. Brownian motion are negligible for the shape, distance between particles and dimensions (>1µm) of BN particles in more concentrated blends (yield stress and shear thinning),[51] which explain the diminution of η when the shear rate is increased. In the neat solution (Newtonian behaviour) and 5 wt. % of BN concentration (pseudoplastic) Brownian diffusion predominates and then the dispersion may be considered dilute.

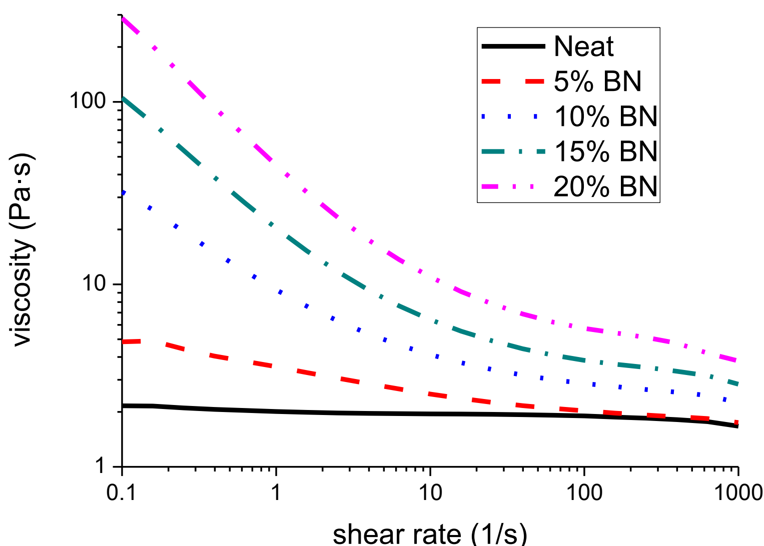

Figure 3. Plot of log η *versus* log v for the different formulations at 35°C from 0.1 to 1000 s^{-1}.

Oscillatory experiments were performed to determine the viscoelastic response of material. It is known that complex viscosity (η*) and the dynamic storage modulus (*G'*) are extremely sensitive to the microstructure variation of filler reinforced polymer mixtures. The Newtonian behaviour is practically kept constant in all the range of strain studied for the base formulation. However, this range becomes shorter and goes to lower strains on increasing the filler content in the strain sweep experiments, where the frequency is fixed (1 Hz) (see **Figure 4A**). The linear viscoelastic region, where the G' are independent of the applied strain, found a critical strain above which the structure starts to breakdown earlier when the amount of filler is raising.[52] Then, the strain was fixed in the linear region for each mixture to perform the oscillatory sweep tests, measuring parameters as function of frequency. As in η plot, η* showed analogous behaviour finding significant change between composites with BN concentration below 5 wt. % and above, nearly Newtonian plateau and shear thinning, respectively, in all the frequency range tested (**Figure 4B**), but more pronounced at low frequencies.

This behaviour is due to the increase in G' and loss modulus (G'') and can be ascribed to the alignment of the particles and their interactions when a stress is applied.

It is interesting to note the small increase in viscosity of the unfilled and low filled compositions when frequency exceeded certain critical value. This apparent increase is associated with the entrance of turbulent regime, but does not mean that viscosity increases, indicates that the degree of turbulence grows.[51] G' (elastic property) and loss G'' (viscous property) curves as a function of frequency of all the formulations are represented in **Figure 5**.

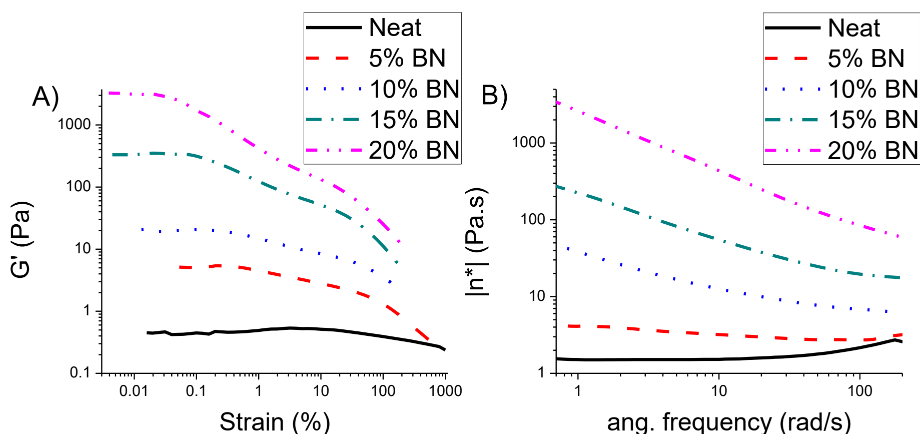

Figure 4. (A) Plot of log G' *versus* log % strain in oscillatory experiments (1 Hz). (B) Plot of log η* *versus* log ω, both at 35°C for all the formulations.

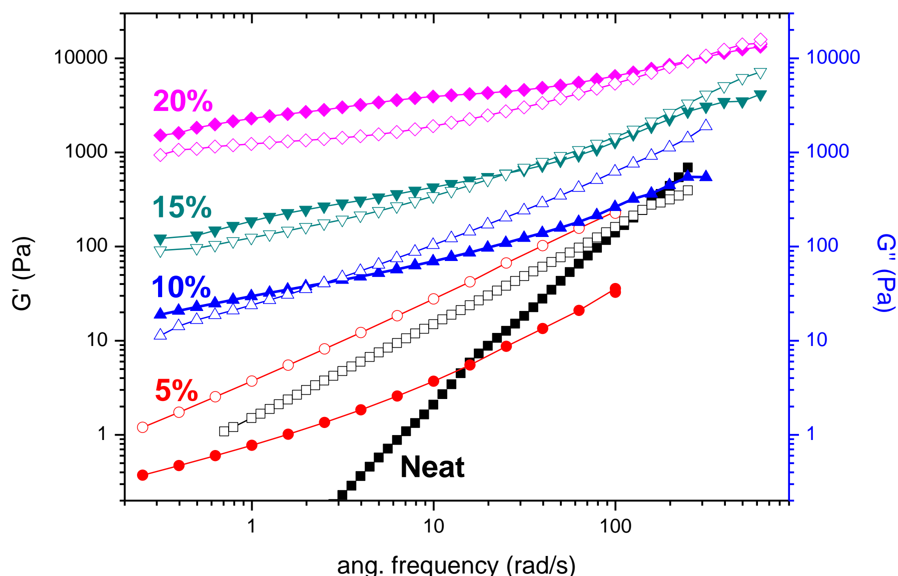

Figure 5. Plots of G' (filled symbols) and G'' (open symbols) against ω of formulations at 35°C.

How is expected, unfilled resin greatly follows the linear rheological theory (G' ∝ ω^2 and G'' ∝ ω^1) at low frequency. Nevertheless, the slopes decrease monotonically with

increasing BN content. When the concentration exceeds 5 wt. % there is a sharp falling in the slope at low angular frequency, indicating a significant variation of the microstructure of composites. G' is observed to be almost independent of the frequency when the filler loading is above that concentration. Also, the change in the liquid like behavior (G' < G'') to solid like (G' > G'') is observed. This change in G' at about 10 wt. %, with a kind of plateau at low frequency, means that composites have reached a rheological percolation. Near the percolation threshold, theory predicts a power law relation that can be used (adapting to mass fraction instead of volume fraction)[53,54] at fixed frequency to determine the threshold of the rheological percolation.[55,56]

$$G' \propto (m - m_c)^{\beta} \quad (10)$$

where G' is the storage modulus, m is the mass fraction of BN composites, m_c is the mass fraction at rheological percolation and β is the critical exponent. This relation is often valid only on a very narrow concentration region.[48] The rheological percolation at 1 rad/s and 10 rad/s was calculated to be 6.9 wt. % and the critical exponent 1.9.

Gelation is an irreversible phenomenon taking place during curing and processing of epoxy formulations that corresponds to the point at which the initial network is formed. Then, the gel fraction extends and increases crosslinking as the curing advances leading to an insoluble and three-dimensional network at the end of the curing process. Macroscopically, there is an abrupt change from a liquid-like to a solid-like behaviour and the viscosity tends to infinite. The material ceases to flow and starts to build up mechanical properties.[32] The knowledge of the conversion and gelation time is of capital importance from the industrial processing point of view that takes into account temperature, time and the minimum viscosity for injection or transfer moulding for computer chip packaging systems. Whereas, the prediction of the conversion at the gelation in polycondensation processes is quite easy by applying the Flory equation,[57] in chain-wise polymerization the conversion at the gelation depends in a complex way on the relative rate of initiation, propagation and termination and also on the amount of initiator. Increasing the initiator concentration results in shorter primary chains and a corresponding increase in the gel conversion, similarly occurs when increasing amounts of hydroxylic compounds are added to the formulation.[21] Since, ring-opening polymerization results from an initiation step starting at different times and positions in the curing mixture, the process is not as homogenous as in polycondensation mechanisms and inhomogeneities, called microgels, appear in the reactive mixture, leading sometimes to gelation at lower conversion than expected.[58]

The addition of BN to the formulation can influence both gel time and conversion at the gelation and the values obtained experimentally are collected in **Table 4**.

From the results obtained, it can be observed that there is a tendency to the reduction of the gel time on increasing BN concentration. The same behaviour was established by several authors when examined an epoxy resin system with silica

filler.[59,60] Moreover, the conversion at the gelation diminishes on increasing the proportion of BN in the formulation. The decrease in the gelation time with increased filler concentration can be related to the fact that the conversion at gelation has decreased by the effect of the BN particles. This decrease could be related to the reaction of -OH and $–NH_2$ groups at the edge of the BN platelets, which can reduce the primary chain length.

Table 4. Gelation data from rheometric monitoring of the curing of the formulations at 90°C.

% BN	t_{gel}[a] (min)	X_{gel}[b] (%)
0	11.0	34
5	10.0	30
10	10.0	30
15	9.5	25
20	8.0	23

[a] Gel time determined from the frequency independent crossover of tan δ.
[b] Determined as the conversion reached by rheometry and DSC test at 10°C/min.

3.3. Thermal characterization of the BN-composites

The addition of inorganic fillers, like BN, can modify the thermal behaviour of the polymeric matrix. Therefore, the thermal stability and the thermomechanical characteristics of the new BN composites were evaluated by TGA and DMTA. The most characteristic data obtained by TGA are collected in **Table 5**.

Table 5. Thermogravimetric data for the thermosets prepared by varying the concentration of BN.

% BN	$T_{5\%}$[a] (°C)	T_{max}[a] (°C)	Char Yield[b] (%)	$T_{5\%}$[c] (°C)	T_{max}[c] (°C)	Char Yield[d] (%)
0	390	433	13.4	343	429	0.0
5	393	434	18.1	368	429	4.9
10	392	433	23.1	369	428	10.4
15	394	433	28.1	373	429	15.1
20	393	432	32.6	379	430	20.0

[a] Temperatures of 5% weight loss and maximum decomposition rate determined by TGA in N_2 at 10°C/min.
[b] Char residue at 600°C (in N_2).
[c] Temperatures of 5% weight loss and the maximum decomposition rate determined by TGA in air at 10°C/min.
[d] Char residue at 800°C (in air).

From the TGA it can be confirmed that composites show the same degradation pattern that the neat epoxy matrix, indicating that the addition of BN does not affect the degradation mechanism. From the data in the table, it can be seen that the initial

degradation temperature and the temperature of maximum degradation rate are not affected by BN and the biggest difference is shown in the residues after heating at high temperature in inert or oxidizing atmosphere, as expected. The char residue at 800°C in air atmosphere agrees with the percentage of BN in the material. The char yield in nitrogen atmosphere is higher on increasing the BN % due to the formation of carbonaceous residues on the BN filler particles. It is reported a slight increase in thermal stability on increasing the proportion of filler in epoxy-BN composites,[14] but this behaviour was not observed in the composites prepared.

By thermomechanical tests the effect of the presence of BN in the cured materials was observed. Although it was not the aim of the present study, by increasing the BN proportion in the material a notable enhancement of thermomechanical behaviour was proved. **Table 6** collects the values obtained by DTMA of all the composites and the neat material for comparison purposes. **Figure 6** represents the variation of storage modulus and tan δ against temperature for all these materials.

Table 6. Thermomechanical data of composites prepared varying BN concentration.

% BN	Young's Modulus[a] (GPa)	T tan δ[b] (°C)	E'[c] (MPa)	CTE_{glass}[d] ($10^{-6}\cdot K^{-1}$)	CTE_{rubber}[e] ($10^{-6}\cdot K^{-1}$)
0	2.3	138	44	75	183
5	2.6	144	79	73	175
10	2.8	144	95	69	180
15	3.2	145	115	66	179
20	3.5	145	148	58	177

[a] Young's modulus determined with DMTA at 35°C in a controlled force experiment using a three point bending clamp.
[b] Temperature of maximum of the tan δ at 1 Hz.
[c] Relaxed modulus determined at the $T_{\tan\delta}$ + 40°C (in the rubbery state).
[d] Thermal expansion coefficient of glassy state determined between 50-75°C.
[e] Thermal expansion coefficient in the rubber state determined between 170-190°C.

As we can see in the table, Young's modulus increases steadily on increasing the % of BN, which is more than a 50% in the sample with 20 wt. % of BN. It is also noticeable that the storage modulus in the rubbery state goes from 44 to 148 MPa, which is a consequence of the reinforcement produced by the filler. Unlike calorimetric study, by DTMA it was observed that on adding BN to the formulation, the composites showed an increase in the T_g of 6-7 °C, although the final T_g was independent from the thermoset composition. The different evolution of the T_g value by DSC and DMTA can be attributed to the physical basis of both measurements. By calorimetry, only changes in the calorific capacity of the polymeric matrix can be detected while in DMTA, the mechanical effects of the filler in the relaxation phenomena of the polymer matrix can affect T_g values. In a

previous study on DGEBA/BN composites,[14] T_g determined by DMTA was increased in 4-5 °C. The authors attributed this enhancement in the relaxation temperature to the surface functionalization of BN particles made by sol-gel with a reactive amine that increases the interaction filler-matrix. However, similar enhancements were obtained in the present work without any surface modification. Thus, from our results, we can state that a restriction of the chain motions for the presence of BN particles and a certain reaction of groups at the edge of the platelets together with some interface affinity between BN surface and epoxy matrix are the responsible for the improvement of temperature of the α relaxation.

Figure 6A shows in the DMTA curves a steadily increase on storage modulus on increasing the % BN in the material, which affects the vitreous and rubbery state, and a unimodal shape of tan δ curve, which indicates that a homogeneous material is formed even in case of high BN percentages.

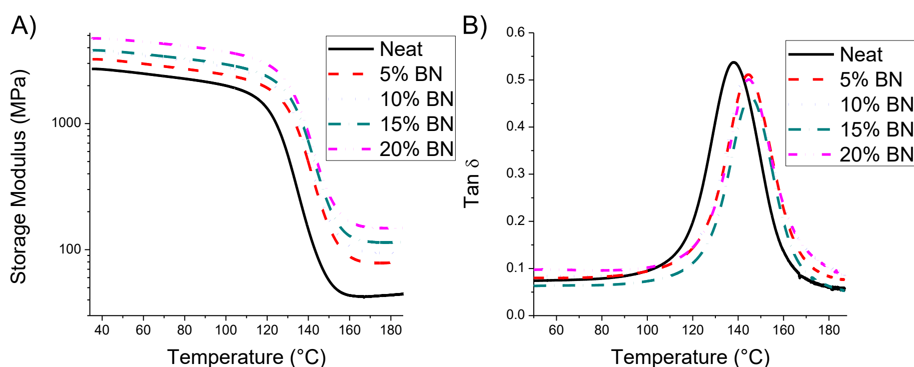

Figure 6. Variation of A) storage modulus and B) tan δ against temperature of the different materials prepared.

Dimensional stability is an important consideration for epoxy materials used in many demanding areas, especially for electrical and electronic applications. Table 6 shows the CTE of the thermosets with different BN contents in the range below and above T_g measured by TMA. As expected, the introduction of the ceramic filler produces a decrease in the CTE. The difference is more remarkable in the vitreous state, which will be the work temperature. This suggests that the mechanical interlock at the organic-inorganic interface may constrain the CTE mismatch of the components.[61] This behaviour, as with the *E* modulus, will be beneficial in the use of these materials as adhesives or encapsulants in printed circuit boards. The more similar will be the properties of composite and metallic substrate, the minimum internal stress and crack will be produced by the temperature fluctuation, ensuring reliability of electronic devices when they run.

3.4. Mechanical characterization and dielectric properties of BN-composites

One of the most important shortcomings of epoxy thermosets is their fragile characteristics, due to the high crosslinking density and therefore, some toughness agents are added to the formulation to improve impact resistance. However, most of these agents decrease the T_g and other thermomechanical properties, reducing the materials performance. In the present work, the addition of a little proportion of glycerol aims to introduce some more flexibility to the network structure and the addition of BN as the filler can also improve toughness by changing the fracture mechanism, especially if some interactions between particles and matrix exist. Toughness characteristics were evaluated by impact test. **Table 7** shows the values of impact strength for all the materials prepared. It can be seen, that the addition of BN leads to an improvement of the neat material in about a 75%, which is quite high. However, on increasing the proportion of BN in the material the increase produced is only slight.

Table 7. Mechanical and dielectric properties of the composites

% BN	Impact strength (kJ/m^2)	KHN[a]	τ^b (MPa)	E_0^c (kV/mm)	β (shape parameter)	Resistivity (Ω·m·10^9)
0	1.45 ± 0.15	21.91 ± 0.44	15.88 ± 1.51	30.8	7.2	5.4
5	2.31 ± 0.25	23.53 ± 0.63	14.99 ±0 .96	35.6	5.8	5.6
10	2.41 ± 0.10	27.93 ± 1.37	15.86 ± 0.56	38.7	6.5	5.8
15	2.51 ± 0.27	25.73 ± 0.87	14.90 ± 0.81	41.9	5.7	6.0
20	2.54 ± 0.25	25.19 ± 0.89	12.83 ± 0.86	42.8	8.7	7.6

[a] Knoop microindentation hardness.
[b] Apparent lap-shear strength.
[c] Scale parameter of Weibull distribution, the dielectric breakdown strength.

The fracture surfaces were examined by ESEM microscopy and **Figure 7** shows their appearance.

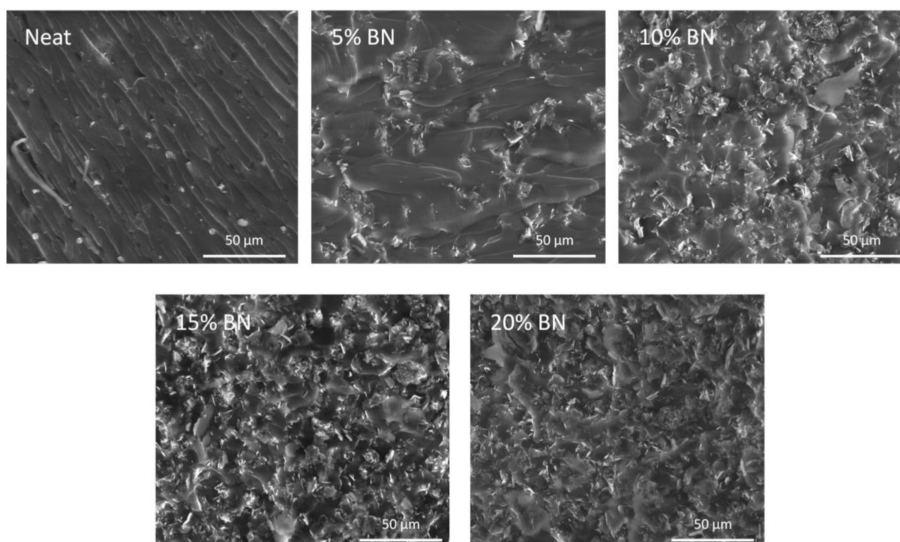

Figure 7. ESEM micrographs for the fracture surfaces of the materials prepared on varying the BN content at 800 magnifications.

It is worth to note the great difference between the micrograph of the neat and of the filled materials. When increasing the filler proportion, the roads of breakage appear shorter and less straight, which explains the increase in the impact strength by having to start new paths of brakeage. Likewise, it can be observed the homogeneity of the materials. There is also a great difference between the samples with 5 and 10% of BN. Whereas in the case of 5% sample, the BN particles are completely isolated and surrounded by the polymeric matrix, in the sample with 10% the particles are close to each other because of the percolation produced at filler contents in between (6.9%).

Microindentation hardness measurements rate the resistance of the material against penetration by static load. This parameter is of interest in the coatings industry. The results obtained using a Knoop microindenter are collected in table 7. As it can be seen, there is a slight tendency to increase hardness on increasing the proportion of BN in the material but it does not follow a linear increase but reach a maximum at 10% of filler added. In any case, BN does not worst but even improve this characteristic.

Adhesion is a complex property that depends on different factors, which include properties of the coating (viscosity, surface energy, etc.), substrate properties (roughness, surface energy, etc.), interfacial properties (internal stress, wettability, etc.) and environmental conditions (humidity, temperature, etc.). Also, differences in thermal expansion coefficients between substrate and coating lead to the reduction of adhesion, especially for epoxy coatings cured at high temperature, since the final decrease of temperature after curing creates internal stresses that leads to the production of microcracks, warping, etc. Internal stress generated during cooling increases proportionally to the differences between T_g and curing temperature.[62] Table 7 shows the apparent shear strength values on steel surfaces for the different materials prepared with different BN content. As we can see, the neat material presents a good adhesion to the metal. This value, in general, does not experiment great changes on adding BN to the formulation, but the addition of a 20% of BN leads to a reduction in a 20% of this value. Taking into account that CTE decreases on increasing BN content (see Table 6), the slight reduction of lap-shear strength observed in table 7 could be related with the lower adhesion of BN particles to the metal than epoxy matrix.

Dielectric breakdown strength measurements were performed to determine the highest voltage which samples can stand before they fail electrically, divided by sample thickness. Weibull plots are presented in **Figure 8**. The addition of BN presented a clear trend to enhance electrical breakdown strength (E_0), also presented in table 7, in increasing the order of filled composites (5 to 20 wt. %). Relative small shape parameters are attributed to imperfections such as imperceptible bubbles, microcracks or tiny fissures created during curing of the thin films.

Despite the fact that the introduction of defects can reduce the electric resistance, the addition of BN particles show a favorable behavior on growing their proportion. The increasing trend observed is according to previous published results.[13,63]

The same pattern was observed in the electrical resistivity of the composites (see table 7). This is the intrinsic property of materials that quantify the opposition to the current flow, another important property in the thermal management in electronic packaging giving them security and stability to the electronic components. Voltage of 5 kV was applied to obtain the best determinations according to the capacity of the tester. As can be seen in the table the resistivity increases with the amount of BN in the material, although slightly. However, when the material contained a 20% of BN this parameter increases notably, reaching an increase of 40% in reference to the neat material. Both dielectric strength and electrical resistivity confirm the tendency that increasing the amount of BN particles, dielectric properties improve, because of the intrinsic properties of boron nitride.

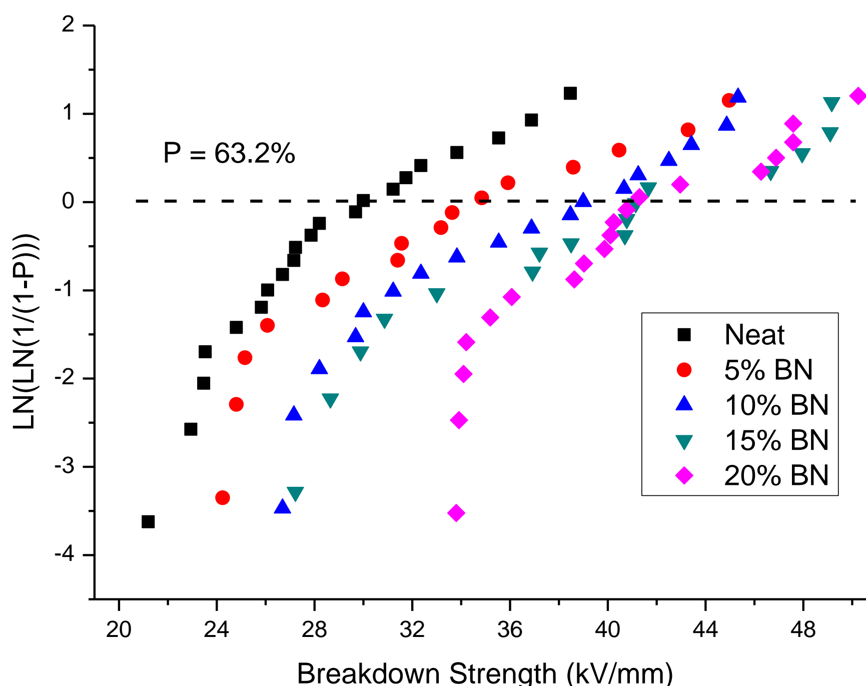

Figure 8. Weibull plots of breakdown strength for neat epoxy and the composites.

3.5. Thermal conductivity

Figure 9 shows the variation of thermal conductivity with the filler content for BN resins. In general, the thermal conductivities of BN filled epoxy resins are enhanced with the increase of filler content. Although, h-BN has a high thermal conductivity (390 W/m·K in basal plane direction; and 2 W/m·K in the c-axis),[64] only limited amount of it is shared by the composite due to the presence of epoxy (k=0.2 W/m·K) used as the matrix. The thermal conductivity of the composites prepared in the present work improved linearly with the concentration of BN added getting a maximum of 0.61 W/m·K

Composites: Part A ***2017**, 103, 35-47*

with the maximum concentration, 20% wt. (13.4 % in volume fraction). This constitutes an enhancement of more than 300% in reference to the neat epoxy.

The thermal conductivity achieved an increase of 300% with the only addition of 20 wt% of BN to the formulation. If we compare the maximum conductivity achieved (with 13.4% of BN in volume) with other authors[14,63] we find equal or even better thermal transport characteristics. These authors stated that there was a great increasing when the addition of filler exceeded 20% in volume, which could not be accomplished in the present case because of the loss of homogeneity in the preparation of the mixtures, due to the high viscosity of the formulation. Taking into account the improvement of thermal conductivity along with other thermal, mechanical and electrical characteristics, it can be confirmed that the compounds prepared in this study are excellent materials for thermal dissipation applications.

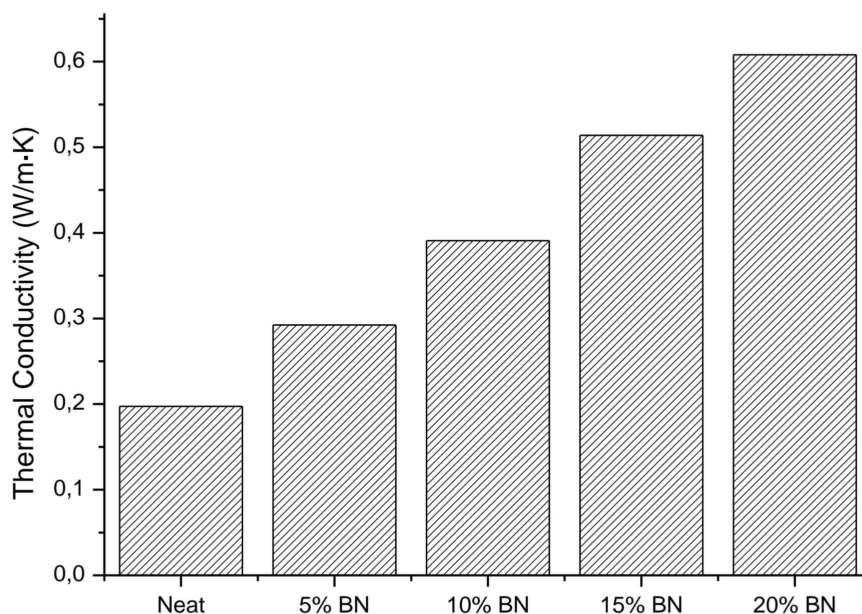

Figure 9. Thermal conductivity of the materials prepared on varying the BN content.

4. Conclusions

A new latent cationic curing system for diglycidylether of bisphenol A was optimized. The curing behavior was not highly influenced by the addition of BN particles and it keeps the latency for a period of three months. The viscosity of the formulation raised with the addition of BN, which can explain, along with the dilution effect exerted by BN, the curing retardation experimented at lower temperatures. Rheological studies allowed to determine that the Newtonian range became shorter and went to lower strains on increasing the filler content. The rheological percolation was calculated to be 6.9 wt. %.

On increasing the amount of BN in the formulation both the conversion at the gelation and the gelation time are reduced which seems to be related to the presence of OH and NH_2 groups in the BN structures which can reduce the primary chain length.

Glass transition temperatures, determined by DSC, were unaltered on increasing the BN proportion in the material, but slightly increased the tan δ temperature, because of the mechanical effect of the particles on relaxation phenomena. Young modulus and rubbery modulus increased steadily on increasing the % of BN.

The introduction of the ceramic filler produced a decrease in the thermal expansion coefficient, more remarkable in the vitreous state.

Mechanical characteristics were maintained or even improved. The addition of BN led to an enhancement in impact strength up to 75% in reference to the neat material. This effect was also confirmed by the SEM inspection of the fracture surface. Microindentation hardness reach a maximum at 10% of filler added in reference to the neat thermoset. Adhesion did not experiment great changes on adding BN to the formulation, but the addition of a 20% of BN led to a reduction in a 20% of this value.

Thermal conductivity enhancements of more than 300% in reference to the neat epoxy was reached, which increased proportionally to the % BN content. Both dielectric strength and electrical resistivity confirm the tendency that increasing the amount of BN particles, dielectric properties improved, because of the intrinsic properties of boron nitride added to the formulation.

5. Acknowledgments

The authors would like to thank MINECO (MAT2014-53706-C03-01 and 02) and Generalitat de Catalunya (2014-SGR-67) for the financial support. We thank the support of Miguel Angel Acebo in performing calculations and John Hutchinson for helping us in thermal conductivity measurements. Gabriel Benmayor S.A. is acknowledge for giving us the BN used in this work.

6. References

[1] Thermal Conductivity: Theory, Properties, and Applications. Tritt TM, editor. Springer US, Kluver Academic/Plenum Press, New York, 2004.
[2] Burger N, Laachachi A, Ferriol M, Lutz M, Toniazzo V, Ruch D. Review of thermal conductivity in composites: Mechanisms, parameters and theory. Prog. Polym. Sci. 2016; 61: 1-28.
[3] Chen H, Ginzburg VV, Yang J, Yang Y, Liu W, Huang Y, Du L, Chen B. Thermal conductivity of polymer-based composites: Fundamentals and applications. Prog. Polym. Sci. 2016; 59: 41-85.
[4] Im H, Kim J. Thermal conductivity of a graphene oxide-carbon nanotube hybrid/epoxy composite. Carbon 2012; 50: 5429-5440.

[5] Huang X, Jiang P. A Review of dielectric polymer composites with high thermal conductivity. IEEE Electric. Insul. Mag. 2011; 27: 8-16.
[6] Donnay M, Tzavalas S, Logakis E. Boron nitride filled epoxy with improved thermal conductivity and dielectric breakdown strength. Compos Sci. Technol. 2015; 110: 152-158.
[7] Yung KC, Zhu BL, Yue TM, Xie CS. Development of epoxy-matrix composite with both high-thermal conductivity and low-dielectric constant via hybrid filler system. J. Appl. Polym. Sci. 2010; 116: 518-527.
[8] Thermosets: Structure, properties and applications. Guo Q, editor. Woodhead Publishing Limited, 2012, Cambridge.
[9] Mir I, Kumar D. Recent advances in isotropic conductive adhesives for electronics packaging applications. Int. J. Adhes. Adhes. 2008; 28: 362–371.
[10] Gu H, Ma C, Gu J, Guo J, Yan X, Huang J, Zhang Q, Guo Z. An overview of multifunctional epoxy nanocomposites. J. Mater. Chem. C. 2016; 4: 5890-5906.
[11] Rybak A, Gaska K. Functional composites with core-shell fillers: I. Particle synthesis and thermal conductivity measurements. J. Mat. Sci. 2015; 50: 7779-7789.
[12] Yang K, Gu M. Enhanced thermal conductivity of epoxy nanocomposites filled with hybrid filler system of triethylenetetramine-functionalized multi-walled carbon nanotubes/silane-modified nano-sized silicon carbide. Composites: Part A 2010; 41: 215-221.
[13] Yu J, Mo H, Jiang P. Polymer/boron nitride nanosheet composite with high thermal conductivity and sufficient dielectric strength. Polym. Adv. Technol. 2015; 26: 514-520.
[14] Hou J, Li G, Yang N, Qin L, Grami ME, Zhang Q, Wang N, Qu X. Preparation and characterization of surface modified boron nitride epoxy composites with enhanced thermal conductivity. RSC Advances 2014; 4: 44282-44290.
[15] Pu X, Zhang H-B, Li X, Gui C, Yu Z-Z. Thermally conductive and electrically insulating epoxy nanocomposites with silica-coated graphene. RSC Advances 2014; 4: 15297–15303.
[16] Song SH, Park KH, Kim BH, Choi YW, Jun GH, Lee DJ, Kong B-S, Paik K-W, Jeon S. Enhanced Thermal Conductivity of Epoxy–Graphene Composites by Using Non-Oxidized Graphene Flakes with Non-Covalent Functionalization. Adv. Mater. 2013; 25: 732–737.
[17] Chatterjee S, Wang JW, Kuo WS, Tai NH, Salzmann C, Li WL, Hollertz R, Nüesch FA, Chu BTT. Mechanical reinforcement and thermal conductivity in expanded graphene nanoplatelets reinforced epoxy composites. Chem. Phys. Lett. 2012; 531: 6–10.
[18] Pashayi K, Fard HR, Lai F, Iruvanti S, Plawsky J, Borca-Tasciuc T. High thermal conductivity epoxy-silver composites based on self-constructed nanostructured metallic networks. J. Appl. Phys. 2012; 111: 104310.
[19] Xu Y, Chung DDL, Mroz C. Thermally conducting aluminium nitride polymer-matrix composites. Composites: Part A. 2001; 32: 1749-1757.
[20] Wang Z, Iizuka T, Kozako M, Ohki Y, Tanaka T. Development of epoxy/BN composites with high thermal conductivity and sufficient dielectric breakdown strength. Part I-Sample preparations and thermal conductivity. IEEE Trans. Dielectr. Electr. Insul. 2011; 18: 1963-1972.
[21] Vidil T, Tournilhac F, Musso S, Robisson A, Leibler L. Control of reactions and network structures of epoxy thermosets. Prog. Polym. Sci. 2016; 62: 126–179.

[22] Epoxy Polymers: New Materials and Innovations, Pascault JP, Williams RJJ, editors. Wiley-VCH, Weinheim, 2010.
[23] Nakano S, Endo T. Cationic polymerization of glycidyl phenyl ether by benzylammonium salts. J. Polym. Sci.: Part A: Polym. Chem. 1995; 33: 505-512.
[24] Nakano S, Endo T. Thermal cationic curing by benzylpyridinium salts. Prog. Org. Coat. 1994; 23: 379-385.
[25] Park S-J, Heo G-Y, Suh D-H. Thermal properties and fracture toughness of epoxy resins cured by phosphonium and pyrazinium salts as latent cationic initiators. J. Polym. Sci.: Part A: Polym. Chem. 2003; 41: 2393-2403.
[26] Jang ES, Khan SB, Seo J, Akhtar K, Nam YN, Seo KW, Han H. Preparation of cationic latent initiators containing imidazole group and their effects on the properties of DGEBA epoxy resin. Macromol. Res. 2011; 19 (10): 989-997.
[27] Toneri T, Watanabe K, Sanda F, Endo T. Synthesis and the initiator activity of fluorenyltriphenylphosphonium salts in the cationic polymerization of epoxide. Novel thermally latent initiators. Macromolecules, 1999; 32: 1293-1296.
[28] Endo T, Sanda F. Design of latent catalysts and their application to polymer synthesis. Macromol. Symp., 1996; 107: 237-242.
[29] Nakano S, Endo T. Thermal cationic curing with benzylammonium salts-2. Prog. Org. Coat. 1996 28: 143-148.
[30] Coats AW, Redfern JP. Kinetic Parameters from Thermogravimetric Data. Nature 1964; 201: 68-69.
[31] Ramis X, Salla JM, Mas C, Mantecón A, Serra A, Kinetic Study by FTIR, TMA, and DSC of the Curing of a Mixture of DGEBA Resin and γ-Butyrolactone Catalyzed by Ytterbium Triflate, J. Appl. Polym. Sci. 2004; 92: 381-393.
[32] Thermosetting Polymers, Pascault JP, Sauterau H, Verdu J, Williams RJJ, editors. Marcel Dekker, New York, 2002.
[33] Shugg WT. Handbook of electrical and electronic insulating materials. Van Nostrand Reinhold, New York, 1986.
[34] Ueki MM, Zanin M. Influence of additives on the dielectric strength of high-density polyethylene. IEEE Transactions on Dielectrics and Electrical Insulation 1999; 6: 876-881.
[35] Ross R. Graphical methods for plotting and evaluating Weibull distribution data. Proc. IEEE. 1994; 1: 250-253.
[36] Kubisa P, Penczeck S, Cationic activated monomer polymerization of heterocyclic monomers. Prog. Polym. Sci. 1999; 24: 1409-1437.
[37] Matejka L, Chabanne P, Tighzert L, Pascault JP. Cationic polymerization of diglycidyl ether of bisphenol A. J. Polym. Sci. Part A: Polym. Chem. 1994; 32: 1447-1458.
[38] Salla JM, Fernández-Francos X, Ramis X, Mas C, Mantecón A, Serra A. Influence of the proportion of ytterbium triflate as initiator on the mechanism of copolymerization of DGEBA epoxy resin and ϒ-butyrolactone. J. Therm. Anal. Calorim. 2008; 91: 385-393.
[39] Arnebold A, Thiel K, Kentzinger E, Hartwig A. Morphological adjustment determines the properties of cationically polymerized epoxy resins. RSC Advances 2015; 54: 2482-42491.
[40] Biedron T, Szymanski R, Kubisa P, Penczek S, Kinetics of polymerization by activated monomer mechanism. Macromol. Chem. Macromol. Symp. 1990; 32: 155-168.
[41] Ivin KJ. Polymer Handbook. Brandrup J, Immergut EH, editors. Wiley, New York, 1975.

[42] Santiago D, Morell M, Fernández-Francos X, Serra A, Salla JM, Ramis X. Influence of the end groups of hyperbranched poly(glycidol) on the cationic curing and morphology of diglycidylether of bisfenol A thermosets. React. Funct. Polym. 2011; 71: 380–389.
[43] Yu J, Huang X, Wu C, Wu X, Wang G, Jiang P. Interfacial modification of boron nitride nanoplatelets for epoxy composites with improved thermal properties. Polymer 2012; 53: 471-480.
[44] Sato K, Horibe H, Shirai T, Hotta Y, Nakano H, Nagai H, Mitsuishi K, Watari K. Thermally conductive composite films of hexagonal boron nitride and polymide with affinity-enhanced interfaces. J. Mat. Chem. 2010; 20: 2749-2752.
[45] Vyazovkin S, Wight CA. Kinetic in Solids, Annu. Rev. Phys. Chem. 1997; 48: 125-149.
[46] Carreau PJ, De Kee DCR, Chhabra RP. Rheology of Polymeric Systems: Principles and Applications. Hanser Publishers, Munich, 1997.
[47] Han CD. Rheology and Processing of Polymeric Materials. Vol. 1. Oxford University Press, New York, 2007.
[48] Kamal MR, Mutel A. Rheological Properties of Suspensions in Newtonian and Non-Newtonian Fluids. J. Polym. Eng. 1985; 5: 293-382.
[49] Han C, Lem K. Rheology of unsaturated polyester resins. II. Thickening behavior of unsaturated polyester and vinyl ester resins. J. Appl. Polym. Sci. 1983; 28: 763-778.
[50] Ren J, Krishnamoorti R. Nonlinear Viscoelastic Properties of Layered-Silicate-Based Intercalated Nanocomposites. Macromolecules 2003; 36: 4443-4451.
[51] Macosko CW, RG Larson. Rheology: Principles, measurements, and applications. Wiley-VCH, New York, 1994.
[52] Tadros TF. Rheology of Dispersions: Principles and Applications. Wiley-VCH, Weinheim, 2010.
[53] Du F, Scogna RC, Zhou W, Brand S, Fisher JE, Winey KI. Nanotube Networks in Polymer Nanocomposites: Rheology and Electrical Conductivity. Macromolecules 2004; 37: 9048-9055.
[54] Hu G, Zhao C, Zhang S, Yang M, Wang Z. Low percolation thresholds of electrical conductivity and Rheology in poly(ethylene terephthalate) through the networks of multi-walled carbon nanotubes. Polymer 2006; 47: 480-488.
[55] De Gennes PG. Scaling theory of polymer adsorption. J. Phys. 1976; 37: 1445-1452.
[56] Feng S, Sen PN, Halperin BI, Lobb CJ. Percolation on two-dimensional elastic networks with rotationally invariant bond-bending forces. Phys. Rev. B. 1984; 30: 5386-5389.
[57] Flory PJ. Molecular size distribution in three dimensional polymers I. Gelation. J. Am. Chem. Soc. 1941; 63: 3083-3090.
[58] Dusek K, Duskova-Smrckova M, Network structure formation during crosslinking of organic coating systems. Prog. Polym. Sci. 2000; 25: 1215-1260.
[59] Ng H, Manas-Zloczower I. Chemorheology of unfilled and filled epoxy-resins. Polym. Eng. Sci. 1993; 33: 211-216.
[60] Becker O, Simon GP, Bailey RJ. Layered silicate nanocomposites based on various high functionality epoxy resins: The influence of an organoclay on resin cure. Polym. Eng. Sci. 2003; 43: 850-862.
[61] Yung C, Liem H. Enhanced thermal conductivity of boron nitride epoxy-matrix composite through multi-modal particle size mixing. J. Appl. Polym. Sci. 2007; 106: 3587-3591.

[62] Zhang Y. Adhesion of epoxy coatings to an alloy-coated steel sheet. Doctor of Philosophy Thesis. Department of Materials Engineering, University of Wollongong 1995 http:/ro.uow.edu.au/theses/1481. Access on March 23th 2017
[63] Fang L, Wu C, Quian R, Xie L, Yang K, Jiang P. Nano-micro structure of functionalized boron nitride and aluminium oxide for epoxy composites with enhanced thermal conductivity and breakdown strength. RSC Advances, 2014; 4: 21010-21017.
[64] Alam MT, Bresnehan MS, Robinson JA, Haque MA. Thermal conductivity of ultra-thin chemical vapor deposited hexagonal boron nitride films. Appl. Phys. Lett. 2014; 104: 13113-13118.

Chapter 4

New epoxy composite thermosets with enhanced thermal conductivity and high T_g obtained by cationic homopolymerization

Polymer Composites ***2018****, 39, 1760-1769*

New epoxy composite thermosets with enhanced thermal conductivity and high T_g obtained by cationic homopolymerization

Isaac Isarn[a], Francesco Gamardella[b], Lluís Massagués[c], Xavier Fernàndez-Francos[d], Àngels Serra[b], Francesc Ferrando[a]

a. Department of Mechanical Engineering, Universitat Rovira i Virgili, C/Av. Països Catalans, 26, 43007 Tarragona, Spain.
b. Department of Analytical and Organic Chemistry, Universitat Rovira i Virgili, C/Marcel·lí Domingo s/n, 43007 Tarragona, Spain.
c. Department of Electronic, Electric and Automatic Engineering, Universitat Rovira i Virgili, C/Av. Països Catalans, 26, 43007 Tarragona, Spain.
d. Thermodynamics Laboratory, ETSEIB, Universitat Politècnica de Catalunya, C/Av. Diagonal 647, 08028 Barcelona, Spain.

Abstract

Thermal dissipation is a critical aspect for the performance and lifetime of electronic devices. In this work, novel composites based on a cycloaliphatic epoxy matrix and BN fillers, obtained by cationic curing of mixtures of 3,4-epoxy cyclohexylmethyl 3,4-epoxy cyclohexane carboxylate (ECC) with several amounts of hexagonal boron nitride (BN) were prepared and characterized. As cationic initiator a commercial benzylanilinium salt was used, which by addition of triethanolamine (TEA), exhibited an excellent latent character and storage stability. The effect of the formulation composition was studied by calorimetry and rheological measurements. The variation of thermal conductivity, thermal stability, thermal expansion coefficient and thermomechanical and mechanical properties of the composites with the load of BN filler (ranging from 10 to 40 wt%) was evaluated. An improvement of an 800 % (1.04 W/m·K) in thermal conductivity was reached in materials with glass transition temperatures higher than 200°C without any loss in electrical insulation.

Keywords

Cycloaliphatic epoxy resin; polymer composites; thermal conductivity; boron nitride; latency.

1. Introduction

The use of high frequencies in electronic devices, with a great electric current, leads to an increase in their temperature caused by the Joule effect. Limiting their work temperature favors their performance, lifetime and reliability and therefore the thermal management of these materials has become an important issue [1]. To dissipate the heat produced during their operation, thermal conductive materials are

required and, since many parts of the devices are usually coated or packaged with epoxy resins, which are thermal insulators, the increase in their thermal conductivity is of utmost importance [2]. Epoxy thermosets are widely used because of the versatility in their properties [3,4]. They are used in electrical and electronic applications because of their good compatibility with a large variety of materials, high electrical insulation and good thermal, corrosion and chemical resistance [5]. However, epoxy thermosets exhibit poor thermal conductivity, in the range 0.1 to 0.3 W/m·K. The addition of thermal conductive but electrically insulating fillers to the resin is one of the easiest methods for effectively dissipating heat in such devices at the lowest price. In last years, many efforts and studies have been intended to increase the thermal conductivity of these resins [6-9].

Cycloaliphatic epoxy resins are preferred in electronic applications for their low viscosity, which permit to impregnate zones with small and abrupt morphology. They have excellent weathering and electrical performance with a low dielectric loss and high electrical resistivity, up to or above their glass transition temperatures, which provide high performance and reliability in both AC and DC circuitry. Their inherent low viscosity enables them to be formulated with higher levels of inorganic fillers, which enhances mechanical and electrical track resistance for electric materials. According to that, in the present study we have selected 3,4-epoxy cyclohexylmethyl 3,4-epoxy cyclohexane carboxylate (ECC) as epoxy monomer. Cycloaliphatic epoxy resins are mainly cured with anhydrides, which show some drawbacks such as toxicity, sensitivity to humidity, yellowing, high viscosities or too short pot life that are serious problems for electronic applications that require high working temperatures [10]. As an alternative, cationic ring-opening polymerization was studied and developed intensively, since the stereoelectronic nature of the epoxy group lead to an extremely low reactivity towards common nucleophilic crosslinkers [11]. Among the cationic curing agents, amino complexes of BF_3 can be used with a moderate latency at room temperature but the electrical properties of cured resins tend to deteriorate at high temperature and high humidity [12]. Lanthanide triflates were also proposed, but the T_gs of the cured materials were lower, although the enthalpy evolved during curing was higher [13]. Endo's group has been one of the major contributors to the field of latent thermal initiators and they observed that the activity can be effectively controlled through the change of electronic and steric properties of the substituents and varying the nucleophilicity of the counteranion in onium salts [14,15]. Among thermal latent initiators, sulfonium, ammonium, phosphonium and hydrazinium salts were reported [11]. In the present study, a commercial anilinium salt, N-(4-methoxybenzyl)-N,N-dimethylanilinium hexafluoroantimonate [16], which to the best of authors' knowledge had not been previously reported to be used to crosslink cycloaliphatic epoxy resins, was selected as initiator and modified with triethanolamine (TEA) to reach a high latency. Many latent systems already exist for cycloaliphatic epoxy resins [17,18] but generally, they are photochemically activated,

Polymer Composites ***2018**, 39, 1760-1769*

which limits their use to the preparation of thin coatings and present some drawbacks in the curing of shadowy parts.

As filler, we selected hexagonal boron nitride (BN), which has gained great popularity in recent years in the field of high thermal conductivity. This is due to the combination of properties: high thermal conductivity in planar direction, good dielectric properties, low thermal expansion coefficient (CTE) and density below other kind of particles [19,20]. We recently studied similar curing processes based on a diglycildylether of bisphenol A (DGEBA) resin [7]. The low viscosity and the higher reactivity of cycloaliphatic epoxides towards cationic initiators, together with the compact structure, are expected to be advantageous to get highly crosslinked materials with high T_g and thermal conductivity. The mechanical and thermal properties of BN composites have been determined by thermogravimetric and thermomechanical analysis (TMA). Mechanical properties such as hardness or adhesion were also tested. Electrical resistivity and thermal conductivity were also measured.

2. Materials and methods

2.1. Materials

ECC (ERL-421D, EEW=126.15 g/eq) was provided by Dow Chemical Company. Initiator CXC1612 from King Industries Inc., USA, which was determined to be N-(4-methoxybenzyl)-N,N-dimethylanilinium hexafluoroantimonate, was solubilised in propylene carbonate at 50 wt%. Propylene carbonate and TEA were provided by Sigma-Aldrich and purified by distillation. Platelets of h-BN were supplied by ESK Ceramics GmbH, TPC 006, with an average particle size of 6 µm in length (Fig. 1).

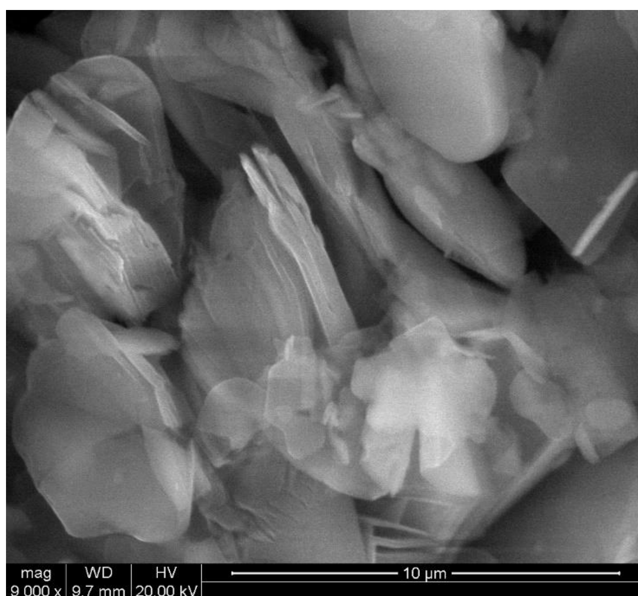

Figure 1. ESEM micrographs of the BN particles used in the study.

2.2. Sample preparation

The mixtures were prepared by mixing ECC with 1 phr (parts of initiator per hundred parts of resin) and 0.1 phr of TEA. For composite samples, the required amount of BN was added in wt% to the previous formulation. The mixtures were manually stirred until homogeneity (10 min) and degassed under vacuum to prevent the appearance of bubbles during the curing process. Finally, the samples were poured onto aluminium molds and cured following a multi-step temperature schedule at 100, 120, 150, 180 and 200 °C, with a dwelling time of 1 hour at each temperature.

2.3. Characterization techniques

A differential scanning calorimeter (DSC) Mettler DSC-821e calibrated using an In standard (heat flow calibration) and an In-Pb-Zn standard (T calibration) was used to study the cure. Samples of approx. 5-10 mg were tested in aluminum pans with a pierced lid in N_2 atmosphere with a gas flow of 100 mL/min. The dynamic studies were performed between 30-250 °C with a heating rate of 10 °C/min. The reaction enthalpy (Δh) was integrated from the calorimetric heat flow signal (dh/dt) using a straight baseline, with the help of the STARe software.

Rheometric measurements were carried out in a TA Instruments AR G2 rheometer, equipped with electrical heated plates (EHP). Parallel plate geometry (25 mm diameter disposable aluminum plates) was used. Complex viscosity (η^*) and viscoelastic properties of the mixtures were recorded as function of angular frequency ω (rad/s) in the range of linear viscoelasticity, obtained from constant shear storage modulus (G') in a strain sweep experiment at 1 Hz at 30 °C.

The thermal stability of cured samples was determined using a Mettler thermogravimetric device (TGA)/SDTA 851e thermobalance under inert atmosphere (N_2 at 100mL/min) and Mettler Toledo TGA/DSC 1 under air (synthetic air at 50 mL/min). Pieces of cured samples of 10-15 mg were degraded between 30 and 600 °C at a heating rate of 10 °C/min. Dynamic mechanical thermal analyses (DMTA) were performed with a TA Instruments DMA Q800 analyser. Prismatic rectangular samples (15 x 6 x 2.3 mm^3) were analyzed by three-point bending at a heating rate of 3 °C/min from 35 to 300 °C using a frequency of 1 Hz and oscillation of 0.1 % of sample deformation. The Young modulus (E) was determined at 30 °C as explained in a previous paper [7]. TMAs were carried out on a Mettler TMA40 thermomechanical analyzer. Cured samples (12 x 12 x 2.3 mm^3) were supported by the clamp and one silica disc to distribute uniformly the force and heated at 5 °C/min from 35 to 150 °C by application of a force 0.01 N, a minimum force to avoid distortion of the results [7].

Knoop microindentation hardness was measured as reported before with a Wilson Wolpert 401 MAV device following ASTM D1474-13 [7]. For each material a minimum of 20 determinations were made with a confidence level of 95%. Adhesion

tests of different mixtures on rectangular steel plates were done as previously reported [7] by tensile lap-shear strength of bonded assemblies using a Houndsfield H10KS universal test machine with 10 kN load cell, following ASTM D1002-10 method. At least seven samples were tested for each mixture. Surface fracture was examined with a FEI Quanta 600 environmental scanning electron microscope (ESEM) that allows collecting electron micrographs at 10-20kV and low vacuum mode of uncoated specimens with low electron conductivity.

X-ray diffraction (XRD) measurements were made using a Siemens D5000 diffractometer (Bragg-Bretano parafocusing geometry and vertical ϴ-ϴ goniometer) fitted with a curved graphite diffracted-beam Soller slits, a 0.06° receiving slit and scintillation counter as a detector. The angular 2ϴ diffraction range was between 5 and 70°. The data were collected with an angular step of 0.05° at 3 s per step and sample rotation. $Cu_{k\alpha}$ radiation was obtained from a copper X-ray tube operated at 40 kV and 30 mA.

Volume resistivity of samples was measured on a Megohmmeter Burster model 24508 insulation tester at room temperature following ASTM D257-14 as reported before [7]. Pieces of 12 x 12 x 2.3 mm^3 were essayed between two stainless steel electrodes with an area of 19.635 mm^2 each one. The applied voltage to the thermosetting composites was 500 V during 1 min. Thermal conductivity was measured using the Transient Hot Bridge method by a THB 100 device from Linseis Messgeraete GmbH. A HTP G 9161 sensor was used with a 3 x 3 mm^2 of area calibrated with polymethyl methacrylate (PMMA), borosilicate crown glass, marble, Ti-Al alloy and titanium. Two equal polished rectangular samples (12 x 12 x 2.3 mm^3) were placed in each one of the faces of the sensor. Due to the small size of sensor, side effect can be neglected. A measuring time of 100 s with a current of 10 mA was applied to each of the five measures done for the different formulations.

3. Results and discussion

3.1. Optimization of the curing process of the neat and BN filled formulations

Initiators play an important role in the curing of epoxies mainly for two reasons: they have a catalytic effect and decrease the activation energies accelerating the reaction, and give to thermosets specific properties. The choice of cationic initiators with low-nucleophilicity counter-anions can significantly enhance the reactivity of cationic curing systems [21]. In this study, we have selected as initiator the commercial compound, CXC1612, which by NMR spectroscopy was disclosed to be N-(4-methoxybenzyl)-N,N-dimethylanilinium hexafluoroantimonate [15]. However, this cationic curing system has not been reported so far in cycloaliphatic epoxies.

To study the curing process of ECC with CXC1612, different amounts of initiator were tested, from 1 to 4 phr. **Figure 2** shows the dynamic calorimetric curves for the formulations studied. The main data extracted from DSC are shown in **Table 1**.

The figure shows that on increasing the proportion of initiator the exotherm shifts at lower temperature because of the catalytic effect. The enthalpy released, given in Table 1, is similar for all the formulations in spite of the amount of initiator. It is worth noting that the curves are quite complex with two broad and partially overlapped exotherms probably due to the different polymerization mechanisms: activated monomer and activated chain end, which are competitive in cationic systems [22]. Moreover, the curing starts at low temperature, which can lead to a premature curing and too short pot life.

Table 1. Calorimetric data from formulations with some proportions of initiator and TEA.

Initiator (phr)	**TEA** (phr)	T_{onset}[a] (°C)	T_{peak}[b] (°C)	Δh[c] (J/g)	Δh[c] (kJ/ee)
1	0	87	109	596	75
2	0	83	107	571	72
3	0	80	105	569	71
4	0	77	103	599	76
1	0.1	116	119	698	88
1	0.2	125	129	541	68

[a] Onset temperature of the exothermic curve.
[b] Temperature of the maximum of the peak of the curing exotherm.
[c] Enthalpy of the curing process by gram of mixture or by epoxy equivalent.

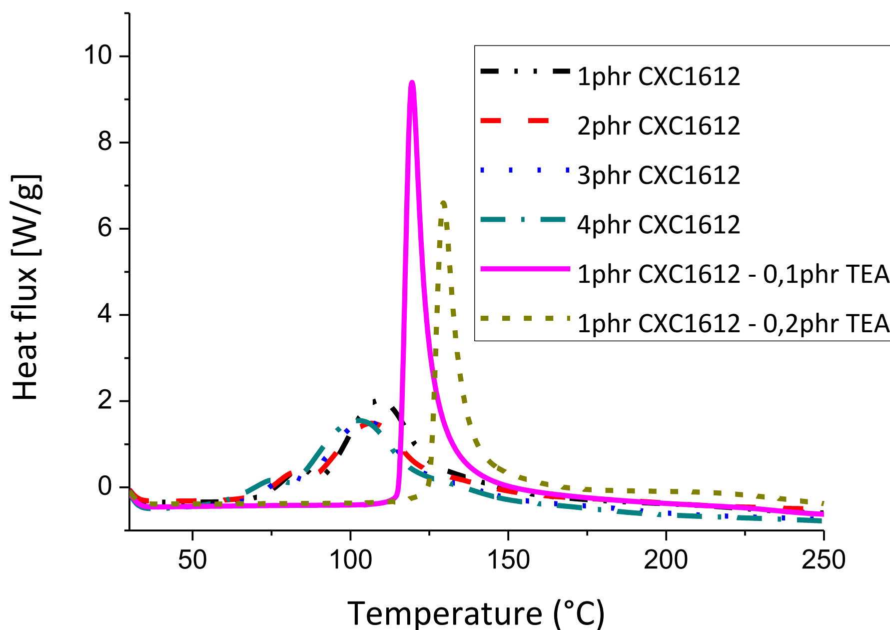

Figure 2. DSC scans of ECC formulations with several proportions of initiator and amine.

To reduce these drawbacks we added small proportions of TEA to the formulation, since it has been reported that it is an efficient inhibitor of low temperature polymerization in cationic systems [23]. The addition of TEA to formulations with 1 phr of initiator leads to curves with a sharp and narrow shape,

Polymer Composites ***2018***, *39, 1760-1769*

starting a fast reaction at high temperature, which is characteristic of latent curing systems. Moreover, the addition of 0.1 phr of TEA produces an increase of the heat evolved during curing up to 88 kJ/ee, but a further increase of the amount of inhibitor, which act as a poison for the cationic curing, shifted the curing onset to higher temperatures but this delay in the curing process resulted in incomplete cure. Therefore, we selected as the best catalytic system the mixture of ECC with 1 phr of CXC1612 and 0.1 phr of TEA.

Once selected the base formulation, we performed periodic DSC scans to evaluate the stability of the mixture stored at room temperature. The curves were almost overlapped confirming the excellent stability of the system. The mixture perfectly preserves the latent characteristic and has a minimal diminution of the temperature peak (see **Table 2**). After four months stored at room temperature, only a loss of 6% of the curing enthalpy was observed. The mixture also kept the same viscosity during this period, without any sign of polymerization. Then, it can be confirmed that this optimized curing system may be advantageous for industrial applications, since in addition to the instantaneous curing at the triggering temperature, the mixtures can be easily stored for long time without loss in their characteristics.

Table 2. Calorimetric data of formulation after various times to be prepared.

Time	T_{peak}[a] (°C)	Δh[b] (J/g)	Δh[b] (kJ/ee)
First day	119	698	88
1 week	118	691	87
4 weeks	118	683	86
6 weeks	117	675	85
8 weeks	117	673	85
12 weeks	117	670	84
16 weeks	116	660	83

[a] Temperature of the maximum of the peak of the curing exotherm.

[b] Enthalpy of the curing process by gram of mixture or by epoxy equivalent.

In order to improve the thermal conductivity and to evaluate the effect on the different characteristics of the composites, different percentages of BN were added to the epoxy formulation. The maximum proportion of BN added to the formulation was 40 wt%, since higher amounts of filler increased the viscosity of the formulation too much and generated big difficulties to prepare homogeneous mixtures. It should be commented that in the previous study, based on DGEBA resins, the maximum amount of BN added was only 20 wt% because of the higher viscosity of DGEBA resin. The curing evolution of the formulations was investigated by DSC, as shown in **Figure 3**.

It can be observed that on increasing the proportion of filler there is a decrease in the height of the exotherms, indicating a diminution in the curing rate. However,

the shape of the curves is similar, confirming that the latency is kept unaltered. The heat released decreases from 88 to 68-69 kJ/ee (see **Table 3**) on adding BN to the formulation but an increase in the proportion no longer affects the released enthalpy. Thus, from the point of view of the curing mechanism it can be stated that BN has an inert character in the cationic homopolymerization. Nevertheless, it affects the final curing degree achieved in dynamic DSC experiments, probably due to topological restrictions caused by the BN particles, which can hinder the growing of the polymer chain, leading to a decrease of the curing enthalpy.

Table 3. Calorimetric data on varying the BN proportion in ECC formulation with 1 phr of initiator and 0.1 phr of TEA.

% BN (in weight)	**% BN** (in volume)	T_{peak} [a] (°C)	**Δ*h*** [b] (J/g)	**Δ*h*** [b] (kJ/ee)
0	0	119	698	88
10	5.6	119	488	69
20	11.7	119	436	68
30	18.9	119	378	68
40	26.0	118	330	69

[a] Temperature of the peak of the curing exotherm.
[b] Enthalpy of the curing process by gram of mixture or by epoxy equivalent.

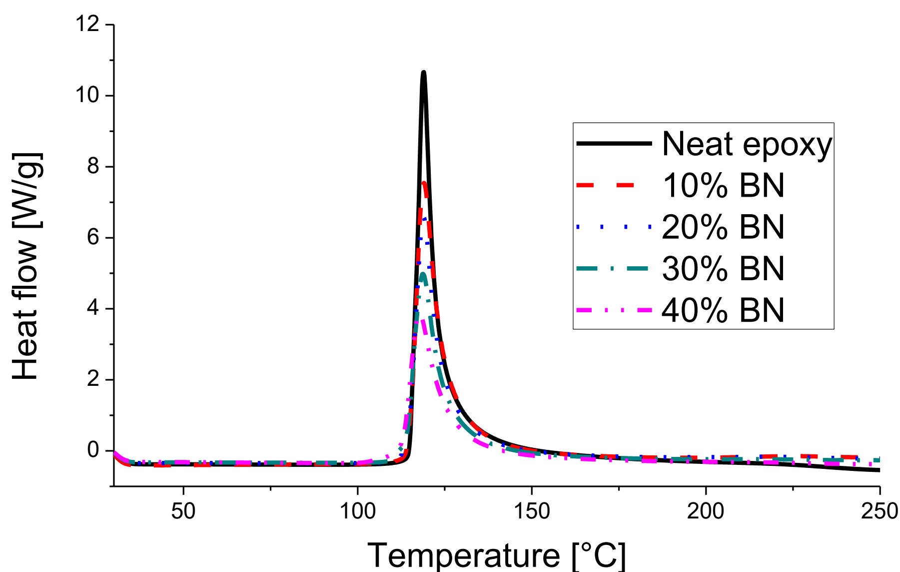

Figure 3. DSC scans of formulations with several proportions of BN in wt%.

3.2. Rheological study of the formulations

Rheological analysis provides important information on the evolution of the structure and consequently, on the interaction between the filler and matrix. Viscosity

is the most important property affecting the applicability of encapsulation resins. For this reason, measurements of viscosity are essential for understanding the processability, to control and optimize process conditions and product performance [24]. Thus, the formulations were studied by performing oscillatory experiments to determine their viscoelastic response.

To determine viscoelastic constants in this kind of mixtures we must firstly establish the linear viscoelastic region (LVR) or Newtonian range to work on it, which means a constant shear storage modulus (*G′*) in strain sweep experiment with the frequency fixed (1 Hz). **Figure 4A** shows how the LVR is shifted to lower strains when the filler content rises while neat epoxy formulation maintained a practically constant *G′* in all the strain range tested, a Newtonian behavior as expected for the unfilled resin. Filled mixtures found a critical strain above which the structure starts to breakdown earlier when the amount of filler increases [25].

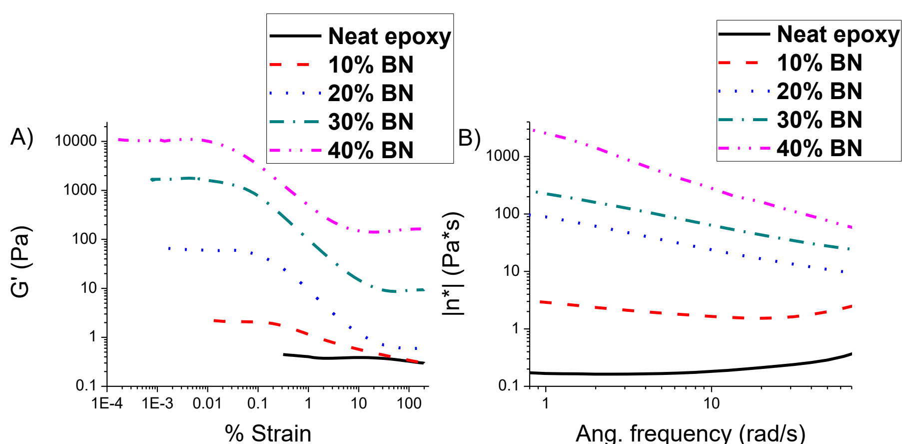

Figure 4. (A) Plot of log G′ versus log % strain in oscillatory experiments (1 Hz). (B) Plot of log η* versus log ω, both at 30 °C for all the uncured formulations studied.

The complex viscosity $|\eta^*|$ of unfilled resin (**Figure 4B**) presents an almost constant value on varying the frequency, and a low frequency dependence for the mixture with 10 wt% of BN which could be considered as a dilute solution. However, upon adding 20 wt% of filler or more, the complex viscosity becomes more dependent on the applied frequency, resulting in a more pronounced low frequency shear thinning response typical of layered particles mixtures [26], indicating a significant change in their microstructure. The shear thinning is the decrease of viscosity with the angular frequency that is determined by the balance of hydrodynamic forces, which tends to align the particles with the flow, and rotary Brownian motion that tends to randomize the orientation [27]. It is worth to note, that the increase of $|\eta^*|$ exceeds more than four orders of magnitude on adding 40% wt of BN to the formulation. In addition, an apparent increase of this value is observed in the dilute mixtures, when frequency exceeded a certain critical value, which is associated with the device inertia.

The significant change in the microstructure can also be evaluated by the study of storage modulus (*G'*) and loss modulus (*G''*), which determine the elastic and viscous properties, respectively. **Figure 5** shows how on increasing the BN content, the slope of *G'* decreases transforming it to a nearly constant value, independent of the angular frequency, with the addition of 40 wt% of BN.

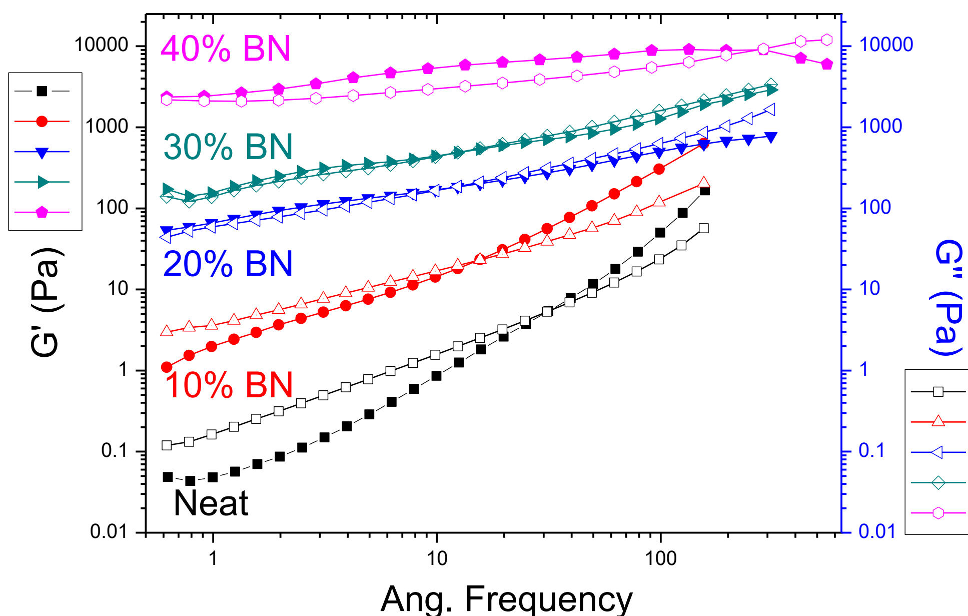

Figure 5. Plots of G' (filled) and G'' (open symbols) against ω of uncured formulations at 30 °C.

Also, the change in the liquid like behavior (*G'<G''*) to solid like (*G'>G''*) is observed. This change in the storage modulus at about 20% of BN, with a kind of plateau at low frequency, means that the filled mixture has reached the rheological percolation. Near the percolation threshold (the point in which a pathway of interconnected particles that extends throughout the network is formed) the theory predicts a power law ratio that can be used at a fixed low frequency to determine it [28,29]:

$$G' \propto (m - m_C)^{\beta} \qquad \text{(Eq. 1)}$$

where *G'* is the storage modulus, *m* is the mass fraction of BN composites, m_C is the mass fraction at rheological percolation and *β* is the critical exponent. This relation is often valid only on a very narrow concentration region [7]. The rheological percolation at 1 rad/s was calculated to be 14.4 wt % of BN and the critical exponent 0.84. It should be commented, that the percolation of BN particles in DGEBA formulations was reached at an only 6.9 wt %.

3.3. Thermal and thermomechanical characterization of the BN composites

The contribution of BN particles to the composite's behaviour was evaluated through different techniques such as TGA, DMTA and TMA and compared with the neat epoxy matrix.

TGA analyses under inert atmosphere showed an only degradation step (**Fig. 6A)** and the most representative data are collected in **Table 4**.

Table 4. Thermogravimetric data of thermosets with several BN contents in N_2 atm.

% BN (in weight)	$T_{2\%}$[a] (°C)	T_{max}[b] (°C)	Char Yield[c] (%)
0	273	415	1
10	298	417	13
20	310	418	22
30	315	419	31
40	342	420	42

[a] Temperature of 2% of weight loss.
[b] Temperature of the maximum decomposition rate.
[c] Char residue at 600 °C.

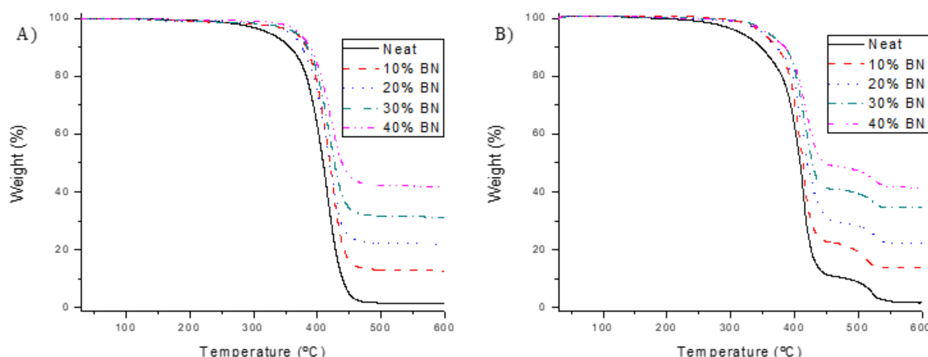

Figure 6. (A) TGA plots of samples under N_2 atmosphere and (B) under synthetic air.

TGA analyses show a great increase of the temperature of 2% of weight loss on increasing the proportion of filler in the material, about 70 °C in reference to the neat epoxy on adding 40% of BN, indicating a stabilization effect caused by the increasing proportion of filler and possible filler-polymer chain interactions. Moreover, the temperature of maximum degradation rate is kept constant which indicates that the degradation mechanism is not affected by the presence of BN. It is worth mentioning that the char residues are in agreement with the percentages of BN in the composites, since the aliphatic nature of ECC leads to a scarce residue after the complete degradation.

By DMTA analysis, we observed the effect of the particles in the mechanic behaviour of the cured materials and evaluated the glass transition temperatures of the composites, which could not be easily determined by DSC due to the high

crosslinking density of the network which minimise ΔCp. **Figure 7A** shows the evolution of storage modulus (E') and **Figure 7B** shows the evolution of the loss factor tan δ with temperature. It can be observed that the relaxation process takes place at high temperatures and this prevented us from determining the modulus after relaxation, since at 300 °C the materials were still relaxing but degradation would have already started. **Table 5** collects the main parameters extracted from the thermomechanical study.

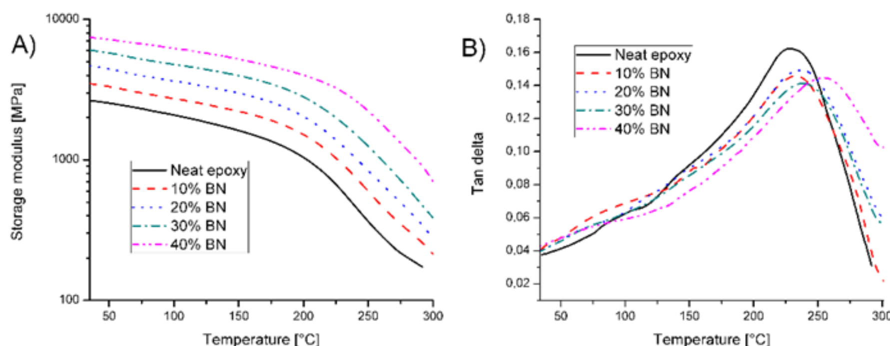

Figure 7. (A) Storage modulus and (B) tan δ against temperature of the different materials prepared.

Table 5. Thermomechanical data for the thermosets with different BN content.

% BN (w/w)	Young's modulus[a] (GPa)	$T_{\tan\delta}$[b] (°C)	CTE[c] ($10^{-6}\cdot K^{-1}$)
0	2.4	227	115
10	3.2	232	65
20	4.1	237	66
30	5.1	240	59
40	6.5	254	55

[a] Young's modulus determined by DMTA at 30 °C using three point bending clamp.
[b] Temperature of maximum of tan δ at 1 Hz.
[c] Coefficient of thermal expansion in the vitreous state determined by TMA, between 50 and 75 °C.

In Figure 7B and Table 5 it can be seen that the glass transition temperatures follow an increasing tendency on increasing the filler proportion until temperatures higher than 250 °C are reached, extremely large for this type of matrix with an ester group in the network structure, which may undergo β-elimination processes. Similar T_g values were found by Sangermano et al [30] with the same ECC photochemically cured but very different compared with samples obtained by cationic homopolymerization with lanthanide triflates, which were not higher than 150 °C [13]. The tan δ curves in Figure 7B are very broad indicating a slow relaxation process and have a low intensity indicating low homogeneity in the network structure due the high crosslinking density and to the inherent inhomogeneity caused by the ring-opening polymerization mechanism [3]. The shift of the tan δ peak with increasing BN content indicates there is an interaction between the polymer matrix and the particles further reducing the mobility of the network structure. The increase of Young modulus,

*Polymer Composites **2018**, 39, 1760-1769*

although it was not the aim of the present study, reached a 160% of improvement thanks to the reinforcement role of the filler that will be beneficial for the material resistance and its durability.

By TMA, CTE's were measured to assess the dimensional stability of the materials. It can be seen that the addition of filler reduces by more than 50% this value, which could be favorable for the purposes required in electronic industry. These thermosets usually cover metallic or ceramic substrates with a lower CTE than the polymers and the smaller the difference between their coefficients, the lower internal stresses will be as the working temperature changes leading to a lower thermal fatigue [31].

3.4. Mechanical characterization and morphology

Coatings applications for electronic devices require a high hardness to keep good appearance of the surface and the protective capacity. To evaluate the resistance against penetration by a static force, we performed microindentation tests. The results obtained using a Knoop microindenter are given in **Table 6**. It is observed that as the amount of BN increases, the hardness of the composite increases, reaching a maximum value of 26.6 KHN, more than twice the neat matrix.

Table 6. Mechanical and electrical properties of the neat materials and composites

% BN (w/w)	KHN[a]	τ^b (MPa)
0	11.7 ± 0.58	2.34 ± 0.46
10	15.3 ± 0.57	3.11 ± 0.47
20	18.8 ± 0.76	7.58 ± 0.66
30	22.0 ± 0.90	10.65 ± 0.89
40	26.6 ± 1.03	9.96 ± 0.44

[a] Knoop microindentation hardness.
[b] Apparent lap-shear strength over steel surface.

Adhesion is a complex property that depends on many different factors such as the properties of the coatings and substrates, interfacial interactions or environmental conditions. In addition, differences in CTE's between substrate and coating can lead to the reduction of the adhesion, especially for epoxy cured at high temperature, since the final decrease of temperature after curing creates internal stresses that leads to the production of microcracks or warping. Table 6 shows the apparent shear strength values on steel surfaces for the different materials prepared with different BN content. It can be seen that the shear strength increases with the BN content until reached a maximum with the 30% of BN. The reduction of adherence with 40% of BN is related to the diminution of epoxy content. When comparing the observed trends of these properties with those previously reported in DGEBA composites, a different behaviour was observed, since the microhardness was only

slightly improved and the adhesion remained constant up to 15% of BN content and then decreased [7].

Fracture surfaces were examined by ESEM microscopy. In **Figure 8** it can be clearly observed the phenomenon of the percolation in the transition from 10 to 20% of BN in the material, since the isolated particles in the 10% BN sample collapse in the 20% BN composite. Moreover, in the transition from the neat material to the filled samples it can be seen that the fairly well defined fracture lines in the neat material are transformed into tortuous fracture cracks because of the plans of the BN particles deviate them, producing the consequent enhancement in toughness.

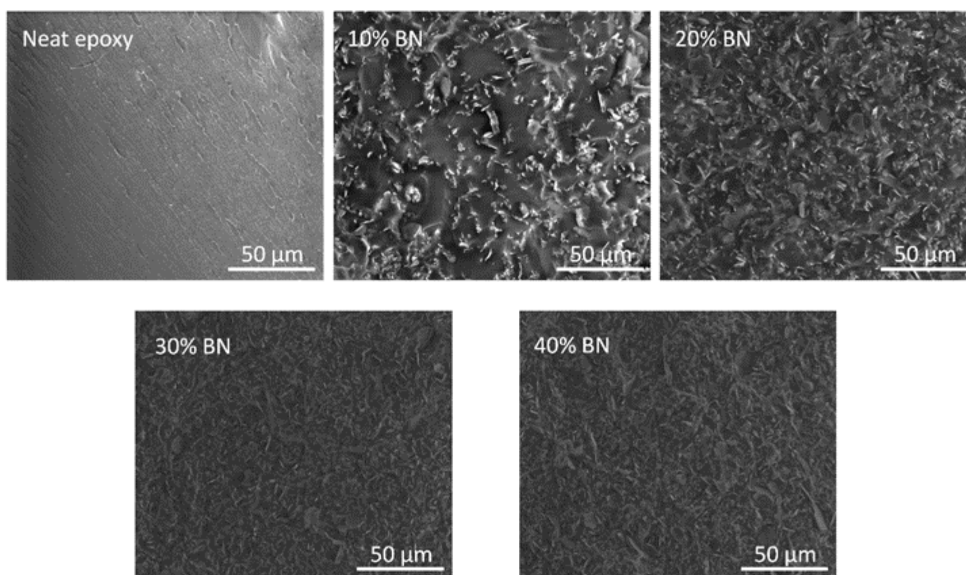

Figure 8. ESEM micrographs of the fracture surfaces of materials at 800 magnifications.

3.5. XRD Diffraction

The XRD is a powerful technique to study the internal structure of materials and to determine the degree of crystallinity of semicrystalline polymers. **Figure 9A** shows the spectrum of the filler used in the study and the peaks correspond exactly to the hexagonal structure pattern of the BN in the database (01-073-2095 (A)).

The composite with 40 wt. % (**Fig. 9B**) was also analyzed. All the peaks related to BN powder are maintained but they show a small widening due to the presence of resin. It is worth mentioning that a wide peak is observed around 17° of 2Θ due to the amorphous structure of the polymer.

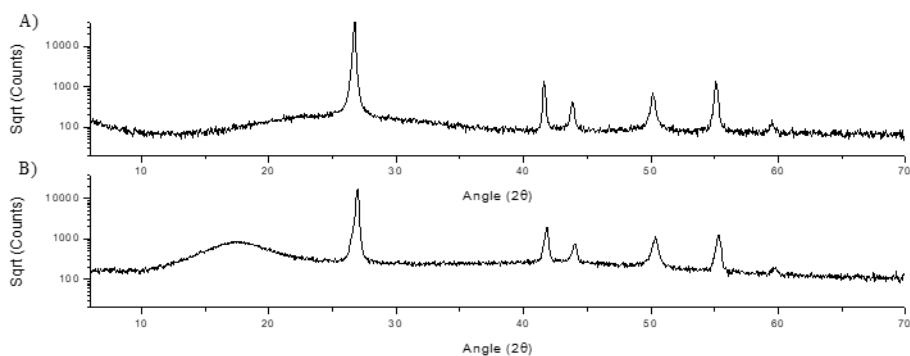

Figure 9. (A) XRD diffractogram of BN particles and (B) 40 wt. % composite.

3.6. Thermal conductivity and electrical resistivity

The main goal of this research was to improve thermal conductivity of a cycloaliphatic epoxy thermoset by the addition of BN without negatively affect the electrical insulation. Different materials with increasing BN content were investigated by thermal conductivity analysis. The values obtained are represented in **Figure 10**. As we can see, the thermal conductivity of the neat resin is highly improved with the increase of BN content. For the sample with 40 wt % of BN (26.0 % vol.) the thermal conductivity reaches 1.04 W/m·K, implying an increase of more than 800%. Chiang and Hsieh obtained similar values of thermal conductivity by using a cycloaliphatic-anhydride system with 25.7% vol. of BN as filler [6]. In addition, a larger increase is observed once percolation is reached. In the previous study on DGEBA composites, a maximum value of 0.61 W/m·K was reached with a 20% wt of BN [7]. Therefore, our hypothesis that the lower viscosity of ECC allows to reach a higher thermal conductivity, because of the possibility to increase the BN % is confirmed.

It should be mentioned, however, that in the literature it can be found references for similar BN contents that reach much higher conductivities [32, 33]. Differences in the curing procedure (using pressure for example), the size and shape of particles, their surface area, and so forth, play a very important role in the increase of thermal conductivity.

Another important parameter in electronic fabrication is the electrical resistance of the thermoset, which quantify the opposition to the current flow. In Figure 10 the resistivity of each material, resulting of the appliance of 500 V during one minute to the samples, are represented. All the results obtained are over 10^8 Ω·m, enough for electronic industry and they do not depend on the content of BN as other authors have found for electrical conductivity [34].

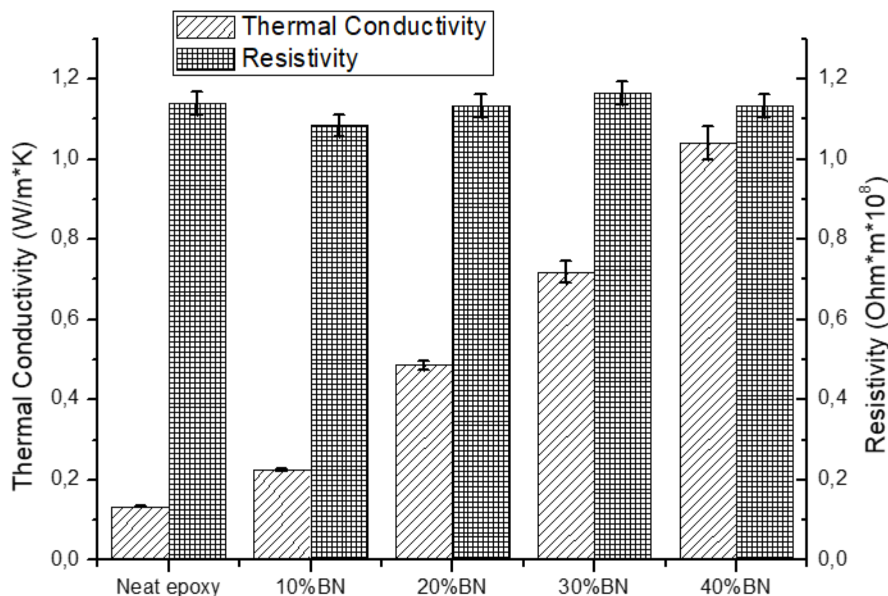

Figure 10. Thermal conductivity and electric resistivity of the materials prepared on varying the proportion of BN.

4. Conclusions

A new latent cationic curing system for ECC was optimized using 1 phr of a benzylammonium salt with 0.1 phr of TEA. This system allows the curing to proceed very quickly on reaching temperatures about 120 °C and the formulation can be stored for more than four months at room temperature without appreciable change. The addition of BN particles did not lead to any effect on the latency.

Rheological studies allow monitoring the increasing viscosity of mixtures on raising the BN proportion. The percolation threshold was determined at 14.4 wt % of BN in the formulation.

Glass transition temperatures, determined by DMTA, are higher than 200 °C and increased slightly with the BN proportion in the materials. Young moduli also shows a similar trend. CTEs decrease more than 50% on adding the filler, which is beneficial for the reduction of thermal stresses.

Microindentation hardness and apparent shear strength increases with the proportion of BN, but adhesion presents a maximum value with a 30% of BN in the material.

Electronic microscopy inspection allows confirming that the percolation occurred between 10 and 20% of BN content. A more tough fracture can be observed in the composites because of the higher tortuosity of crack propagation.

Polymer Composites ***2018****, 39, 1760-1769*

Thermal conductivities of composites were increased in an 800% with the addition of 40 wt % BN filler. According to all these results, the curing system and the materials obtained are very promising for thermal management application and electronic encapsulation.

5. Acknowledgments

The authors would like to thank MINECO (MAT2014-53706-C03-01 and 02) and Generalitat de Catalunya (2014-SGR-67) for the financial support. Xavier F.-F also acknowledges the Serra-Húnter programme (Generalitat de Catalunya). Gabriel Benmayor S.A. is acknowledged for giving us the BN used in this work.

6. References

1. H. Chen, V.V. Ginzburg, J. Yang, Y. Yang, W. Liu, Y. Huang, L. Du, B. Chen, *Prog. Polym. Sci.*, **59**, 41-85 (2016).
2. X.C. Tong, *Advanced materials for thermal management of electronic packaging*. Springer, New York, p. 616 (2011).
3. J.P. Pascault, H. Sauterau, J. Verdu, R.J.J. Williams (Ed.), *Thermosetting Polymers*. Marcel Dekker, New York (2002).
4. X. Huang, P. Jiang, T. Tanaka, *IEEE Electr. Insul. Mag„* **27**, 8-16 (2011).
5. C.A. May, *Epoxy Resins: Chemistry and Technology*, Marcel Dekker Inc., New York (1988).
6. T.H. Chiang, T.-E. Hsieh, *J. Inorg. Organomet. Polym. Mat.*, **16**, 175-183 (2006).
7. I. Isarn, L. Massagués, X. Ramis, A. Serra, F. Ferrando, *Composites Part A*, **103**, 35-47 (2017).
8. K. Yang, M. Gu, *Composites Part A*, **41**, 215-221 (2010).
9. X. Huang, P. Jiang, T. Tanaka, *IEEE Elect. Insul. Mag.*, **27**, 8-16 (2011).
10. W. Green, *Industrial photoinitiators. A technical guide*. CRC Press, Boca Raton (2010).
11. T. Vidil, F. Tournilhac, S. Musso, A. Robisson, L. Leibler, *Prog. Polym. Sci.*, **62**, 126-179 (2016).
12. M. Tokizawa, H. Okada, N. Wakabayashi, *J. Appl. Polym. Sci.*, **50**, 875-884 (1993).
13. C. Mas, A. Serra, A. Mantecón, J.M. Salla, X. Ramis, *Macromol. Chem. Phys.*, **202**, 2554-2564 (2001).
14. S. Nakano, T. Endo, *Prog. Org. Coat.*, **23**, 379-385 (1994).
15. S. Nakano, T. Endo, *Prog. Org. Coat.*, **28**, 143-148 (1996).
16. S. Nakano, T. Endo, *J. Polym. Sci. Part A: Polym. Chem.*, **33**, 505-512 (1995).
17. J.V. Crivello, S. Liu, *J. Polym. Sci. Part A: Polym. Chem.*, **38**, 389-401 (2000).
18. H. Lützen, T.M. Gesing, B.K. Kim, A. Hartwig, *Polymer*, **53**, 6089-6095 (2012).
19. M. Donnay, S. Tzavalas, E. Logakis, *Compos. Sci. Technol.*, **110**, 152-158 (2015).
20. J. Yu, H. Mo, P. Jiang, *Polym. Adv. Technol.*, **26**, 514-520 (2015).
21. S. Nakano, T. Endo, *Prog. Org. Coat.*, **22**, 287-300 (1993).
22. L. Matejka, P. Chabanne, L. Tighzert, J.P. Pascault, *J. Polym. Sci. Part A: Polym. Chem.*, **32**, 1447-1458 (1994).

23. M. Tejkl, J. Valis, M. Kaplanová, B. Jasúrek, T. Syrový, *Prog. Org. Coat.*, **74**, 215-220 (2012).
24. M.R. Kamal, A. Mutel, *J. Polym. Eng.*, **5**, 293-382 (1985).
25. T.F. Tadros, *Rheology of Dispersions: Principles and Applications*. Wiley-VCH, Weinheim, 76-77 (2010).
26. J. Ren, R. Krishnamoorti, *Macromolecules*, **36**, 4443-4451 (2003).
27. C.W. Macosko, R.G. Larson, *Rheology: Principles, measurements, and applications*. Wiley-VCH, New York, p. 440 (1994).
28. G. Hu, C. Zhao, S. Zhang, M. Yang, Z. Wang, *Polymer*, **47**, 480-488 (2006).
29. P.G. De Genes, Scaling theory of polymer adsorption. *Journal de Physique*, **37**, 1445-1452 (1976).
30. M. Sangermano, Y. Yagci, G. Rizza, *Macromolecules*, **40**, 8827-8829 (2007).
31. D.D.L. Chung, L. Li, *Materials for electronic packaging*. Butterworth-Heinemann, Newton, p. 168 (1995).
32. A. Rybak, K. Gaska, C. Kapusta, F. Toche, V. Salles, *Polym. Adv. Technol.*, **28**, 1676 (2017).
33. K. Gaska, A. Rybak, C. Kapusta, R. Sekula, A. Siwek, *Polym. Adv. Technol.*, **26**, 26 (2015).
34. Y.S. Perets, L.Y. Matzui, L.L. Vovchenko, Y.I. Prylutskyy, P. Scharff, U. Ritter, *J. Mat. Sci.*, **49**, 2098-2105 (2014).

UNIVERSITAT ROVIRA I VIRGILI
NEW EPOXY COMPOSITES WITH ENHANCED THERMAL CONDUCTIVITY KEEPING ELECTRICAL INSULATION.
Isaac Isarn Garcia

Chapter 5

Thermoconductive thermosetting composites based on boron nitride fillers and thiol-epoxy matrices

Polymers ***2018****, 10, 277-292*

Thermoconductive Thermosetting Composites Based on Boron Nitride Fillers and Thiol-Epoxy Matrices

Isaac Isarn[1], Xavier Ramis[2], Francesc Ferrando[1] and Angels Serra[3]

1. Department of Mechanical Engineering, Universitat Rovira i Virgili, C/Av. Països Catalans, 26, 43007 Tarragona, Spain.
2. Thermodynamics Laboratory, ETSEIB Universitat Politècnica de Catalunya, Av. Diagonal 647, 08028 Barcelona, Spain.
3. Department of Analytical and Organic Chemistry, Universitat Rovira i Virgili, C/Marcel·lí Domingo s/n, 43007 Tarragona, Spain.

Abstract

In this work, the effect of the addition of boron nitride (BN) fillers in a thiol-cycloaliphatic epoxy formulation has been investigated. Calorimetric studies put into evidence that the kinetics of the curing has been scarcely affected and that the addition of particles does not affect the final structure of the network. Rheologic studies have shown the increase in the viscoelastic properties on adding the filler and allow the percolation threshold to be calculated, which was found to be 35.5%. The use of BN agglomerates of bigger size increases notably the viscosity of the formulation. Glass transition temperatures are not affected by the filler added, but Young's modulus and hardness have been notably enhanced. Thermal conductivity of the composites prepared shows a linear increase with the proportion of BN particle sheets added, reaching a maximum of 0.97 W/K·m. The addition of 80 µm agglomerates, allowed to increase this value until 1.75 W/K·m.

Keywords

cycloaliphatic epoxy resin; composites; thermal conductivity; boron nitride; thiol-epoxy

1. Introduction

Nowadays, electronic and electrical industries have an increasing need to dissipate the heat of devices, which is produced by the Joule effect. This leads to a continuous demand of thermal conductive coatings and adhesives, with high electrical insulation capability. This demand is originated by the constant miniaturization, integration and functionalization of electronics and the appearance of new applications such as flexible electronics, light emitting diodes, etc. In this sense, heat management is of special interest in electronic components since they can be deserved for greater power output, improved efficiency and lengthening of half-life time and prevention of premature failures of devices [1]. These kind of thermally

conductive polymers finds also usage in other applications like aerospace industry, heat exchangers and corrosion-resistant coatings and therefore the research in these materials is in constant development [2].

Thermal energy is defined by the existence of microscopic vibrations of particles. The temperature, describing the state of a body, is a physical property quantifying those microscopic thermal vibrations of the particles. Heat is directly related to the thermal conductivity (TC) and has been defined as the thermal energy transfer from a specific point to its surroundings due to the temperature gradient [3]. Thus, temperature is produced by particles vibration and heat evaluates how much of this energy is transferred, how fast and in what direction.

Although epoxy resins are extremely valuable materials in coatings and adhesion applications, thermal conductivity of these polymer resins is in the low range from 0.1 to 0.3 W/m·K. The addition of inorganic filler particles into the epoxy material can significantly improve the TC and can also affect the mechanical properties of the composite. However, this constitutes the easiest way to reach the aimed technological goals such as heat dissipation [4–6]. Among inorganic fillers, hexagonal boron nitride (BN) is structurally analogous to graphite and has similar thermal conductivity [7,8]. However, for potential electric/electronic applications, BN composites have several advantages over those based on graphene, because of BN is a non-electrically conductor [9].

It has been reported that the filler type, loading level, filler size, and filler shape have a strong influence on the thermal conductivity of polymer composites. Creating a continuous filler network is the key point to reach high TC in composite structures. Network formation usually takes place at high filler loading levels and it is related to the percolation threshold that can be calculated by rheological measurements. It should be noticed that a too high filler content worsens the processability and mechanical properties and increase unnecessarily costs and densities.

The interaction between filler and polymer matrix is also important in terms of TC enhancement [10]. Phonons are the responsible of heat transmission in amorphous polymers. Because of the mismatches between BN surfaces and the polymer, the interface will result in phonon scattering and hinder the heat transfer. Therefore, improving polymer-filler interfacial interaction can increase the overall composite TC substantially [11]. Several authors reported the modification of BN nanosheets [12,13]. Hexagonal BN particles have a smooth plate-like shape with no available surface functional groups for chemical bonding, but BN particles have hydroxyl and amino groups at the edge planes. Using a simple sol–gel process by reaction with a functional silane compound a higher adhesion between particles and polymeric matrix can be reached with a notable enhancement in TC [13,14].

Recently, Hutchinson et al. [15] reported a notable increase in TC in thiol-epoxy materials filled with BN, without the need of functionalization of the particles. In fact, the thermal conductivities of thiol-epoxy materials were superior to those of the epoxy cured with Jeffamine, which was attributed to a better interface interaction between particles and matrix. They also reported that the increase in TC with filler content was also quicker in thiol-epoxy systems, although high proportions of filler could not be investigated because of the bad workability of the mixture caused by the high viscosity.

Taking into account the improvement in TC of thiol-epoxy materials and the need of a low viscosity of the reactive mixture, we proposed in the present work the use of a cycloaliphatic epoxy resin (ECC) with a commercial tetrathiol (PETMP) as the starting reactive mixture, filled with different proportions of BN filler. The curing of cycloaliphatic resin with thiols in the presence of a tertiary amine, acting as a base, has been previously developed in our research group [16]. The reactive mixture has a low viscosity, which allows adding a high content of BN to the formulations and the materials obtained have a good transparency. As demonstrated in previous publications, this curing system is very versatile since the curing rate and properties of the materials can be tailored by changing the type of amine and the epoxy and thiol structures, respectively [17,18]. Moreover, the polycondensation type polymerization mechanism allows the preparation of more homogeneous networks than those obtained by cationic polyetherification of cycloaliphatic epoxy resins [19]. In that work, the low viscosity of the cycloaliphatic epoxy resin allowed us to reach a 800% of TC enhancement by adding a 40% of unmodified BN as the filler.

Gaska et al. [4] reported that larger particle sizes as agglomerates can lead to higher TC values, according to that, we also try in the present work to improve thermal conductivity by increasing the size of the BN particles. However, the addition of larger particles can negatively affect other properties, like the mechanical performance or viscosity of the formulation.

The effect of the BN content and the increase in the size of the BN particles on the curing kinetics, viscosities, rheological behavior and gelation phenomena is reported in the present paper together with the thermal and mechanical characterization of the composites obtained.

2. Materials and Methods

2.1. Materials

3,4-Epoxy cyclohexylmethyl 3,4-epoxycyclohexane carboxylate (ECC) (ERL-421D, EEW=126.15 g/epoxy eq) was provided by Dow Chemical Company (Midland, MI, USA). 4-(*N*,*N*-dimethylamino)pyridine (DMAP) was used as initiator, grinded before use and provided by Fluka Analytical (Neu-Ulm, Germany). Pentaerythritol tetrakis (3-mercaptopropionate) (PETMP) (ETW=122.165 g/thioleq) was purchased by

Sigma-Aldrich (Darmstadt, Germany) and used without further purification. Platelets of hexagonal boron nitride (BN) were supplied by ESK Ceramics GmbH (Kempten, Germany), TPC 006, with an average particle size of 6 µm and an agglomerate of 80 µm average, PCTL5MHF, was supplied by Saint-Gobain (Valley Forge, PA, USA) and both were used as received.

2.2.Sample Preparation

The neat mixture was prepared by mixing stoichiometric proportions of ECC and PETMP and adding 1 phr (parts per hundred of resin) of initiator. For composite samples, the required amount of BN was added in wt. % to the neat formulation before curing. The mixtures were mechanically stirred until homogeneity was reached. Finally, the samples were poured onto aluminum molds and cured at 120 °C during 1h, followed by a post-curing at 150 °C for another 1h and a final step at 200 °C for half an hour.

2.3. Characterization Techniques

To analyze the curing evolution of the epoxy system, a differential scanning calorimeter (DSC) Mettler DSC-821e (Mettler Toledo, Columbus, OH, USA) was used. The device was calibrated using an indium standard (heat flow calibration) and an indium-lead-zinc standard (temperature calibration). Samples of about 5–10 mg were essayed in aluminum pans with a pierced lid in N_2 atmosphere with a gas flow of 100 mL/min. The scans were performed in the temperature range of 30 to 250 °C with a heating rate of 10 K/min. Curing enthalpies (Δh) of the different samples were calculated by integration of the calorimetric signal. Glass transition temperatures (T_g) of cured samples were evaluated by a second scan as the temperature of the half-way point of the jump in the heat capacity curve. The estimated error was considered to be ±1 °C.

Thermal stability of neat and composite materials was evaluated by thermogravimetric analysis (TGA), using a Mettler-Toledo TGA/DSC 1 Star system (Mettler Toledo). Experiments were performed under N_2 atmosphere (flux 50 mL/min). Pieces of cured samples of 5–10 mg were degraded between 30 and 600 °C at a heating rate of 10 K/min.

Dynamic mechanical thermal analyses (DMTA) were performed by employing a TA Instruments DMA Q800 device (TA Instruments, New Castle, DE, USA). Samples were isothermally cured in an aluminum mold at120 °C for 1 h, then at150 °C for 1 h and finally post-curing at 200 °C for 30 min. Prismatic rectangular samples (15 × 5.0 × 2.3 mm^3) were tested in 3-point bending mode at a heating rate of 3 K/min in the temperature range from 35 to 125 °C, with a frequency of 1 Hz and oscillation amplitude of 0.1% of sample deformation. The Young's moduli (E) were determined at 30 °C by using a force ramp at a constant rate, 1 N/min, never exceeding 0.25% of

deformation to be sure that only elasticity was evaluated. The slope between 0.1% and 0.2% of deformation was taken. *E* was calculated from the slope of the load deflection curve according to the following equation:

$$E = \frac{L^3 m}{4bt^3} \qquad (1)$$

where *E* is the elastic modulus of the sample (MPa), *L* is the support span (mm), *b* and *t* are the width and the thickness, respectively, of the sample tested (mm) and *m* is the gradient of the slope in the linear region (N/mm).

Thermomechanical analyses (TMA) were performed on a Mettler TMA40 thermomechanical device (Mettler Toledo). Thermosetting samples (9 × 9 × 2.3 mm^3) were supported by the clamp and one silica disc to uniformly distribute the force and heated at 5 °C/min from 32 up to 120 °C by application of a minimum force of 0.01N, to not distort the results. Two heating scans were performed, being the first to erase the thermal history and the second to determine the thermal expansion coefficients (CTEs), below and above the T_g. They were calculated according to the following equation:

$$CTE = \frac{1}{L_0} \cdot \frac{dL}{dT} = \frac{1}{L_0} \cdot \frac{dL/dt}{dT/dt} \qquad (2)$$

where *L* is the sample thickness, $L_0$the initial length, *t* the time, *T* the temperature and *dT*/*dt* the heating rate.

Surface fractures were examined by using a FEI Quanta 600 environmental scanning electron microscope (ESEM, FEI Company, Hillsboro, OR, USA) that allows collecting electron micrographs at 20kV and low vacuum mode of uncoated specimens with low electron conductivity. A working distance (WD) of ca. 10 mm was used.

Microindentation Knoop hardness was evaluated by using a Wilson Wolpert 401 MAV apparatus according to ASTM D1474-13 (Wolpert Wilson Instruments, Aachen, Germany). A minimum of 20 determinations were made for each material with a confidence level of 95%. The Knoop microindentation hardness (KHN) was calculated by using the equation:

$$KHN = \frac{L}{A_P} = \frac{L}{l^2 C_P} \qquad (3)$$

where *L* is the load applied to the indenter (0.025 Kg), A_P is the projected area of indentation in mm^2, C_P is the indenter constant (7.028 × 10^{-2}) relating l^2 to A_P.

Rheometric experiments were done in parallel aluminum plates (geometry of 25 mm Ø) mode by using a TA AR G2 rheometer (TA Instruments, New Castle, DE, USA), with electrical heated plates (EHP). Viscoelastic characteristics, *G′* (shear elastic modulus) and *G″* (viscous modulus), were determined with a constant deformation in the linear viscoelasticity range for each formulation, obtained from constant *G′* in a

strain sweep experiment at 1 Hz, at 30 °C. The curing was followed at 85 °C to determine gel point and conversion at gelation. Gel time was taken as the point where tan δ is independent of frequency [20]. The conversion at the gelation (x_{gel}) was determined by stopping the rheology experiment when gelation occurred and the sample was quenched in liquidN_2.Then, the remaining enthalpy was evaluated by a dynamic DSC experiment at 10 K/min. The degree of conversion in the gelation was calculated according to the following equation:

$$x_{gel} = 1 - \frac{\Delta h_g}{\Delta h_T} \qquad (5)$$

where Δh_g is the heat released up of gelled samples, obtained by integration of the calorimetric curve, and Δh_T is the heat associated with the complete curing.

The volumetric content of BN of the different materials prepared was calculated taking into account the densities of the composites determined by means of a liquid pycnometer. The densities of pure BN were taken from the data sheet published by the commercial source company.

Thermal conductivity was determined using the Transient Hot Bridge method by a THB 100 device from Linseis Messgeräte GmbH (Selb, Germany). A HTP G 9161 sensorwith a 3 × 3 mm^2 of area was used. The sensor was calibrated with poly(methylmethacrylate) (PMMA), borosilicate crown glass, marble, Ti-Al alloy and titanium. Two equal rectangular samples, perfectly polished, with size of 12 × 12 × 2.3 mm^3 were placed at both faces of the sensor. Because of the small size of sensor, the side effects can be neglected. Measuring times of 100 s with a current of 10 mA were applied. Five measures were taken for each material.

3. Results and Discussion

3.1.Study of the Curing Process

Our research team reported for the first time the thermal curing of biscycloaliphatic epoxy compounds by thiols in the presence of tertiary amines to form new thiol-epoxy thermosets [16]. In our previous publication, we showed that among other tertiary amine catalysts, DMAP was the most suitable to reach the controlled curing of those stoichiometric systems by this thiol-epoxy click reaction. In diglycidylether of Bisphenol A (DGEBA) resins, Hutchinson et al. [15] observed that the reaction kinetics of a thiol-epoxy system was affected by the amount of BN filler added to the formulation, showing an unexpected trend, firstly increasing the curing rate and then retarding it as the filler content increases, without affecting the final cured epoxy network structure. The variations in the reaction kinetics were attributed to an improvement of the interface forces between particles and matrix as a consequence of a Lewis acid-base interaction which finally led to a notable enhancement in the thermal conductivity [15].

The lower viscosity of cycloaliphatic epoxies in front of DGEBA resins opens the possibility to increase the BN content in the formulation and that led us to start the study of a new BN-filled thiol epoxy system. In this study, we have used 1 phr of DMAP in a stoichiometric formulation of ECC/PETMP with different amounts of BN (10–40 wt. %) of 6 µm average. With the aim to corroborate that the size of the particles plays an important role in the TC we have also prepared a composite with greater particles of BN (80 µm agglomerates). In **Scheme 1** the chemical structures of the monomers selected and the network formed are represented.

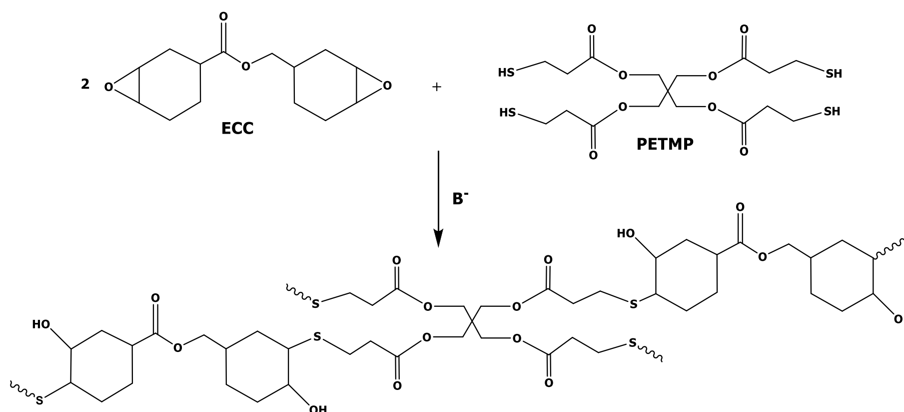

Scheme 1. Chemical structures of the monomers used and the network formed during the curing process.

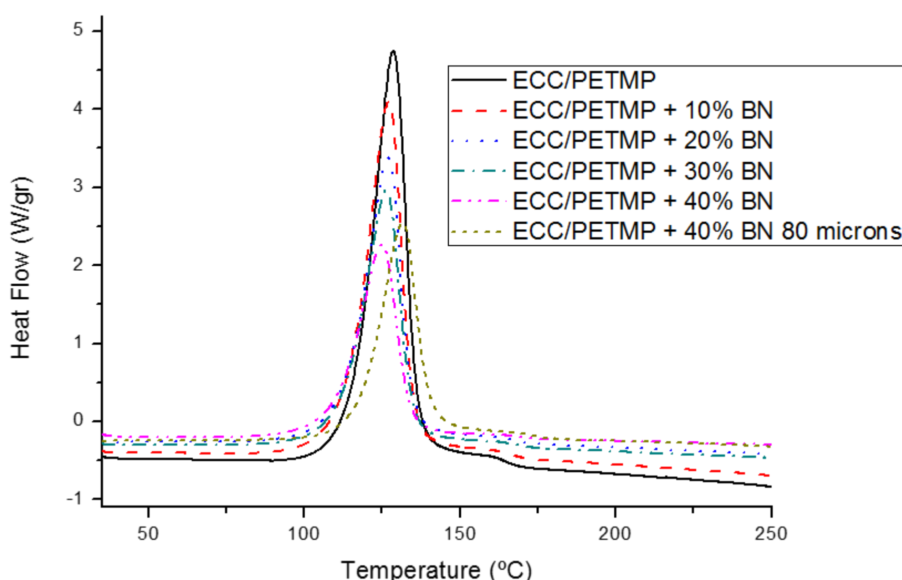

Figure 1. DSC curves showing the effect of the addition of different proportions of BN in wt. % to the formulation.

As we can see, on increasing the proportion of BN in the formulation no much effect is observed, only a slight shift of the maximum of the curing exotherm to lower temperatures and a decrease in the height of the curve, indicating a reduction in the curing rate of the system. However, the addition of the filler with bigger particle size provokes a greater effect, since a displacement of the maximum of the exotherm of 7 °C in reference to the formulation with the same proportion of 6 µm BN is clearly detected. In previous studies of our group in the preparation of BN composites by the cationic homopolymerization of epoxy resins [19,21] we observed much variation in the kinetics of DGEBA matrices than in ECC. As reported, the addition of BN to thiol-DGEBA resins led also to kinetics influence [15]. All these results seem to suggest that DGEBA resin systems are likely to interact better with BN. From the values of the table, it can be seen that the addition of particles does not affect the final structure of the network. This is explained, because of the heat evolved during the dynamic calorimetric scans and the glass transition temperatures (T_g) determined remain practically constant for all the formulations, with a slight decrease in the enthalpy released at the highest proportion of BN, probably due to topological restrictions in curing.

Table 1. Calorimetric data of formulations ECC/PETMP with several proportions of BN.

BN (wt. %)	T_{max}[a] (°C)	Δ*h*[b] (J/g)	Δ*h*[b] (kJ/ee)	T_g[c] (°C)
0	127	479	120	58
10	126	436	121	58
20	126	376	118	57
30	125	337	121	57
40	124	272	114	57
40 (80 µm)	131	276	116	58

[a] Temperature of the maximum of the curing exotherm.
[b] Enthalpy of the curing process by gram of mixture or by epoxy equivalent.
[c] Glass transition temperature determined by the second scan by DSC after a dynamic curing.

3.2. Rheological Study of the BN Formulations

Any material that cannot be classified as purely elastic or as viscous has a viscoelastic behavior. Polymeric systems, especially those with two or more components, do not obey the Newton's law of viscosity and present different phenomena since they are considered structured fluids. The design of many industrial processing operations requires taking into account several of these phenomena [22], since their behaviour is generally dictated by the interactions among the components.

The study of filled uncured formulations is recommended to be done by oscillatory experiments and must be performed in the material's linearity region (LVR) to determine the viscoelastic properties. Thus, a good initial step is to measure the storage and loss moduli (*G'*, *G''*) dependence with the strain amplitude. **Figure 2** represents *G'* (more sensitive than *G''*) versus percentage of strain applied at 30 °C for

mixtures without base catalyst to prevent any reaction. It can be observed how the unfilled formulation presents an almost constant storage modulus in all the strain range tested, which means that it has a Newtonian behavior. With the increasing filler content, the Newtonian plateau is shifted to lower strains and became shorter as observed in previous studies [19,21]. However, there is a significant difference at high deformations in the more filled formulations when comparing with these previous studies: it is an increase of the *G′* with a shoulder shape. Some materials show this behavior due to structure reorganization as the result of the applied deformation, as reported by Laun in polystyrene-ethylacrylate latex particles in water [23]. In our case, the fact that the only difference is the presence of thiol monomer in the mixture, could mean that there was an interaction of thiols with the BN particles. In contrast, the agglomerates only present the typical shear thinning of systems loaded with particles, almost in the frequency range tested, and the plateau is moved even to lower strain. According to the results, the strain was fixed in the LVR for each mixture to perform the oscillatory sweep tests, measuring parameters as function of frequency (ω).

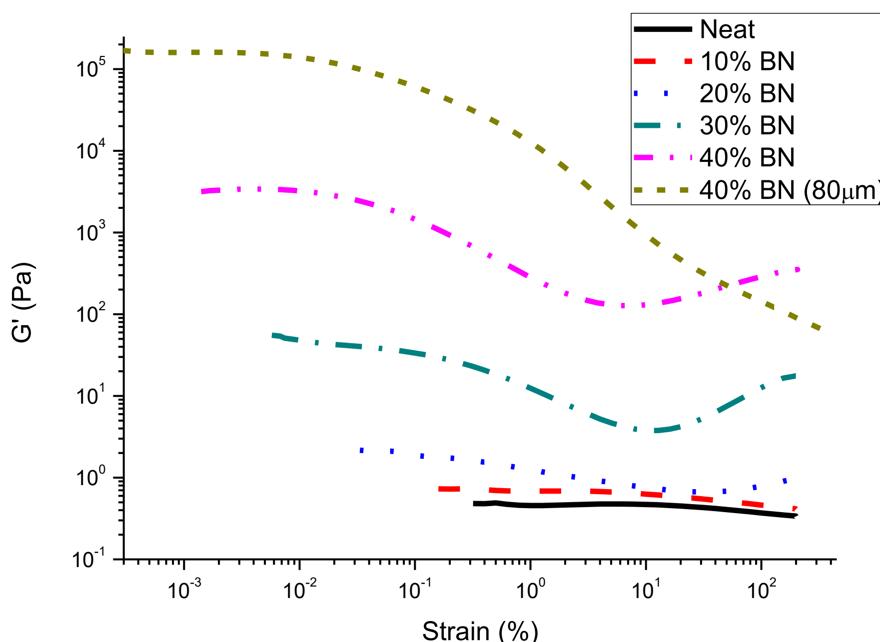

Figure 2. Plot of log *G′* versus log % strain in oscillatory experiment (1 Hz) of uncured formulations.

To reach good thermal conductivities and to go deeply in the knowledge of our filled system it is interesting to determine the viscoelastic percolation threshold. Percolation is the point in which the particles contact and create a network structure, and the percolation threshold is the minimum filler content in the matrix that produces this network. At this filler percentage a notable change in thermal conductivities and some other properties, can be in principle being observed. To determine this value we have represented *G′* (elastic property) and *G″* (viscous property) curves as function of

frequency (**Figure 3**) for all the mixtures studied. We have also included two new mixtures (35 and 38 wt. %) to determine the percolation value more accurately.

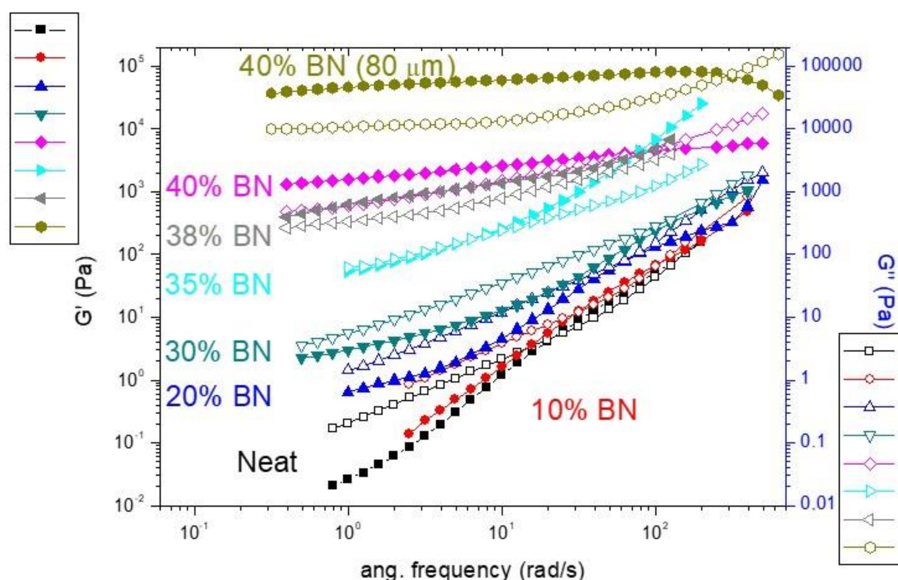

Figure 3. Plots of *G'* (filled symbols) and *G"* (open symbols) against *ω* for all the formulations at 30 °C.

First, it can be seen in the figure that the effect of BN particles in the mixture on *G'* and *G"* is not significant at high frequencies (Rouse dynamic region). However, in the region related to reptation dynamics, at low frequencies, the effect is quite important [24]. Moreover, how it was expected, unfilled resin greatly follows the linear viscoelastic rule [25] ($G'\propto\omega^2$ and $G''\propto\omega^1$) at low frequencies, but with the increasing content of BN, the slopes continuously decline until the maximum concentration of filler added (40 wt. %), where *G'* is practically constant on varying the frequency which means that percolation threshold is overpassed.

Above the percolation threshold, the point at which an interconnected network of particles through the whole material is formed, the behavior of the mixtures should obey the scaling law relation at a fixed frequency, that can be used to determine the rheological percolation [26,22]:

$$G' \propto (m - m_c)^{\beta} \qquad (5)$$

where *G'* is the storage modulus, *m* is the mass fraction of BN composites, m_c is the mass fraction at the rheological percolation and β is the critical exponent. The threshold was calculated to be 35.5 wt. % and the critical exponent 2.4 at 1 rad/s.

It is worth noting that the BN percentage in the percolation threshold is much higher in this system than in the previous study based on BN composites with cationically homopolymerized epoxy matrices (14.4% for ECC and 6.9% for DGEBA)

[19,21]. For this reason, two stablished criteria were utilized to confirm the proportion of BN at the percolation calculated previously.

Numerous studies take as valid the criterium for percolation of $G' \sim \omega^{0.5}$ in the terminal region in small amplitude oscillatory shear (SAOS) experiments [24,27–28]. The slope in *G′* versus frequency reach a value of 0.5 between formulations with a filler content of 35% and 38% (see **Table 2**), agreeing this range with the previous calculations.

Finally, the second criterium employed is an interpretation of Rouse-like behavior: at percolation *G′* and *G″* at low frequencies become equal (see Figure 3) [24]. Then, the rheological response at the percolation threshold must show the transition from liquid-like behavior (*G″*>*G′*) to a solid-like behavior (*G′*>*G″*). This change is also observed in **Figure 3** between the formulations with 35 and 38 wt. % of BN.

Table 2. Rheological fitting results at 30 °C and gelation data from rheometric monitoring of the curing of the formulations at 85 °C.

BN (wt. %)	G'_{slope} [a] (Low Freq.)	G''_{slope} [a] (Low Freq.)	t_{gel} [b] (Min.)	x_{gel} [c] (%)
0	1.81	1.02	16.3	59
10	1.77	1.06	17.8	62
20	1.34	0.99	18.3	60
30	0.62	0.84	18.4	55
35	0.57	0.66	-	-
38	0.36	0.27	-	-
40	0.22	0.24	19.5	55
40 (80 µm)	0.11	0.08	-	-

[a] Slopes of viscoelastic properties at low frequencies (potential functions in log-log diagrams).
[b] Gel time determined from the frequency independent crossover of tan δ.
[c] Determined as the conversion reached by rheometry and DSC test at 10 °C/min.

Comparing the rheological behavior of these systems with those previously reported, it is possible to predict a better application as a coating with the same filler loading.

From a practical point of view, it is quite important to know about the gelation phenomenon produced during curing. Gelation occurs when soluble reactants are irreversibly transformed into a three dimensional, infusible and insoluble network. At this point, the system loses its ability to flow and therefore it must be avoided during industrial processing before the shaping of the final material. The polycondensation mechanism in the present thiol-epoxy system must obey the Flory equation and the conversion in the gelation should depend only on the functionality of the monomeric compounds involved in the curing process. Thus, large differences are not expected if BN particles do not play a role in the network formation (although they can be reactive

by the presence of reactive groups in the edges of BN sheets). Table 2 shows the data obtained from the gelation studies by rheological measurements at 85 °C. Since filler contents of 35% and 38% were only added to calculate percolation thresholds, the gelation data of these formulations have not been evaluated.

As we can see, there is an increasing trend, although small, in gelation time on increasing the BN proportion. This behavior contrasts with the observed in previous studies on polymeric systems with particle additions [21,29]. This delay to reach the gelation could be attributed to the steric hindrance caused by the BN particles in the formation of the three-dimensional network structure. Moreover, as expected, the conversions at the gelation are kept practically constant for all the mixtures, which confirms that BN particles only act as filler and that the ending groups in the edges of the BN sheets does not participate in the curing. The results obtained in the gelation studies are interesting from the point of view of the application, since the addition of particles allows increasing the pot life of the reactive mixture and does not reduce the conversion at the gelation, in contrast with the results reported in our previous study [21]. In the previous work, the cationic ring-opening homopolymerization mechanism of curing led to a reduction in the conversion at the gelation and to a shorter gelation time. It is important to note that after gelation the material loses its mobility and stresses and small defects could appear because of the shrinkage produced. These problems will be reduced when gelation occurs at higher conversion. The gel point of formulation prepared with 80 µm agglomerates was not evaluated by this technique because of the lack of comparison with other proportions.

3.3. Thermal and Mechanical Characterization of BN Composites

Thermogravimetric analysis is the most powerful tool to characterize the thermal stability of the polymeric materials once cured. **Figure 4** represents the degradation curves under inert atmosphere.

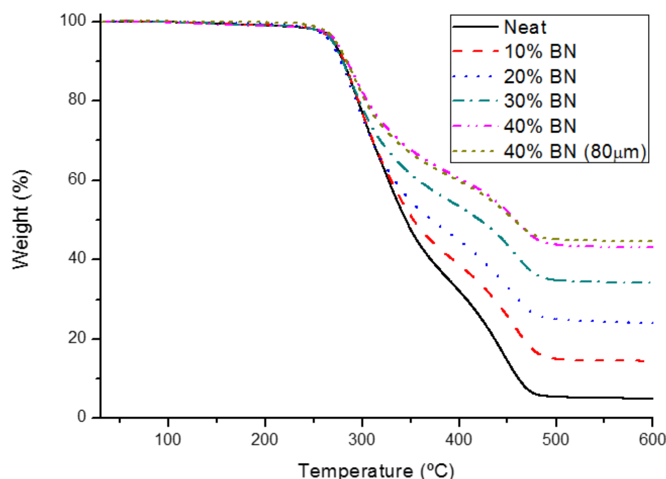

Figure 4. Degradation curves of thermosets obtained by TGA under inert atmosphere at 10 K/min.

All the curves show a similar shape, only differentiated in the final residue that results in accordance with the quantity of filler added and a slight increase of the temperature of maximum degradation rate on increasing the BN content in the material (see **Table 3**). Thus, it can be considered that the degradation mechanism is not affected by the presence of BN, since the network structure of the matrix does not change. In the curves, it can be observed two degradation steps because of the presence of ester groups, both in PETMP and in ECC. The lowest temperature degradation step is related to the decomposition of these ester groups by a β-elimination process that leads to the breakage of the network structure at lower temperatures, and the second one to the scission of the other bonds that occurs simultaneously. It was found in a previous study that the addition of BN to a homopolymerized DGEBA matrix did not significantly affect the thermal stability of composites [21] but in contrast, the temperature of initial degradation suffered an increase of 70 °C on adding a 40% of BN to the cationic homopolymerized ECC matrix [19]. The change in the particle size does not produce great significant changes in the thermal stability behavior of the composites, but only a slight enhancement in the initial degradation temperature and char yield.

Table 3. Thermal data of composites extracted from TGA and TMA analysis.

BN (wt. %)	BN (vol %)	$T_{2\%}$ [a] (°C)	Char Yield [b] (%)	CTE_{glass} [c] ($10^{-6}\cdot K^{-1}$)	CTE_{rubber} [c] ($10^{-6}\cdot K^{-1}$)
0	0	249	5.0	69	195
10	6.0	250	14.4	68	192
20	12.8	249	24.0	66	166
30	20.2	250	34.2	67	157
40	28.2	252	43.0	55	134
40 (80 µm)	27.4	259	44.7	43	135

[a] Temperature of 2% weight loss determined by TGA in N_2 at 10 °C/min.

[b] Char residue at 600 °C.

[c] Thermal expansion coefficient in the glassy state determined between 38–52 °C and in the rubbery state between 70–90 °C.

Dimensional stability is an important issue when epoxy resins are applied as coatings on any surface, usually metals or ceramics, with a CTE lower than polymers. Oscillating temperature changes can produce premature failures such as separation, blistering, delamination, etc., because of the internal stresses produced by the disparity in their thermal expansion coefficients. To reduce that difference will be beneficial for coating materials to prevent failures and it is known that the addition of BN ceramic particles must positively affect this characteristic [30]. Table 3 presents the CTE values obtained by TMA in the vitreous and in the rubbery state. In the glassy state, there is not a significant change until the value reached for the sample with a 30% BN with a great reduction at 40%, which is the maximum concentration achieved in the composite. This important reduction in CTE between 30 and 40 wt. % of BN

could be related to the percolation achieved between these proportions that could lead to a restricted expansion. It has been reported [31] that filler size is an important factor influencing the CTE of composites and that small particles can function effectively to lower the CTE of composites. However, the contrary effect was observed in the present study and the lower CTE was obtained by adding 80 m BN agglomerates. In the rubbery state, where the matrix is completely relaxed, the diminution is significant above 20 wt. %. Contrary to what observed in the glassy state, there is no difference with the use of bigger agglomerates.

Thermomechanical analysis was performed with DMTA. The filler play the role of matrix reinforcement conferring to material better mechanical performance. **Table 4** reports the most important information extracted from the study.

Table 4. Thermomechanical data of composites varying BN concentration.

BN (wt. %)	Young's Modulus[a] (GPa)	$T_{\tan\delta}$[b] (°C)	E'_{rubber}[c] (MPa)	$Peak_{area}$[d]	FWHM[e] (°C)
0	2.3	75	6.9	1.37	13.7
10	2.4	74	10.4	1.28	14.6
20	3.6	73	19.6	1.27	14.8
30	4.5	73	31.9	1.13	16.0
40	5.6	74	61.2	0.90	16.8
40 (80 μm)	4.0	71	78.5	0.88	19.3

[a] Young's modulus determined with DMTA at 30 °C in a controlled force experiment using three point bending clamp.
[b] Temperature of maximum of the tan δ peak at 1 Hz.
[c] Relaxed modulus determined at the $T_{\tan\delta}$+ 40 °C (in the rubbery state.
[d] Area of tan δ peak between 40 and 120 °C.
[e] FWHM stands for full width at half maximum.

As we can see, Young's modulus gradually increases with the proportion of particles added. The composite with 40 wt. % of BN shows an improvement higher than 140% in rigidity compared to unfilled material. This is thanks to the anisotropic shape of the BN sheets and to the larger specific surface of these particles. As opposed, the spherical shape of the agglomerates leads to a different behavior when they act as reinforcement. Thus, with agglomerates, the enhancement in Young's modulus is about 74% compared with the neat resin.

Figure 5A shows the variation in the storage modulus with the temperature for the different filler proportions. As we can see, *E'* is closely related with the filler content because the applied stress is transferred from the polymeric matrix to the BN particles, that have an inherent high modulus. Moreover, the storage modulus in the rubbery state reaches a higher value in the composite obtained with the big agglomerates. This is because in the rubber state, the movement of larger particles is restricted by the other adjacent, while small particles have more freedom of movement and therefore, the material is softer and more deformable.

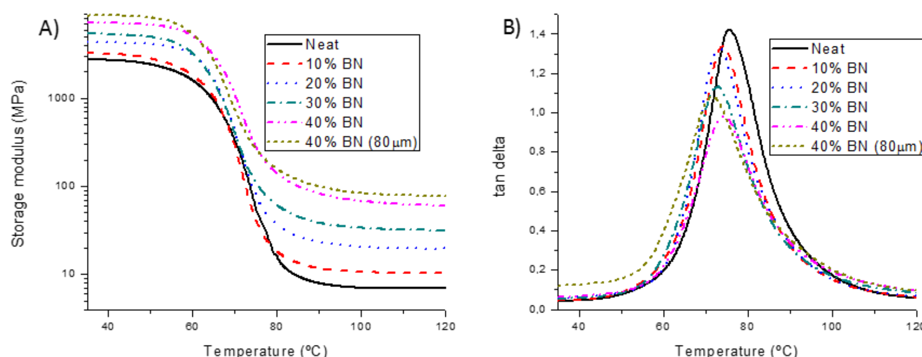

Figure 5. Variation of storage modulus (**A**) and tan δ (**B**) against temperature of the different materials prepared.

In the representation of tan δ against temperature shown in **Figure 5B** we can see that all the composites filled with BN sheets have a quite similar shape and a similar temperature of the maximum (see Table 4) and no much differences were observed in the curves obtained with the composite with agglomerates. The fact that tan δ peak temperatures are not affected by the BN content seems to confirm that no important interactions between filler and matrix exist. This behavior is contrary to that observed previously by us for homopolymerized ECC matrices [19], with enhancement in tan δ values of more than 25 °C. The area of the tan δ peak, which can be associated to the damping characteristics, is decreasing with the increasing amount of filler according to the lower polymer content that can be relaxed. The peak broadens on increasing the BN content, which can be related to the increasing inhomogeneity of the material.

Since hardness is a desired property for resistance and durability of coatings we have rated how the addition of BN to the neat material affects it. In Figure 6 the Knoop hardness has been represented for all the materials prepared. The increase of BN proportion in the composite leads to an increasing tendency of this characteristic and the maximum is achieved at 40% of BN content. As occurs in the Young's modulus behavior the addition of agglomerate particles of BN worsens hardness characteristics, due to their big size and less surface of interaction that leads to a smaller reinforcement effect. When comparing these materials to the ones based on homopolymerized ECC (from 11.7 to 26.6), we can see that the reaction with thiols reduced hardness characteristics, because of their flexibility and to the more open network structure formed. Moreover, the increase in hardness with the proportion of BN is much lower in thiol-epoxy materials (50% in front of 150% at 40 wt. % of BN content) [19].

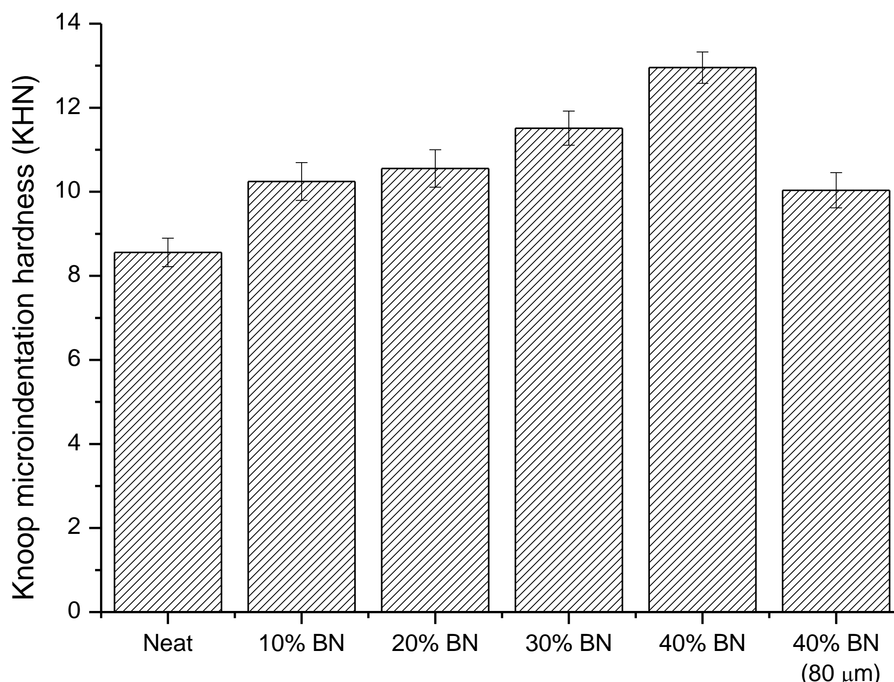

Figure 6. Dependence of the microindentation hardness of ECC/thiol thermosets with different weight percentages of BN.

3.4.Morphology Inspection of BN Composites

Fracture surfaces were analyzed by ESEM, and the most representative micrographs are collected in **Figure 7**. Neat polymer has not-linear rupture trajectories with thicker breaks and river-like cracks that accounts for a plastic rupture. On increasing the amount of BN in the formulation, the rupture lines become shorter and more complex due to the action of BN particles that leads to start new paths of breakage. This variation should produce an increase in resilience, the energy absorbed in an impact. If we look at the micrograph of the sample with 10% of BN we can state that it presents a fairly good homogeneity of particle distribution. On increasing the amount of BN the distribution remains homogeneous, but the sample with 40% of BN seems to present a more fragile rupture, that agrees with the percolation achieved in the BN network. As we can see in the corresponding micrograph, the addition of a 40% BN agglomerates leads to a quite inhomogeneous material with a fragile fracture due to the presence of bigger and smaller particles and agglomerates and low adhesion between both organic and inorganic phases.

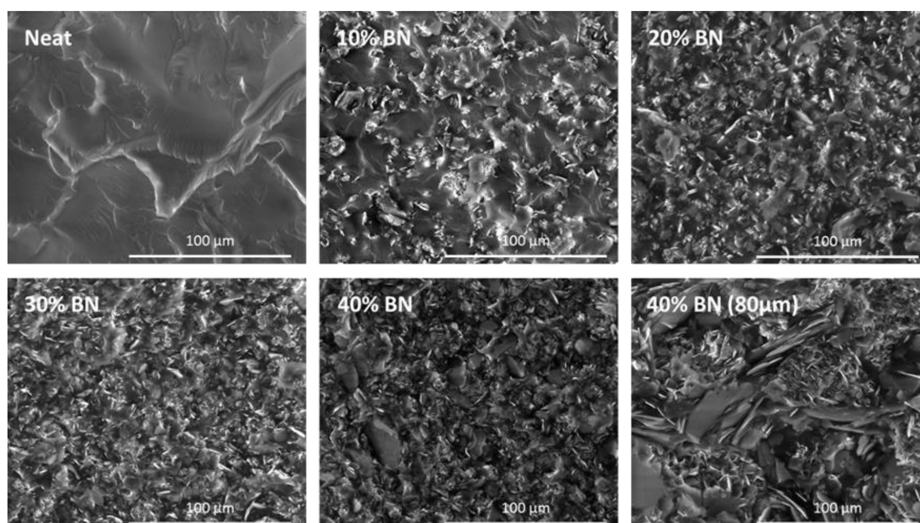

Figure 7. ESEM micrographs of fracture surfaces of the materials prepared at 800 magnifications.

3.5. Thermal Conductivity of BN Composites

The final goal of this study is to increase thermal conductivities of thiol-epoxy matrices by addition of BN. Thus, the thermal conductivity of the thermosets prepared has been measured and the values are represented in **Figure 8**.

As we can see, there is a regular improvement in the thermal conductivities with the proportion of BN and at the proportion of 40% an increase of about 400 % has been reached. This value of thermal conductivity (0.97 W/K·m) is close to that determined for homopolymerized ECC resins with the same proportion of BN (1.04 W/K·m) [19]. The difference can be attributed to the different particle-matrix interaction in both materials, better in homopolymerized ECC according to the participation of hydroxyl end-groups in the BN in the homopolymerization mechanism.

The conductivities measured in this study do not reach the values obtained by Hutchinson et al. [15] in DGEBA-thiol systems, which are higher than 2 W/K·m using the same type of BN as filler. However, the values obtained in the present study are similar or even higher than some reported in the literature [13,32–34].

It is worth noting that the addition of bigger agglomerate particles has led to a notable improvement in this characteristic and the value of 1.75 W/K·m (775% increase) has been reached. The enhanced value can be explained according to that reported by Gaska et al. [4] who reached high values by using bigger particle sizes, because of heat transfer through the polymer matrix is much less efficient than through the crystalline filler. Since the main reason of the low thermal conductivity in polymer composites is the phonon scattering, especially at the interfaces, it is foreseeable that at a determined filler loading the thermal conductivity increases with

increasing particle size due to the smaller interfacial area between filler and matrix [31]. In contrast, many authors have reported that nanoparticles produces better enhancements in thermal conductivity [31,35]. This improvement is probably due to an increase of the intrinsic thermal conductivity of fillers, connected to a symmetry-based selection rule that strongly suppresses phonon-phonon scattering in 2D particles [36]. However, the use of nanoparticles enlarges the amount of filler-matrix interfaces and they seem not to be the best choice to obtain high thermal conductivity composites [3].

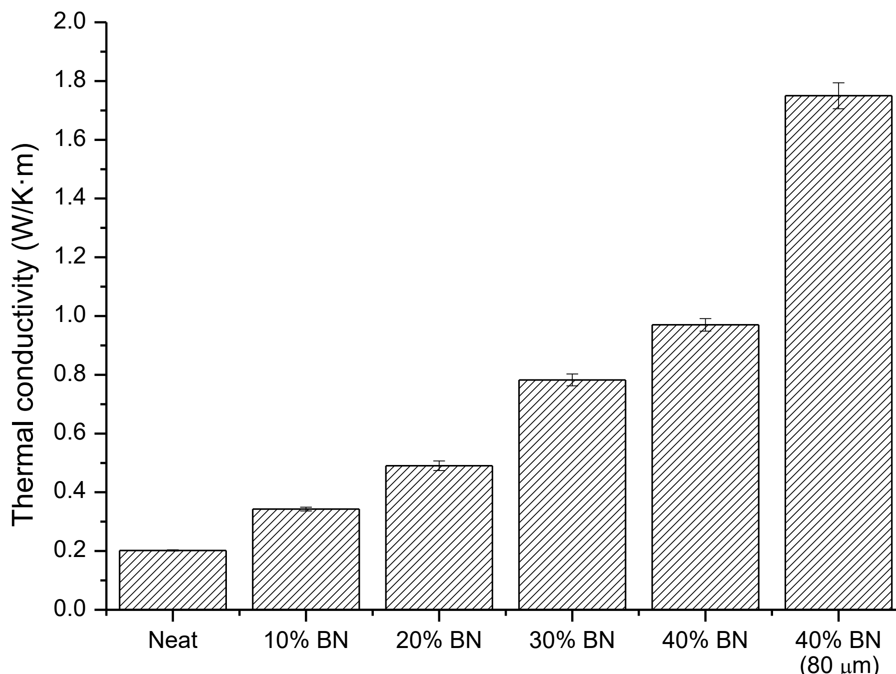

Figure 8. Thermal conductivity of the neat material and composites prepared.

In our case, by using 80 μm agglomerates, there is a great dispersion in particle sizes and a big amount of interphases, which can reduce the expected increase in thermal conductivity if the particles were purely crystalline. **Figure 9** shows the ESEM micrographs of the pure BN agglomerates.

After curing (see Figure 7) both agglomerates and separated nanosheets can be observed dispersed in the polymeric matrix, in which big and small BN particles are well distributed. It is foreseeable that inside the agglomerates may not have penetrated the resin, subsequently reducing the interaction area in comparison to what happens in the BN sheets.

Polymers **2018**, *10*, 277-292

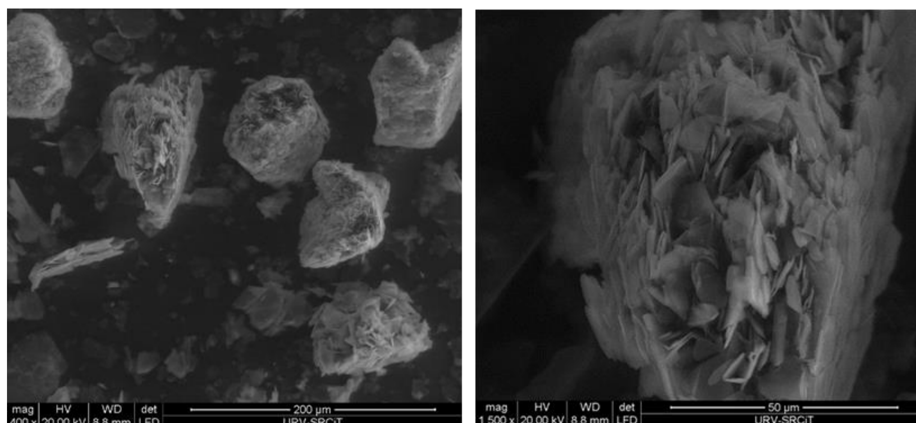

Figure 9. ESEM micrographs of the pure BN agglomerates at 400 (**left**) and 1500 (**right**) magnifications.

4. Conclusions

Calorimetric studies put into evidence that the kinetics of the curing was scarcely affected and that the addition of particles did not affect the final structure of the network. There is an increasing trend, although small, in gelation time on increasing the BN proportion in the formulation but no differences were observed in the conversion at the gelation, which indicates that BN particles did not play a role in the curing mechanism.

The percolation threshold was calculated by rheometry to be 35.5 wt. % and the critical exponent 2.4 at 1 rad/s.

The thermal stability and the degradation mechanism were not affected by the presence of BN. The addition of BN to the formulation reduced the thermal expansion coefficient of the final materials. Bigger BN particles results advantageous in this reduction.

Young's modulus gradually increased with the proportion of BN particles added, but the addition of BN agglomerates had a lower reinforcing effect, due to the different shape and size of fillers. The same trend was observed in the hardness enhancement. Glass transition temperature did not vary on increasing the BN proportion, but storage modulus increased due to the reinforcement of particles. On increasing the amount of BN in the material damping characteristics and homogeneity were reduced.

By ESEM inspection, it was possible to see that on increasing the amount of BN in the formulation, the rupture lines became shorter and more complex due to the action of BN particles that led to start new paths of breakage. This variation should produce an increase in resilience, the energy absorbed in an impact.

The addition of BN particles to the thiol-epoxy matrix resulted in a substantial increase in thermal conductivity of about 400% (0.97 W/K·m) at the highest

proportion added. This value was highly improved (1.75 W/K·m, 775% increase) if 80 µm agglomerates were added.

Acknowledgments: The authors would like to thank MINECO (Ministerio de Economia, Industria y Competitividad, MAT2017-82849-C2-1-R and 2-R) and Generalitat de Catalunya (2014-SGR-67) for the financial support. Gabriel Benmayor S.A. is acknowledged for giving us the BN used in this work.

Author Contributions: Francesc Ferrando and Angels Serra conceived and designed the experiments, which were performed by Isaac Isarn. Xavier Ramis helps in calorimetric and thermomechanical analyses. The results were discussed and the article written and revised by all the authors.

Conflicts of Interest: The authors declare no conflict of interest. The founding sponsors had no role in the design of the study.

References

1. Cengel, Y.A.; Ghajar, A.J. *Heat and Mass Transfer: Fundamentals and Application*, 5th ed.; McGraw-Hill: New York, NY, USA, 2015; ISBN-13 978-0073398181.
2. Zhang, S.; Zhao, D. (Eds.) *Aerospace Materials Handbook*; CRC Press: Boca Ratón, FL, USA, 2013; ISBN 9781439873298.
3. Burger, N.; Laachachi, A.; Ferriol, M.; Lutz, M.; Toniazzo, V.; Ruch, D. Review of thermal conductivity in composites: Mechanisms, parameters and theory. *Prog. Polym. Sci.* **2016**, *61*, 1–28, doi:10.1016/j.progpolymsci.2016.05.001.
4. Gaska, K.; Rybak, A.; Kapusta, C.; Sekula, R.; Siwek, A. Enhanced thermal conductivity of epoxy–matrix composites with hybrid fillers. *Polym. Adv. Technol.* **2015**, *26*, 26–31, doi:10.1002/pat.3414.
5. Song, W.-L.; Wang, P.; Cao, L.; Anderson, A.; Meziani, M.J.; Farr, A.J.; Sun, Y.-P. Polymer/Boron Nitride Nanocomposite Materials for Superior Thermal Transport Performance. *Angew. Chem. Int. Ed.* **2012**, *51*,6498–6501, doi:10.1002/anie.201201689.
6. Chen, H.; Ginzburg, V.V.; Yang, J.; Yang, Y.; Liu, W.; Huang, Y.; Du, L.; Chen, B. Thermal conductivity of polymer-based composites: Fundamentals and Applications. *Prog. Polym. Sci.* **2016**, *59*, 41–85, doi:10.1016/j.progpolymsci.2016.03.001.
7. Stankovich, S.; Dikin, D.A.; Dommett, G.H.B.; Kohlhaas, K.M.; Zimney, E.J.; Stach, E.A.; Piner, R.D.; Nguyen, S.T.; Ruoff, R.S. Graphene-based composite materials. *Nature* **2006**, *442*, 282–286, doi:10.1038/nature04969.
8. Golberg, D.; Bando, Y.; Huang, Y.; Terao, T.; Mitome, M.; Tang, C.C.; Zhi, C.Y. Boron Nitride Nanotubes and Nanosheets. *ACS Nano***2010**, *4*, 2979–2993, doi:10.1021/nn1006495.
9. Alam, M.T.; Bresnehan, M.S.; Robinson, J.A.; Haque, M.A. Thermal conductivity of ultra-thin chemical vapor deposited hexagonal boron nitride films. *Appl. Phys. Lett.* **2014**, *104*, 013113, doi:10.1063/1.4861468.

10. Li, A.; Zhang, C.; Zhang, Y.-F. Thermal Conductivity of Graphene-Polymer Composites: Mechanisms, Properties, and Applications. *Polymers* **2017**, *9*, 437, doi:10.3390/polym9090437.
11. Yu, J.; Huang, X.; Wu, C.; Wu, X.; Wang, G.; Jiang, P. Interfacial modification of boron nitride nanoplatelets for epoxy composites with improved thermal properties. *Polymer* **2012**, *53*, 471–480, doi:10.1016/j.polymer.2011.12.040.
12. Seyhan, A.T.; Göncü, Y.; Durukan, O.; Akay, A.; Ay, N. Silanization of boron nitride nanosheets (BNNSs) through microfluidization and their use for producing thermally conductive and electrically insulating polymer nanocomposites. *J. Solid State Chem.* **2017**, *249*, 98–107, doi:10.1016/j.jssc.2017.02.020.
13. Fang, L.; Wu, C.; Qian, R.; Xie, L.; Yang, K.; Jiang, P. Nano–micro structure of functionalized boron nitride and aluminum oxide for epoxy composites with enhanced thermal conductivity and breakdown strength. *RSC Adv.* **2014**, *4*, 21010–21017, doi:10.1039/C4RA01194E.
14. Kim, K.; Kim, M.; Hwang, Y.; Kim, J. Chemically modified boron nitride epoxy terminated dimethylsiloxane composite for improving the thermal conductivity. *Ceram. Int.***2014**, *40*, 2047–2056, doi:10.1016/j.ceramint.2013.07.117.
15. Hutchinson, J.M.; Román, F.; Cortés, P.; Calventus, Y. Epoxy composites filled with boron nitride and aluminium nitride for improved thermal conductivity. *Polimery* **2017**, *62*, 764–770, doi:10.14314/polimery.2017.560.
16. Guzmán, D.; Mateu, B.; Fernández-Francos, X.; Ramis, X.; Serra, A. Novel thermal curing of cycloaliphatic resins by thiol–epoxy click process with several multifunctional thiols. *Polym. Int.* **2017**, *66*, 1697–1707, doi:10.1002/pi.5336.
17. Guzmán, D.; Ramis, X.; Fernández-Francos, X.; Serra, A. New catalysts for diglycidyl ether of bisphenol A curing based on thiol-epoxy click reaction. *Eur. Polym. J.* **2014**, *59*, 377–386, doi:10.1016/j.eurpolymj.2014.08.001.
18. Guzmán, D.; Ramis, X.; Fernández-Francos, X.; Serra, A. Enhancement in the glass transition temperature in latent thiol-epoxy click cured thermosets. *Polymers* **2015**, *7*, 680–694, doi:10.3390/polym7040680.
19. Isarn, I.; Gamardella, F.; Massagués, L.; Fernández-Francos, X.; Serra, A.; Ferrando, F. New epoxy composite thermosets with enhanced thermal conductivity and high T_g obtained by cationic homopolymerization. *Polym. Compos.* **2018**, in press.
20. Pascault, J.P.; Sauterau, H.; Verdu, J.; Williams, R.J.J.*Thermosetting Polymers*; Marcel Dekker: New York, NY, USA, 2002; ISBN 0-8247-0670-6.
21. Isarn, I.; Massagués, L.; Ramis, X.; Serra, A.; Ferrando, F. New BN-epoxy composites obtained by thermal latent cationic curing with enhanced thermal conductivity. *Compos. Part A* **2017**, *103*, 35–47, doi:10.1016/j.compositesa.2017.09.007.
22. Carreau, P.J.; De Kee, D.C.R.; Chhabra, R.P. *Rheology of Polymeric Systems: Principles and Applications*; Hanser Publishers: München, Germany, 1997; ISBN-13 978-1569902189.
23. Laun, H.M. Rheological properties of aqueous polymer dispersion. *Angew. Makromol. Chem.* **1984**, *123/124*, 335–359, doi:10.1002/apmc.1984.051230115.

24. Jouault, N.; Vallat, P.; Dalmas, F.; Said, S.; Jestin, J.; Boué, F. Well-dispersed fractal aggregates as filler in polymer-silica nanocomposites: Long-range effects in rheology. *Macromolecules* **2009**, *42*, 2031–2040, doi:10.1021/ma801908u.
25. Ferry, J.D. *Viscoelastic Properties of Polymers*, 3rd ed.; Wiley: New York, NY, USA, 1980; ISBN 0-471-048941-1.
26. De Gennes, P.G. Scaling theory of polymer adsorption. *J. Phys.* **1976**, *37*, 1445–1452, doi:10.1051/jphys:0197600370120144500.
27. Zhang, Q.; Rastogi, S.; Chen, D.; Lippits, D.; Lemstra, P.J. Low percolation threshold in single-walled carbon nanotube/high density polyethylene composites prepared by melt processing technique. *Carbon* **2006**, *44*, 778–785, doi:10.1016/j.carbon.2005.09.039.
28. Hassanabadi, H.M.; Wilhelm, M.; Rodrigue, D. A rheological criterion to determine the percolation threshold in polymer nano-composites. *Rheol. Acta* **2014**, *53*, 869–882, doi:10.1007/s00397-014-0804-0.
29. Ng, H.; Manas-Zloczower, I. Chemorheology of unfilled and filled epoxy-resins. *Polym. Eng. Sci.* **1993**, *33*, 211–216, doi:10.1002/pen.760330404.
30. Hamerton, I. *Recent Developments in Epoxy Resins*; Smithers Rapra Technology: Shawbury, UK, 1996; Volume 8, ISBN-13 978-1859570838.
31. Huang, X.; Jiang, P.; Tanaka, T. A review of dielectric polymer composites with high thermal conductivity. *IEEE Electr. Insul. Mag.* **2011**, *27*, 8–16, doi:10.1109/MEI.2011.5954064.
32. Teng, C.-C.; Ma, C.-C.M.; Chiou, K.-C.; Lee, T.-M.; Shih, Y.-F. Synergetic effect of hybrid boron nitride and multi-walled carbon nanotubes on the thermal conductivity of epoxy composites. *Mater. Chem. Phys.* **2011**, *126*, 722–728, doi:10.1016/j.matchemphys.2010.12.053.
33. Pak, S.Y.; Kim, H.M.; Kim, S.Y.; Youn, J.R. Synergistic improvement of thermal conductivity of thermoplastic composites with mixed boron nitride and multi-walled carbon nanotube fillers. *Carbon* **2012**, *50*, 4830–4838, doi:10.1016/j.carbon.2012.06.009.
34. Chiang, T.H.; Hsieh, T.-E. A study of Encapsulation Resin Containing Hexagonal Boron Nitride (hBN) as Inorganic Filler. *J. Inorg. Organomet. Polym. Mater.* **2006**, *16*, 175–183, doi:10.1007/s10904-006-9037-8.
35. Yu, J.; Mo, H.; Jiang, P. Polymer/boron nitride nanosheet composite with high thermal conductivity and sufficient dielectric strength. *Polym. Adv. Technol.* **2015**, *26*, 514–520, doi:10.1002/pat.3481.
36. Lindsay, L.; Broido, D.A. Enhanced thermal conductivity and isotope effect in single-layer hexagonal boron nitride. *Phys. Rev. B* **2011**, *84*, 155421–155426, doi:10.1103/PhysRevB.84.155421.

Chapter 6

Thermal conductive composites prepared by addition of several ceramic fillers to thermally cationic curing cycloaliphatic epoxy resins

Polymers **2019**, *11, 138-151*

Thermal conductive composites prepared by addition of several ceramic fillers to thermally cationic curing cycloaliphatic epoxy resins

Isaac Isarn[1], Francesco Gamardella[2], Xavier Fernàndez-Francos[3], Àngels Serra[2] and Francesc Ferrando [1]

1. Department of Mechanical Engineering, Universitat Rovira i Virgili, C/Av. Països Catalans, 26, 43007 Tarragona, Spain.
2. Department of Analytical and Organic Chemistry, Universitat Rovira i Virgili, C/Marcel·lí Domingo s/n, 43007 Tarragona, Spain.
3. Thermodynamics Laboratory, ETSEIB, Universitat Politècnica de Catalunya, C/Av. Diagonal 647, 08028 Barcelona, Spain.

Abstract

Novel composite coatings prepared from 3,4-epoxy cyclohexylmethyl 3,4-epoxycyclohexane carboxylate (ECC) and different ceramic fillers have been prepared to improve the thermal dissipation of electronic devices. As latent cationic initiator, a benzylanilinium salt with triethanolamine has been used, which leads to a polyether matrix. Different proportions of Al2O3, AlN and SiC as fillers were added to the reactive formulation. The effect of the fillers selected and their proportions on the evolution of the curing was studied by calorimetry and rheometry. The thermal conductivity, thermal stability, thermal expansion coefficient and thermomechanical and mechanical properties of the composites were evaluated. An improvement of 820% in thermal conductivity in reference to the neat material was reached with a 75 wt % of AlN, whereas glass transition temperatures higher than 200 °C were determined in all the composites.

Keywords

Cycloaliphatic epoxy resin; composites; thermal conductivity; latency; ceramic fillers.

1. Introduction

Epoxy thermosets are widely used in electric and electronic industries and other engineering applications. Usually, they are applied as adhesives or protective coatings, due to their good processability before curing, good compatibility with a large number of materials, high electrical insulating characteristics, and good thermal, corrosion and chemical resistance [1]. However, unmodified epoxy thermosets show low thermal conductivity, typically around 0.2 W/m·K, which may limit their use when thermal dissipation is required [2]. It must be noticed, that the dissipation of heat generated becomes a non-ignorable issue in the miniaturization of electronic devices. The increasing temperature, as the result of the generated heat in specific parts of the

devices, greatly affects the performance of the electronic equipment, leading to malfunction, poor reliability, and premature failures. The dissipation of heat is usually done by applying a heat sink, for example, a metal plate, and a cooling fan to blow away local heat. In order to keep good thermal contact between heat sources and heat sinks and to improve heat transfer efficiency, materials with high thermal conductivity, but electrically insulating, are needed to fill the gaps [3].

One of the easiest methods to solve the inherent low conductivity of epoxy resins, with the lowest cost and effectiveness, is to introduce fillers with high thermal conductivity combined with electrical insulating properties. Among them, boron nitride (BN) is one of the most used fillers, which combines properties such as high thermal conductivity, high dielectric strength, low thermal expansion coefficient (CTE) and low density [4,5]. However, some authors reported the use of other fillers to get those improvements [6]. Among them, ceramics such as aluminum oxide (Al_2O_3) [7] and aluminum nitride (AlN) [8], silicon nitride (Si_3N_4) [9], silicon carbide (SiC) [10] and graphene oxide (GO) [11] are ideal candidates in terms of their wide band gap and high thermal conductivity [3].

In the present paper, we have selected three of them: aluminum oxide and nitride and silicon carbide and they are added as fillers in cycloaliphatic epoxy resin formulations. Al_2O_3 particles are widely used in the electronic field, because of their cheaper price compared to other ceramic fillers, despite their relatively lower thermal conductivity (38–42 W/m·K) [12]. Its CTE is reported to be 7 ppm/°C. AlN particles are relatively expensive but show higher thermal conductivity (150–220 W/m·K) and lower thermal expansion coefficient (CTE) (2.5–5 ppm/°C) [12]. Finally, SiC has an intermediate thermal conductivity of 85 W/m·K [12] and CTE on the range 4.1–4.7 ppm/°C [3]. With regards to the cycloaliphatic epoxy, few studies are based on this. The combination of small and compact structure and high oxirane content gives resins with low viscosity and thermosets with high weatherability, low dielectric constant, in addition to high T_g [1]. This class of epoxy is popular for diverse end uses including auto topcoats, weatherable high-voltage insulators, ultraviolet (UV) coatings and encapsulants for electronic and optoelectronic applications, and in the last times there is an interest in growing applications including lithographic inks and photoresists for the electronics industry [13]. The inherent low viscosity of these resins enables them to be formulated with higher levels of inorganic fillers. This enhances mechanical and electrical track resistance for electrical and electronic components [14]. In the present work, we have used as thermal curing agent an ammonium salt (CXC1612) with a small proportion of triethanolamine (TEA) that confers a latent character to the curing system. In a previous work, it has been proved its latency and the fact that it leads to thermosets with high glass transition temperature (T_g) [15].

By the use of different fillers, this study aims at reaching better results than those obtained in a previous study in which BN was used [15]. In that study, an increase of

Polymers **2019**, *11, 138-151*

800% in thermal conductivity was obtained by adding 40 wt % of BN to the formulation. The materials obtained presented T_g values higher than 200 °C, reductions in CTE up to 50% in reference to the neat epoxy material and improved shear strength and microindentation hardness. The addition of BN filler did not compromise the latency of the curing system, due to their inert character in this polymerization mechanism. The different chemical characteristics of the fillers selected in the present study could affect the curing kinetics, and it is foreseeable they greatly influence the thermal and mechanical characteristics of the final composites.

2. Materials and Methods

2.1. Materials

3,4-epoxy cyclohexylmethyl 3,4-epoxycyclohexane carboxylate (ECC) (ERL-421D, EEW = 126.15 g/eq) was provided by Dow Chemical Company (Midland, MI, USA). Initiator CXC1612 from King Industries Inc., Norwalk, CT, USA, which was determined to be *N*-(4-methoxybenzyl)-*N*,*N*-dimethylanilinium hexafluoroantimonate, was dissolved in propylene carbonate at 50 wt %. Propylene carbonate and triethanolamine (TEA) were provided by Sigma-Aldrich (Darmstadt, Germany) and purified by distillation. Aluminum oxide (Al_2O_3) from Showa Denko (Tokyo, Japan) with a particle size of 1–5 µm (ρ = 3.95 g/cm^3), aluminum nitride (AlN) from Sigma Aldrich (Darmstadt, Germany) with a particle size of 0.5–3 µm (ρ = 3.26 g/cm^3) and silicon carbide (SiC) 1D 99/CM101/F1200 from Shengli Abrasives (Dongying, China) with approximate size of 4–8 µm (ρ = 3.21 g/cm^3).

2.2. Sample Preparation

The mixtures were prepared by mixing ECC with 1 phr of CXC1612 (parts of initiator per hundred parts of resin) and 0.1 phr of TEA. For composite samples, the required amount of filler was added in wt % to the previous formulation. The mixtures were stirred mechanically until homogeneity and degassed under vacuum to prevent the appearance of bubbles during the curing process. Finally, the samples were poured onto aluminum molds coated with Teflon and cured following a multi-step temperature schedule at 100, 120, 150, 180 and 200 °C, with a dwelling time of 1 h at each temperature.

2.3. Characterization Techniques

Differential scanning calorimetry (DSC, Mettler Toledo, Columbus, OH, USA) was used to study the curing evolution by using a Mettler DSC-821e calibrated using an In standard (heat flow calibration) and an In-Pb-Zn standard (T calibration). Samples of approx. 5–10 mg were tested in aluminum pans with a pierced lid in N_2 atmosphere with a gas flow of 100 mL/min. The dynamic studies were performed between 30–250 °C with a heating rate of 10 °C/min. The reaction enthalpy (Δh) was integrated from the

calorimetric heat flow signal (*dh/dt*) using a straight baseline, with the help of the STARe software.

Rheometric measurements were carried out in a TA Instruments AR G2 rheometer (New Castle, DE, USA), equipped with electrical heated plates (EHP) with parallel plate geometry (25 mm diameter disposable aluminum plates). Complex viscosity (η^*) and viscoelastic properties of the mixtures prepared were recorded as function of angular frequency ω (rad/s) in the linear range of viscoelasticity, obtained from constant shear storage modulus (G') in a strain sweep experiment at 1 Hz at 30 °C. Thermal stability of cured samples was evaluated in a Mettler thermogravimetric analysis/simultaneous difference thermal analysis (TGA/SDTA) 851e thermobalance (Columbus, OH, USA). All the experiments were carried out under N_2 atmosphere (100 mL/min). Pieces of cured samples of 5–10 mg were heated between 30 and 600 °C at a heating rate of 10 °C/min. Dynamic mechanical thermal analyses (DMTA) were performed by using a TA Instruments DMA Q800 analyzer (New Castle, DE, USA). Prismatic rectangular samples (15 × 6 × 2.3 mm^3) were analyzed by 3-point bending at a heating rate of 3 °C/min from 35 to 300 °C using a frequency of 1 Hz and oscillation of 0.1% of sample deformation. The Young's modulus (E) was determined at 30 °C in a controlled force experiment using a three point bending clamp, as explained in a previous paper [4]. Thermomechanical analyses (TMA) were carried out on a Mettler TMA40 thermomechanical analyzer (Columbus, OH, USA). Cured samples (12 × 12 × 2.3 mm^3) were supported by the clamp and one silica disc to distribute uniformly the force and heated at 5 °C/min from 35 to 100 °C by application of 0.01 N, a minimum force to avoid distortion of the results.

Knoop microindentation hardness was measured as reported before with a Wilson Wolpert 401 MVA (Microhardness Vickers Analog) device following ASTM D1474-13 (Wilson Wolpert Instruments, Aachen, Germany). 20 determinations were made for each material to reach a confidence level of 95%. Surface fracture was examined with a FEI Quanta 600 environmental scanning electron microscope (ESEM, FEI Company, Hillsboro, OR, USA) that allows collecting electron micrographs at 10–20 kV and low vacuum mode of uncoated specimens with low electron conductivity.

Thermal conductivity was measured using the Transient Hot Bridge method by a THB 100 device from Linseis Messgeräte GmbH (Selb, Germany). A HTP G 9161 sensor was used with a 3 × 3 mm^2 area calibrated with poly(methyl methacrylate) (PMMA), borosilicate crown glass, marble, Ti-Al alloy and titanium. Two equal polished rectangular samples (12 × 12 × 2.3 mm^3) were placed in each one of the faces of the sensor. Due to the small size of the sensor, side effects can be neglected. A measuring time of 100 s with a current of 10 mA was applied to each of the five measures done for the different formulations.

3. Results and Discussion

3.1. Calorimetric Study of the Curing Process

To ascertain the influence of the different fillers selected in the curing evolution, proportions of 50, 60 and 70 wt % of each type of particle fillers were added to the epoxy resin/initiator formulations and studied by DSC. In the case of AlN, a higher proportion (75 wt %) was added after examining the rheological results obtained. As the curing system, we selected a thermal cationic latent epoxy system previously reported that consist in *N*-(4-methoxybenzyl)-*N*,*N*-dimethylanilinium hexafluoroantimonate with a small proportion of triethanolamine that leads to the homopolymerization of the cycloaliphatic epoxy in a latent manner [15]. **Figure 1** presents the non-isothermal calorimetric curves of the different formulations studied, where we can see the different effects for the fillers selected.

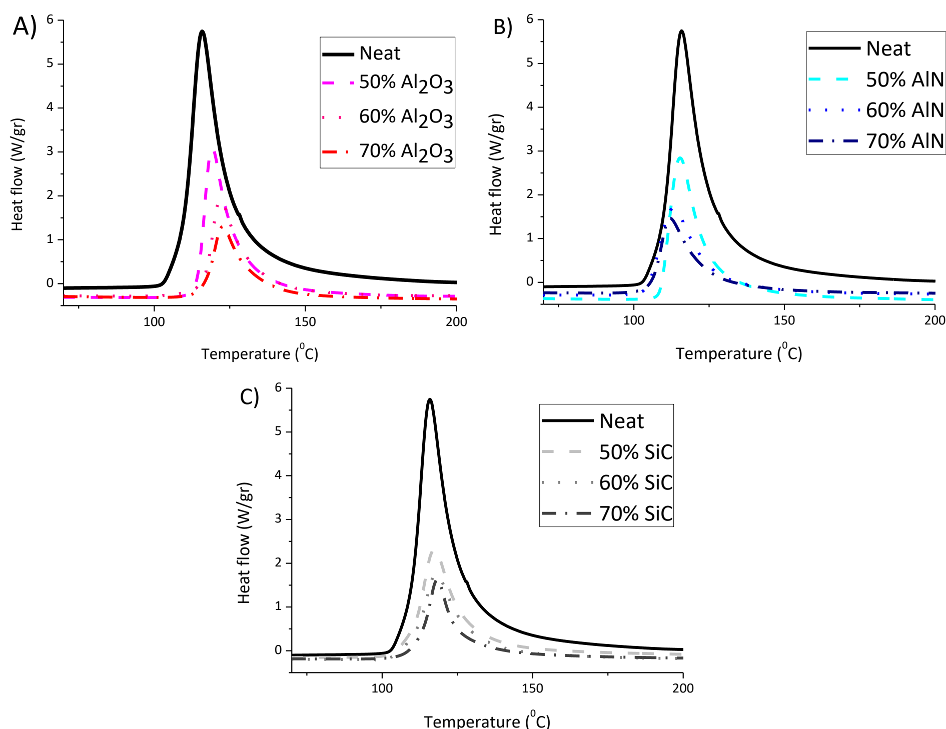

Figure 1. Exothermic curves from differential scanning calorimetry (DSC) analysis of all the mixtures prepared with different fillers: (A) Al_2O_3, (B) AlN, (C) SiC.

In Figure 1A, it can be seen that the addition of alumina produces a delay in the curing process on increasing its proportion in the formulation, which can be related to its basic character that interacts with the growing cationic species, deactivating them. By contrast, AlN shows in Figure 1B a small acceleration of the reaction which is accentuated on rising its concentration. Thus, it seems that AlN structure favors the formation and stability of the cations. The addition of the third filler, SiC in Figure 1C,

leads to practically the same peak temperature as the neat epoxy, which means that it has an inert character in the reaction mechanism and that no interaction between the cationic species formed and the filler structure occurs. The interaction between growing polymer chains and fillers can also play a role in the thermal transmission, because in the interphase phonons are usually scattered, reducing the heat transfer.

The most representative data obtained from the calorimetric analysis are collected in **Table 1**.

Table 1. DSC data of the different formulations studied.

Sample	T_{onset} [a] (°C)	T_{peak} [a] (°C)	*Δh* [b] (J/g)	*Δh* [b] (kJ/ee)
Neat	109	117	596	75.2
50% Al_2O_3	114	120	258	65.2
60% Al_2O_3	116	122	202	63.8
70% Al_2O_3	117	123	147	62.0
50% AlN	109	116	286	72.2
60% AlN	106	113	225	71.0
70% AlN	106	112	172	72.1
75% AlN	106	111	146	73.4
50% SiC	109	118	277	69.9
60% SiC	110	118	221	69.8
70% SiC	112	120	166	69.6

[a] Onset and maximum peak temperatures of the curing exotherm.
[b] Heat evolved during the curing by gram of mixture or by epoxy equivalent.

In addition to the onset and the temperature of the maximum of the peak, the heat evolved by gram or by epoxy equivalent was calculated. This value gives us valuable information about the conversion of epoxide groups achieved in all the composites prepared. The value of enthalpy should approach the one of the neat formulation. As we can see, the heat released in the neat formulation is the highest, which indicates that the addition of filler to the formulation reduces the conversion achieved, probably due to topological restrictions produced by the particles. However, the addition of alumina leads to the lowest enthalpy released, which can be related to the inactivation of the growing cationic species in the basic alumina surface. In previous studies with BN as the

Polymers ***2019***, *11, 138-151*

filler no effect was observed in the kinetics which agrees with the inert chemical character of the BN particles, but there was a reduction in the released enthalpy, independent of the filler content, related to topological hindrance to the homopolymerization reaction [15]. All the cured samples were submitted to a second DSC scan but no T_g could be observed due to the high crosslinking achieved in the epoxy matrix because of the compact structure of the epoxy resin and the homopolymerization produced in the curing.

3.2. Rheological Behavior of Mixtures

Mixtures before curing were essayed by rheology to analyze their viscoelastic behavior. The particle size of the different fillers is in the same range, and the particle shapes are quite similar. These two properties are the ones having the strongest influence on the rheological behavior. Although density differences in the fillers selected lead to a variation on their volumetric content, the similarity between particles allowed us to perform the comparison among the different formulations [16,17]. The linear viscoelastic region (LVR) was determined in oscillatory tests, varying amplitude of deformation with a fixed frequency (1 Hz) at 30 °C. As in previous studies with BN [4,15,18], the LVR is displaced to lower amplitudes when the filler proportion increases. This means that the mixture's microstructure finds a critical strain above which the structure organization starts to breakdown at lower amplitudes when the amount of filler grows [19]. Thus, the amplitude was set at the LVR for each mixture to carry out the frequency sweep experiments. The effect of the filler content for each type of filler on the complex viscosity (η^*) is represented in **Figure 2**.

As we can see in all the mixtures, to a greater or lesser extent, shear thinning is observed. This is due to a diminution of viscosity on increasing the frequency applied, attributable to changes in the microstructure of the mixture, typical of filled blends. In contrast, the neat formulation represents an almost constant value on varying the frequency, which means that it has a Newtonian behavior. Mixtures with alumina and silicon carbide present a very large difference in viscosity between 60 and 70 wt % (3 orders of magnitude) and 5-7 orders of magnitude in reference to the neat formulation. On the other hand, the addition of aluminum nitride does not produce any large effect until the addition of 75 wt %. Thus, from the point of view of the application on surfaces or filling molds, aluminum nitride is the best suited.

Studies on micro and nanoparticle composites showed that the thermal conductivity of the composites is significantly smaller than that of their bulk counterparts due to phonon-interface scattering [20]. Commonly, the used fabrication techniques, such as hot pressing, tend to produce randomly particle distributed composites, forming clusters of particles. When particles with high thermal conductivity are randomly dispersed in a matrix material with low transport properties, the largest cluster can form a percolation network [21]. Thus, the largest cluster of thermally

conductive material can connect the opposite boundaries when the volumetric concentration of particles reaches certain limit. This limit of volumetric concentration, defined as the percolation threshold, is determined by the geometric characteristics of particles. The percolating network can create a low resistance pathway for thermal transport and the conductivity of the composites can increase notably once reached percolation [22]. The significant changes in the microstructure, related to the percolation threshold, can be evaluated by the study of storage modulus (G') and loss modulus (G''), which determine the elastic and viscous properties, respectively. **Figure 3** shows the plots of both moduli on changing the frequency for all the formulations studied.

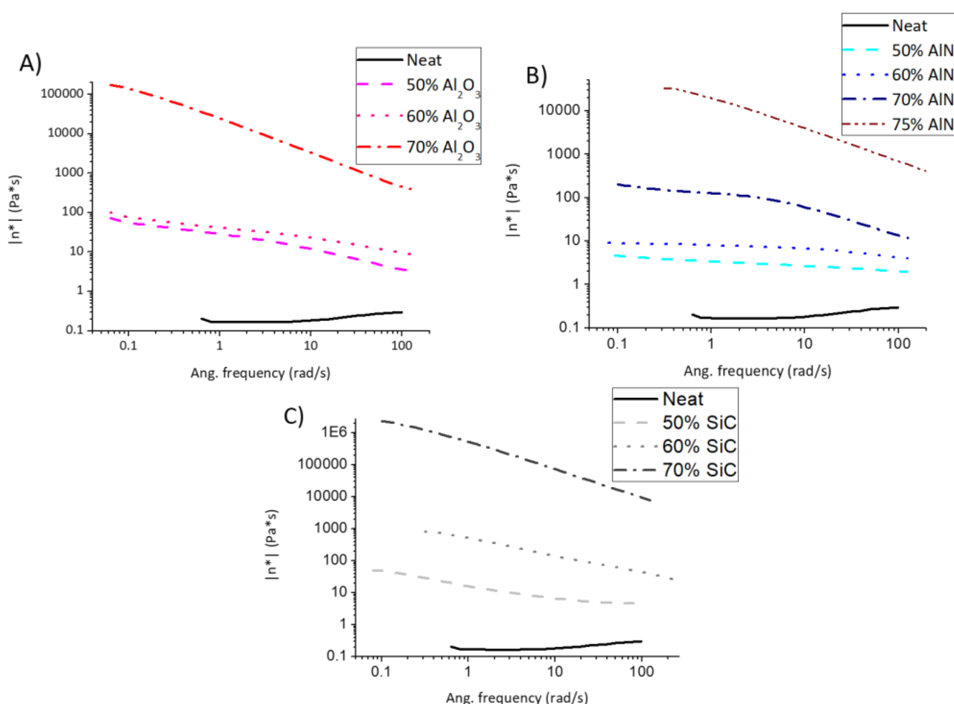

Figure 2. Complex viscosities of mixtures varying frequency in the linear viscoelastic region (LVR) of each formulation at 30 °C with different fillers: (A) Al_2O_3, (B) AlN, (C) SiC.

An interpretation of Rouse-like behavior takes as a criterion that when G' and G'' at low frequencies become equal the percolation threshold has been reached [18,23]. This means the transition from non-percolated to percolated response must be accompanied by the change from the liquid-like behavior (G' < G'') to solid-like behavior (G' > G''). In Figure 3A this change is observed between the mixtures of 60 and 70 wt % of alumina, as corresponds to the large increase in viscosity (Figure 2A). In case of AlN blends (Figure 3B) only liquid like behavior is exhibited until the 70% of filler added. For this reason, a new mixture with the 75% of AlN was also prepared to surpass the rheological percolation. It must be commented, that this is the practical limit for a hand-

mixing procedure. Since all particle sizes are similar, the lower viscosity of AlN formulations could be attributed to the lower specific surface area (SSA) of AlN powder. Finally, the mixtures with 50 and 60 wt % of SiC (Figure 3C) are very close to reach the percolation but this is not surpassed until 70% wt % of SiC. A high increase of viscosity is observed in the transition (Figure 2C). Apart from the high volumetric ratio due to its low density, this high viscosity is assumed to be related to the high SSA.

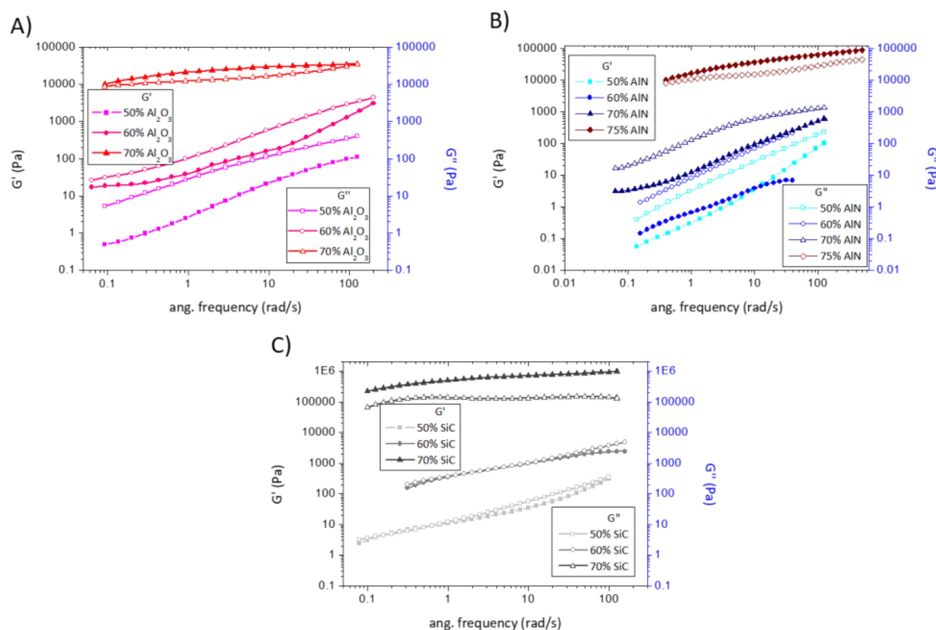

Figure 3. Plots of G' and G'' versus frequency in frequency sweep tests at 30 °C for the different formulations studied with different fillers: (A) Al_2O_3, (B) AlN, (C) SiC.

3.3. Morphological Analysis

The appearance of the different fillers used in this study as well as the fracture surface of the prepared composites was analyzed by ESEM. Representative micrographs are shown in **Figure 4**.

The morphological characteristics of the fillers used in the present study are shown in the first row of the figure. In the next two rows, two images of each type of composite with different filler contents and different magnifications have been also included. As we can see, SiC is formed by particles with a polyhedral shape with smooth surface. In the composite with a 70 wt %, these particles are not well bonded to the polymeric matrix, which agrees with the inert character of SiC in the DSC kinetic study. The particles are very close to each other, which confirms that the percolation has been reached.

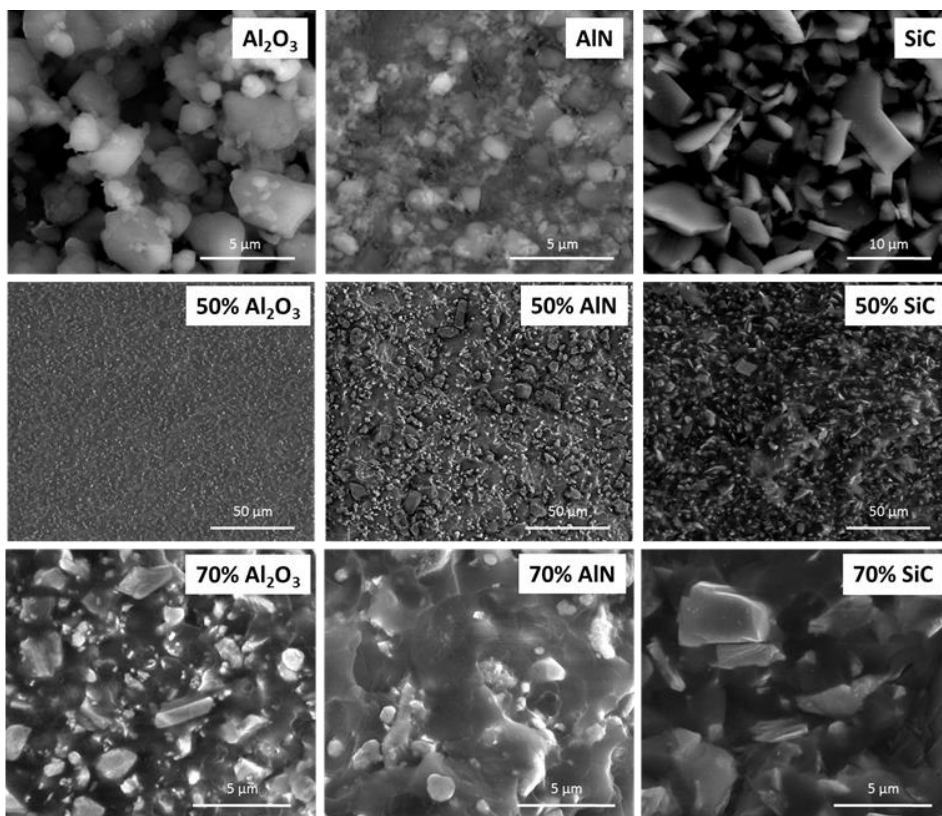

Figure 4. Environmental scanning electron microscope (ESEM) micrographs of fillers and fracture surfaces of composites at different magnifications.

The particles of alumina and AlN are like aggregates and polydisperse in size. However, AlN particles are much smaller and more polydisperse. Both type of particles seems to be quite well bonded to the epoxy matrix as can be seen in the micrographs of the bottom row, which accounts for an interaction of the surface groups with the growing chains, as was deduced from the retardation and acceleration of the curing process detected by calorimetric studies. The micrograph of AlN at 70 wt % composite show that some of the particles are isolated, since at this filler content percolation has not been reached. The inspection of the fracture surfaces of the samples with a 50 wt % of each filler allows confirming the homogeneous distribution of the particles on the epoxy matrix and the tough characteristics of the fracture, since the fracture cracks are very tortuous.

3.4. Thermal and Mechanical Characterization of Composites

The addition of filler can increase some thermomechanical properties of polymeric materials. Particles act as a reinforcement of the polymer network leading to the improvement of some properties as thermal stability, stiffness or hardness.

Polymers **2019**, *11*, 138-151

TGA, DMTA, TMA and microindentation experiments were performed in the composites prepared to evaluate these characteristics and to investigate the effect of each of the fillers on them.

The evaluation of the thermal stability performed by TGA analysis is represented in **Figure 5**. As can be seen, the shape of the curves is similar which implies that the presence of fillers does not influence the degradation mechanism.

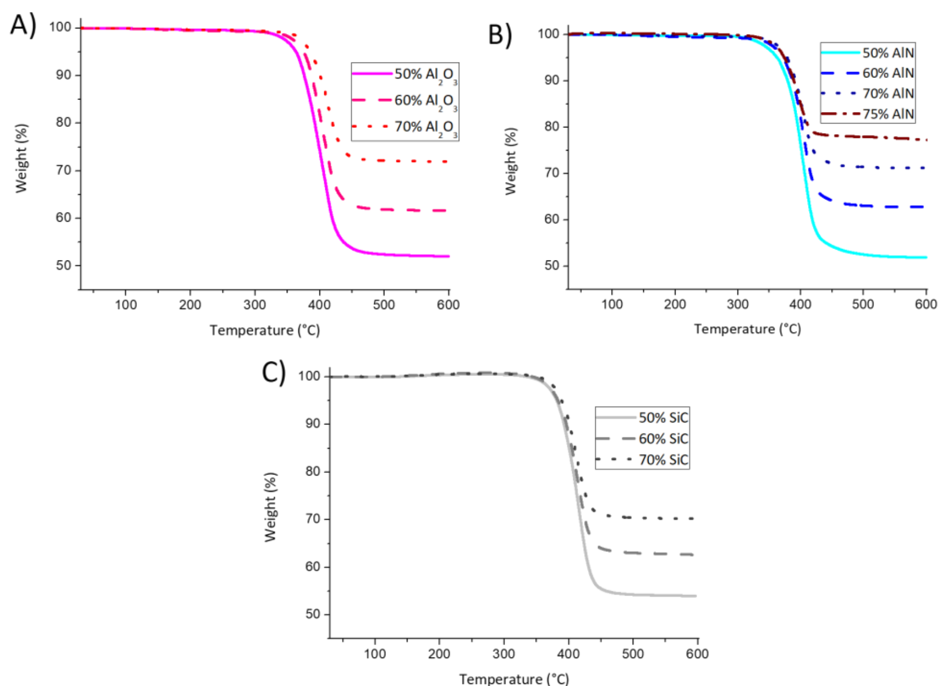

Figure 5. Thermogravimetric analysis (TGA) degradation curves of the different composites obtained by the addition of different fillers: (A) Al_2O_3, (B) AlN, (C) SiC.

Table 2 collects the data of char yields and the temperature of 2% of decomposition ($T_{2\%}$). A large difference can be observed in the $T_{2\%}$ between the neat epoxy and the composites, of around 100 °C. In a previous study [15] using the same epoxy system but adding BN till 40 wt % this increase was more than 70 °C. The reason for this increase is the less resin content to be degraded and therefore $T_{2\%}$ occurs at higher temperature. However, on changing the type of filler these temperatures experiment small variations when the same proportion was added, which could be attributed to differences in the organic network structure. In fact, greater differences on changing the proportion are observable for alumina and AlN composites, in line with the effect of the filler on the curing process observed with DSC. As can be seen in the table, practically the total amount of ECC is decomposed in inert atmosphere and char residues agrees quite well with the proportion of filler added. What can be assumed is that the introduction of particles does not negatively affect the thermal stability of composites.

Table 2. Thermogravimetric and thermomechanical data from the composites prepared.

Sample (wt. %)	Vol. Fract. (%)	$T_{2\%}$[a] (°C)	Char Yield[b] (%)	E[c] (GPa)	T_g[d] (°C)	CTE[e] ($10^{-6}\cdot K^{-1}$)
Neat epoxy	-	273	1.0	2.4	227	115
50% Al_2O_3	22.8	341	52.0	6.1	223	58
60% Al_2O_3	30.8	354	61.6	7.5	223	38
70% Al_2O_3	40.9	368	71.9	11.1	244	36
50% AlN	26.4	337	51.9	7.1	235	56
60% AlN	35.0	351	62.8	7.8	238	38
70% AlN	45.6	359	71.2	12.2	246	35
75% AlN	51.8	353	77.3	14.4	252	22
50% SiC	26.6	368	54.0	7.8	230	52
60% SiC	35.3	370	62.7	10.4	230	48
70% SiC	46.0	377	72.6	11.6	240	32

[a] Temperature of 2% weight loss determined by TGA in N_2 at 10 °C/min.
[b] Char residue at 600 °C (in N_2).
[c] Young's modulus determined by dynamic mechanical thermal analyses (DMTA) at 30 °C.
[d] Temperature of maximum of tanδ at 1 Hz in a DMTA oscillatory experiment using the same clamp.
[e] Thermal expansion coefficient in the glassy state determined between 50–75 °C by thermomechanical analyses (TMA).

Thermomechanical behavior of composites was analyzed by DMTA. Table 2 shows the rigidity and the temperature of the maximum of tan δ peak, related to T_g. Young's modulus measured at 30 °C is highly increased with the addition of filler. This is due to the mechanical reinforcement role played by the particles within the matrix. In **Figure 6**, the tan δ curves are shown.

It can be seen that the relaxation curves are very broad and have low intensity as in ECC-BN composites [15], indicating a slow relaxation process and a low homogeneity in the network structure due the high crosslinking density and to the inherent inhomogeneity caused by ring-opening polymerization mechanism. As DMTA evaluates the thermomechanical characteristics, the results are influenced by the mechanical role played by the particles on the organic matrix. In this way, it can be seen a notable change in the T_g of the materials with alumina and SiC when it exceeds percolation. Conversely,

materials with AlN show a gradual increase of T_g without major changes when percolation is achieved.

The values of the storage modulus (E') in the rubber state could not be determined, since in the tan δ curves we can observe that the complete relaxation of the material is higher than 300 °C, and at this temperature the decomposition of the polymeric matrix has already begun.

The thermal expansion coefficient is an important parameter for the reliability and working life of epoxy materials when they operate as coatings or as thermal interface materials (TIMs) since changes in their working temperature can produce high internal stresses due to the mismatch between the CTE the epoxy coating or TIM, and the substrate, the former being larger [24]. This can provoke de-adhesion between the interfaces they bond, wrapping or any type of defects that finally reduce the durability of the materials. Reducing the CTE of the epoxy coating or TIM would reduce the CTE mismatch and this would result in an enlargement of the working-life of the devices.

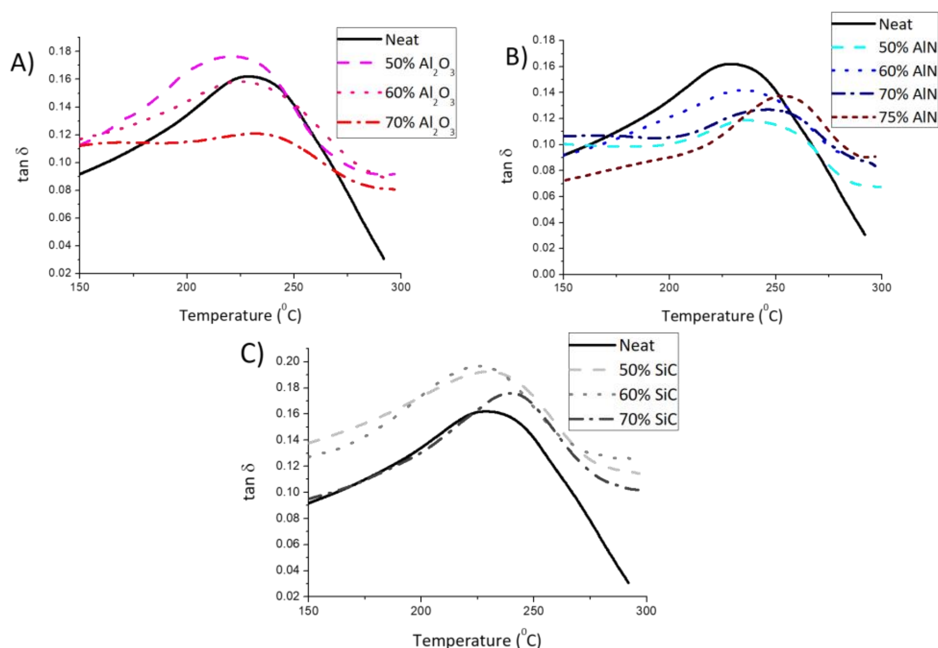

Figure 6. Curves of tan δ for the composites prepared determined by DMTA: (A) Al_2O_3, (B) AlN, (C) SiC.

CTEs were evaluated by TMA and the results are given in Table 2. As expected, on increasing the filler content CTE's are notably reduced. The reduction of this coefficient is gradual with the percentage of filler added. The CTE of the ceramic filler does not affect much the values of the composite materials. However, the addition of 75 wt % of AlN, which has the lowest CTE, leads to the lowest value of 22 ppm/K in all the composites prepared.

Another characteristic that has an effect on the durability of composites is the surface hardness of the materials. By means of microindentation tests, the Knoop hardness of each composite was determined and the values are represented in **Figure 7**.

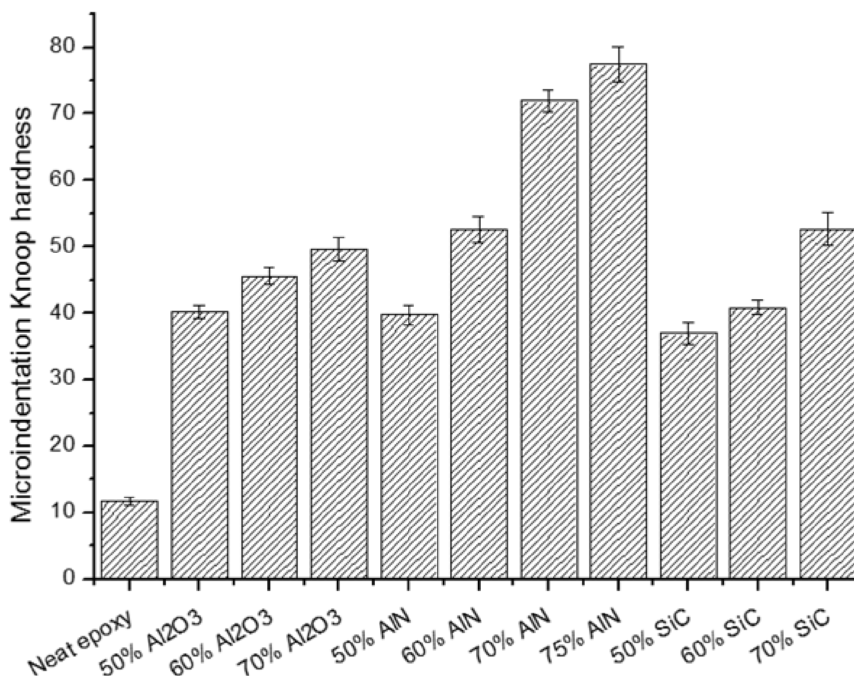

Figure 7. Microindentation Knoop hardness dependence on filler/proportion in the composites.

As in the case of materials with BN [4,15,18], the hardness increased with the filler loading. The change of the type of particles added should also affect in principle, the improvement reached. It is reported that the hardness of the ceramic fillers follows the order SiC > Al_2O_3 > AlN [25]. However, this trend is not followed in our composites, since the greater effect on hardness is originated by AlN, which leads to more than 6-fold improvements on adding a 75 wt % of this filler to the epoxy formulation. These unexpected results could be rationalized in a better interaction between the organic matrix with the filler in case of AlN, or to the particle size and shape that undoubtedly should affect hardness characteristics. In a previous study on composites with the same polymer matrix but a 40 wt % BN filler, the maximum hardness value reached was only 26.6 KHN (Koop Hardness) and the progressive improvement of the hardness with the filler content occurs more smoothly than in the present study [15]. However, in that work the proportion of filler was lower, the percolation was reached at 14.4 wt %, because of the platelet-like shape of the particles. This leads to the conclusion that for hardness improvement, the fillers used in the present study are better than the previous studied h-BN filler, and among them, AlN is the most effective.

Polymers ***2019****, 11, 138-151*

3.5. Thermal Conductivities

The main goal of the study was to increase the thermal conductivity of the cycloaliphatic epoxy matrix by the addition of thermal conductive particles. The results of the thermal conductivity determined for the composites prepared are represented in **Figure 8**.

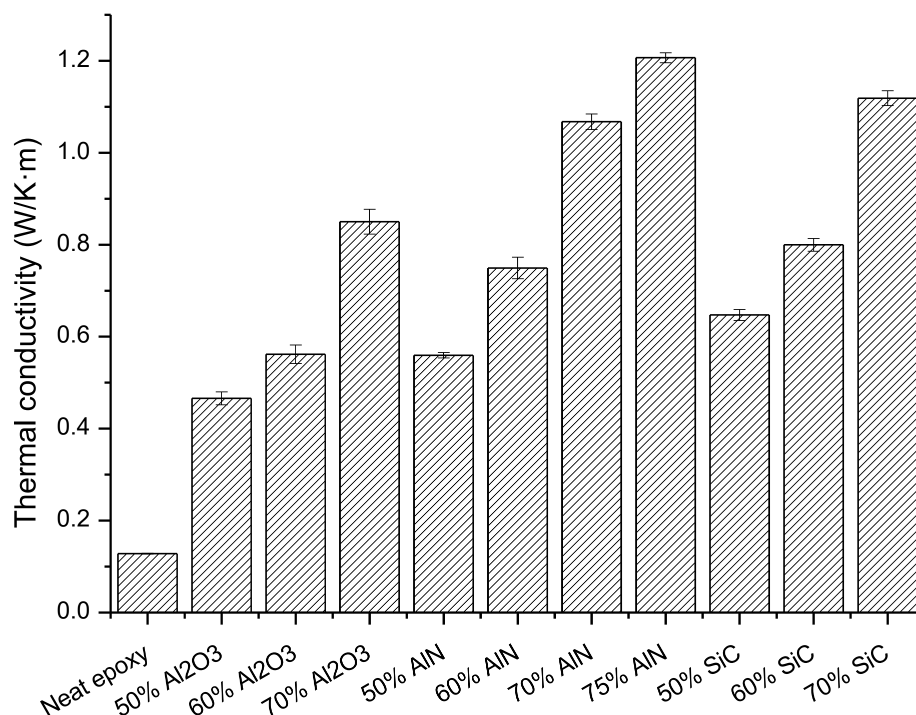

Figure 8. Thermal conductivities of the neat epoxy and the different composites prepared.

The highest conductivity values (1.21 W/m·K) were reached for the sample with a 75 wt % of AlN, followed by the composite with the highest proportion of SiC (1.12 W/m·K). However, it is quite curious that at the same filler content (70%) SiC leads to a higher value of this parameter, although pure AlN has a much higher conductivity than pure SiC. This unexpected result could be explained on the basis of the conductive pathways formed by the filler particles, which is related to the percolation phenomenon, which for AlN has not been achieved at this filler content.

The thermal conductivity obtained in the present study is higher than that obtained in BN composites (1.04 W/m·K) [15]. However, in the present case a higher proportion of filler has been added to the formulation, since the addition of h-BN was limited to 40 wt %, because of the difficulty of the manual preparation of mixtures with a higher proportion of this filler. However, the different shape and size of the filler particles finally leads to big differences in the surface area and on the interactions with

the organic matrix and makes it difficult to come to general conclusions. In a previous study, we could demonstrate the influence of the size and shape of the particles on the thermal conductivity of this type of composites [18].

As we have seen, the higher the proportion of filler, the better is the thermal conductivity, but any big difference is observed between the different particles used, being the most important effect the achievement of the percolation. However, it should be taken into account that mechanical properties and processability can become worse with a high proportion of fillers and both characteristics should also be considered in the improvement of thermal management. For this reason, as an alternative, the use of nanofillers, with high specific surface area that can be chemically modified, will be attempted in the forthcoming studies of our group.

4. Conclusions

The addition of different ceramic fillers to an epoxy cycloaliphatic formulation cured with a latent cationic homopolymerization system led to an acceleration on adding AlN, a delay in the case of alumina, whereas the addition of SiC did not produce any kinetic effect in the curing process. The addition of filler slightly reduced the degree of curing, probably due to topological restrictions. The use of alumina as the filler led to the lowest curing degree, which could be related to the basic character of alumina.

The viscosities of the filled formulations increased significantly on reaching the percolation. The addition of alumina or SiC in a proportion of 70 wt % surpassed the percolation threshold but it is necessary to reach a 75 wt % of AlN to experiment with this phenomenon.

The different fillers did not affect the thermal degradation mechanism of the composites but the initial degradation temperature increased in 100 °C in the highest loaded composites in reference to the neat material.

The materials presented a broad relaxation curve in the DMTA, according to their high crosslinked structure. T_g values increased with the filler content.

Young's moduli and hardness were enhanced significantly by the addition of the reinforcements. The maximum values were reached in the 75 wt % of AlN composite with a 6-fold and a 7-fold increase, respectively, in reference to the neat material. This material showed the lowest CTE value of all the materials prepared.

As a general conclusion, it can be stated that the formulation with a 75 wt % of AlN is the most adequate in terms of applicability (lower viscosity) and the material obtained after curing has the best mechanical performance, the highest T_g, the lowest thermal expansion coefficient, and the highest thermal conductivity.

Author Contributions: Francesc Ferrando and Angels Serra conceived and designed the experiments, which were performed by Isaac Isarn and Francesco Gamardella. Xavier Fernández-Francos improved the curing system used. All authors discussed the results, contributed to the writing of the manuscript and revised the final version.

Funding: The authors would like to thank MINECO (Ministerio de Economia, Industria y Competitividad) (MAT2017-82849-C2-1-R and MAT2017-82849-C2-2-R) and Generalitat de Catalunya (2017-SGR-77 and Serra Húnter programme) for the financial support.

Acknowledgments: Gabriel Benmayor S.A. is acknowledged for giving us the fillers used.

Conflicts of Interest: The authors declare no conflict of interest.

References

1. Pascault, J.P.; Williams, R.J.J.; (Eds.) *Epoxy Polymers: New Materials and Innovations*. Wiley-VCH: Weinheim, Germany, 2010.
2. Guo, Q. (Ed.) *Thermosets. Structure, Properties and Applications*, 2nd ed.; Elsevier: Amsterdam, The Netherland, 2018.
3. Huang, X.; Zhi, C. (Eds.) *Polymer Nanocomposites: Electrical and Thermal Properties*; Springer International Publishing: Cham, Switzerland, 2016.
4. Isarn, I.; Massagués, L.; Ramis, X.; Serra, A.; Ferrando, F. New BN-epoxy composites obtained by thermal latent cationic curing with enhanced thermal conductivity. *Compos. Part A* **2017**, *103*, 35–47, doi:10.1016/j.compositesa.2017.09.007.
5. Yung, K.; Liem, H. Enhanced thermal conductivity of boron nitride epoxy-matrix composite through multi-modal particle size mixing. *J. Appl. Polym. Sci.* **2007**, *106*, 3587–3591, doi:10.1002/app.27027.
6. Xu, Y.; Chung, D. Increasing the thermal conductivity of boron nitride and aluminum nitride particle epoxy-matrix composites by particle surface treatments. *Compos. Interfaces* **2000**, *7*, 243–256, doi:10.1163/156855400750244969.
7. Gao, Z.; Zhao, L. Effect of nano-fillers on the thermal conductivity of epoxy composites with micro-Al_2O_3 particles. *Mater. Des.* **2015**, *66*, 176–182, doi:10.1016/j.matdes.2014.10.052.
8. Choi, S.; Kim, J. Thermal conductivity of epoxy composites with a binary-particle system of aluminum oxide and aluminum nitride fillers. *Compos. Part B* 2013, *51*, 140–147, doi:10.1016/j.compositesb.2013.03.002.
9. Yin, L.; Zhou, X.; Yu, J.; Wang, H.; Ran, C. Fabrication of a polymer composite with high thermal conductivity based on sintered silicon nitride foam. *Compos. Part A* **2016**, *90*, 626–632, doi:10.1016/j.compositesa.2016.08.022.
10. Román-Manso, B.; Chevillotte, Y.; Osendi, M.I.; Belmonte, M.; Miranzo, P. Thermal conductivity of silicon carbide composites with highly oriented graphene nanoplatelets. *J. Eur. Ceram. Soc.* **2016**, *36*, 3987–3993, doi:10.1016/j.jeurceramsoc.2016.06.016.

11. Li, A.; Zhang, C.; Zhang, Y.-F. Thermal Conductivity of Graphene-Polymer Composites: Mechanisms, Properties, and Applications. *Polymers* **2017**, *9*, 437, doi:10.3390/polym9090437.
12. Huang, X.; Jiang, P. A review of dielectric polymer composites with high thermal conductivity. *IEEE Electr. Insul. Mag.* **2011**, *27*, 8–16, doi:10.1109/MEI.2011.5954064.
13. Pham, H.Q.; Marks, M.J. *Ullmann's Encyclopedia of Industrial Chemistry: Epoxy Resins*; Wiley-VCH: Weinheim, Germany, 2012.
14. Hussain, F.; Hojjati, M.; Okamoto, M.; Gorga, R.E. Polymer-matrix Nanocomposites, Processing, Manufacturing, and Application: An Overview. *J. Compos. Mat.* **2006**, *40*, 1511–1575, doi:10.1177/0021998306067321.
15. Isarn, I.; Gamardella, F.; Massagués, L.; Fernández-Francos, X.; Serra, À.; Ferrando, F. New epoxy composite thermosets with enhanced thermal conductivity and high Tg obtained by cationic homopolymerization. *Polym. Compos.* **2018**, *39*, 1760–1769, doi:10.1002/pc.24774.
16. Carreau, P.J.; De Kee, D.C.R.; Chhabra, R.P. *Rheology of Polymeric Systems: Principles and Applications*; Hanser Publishers: Munich, Germnay, 1997.
17. Han, C.D. *Rheology and Processing of Polymeric Materials*; Oxford University Press: New York, NY, USA, 2007; Volume 1.
18. Isarn, I.; Ramis, X.; Ferrando, F.; Serra, À. Thermoconductive thermosetting composites based on boron nitride fillers and thiol-epoxy matrices. *Polymers* **2018**, *10*, 277, doi:10.3390/polym10030277.
19. Tadros, T.F. *Rheology of Dispersions: Principles and Applications*; Wiley-VCH: Weinheim, Germany, 2010.
20. Yang, R.G.; Chen, G. Thermal conductivity modeling of periodic two-dimensional nanocomposites. *Phys. Rev. B* **2004**, *69*, 195316, doi:10.1103/PhysRevB.69.195316.
21. Stauffer, D.; Aharony, A. *Introduction to Percolation Theory*, 2nd ed.; Taylor & Francis: London, England, 1991.
22. Tian, W.; Yan, R. Phonon Transport and Thermal Conductivity Percolation in Random Nanoparticle Composites. *CMES* **2008**, *24*, 123–141.
23. Jouault, N.; Vallat, P.; Dalmas, F.; Said, S.; Jestin, J.; Boué, F. Well-dispersed fractal aggregates as filler in polymer-silica nanocomposites: Long-range effects in rheology. *Macromolecules* **2009**, *42*, 2031–2040, doi:10.1021/ma801908u.
24. Sadhir, R.K.; Luck, R.M. (Eds.) *Expanding Monomers: Synthesis Characterization and Applications*; CRC Press: Boca Ratón, FL, USA, 1992.
25. Coors Tek Amazing Solutions. Available online: www.dynacer.com/hardness (accessed on 1 July 2018).

Chapter 7

Study on the cooperative effect of boron nitride and carbon nanotubes in the improvement of the thermal conductivity of epoxy composites

Submitted to Polymer Composites

Study on the cooperative effect of boron nitride and carbon nanotubes in the improvement of the thermal conductivity of epoxy composites

Isaac Isarn[a], Leïla Bonnaud[b], Lluís Massagués[c], Àngels Serra[d], Francesc Ferrando[a]

a. Department of Mechanical Engineering, Universitat Rovira i Virgili, C/Av. Països Catalans, 26, 43007 Tarragona, Spain.
b. Laboratory of Polymeric and Composite Materials, Center of Innovation and Research in Materials and Polymers (CIRMAP), Materia Nova Research Center & University of Mons, 23 Place du Parc, B-7000, Mons, Belgium.
c. Department of Electronic, Electric and Automatic Engineering, Universitat Rovira i Virgili, C/Av. Països Catalans, 26, 43007 Tarragona, Spain.
d. Department of Analytical and Organic Chemistry, Universitat Rovira i Virgili, C/ Marcel·lí Domingo s/n, 43007 Tarragona, Spain.

Abstract

The enhancement of the thermal conductivity, keeping electrical insulation, of epoxy thermosets through the addition of pristine and oxidized carbon nanotubes (CNTs) and micro-platelets of boron nitride (BN) was studied. Two different epoxy resins were selected: a cycloaliphatic (ECC) and a glycidylic (DGEBA) epoxy resins. The behavior of the composites obtained was studied and compared in terms of thermal, thermo-mechanical, rheological and electrical properties. Two different dispersion methods were used in the addition of pristine and oxidized CNTs depending on the type of epoxy resin used. Slight changes in the kinetics of the curing reaction were observed in the presence of fillers. The addition of pristine CNTs led to a greater enhancement of the mechanical properties of ECC composites whereas the oxidized CNTs presented a higher effect in the DGEBA matrix. The addition of CNTs alone drastically led to a drop of the electrical resistivity of the composites. Nevertheless, in the presence of BN, it is possible to increase the proportion of CNTs in the formulation without deterioration of the electrical resistivity. A low but significant synergic effect was detected when both fillers were added together. Improvements of about 750% and 400% in thermal conductivity were determined in reference to the neat epoxy matrix for the ECC and DGEBA composites, respectively.

Keywords

Thermal conductivity, carbon nanotubes, boron nitride, epoxy resins, composites

1. Introduction

In the last two decades great efforts have been devoted to enhancing the performance capabilities in reinforced epoxy polymers.[1,2] One of the most challenging

issue in this type of materials consists in the enhancement of the thermal conductivity (TC), because of their intrinsically insulating characteristics. To improve the thermal management is crucial in the rapid evolution of modern electronics and other applications that involve the maintenance of a working temperature range.[3] The thermal conductivity of traditional ceramic fillers (Al_2O_3, SiO_2, AlN, BN, SiC…) is becoming insufficient for this purpose, even at high loadings. That is why many studies have been performed using carbon materials including carbon nanotubes (CNTs), carbon nano-fibers, graphene, graphite, expanded graphite (EG), carbon black, etc., as they exhibit an exceptional thermal transport ability.[4]

CNTs are characterized by a high aspect ratio, excellent mechanical properties, remarkable thermal and electric conductivities, low density and good corrosion resistance against oxidative environments.[2,5] Although these properties depend on the synthetic method used (chemical vapor deposition, laser ablation, arch discharge, etc.) and manufacturing quality, CNTs can improve epoxy composite properties such as: Young's modulus, tensile and yield strengths, fracture toughness, hardness, flexibility, adhesion, vibrational damping, hydrophobicity, piezoelectricity for sensors, etc.[5-10] These characteristics make them very interesting materials in the development of nanotechnology, nanoscience and microelectronics. According to their exceptional properties, they can be used in a wide range of different applications in the fields of aerospace, automotive and naval engineering, light emitting diodes (LEDs) and bio-medicine, among others.[11,12] Besides the different synthetic methodologies, chemical vapor deposition appears as the most convenient, since it is the most economical, it is able to grow nanotubes directly on a surface and the obtained nanotubes have more defects, which improves the interaction capability with the matrix, increasing the interface properties.[13,14] One of the main problems to solve in the preparation of composites is the dispersion of CNTs in the matrix due to their high surface area and their strong tendency to agglomerate via Van der Waals forces.[5,7] The other important issue is the high interfacial thermal resistance between the nanofiller and the polymeric matrix.[3,15] Previous published studies[16,17] showed that pristine CNTs at low concentration can enhance TC when good dispersion is reached. Nonetheless, a beneficial method to improve the epoxy-CNT interactions and thus the dispersion of CNTs is their functionalization (usually by oxidizing the surface), which can preserve CNT pristine structure, through the delocalized π-bonds interactions.[5,18] It is important to stress that not all functionalization types contribute in a positive way to the enhancement of TC.[19,20]

Heat transport in carbon materials is dominated by electron transport due to the sp^2 hybridization of carbon atoms, while in polymer composites this phenomenon is governed through phonons.[3,21] Despite the high thermal conductivity of CNTs, composite conductivities presented a much lower values than those estimated by theoretical calculations.[3,22] This fact is caused by the phonon scattering produced in the

CNT-matrix and CNT-CNT interfaces and their high interface thermal resistances. The origin of this resistance is the high difference of the frequency modes that obstruct the phonon-phonon coupling before exchanging heat in each interface.[22,23] Lattice defects and impurities should not be underestimated, since they are points at which phonons can be scattered.[3]

Up to now, there are only few publications combining boron nitride (BN) and CNTs in epoxy matrices. However, a synergistic improvement in the thermal conductivity using these two fillers has been demonstrated in polyphenylene sulfide matrices.[24] This improvement seems to strongly depend on the surface treatment of the MWCNTs. Teng et al.[25] used BN and functionalized MWCNTs to prepare epoxy composites. A synergistic effect in the thermal conductivity was observed in the composite containing 30 vol. % of BN and 1 vol.% of MWCNTs, reaching a value of TC of 1.91 W/m·K. Li et al.[26] studied how the addition of fillers (BN/CNT), fabricated by in-situ growing of CNTs onto BN surfaces, to epoxy resins affects mechanical characteristics and TC. The materials with BN/CNT particles show better thermal performance than pure BN composites even with CNTs loading as low as 2 wt. %. The prepared composites have a large electrical resistivity because BN particles block the current paths of CNTs bonded to the inorganic particles. Mechanical properties of the samples are also improved. The Su's group reported different results when adding BN particles and CNTs to epoxy matrices.[27,28] In both papers, CNTs are modified with amino groups at the surface, whereas BN is modified with iron oxide in one of the works and unmodified in the other. By using a 30 wt. % of modified BN, the addition of CNTs is found to reduce TC, whereas when 35 wt. % of pristine BN is used, a synergistic effect of about 40% of increase is observed.

According to the different results reported and the scarce number of studies on the synergism between BN and CNTs we have considered interesting to go deeper in this topic. Thus, the aim of the present work is the preparation of epoxy composites with a high thermal conductivity keeping electrical insulation using different proportions of these particles. The study also aims to correlate which changes in the matrix and in the fillers affect these characteristics and if there are some kind of cooperative effects among them. As the matrix, two different epoxy systems based on diglycidylether of bisphenol A (DGEBA) and a cycloaliphatic resin (ECC) cationically homopolymerized have been tested, which were previously optimized using a cationic initiator, CXC1612, and adding BN microplatelets as the filler.[29-31] In the present work, BN particles, with a larger size, and pristine and oxidized MWCNT's are selected. The kinetics of the curing of the different formulations have been determined by calorimetry. Rheological studies have allowed us to determine the effect of the addition of fillers to the formulations on their viscoelastic characteristics and to determine the rheological percolation threshold. The materials obtained have been characterized from the thermal and thermomechanical point of view and thermal conductivity and electrical resistivity were also determined.

2. Materials and methods

2.1. Materials

Cycloaliphatic epoxy resin (3,4-epoxy cyclohexylmethyl 3,4-epoxycyclohexane carboxylate, ECC) (EEW=126.15 g/epoxy eq.) was supplied from Sigma Aldrich Inc. (Darmstadt, Germany). Diglycidyl ether of bisphenol A (DGEBA) EPIKOTE Resin 828 (EEW=187g/epoxy eq.) was purchased from Hexion Specialty Chemicals (Stuttgart, Germany). The initiator N-(4-methoxybenzyl)-N,N-dimethylanilinium hexafluoro-antimonate (CXC1612) from King Industries Inc. (Norwalk, CT, USA), was dissolved in propylene carbonate at 50 wt. %. Propylene carbonate and triethanolamine (TEA) were provided by Sigma Aldrich Inc. and both purified by distillation before use. Glycerol (Gly) and hydrogen peroxide solution of 30 wt. % were supplied by Sigma Aldrich Inc. and used as received. Multiwalled carbon nanotubes (MWCNT, see **Figure 1A**) were provided by Nanocyl SA (Sambreville, Belgium), with 9.5 nm and 1.5 µm of diameter and length averages, respectively, and specific surface area (SSA) in the range of 250-300 m^2/g. Platelets of hexagonal boron nitride (BN, **Figure 1B**) with an average size of 30 µm (PCTP30) were purchased from Saint-Gobain (Valley Forge, PA, USA).

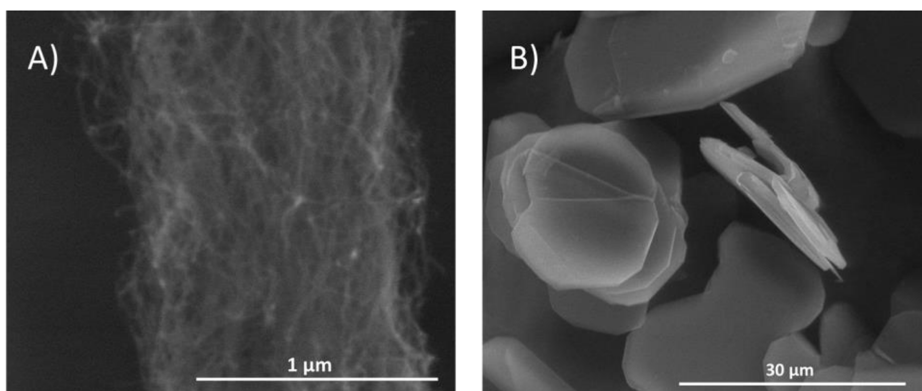

Figure 1. A) Pristine CNT agglomerate in powder form. B) Micro-sized platelets of h-BN.

2.2. Sample preparation

The curing of samples was carried out onto teflonated metallic moulds and following a multi-step temperature schedule at 100, 120, 150, 180 and 200 °C, leaving them 1 h at each temperature.

The cycloaliphatic epoxy system was prepared by mixing 1 phr of CXC1612 (parts of initiator per hundred parts of resin) and 0.1 phr of TEA. Proportions between 0.05-1 wt. % of CNT were added to the epoxy system as is schematized in **Figure 2A**. CNTs were dispersed in the resin by direct sonication (Digital Sonifier 250/450 from Branson Ultrasonic Corporation, Danbury, CT, USA), using 35% of amplitude during 20 s, divided in four equal batches of 5 s. Vacuum at room temperature was applied during 1 h to remove bubbles formed by the dispersion procedure. The mixtures of ECC-CNT were

used to form new mixtures by using 60 wt. % of them with the 40 wt. % of BN particles. In this case, mechanical stirring until homogeneity was done. The curing of the samples was carried out in metallic molds and following an optimized multi-step temperature schedule at 80, 100, 120, 150, 180 and 200 °C, with a dwelling time of 1 h at each temperature.

DGEBA resin formulation was prepared following a previous procedure by mixing 3 phr of CXC1612 and 2 phr of Gly. A maximum proportion of 1 wt. % of CNTs, and 40 wt. % of BN were added. The curing was performed at 120 °C for 1 h, followed by a post curing at 150 °C for 1 h. The preparation procedure is schematized in **Figure 2B**.

CNTs were oxidized following the procedure described by Pak et. al.[24] using a mild treatment of the CNTs with hydrogen peroxide at 30% in a sonicator bath. 1 wt. % of oxidized carbon nanotubes (o-CNTs) was added to neat ECC and DGEBA epoxy formulations, and to these formulations containing a 40 wt. % of BN.

2.3. Characterization techniques

A modulated differential scanning calorimeter (DSC, Mettler Toledo, Columbus, OH, USA) Mettler DSC-3+ was used to analyze the epoxy reaction evolution. Samples of ca. 3-5 mg were tested in aluminum pans with a pierced lid in a nitrogen atmosphere with a gas flow of 50 mL/min. The dynamic studies were performed in the range of 30-250 °C with a heating rate of 10 K/min. Enthalpy released on curing the samples (Δh) was calculated integrating the calorimetric signal (dh/dt) using a straight baseline in the range of the exotherm, with the help of the STARe software.

Rheologic experiments were carried out for ECC-CNT formulations in parallel aluminium plates (20 mm diameter) in oscillatory mode with an AR G2 rheometer equipped with a peltier temperature controller accessory from TA Instruments (New Castle, DE, USA). The linear viscoelastic range (LVR) was determined at 1 Hz and 30 °C varying the strain applied. Viscoelastic properties as shear elastic modulus (G') and viscous modulus (G''), were determined in the LVR in frequency sweep experiments at 30 °C.

Dynamic mechanical thermal analyses (DMTA) were performed with a TA Instruments DMA Q800 analyzer. The prismatic rectangular samples (20 x 4.5 x 2.5 mm3) were analyzed by 3-point bending clamp at a heating rate of 3 K/min from 30 to 300 °C, using a frequency of 1 Hz and an oscillation of 0.1% of sample deformation. The Young's modulus (E) was determined at 30 °C by means of a force ramp at constant rate, 1 N/min, until reaching a deformation that never exceeds 0.25% of strain, to guarantee that only the elastic part of the material is evaluated. E was calculated taken the slope between 0.1 and 0.2 % of the deformation curve in accordance with the equation:

$$E = \frac{L^3 m}{4bt^3} \qquad (1)$$

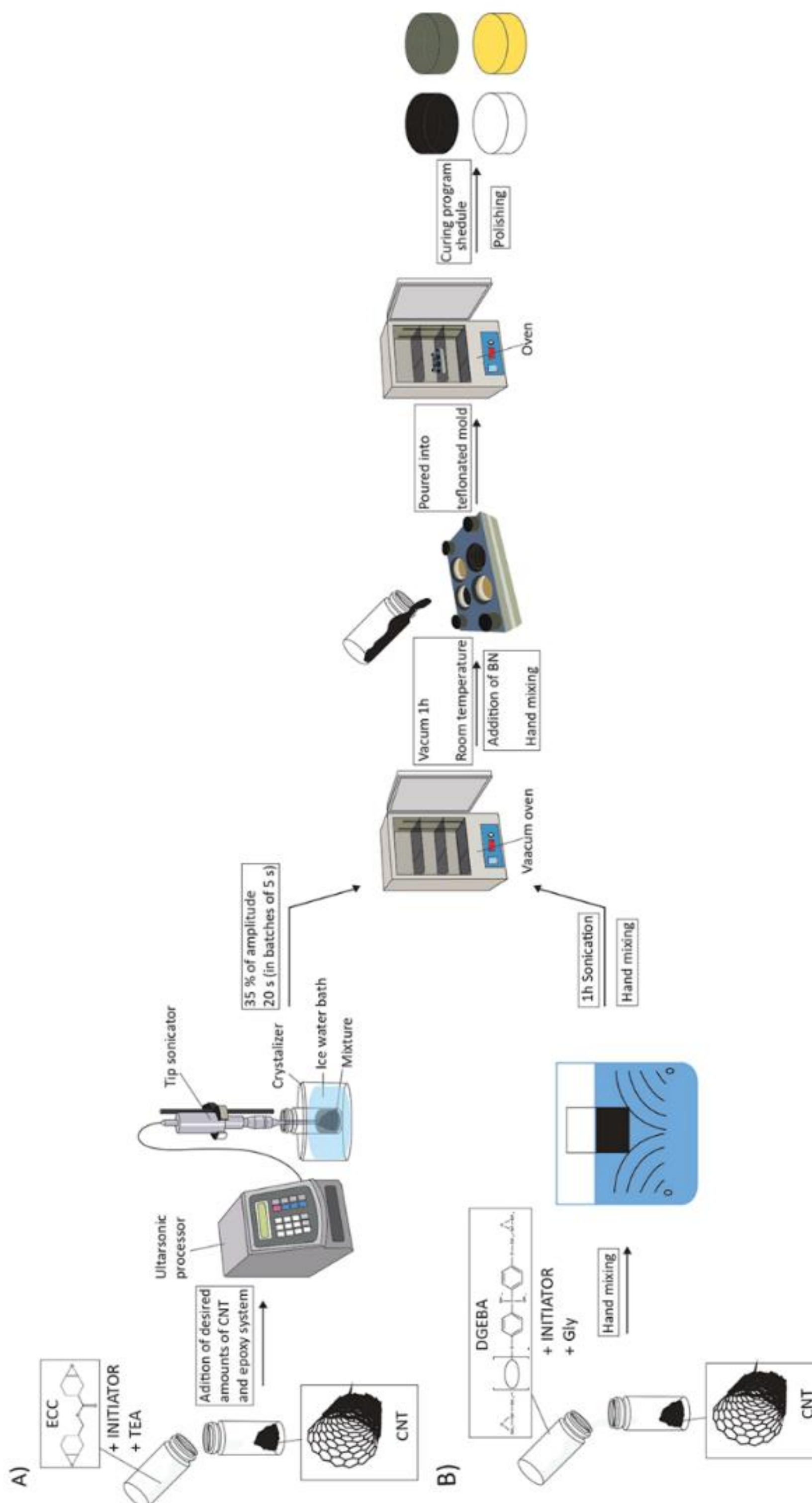

Figure 2. Scheme of sample preparation of ECC (A) and DGEBA mixtures (B).

where E is the elastic modulus of epoxy sample (MPa), L is the support span (mm), b and t are the width and the thickness of test sample (mm) and m is the gradient of the slope (N/mm).

Surface hardness was evaluated through Knoop microindentation analysis being consistent with ASTM D1474-13. A minimum of 12 determinations were considered with a confidence level of 95% for each material. Knoop microindentation hardness (KHN) was calculated as follows:

$$KHN = \frac{L}{A_p} = \frac{L}{l^2 C_p} \qquad (2)$$

where L is the load applied by the indenter (0.025 Kg), A_p is the area of indentation in mm^2 and C_p the indenter constant relating l^2 with A_p.

Thermomechanical analyses (TMA) were carried out on a Mettler TMA40 thermomechanical analyzer. Square cured samples (9 x 9 x 2.3 mm^3) were supported by the clamp and a silica disc to distribute uniformly the force and heated at 5 K/min from 35 to 100 °C. A minimum force of 0.01 N was applied to avoid results distortion. The thermal expansion coefficients (*CTEs*) in the glassy state of the material were calculated as follows:

$$CTE = \frac{1}{L_0} \cdot \frac{dL}{dT} = \frac{1}{L_0} \cdot \frac{dL/dt}{dT/dt} \qquad (3)$$

where L is the thickness of sample, L_0 the initial length, t the time, T the temperature and dT/dt the heating rate.

Thermal stability of cured samples was evaluated in a Mettler TGA2 thermobalance. All the experiments were carried out under N_2 atmosphere (50 mL/min). Pieces of cured samples of 3-6 mg were heated between 30 and 600 °C at a heating rate of 10 °C/min.

Environmental scanning electron microscopy (ESEM) was used to examine the fillers and breaking surfaces of the materials prepared. A Quanta 600 environmental scanning electron microscopy (FEI Company, Hillsboro, OR, USA) allows collect micrographs at 10-20 kV and low vacuum mode without the need to coat the samples with poor electrical conductivity.

Electrical resistance of materials was tested using a multimeter 34410A 6½ Digit from Agilent Technologies (Santa Clara, CA, USA) at room temperature and based on ASTM D257-14. The samples with higher electrical resistance (>10^8 Ω·m) were evaluated with a Megohmmeter Resistomat 24508 (Gernsbach, Germany) at room temperature and the same standard. Samples of approximately 14 mm of diameter were tested between two stainless steel electrodes with a surface area of 19.635 mm^2. A voltage of 500 V during 5 min was applied to thermoset composites. Electrical resistivity (ρ) was determined as follows:

$$\rho = R\frac{A}{l} \qquad (4)$$

where *R* is the electrical resistance measured by the device, *A* the electrode area and *l* the sample thickness.

Thermal conductivity was measured using the Transient Hot Bridge method by a THB 100 device from Linseis Messgeräte GmbH (Selb, Germany). A HTP G 9161 sensor was used with a 3 x 3 mm^2 of area calibrated with poly(methyl methacrylate) (PMMA), borosilicate crown glass, marble, Ti-Al alloy and titanium. Two equal polished rectangular samples (9 x 9 x 2.3 mm^3) were placed in each face of the sensor. Due to the small size of sensor, side effect can be neglected. A measuring time of 100 s with a current of 10 mA was applied to the five measures done for the different formulations.

3. Results and discussion

3.1. Calorimetric analysis by DSC

The initiator selected, CXC1612, has proved to present a markedly thermal latent character in ECC formulation in the presence of TEA until reaching temperatures over 100 °C (determined by DSC).[29] According to that, the formulation presents a long storage stability at room temperature. For this reason, this system was selected for direct sonication to disperse carbon nanotubes, taking advantage of the low viscosity of ECC resin. Ultrasonication is considered an efficient dispersion method, less time consuming compared to other techniques, although it is known to damage CNTs introducing defects and reducing lengths.[20,32] The formation of defects represents an advantage providing bonding sites between the filler and the matrix, to the already imperfect CNT made by CVD. After preliminary investigations it was decided to apply 20 s of ultrasonication, divided in batches of 5 s, at the high amplitude of 35% to all the ECC-CNT mixtures (see compositions in **Table 1**). Lengthen sonication time increased the temperature by the mechanical action and the homopolymerization reaction was initiated despite having the curing system the latent character. CNT suspensions, which were degassed under vacuum, could be stored at room temperature for three months without observing any sign of filler precipitation, which confirmed the good dispersion reached. To ECC-CNT mixtures a 40 wt. % of BN was added, and the compositions of the different formulations are detailed in Table 1.

The curing of the formulations prepared was studied by DSC in dynamic mode. Table 1 contain the most important data extracted from these experiments. It should be mentioned, that the curing exotherms are narrow and high, due to the latent character and quick reaction.[29]

Some authors studied the curing behavior of epoxy systems filled with CNTs.[33] When the filler was well dispersed no variation in the curing process was observed. However, when CNTs agglomerate conflicting results were reported, diminishing or increasing the enthalpy evolved during curing. In Table 1 it can be observed how the addition of CNTs barely change the temperature of the maximum of the exotherm and the heat evolved during the cure, which support the good CNT dispersion. The addition

of o-CNTs does not lead to great differences when added to the curing formulation. In all the CNTs filled formulations the temperature of the maximum of the peak is reduced only in 2 °C, which indicates a slight activation of the curing process as reported previously.[34] The addition of a 40% of BN to the neat epoxy leads to a similar decrease in the temperature of the peak, but there is any influence on the CNTs filled formulations. The sample of 1 wt. % o-CNT/40 wt. % BN seems to be the most reactive, since a reduction of 3 °C in the temperature of the exotherm can be observed in reference to the neat epoxy. It seems to indicate a slight cooperative effect between both fillers. It is known, that the presence of protons, formed in the CNT oxidation, can help to catalyze the ring-opening polymerization.[35,36] It must be mentioned that DSC did not allow to determine the T_g of the cured material, due to the constrained network formed.[29]

Table 1. Composition of the ECC formulations and DSC data for all the mixtures.

Sample	T_{peak} (°C)	Δh (J/g)	Δh (kJ/ee)
Neat epoxy	122.4	603	76.1
0.05% CNT	121.6	599	75.6
0.10% CNT	120.5	594	75.1
0.25% CNT	121.0	592	74.9
0.50% CNT	120.5	594	75.3
0.75% CNT	120.1	593	75.4
1.00% CNT	120.5	593	75.5
1.00% o-CNT	120.4	601	76.5
40% BN	120.2	364	76.5
0.05% CNT / 40% BN	120.9	363	76.4
0.10% CNT / 40% BN	120.6	363	76.4
0.25% CNT / 40% BN	120.8	363	76.7
0.50% CNT / 40% BN	120.2	354	75.0
0.75% CNT / 40% BN	120.8	353	75.3
1.00% CNT / 40% BN	120.9	350	74.8
1.00% o-CNT / 40% BN	118.9	353	75.5

DGEBA formulations were also tested to know the effect of the fillers in their curing behavior. The higher viscosity of DGEBA makes more difficult the CNT dispersion. Since the use of solvents must be avoided, it was decided to combine mechanical mixing and the action of bath sonication to reach a good dispersion (see Figure 2B). In this case, only the formulations with a 1 wt. % of CNT or o-CNTs were studied (see **Table 2**). The addition of fillers to the DGEBA-CNT curing system produces higher differences in the DSC characteristics than in the previous formulations, probably as a consequence of a worst dispersion and the influence of the structure of this resin (**Figure 3** and Table 2). In contrast to ECC mixtures, the storage stability of these formulations is limited to some days. Unlike ECC-CNT samples, in DGEBA formulations the fillers shift the reaction to higher temperatures, delaying the curing. The delay is more noticeable in BN

formulations, which could be explained by the dilution effect of the high quantity of filler. The differences in ECC and DGEBA mixtures could be related to the highest reactivity of ECC resins in cationic polymerizations. The curing achieved in all the formulation seems to be quite similar, because there is no difference in the enthalpies evolved per epoxy equivalent in the different formulations. In these materials, T_g could be appreciated and the filler seems not influence much the values, although the highest T_g was reached in samples containing both BN and CNTs.

Table 2. Composition of the DGEBA formulations and DSC data for all the mixtures.

Sample	T_{peak} (°C)	Δh (J/g)	Δh (kJ/ee)	T_g (°C)
Neat epoxy	121	542	101.3	132
1% CNT	126	530	100.1	132
40% BN	133	318	99.0	130
1% CNT / 40% BN	134	314	99.5	134
1% o-CNT	126	540	102.0	132
1% o-CNT / 40% BN	134	317	100.4	134

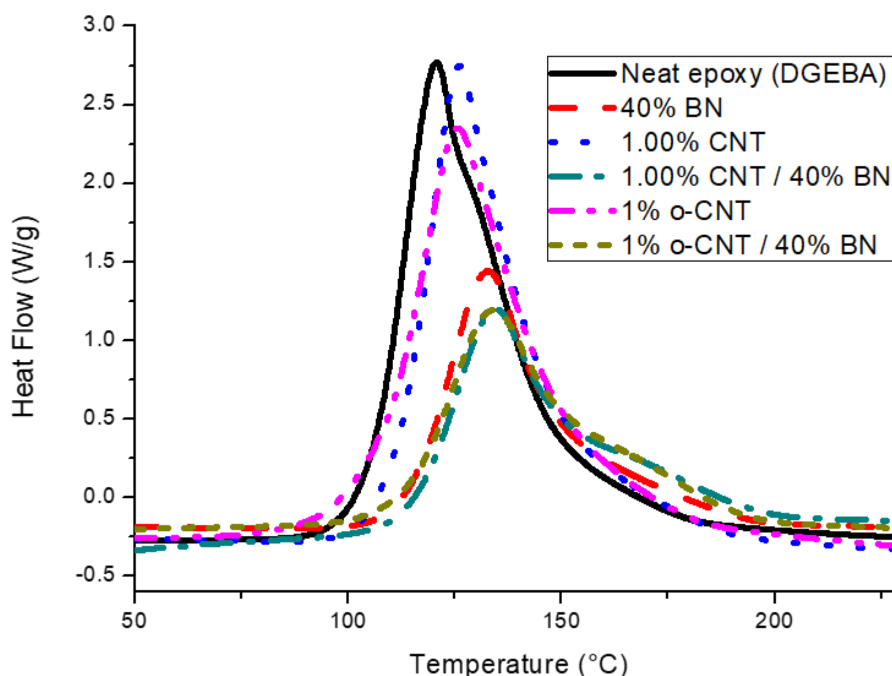

Figure 3. DSC curves of DGEBA formulations.

3.2. Rheologic study

The rheological behavior of polymers loaded with nanoparticles is one of the most important factors when these mixtures have to be processed. From the viscoelastic properties in oscillatory experiments it can be determined at what concentration for each type of particles the percolation is reached. It is known that not only the shape,

particle and matrix interactions, microstructure formed, and dispersion can determine the viscoelastic behavior of polymer-particles mixtures, but temperature is a very important influencing factor, and as consequence, can vary the concentration at the percolation.[37,38]

In the present case, tube-like particles (CNTs) are used as fillers and they can be dispersed randomly or aligned thanks to the high aspect ratio and therefore, percolation threshold is expected to be reached at low concentration. The determination of this point is important since a sudden change in different properties can occur. In this study, the percolation threshold of the CNTs in the ECC solution has been determined, because it is important to be under this threshold to keep the electrical insulation character of the composites prepared. A temperature closely to room temperature (30 °C) was used considering industrial processing. Only the mixtures of ECC-CNT where evaluated since, the amount of BN added (40 wt. %) as filler exceeded the percolation threshold as was determined in a previous study.[29]

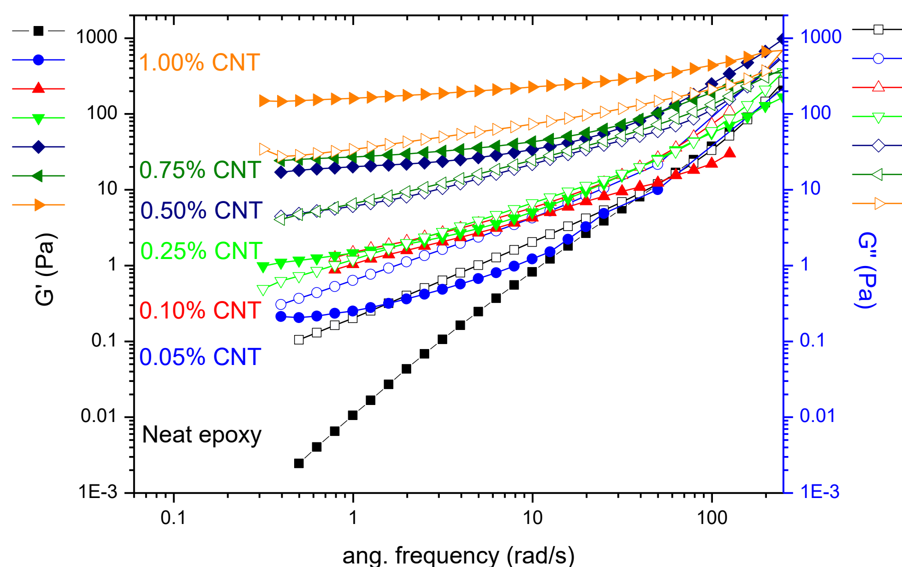

Figure 4. Storage modulus (G’) and loss modulus (G’’) against frequency (ω) of the ECC-CNT mixtures at 30°C.

All the mixtures were tested varying the amplitude at a fixed frequency (1 Hz) to determine the linear viscoelastic range (LVR), mandatory to determine the viscoelastic properties such as storage modulus (*G’*), loss modulus (*G’’*) and complex viscosity (η*) in experiments changing the frequency (ω) applied. **Figure 4** represents *G’* and *G’’* towards the ω for all the mixtures. It can be observed at which concentration *G’* is over *G’’* at low frequencies (<1 rad/s), sign that percolation threshold is surpassed.[31,39] This transition from liquid like behavior (*G’’*>*G’*) to solid like (*G’*>*G’’*) is located between the wt. % of 0.10 to 0.25 of CNT. It must be considered that this behavior is characteristic in this epoxy system with this type of particles used, the dispersion method applied (sonication) and the temperature at which the mixtures were examined.

As expected, the concentration of CNTs necessary to reach the percolation is quite low, common of nanoparticles with high surface area. In contrast, micro-sized particles, like 6 μm hexagonal BN platelets, in the same type of resin and at the same temperature, the percolation was reached at a proportion of 14.4 wt. %.[29]

The plot of η* against ω for 1 wt. % of CNT and o-CNT are represented in **Figure 5**. The plot shows a lower viscosity for the non-oxidized nanotubes. This means that the percolation with this filler would result in higher concentrations than the untreated filler, as it is common with functionalized CNT.[40] The increase of the concentration to achieve the rheological percolation threshold in modified particles is explained as the changes in particles during the processing, the enlargement of particle-matrix interactions and, as consequence, as an improvement of filler dispersion.[38,41]

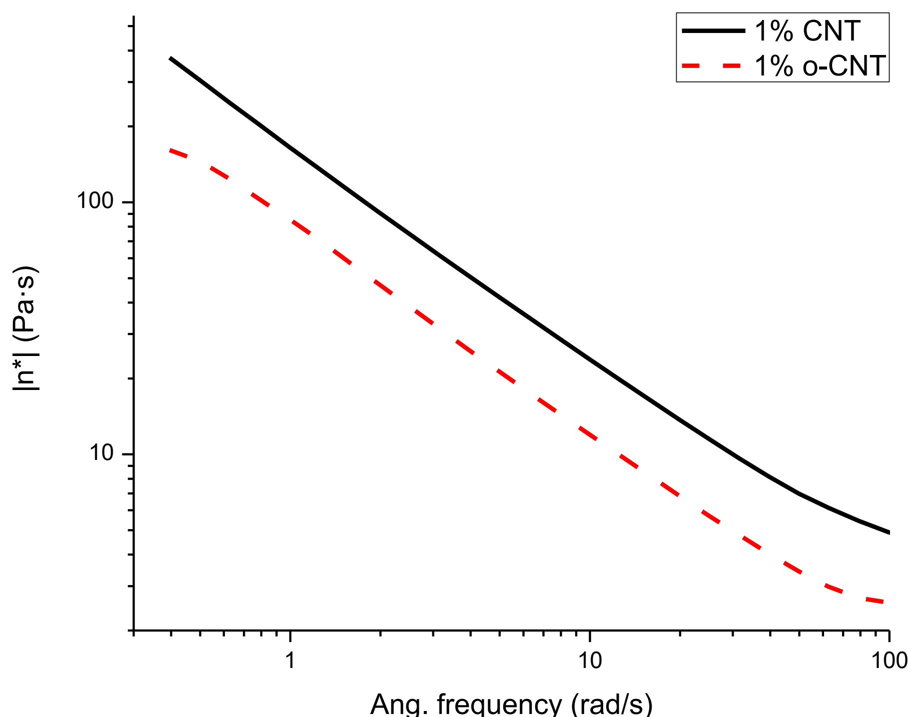

Figure 5. Complex viscosity against frequency of treated and untreated CNT in ECC matrix.

3.3. Thermal and thermomechanical analysis

Thermal and thermomechanical properties were determined in all the cured composites. The most important information of the experiments performed by DMTA, TGA and TMA in the ECC-CNT samples are collected in **Table 3**. Nanoparticles added in polymer matrices and, specifically CNTs in this study, are known to greatly increase a wide range of properties which include mechanical and thermal characteristics using lower concentrations than the conventional micro-sized fillers.[6]

Table 3. Mechanical and thermomechanical characterization of ECC-CNT composites.

Sample	E^a (GPa)	tan δ_{peak}^b (°C)	$T_{5\%}^c$ (°C)	Char yield[c] (%)	KHN[d]	CTE_{glass}^e ($10^{-6}·K^{-1}$)
Neat epoxy (ECC)	2.42 ± 0.02	210	352	1.8	12.9 ± 0.8	108
0.05% CNT	2.73 ± 0.08	209	346	2.0	18.0 ± 0.9	101
0.10% CNT	2.95 ± 0.04	214	342	1.8	21.4 ± 0.8	100
0.25% CNT	3.04 ± 0.02	212	336	2.8	21.8 ± 0.9	100
0.50% CNT	3.06 ± 0.04	214	330	3.1	22.9 ± 0.7	87
0.75% CNT	3.33 ± 0.05	214	332	3.5	26.0 ± 0.9	85
1.00% CNT	3.17 ± 0.03	215	329	3.6	25.2 ± 1.2	83
1.00% o-CNT	2.92 ± 0.01	214	318	3.1	25.0 ± 1.3	82
40% BN	6.50 ± 0.11	215	361	41.9	22.7 ± 0.7	78
0.05% CNT / 40% BN	6.58 ± 0.12	212	359	44.1	24.3 ± 1.4	77
0.10% CNT / 40% BN	6.61 ± 0.16	211	357	43.8	25.1 ± 1.8	72
0.25% CNT / 40% BN	6.98 ± 0.39	210	351	44.4	25.0 ± 1.2	69
0.50% CNT / 40% BN	7.01 ± 0.47	211	346	43.4	25.8 ± 1.6	69
0.75% CNT / 40% BN	7.16 ± 0.14	212	342	45.0	25.9 ± 1.4	67
1.00% CNT / 40% BN	6.68 ± 0.11	215	343	44.3	24.9 ± 1.1	64
1.00% o-CNT / 40% BN	6.61 ± 0.41	212	340	44.1	24.0 ± 1.0	65

[a] Young's modulus determined at 30°C in DMTA with a controlled force experiment in the elastic material range.

[b] Temperature of the maximum of the tan δ peak determined at 1 Hz in an oscillatory experiment by DMTA.

[c] Temperature of 5 wt.% loss and final residue in TGA test at 10 K/min in nitrogen atmosphere.

[d] Microindentation Knoop hardness.

[e] Coefficient of thermal expansion (CTE) in the glassy state (50-75°C) determined by TMA.

The values of Young's modulus show an enhancement with the increasing addition of CNTs, up to a maximum at the proportion of 0.75 wt. % of CNT with an improvement of a 37.5 % in reference to the neat epoxy sample. Similar results were described by Ulus et al. were small proportions of CNT results in better mechanical behavior than increasing the concentration of nanofillers.[42,43] On increasing the CNT content the viscosity of the formulation becomes higher and the possibility of the formation of agglomerates increases, which influence the processing and the final properties.[44] The use of o-CNT leads to a diminution of the rigidity, probably due to the deterioration of the structure of the particles. This seems to indicate that the hydroxyl and acids groups on the surface does not produce any improvement in the interaction. With the addition of 40 wt. % of BN the rigidity is highly improved, more than twice of neat material as observed in previous studies[29,39] as the result of the reinforcing role of the filler. The use of both CNTs and BN particles has a complementary effect in the

rigidity of the samples, slightly increasing their value with the same trend as the composites with only CNT as filler, which reach the maximum rigidity at 0.75 wt. % proportion.

The rigidity of the composites with DGEBA as the matrix was also determined and the values obtained are collected in **Table 4**.

Table 4. DMTA, TGA and TMA results from DGEBA-CNT composites.

Sample	E[a] (GPa)	tan δ_{peak}[b] (°C)	$T_{5\%}$[c] (°C)	Char yield[c] (%)	KHN[d]	CTE_{glass}[e] (10^{-6}·K^{-1})
Neat DGEBA	2.17 ± 0.05	131	376	13.1	21.9 ± 0.9	80
1% CNT	2.26 ± 0.04	145	372	18.9	21.9 ± 0.7	78
1% o-CNT	2.37 ± 0.03	144	381	17.5	25.7 ± 1.0	72
40% BN	5.49 ± 0.12	148	399	48.8	24.5 ± 1.3	72
1% CNT/40%BN	5.63 ± 0.09	146	386	48.2	24.6 ± 1.1	56
1% o-CNT/40%BN	6.26 ± 0.21	145	395	51.0	25.7 ± 0.9	57

[a] Young's modulus determined at 30°C in DTMA with a controlled force experiment in the elastic materials range.
[b] Temperature of the maximum of the tan δ peak determined at 1 Hz in an oscillatory experiment by DMTA.
[c] Temperature of 5 wt.% loss and final residue in TGA test at 10 K/min in nitrogen atmosphere.
[d] Microindentation Knoop hardness.
[e] Coefficient of thermal expansion (CTE) in the glassy state (50-75°C) determined by TMA.

Young modulus barely increases with the addition of 1 wt. % of CNT. However, the oxidation of CNTs leads to a slightly higher rigidity. The results obtained seems to indicate that there is no interaction between the electronic density of phenylene rings in the resin and electronic density of CNTs on the contrary to our expectations, but the presence of reactive groups in o-CNTs can lead to covalent bonding with the resin to some extent.

The T_gs of the composites derived from ECC (Table 3), which could not be determined by DSC due to the tight network formed, could be visualized by DMTA. The values remained within a narrow range of temperatures (209-215 °C) according to the rigidity and high crosslinking density of the epoxy matrix. The small variation by the addition of filler confirms the low interaction between fillers and the matrix. On the other hand, the temperature of tan δ peaks of DGEBA materials (Table 4) shows an increase of about 15 °C when the fillers are added, but in this case the temperatures were lower (131-148 °C). Both the addition of 1 wt. % of pristine and oxidized CNTs affects the tan δ values in a similar way than 40 wt. % of BN and any synergetic effect between the filers could be appreciated. In DGEBA composites the addition of fillers increase more the tan δ temperature than the T_g determined by DSC (Table 2). This can be related to the fact that these fillers somehow interact with the resin producing a more pronounced effect on thermomechanical tests than in techniques based on the change of the heat capacity, indicating their higher mechanical effect close to the relaxation temperature range.

The thermal stability of the composites was studied by TGA under inert atmosphere (see Tables 3 and 4). This is an important characteristic which determine the service life of a material when it is exposed to high temperature. It is known that the addition of CNTs to polymer matrices increases the thermal resistance of the composites mainly attributable to the good dispersion and interactions between the filler and the polymer matrix.[45,46] Nevertheless, the impurities that remain in the nanofiller, due to the manufacturing technique, can accelerate the degradation process.[47] The two types of composite matrices present a monomodal decomposition derivative plot, with an only pronounced step of weight loss. In Table 3, the TGA data for ECC samples are collected. As we can see, the initial decomposition temperature ($T_{5\%}$) decreases proportionally to the amount of CNTs added, but the addition of BN particles delays the decomposition process. The addition of the partially oxidized CNTs accelerates even more the degradation. The char yield exhibits its dependence with the amount of filler. It should be noted the carbonaceous residue that promotes the addition of pristine CNTs. In contrast, although the addition of CNTs accelerates the degradation process and BN particles stabilize thermally the composites, the addition of o-CNTs increases moderately their thermal stability, which is sign that functionalization of nanotubes is more valuable with aromatic epoxy matrices. The notable difference of residue formed with ECC and the DGEBA composites leads to a predictable higher flame retardancy for the latter.

For coating applications, the surface hardness is one of the main characteristics to ensure durability. The values determined for both types of composites are collected in the previous tables. In the case of ECC composites, the minimum addition of CNTs greatly increases the hardness, from 12.9 to 18.0 KHN and there is progressive increase, reaching a maximum at the 0.75 wt. % CNT proportion (26.0 KHN). When BN is added, the enhancement in hardness on adding increasingly proportions of CNTs get lost, and the maximum value is limited to 25.9 KHN with a 0.75 wt. % of CNT. The results with DGEBA resin make a difference. The addition of CNTs did not produce any change in hardness in reference to the neat epoxy (21.9 KHN). However, when o-CNTs are added, there is a notable enhancement (25.7 KHN), showing again that the modification has a greater effect when DGEBA is used as the matrix.

The thermal expansion coefficient of the composites was analyzed by TMA experiments. The reduction of this coefficient is desirable since polymers expand more than metals or ceramics on increasing temperature. Thus, when they are used to join or coat surfaces of metallic or ceramic materials, temperature fluctuations can cause deadhesion, warping, cracking or the creation of internal stresses that over time can result in critical failures. In Table 3 it can be seen a reducing trend in the CTE with the addition of both type of fillers. The most important change in CTE was found on adding 0.25-0.50 wt. % of CNT. A 40 wt. % of BN leads to a high reduction of the CTE value but proportionally, CNTs play a more important role in this improvement. In fact, the size

and shape of the particles greatly affect this property, since in previous studies with the same epoxy system, using a 6 µm sized BN, the reduction was greater.[29] DGEBA materials have a lower CTE value and is slightly reduced by the presence of one of the fillers. The combination of CNT and BN has a synergistic effect on the CTE reduction. The CTE of neat DGEBA drops in a 30 % when both fillers are added.

3.4. Microscopic inspection of composites

It has been explained previously, that the dispersion of fillers in the matrix is one of the most important requirements to improve the final composite characteristics. To prove that a good dispersion has been reached, electronic microscopy inspection (ESEM) is highly recommended. **Figure 6** shows some of the most representative micrographs of the fracture surface of the materials prepared with ECC as the matrix.

As we can see, there is a good dispersion of oxidized nanotubes in the matrix (Figure 6A). When both pristine CNTs and BN were added to composites, both fillers are well dispersed in the matrix (micrograph not shown), but which is intriguing is the distribution of nanotubes on the BN surface. Figure 6B shows the surface of a BN platelet (in the inner of the composite) with a thin layer of resin containing nanotubes, and Fig 6C shows an amplification of the BN particle surface. It can be observed how nanotubes are well distributed forming a co-continuous morphology of CNT-ECC matrix. It is also clear that CNTs have surpassed the percolation threshold.

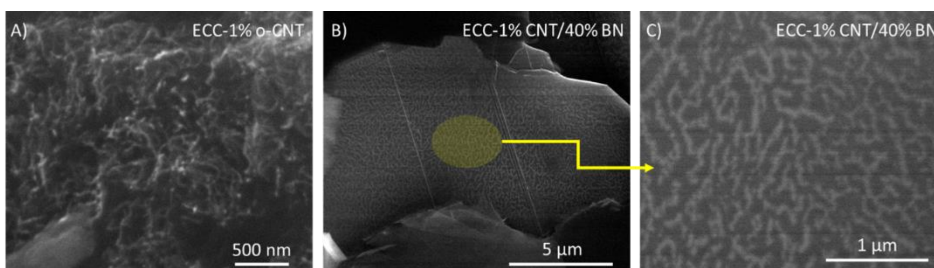

Figure 6. A) ECC with 1 wt. % of o-CNTs at 50k magnifications. B) ECC with 1 wt. % of pristine CNTs and 40 wt. % of BN at 10k magnifications, and the amplification of the same sample at 50k magnifications.

Figure 7 shows some selected micrographs of broken surfaces of DGEBA composites.

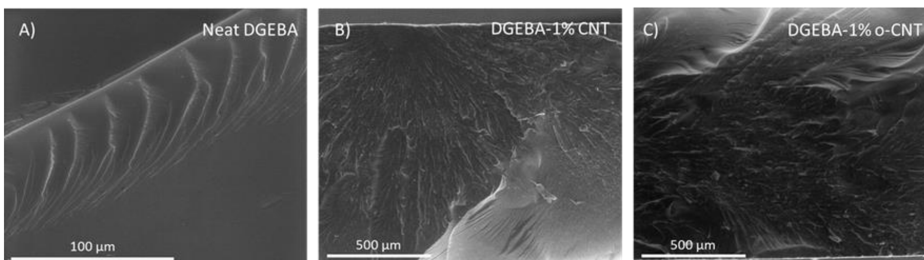

Figure 7. A) Neat DGEBA resin at 800 magnifications. B) DGEBA composite with pristine CNTs at 100 magnifications. C) DGEBA composite with o-CNTs at 100 magnifications.

The figures show in this case that the addition of pristine and oxidized CNTs leads to an improvement of toughness, since the crack propagation in Figures 7B and 7C, is more complex with more tortuous ways. In case of DGEBA, although a good dispersion of the nanotubes in the matrix could be observed, it was not possible to get clear images of them with this technique.

3.5. Electrical resistivity

The technological application of the materials developed in the present work requires the achievement of a maximum thermal conductivity without affecting electrical insulating character. For this reason, it is imperative to know the maximum amount of CNTs able to keep electrical insulation. By rheology we could determine that the percolation threshold in ECC/CNT mixtures was between 0.10 and 0.25 wt. %. However, this value can slightly differ from the proportion of CNTs to reach the electrical percolation. Thus, we selected different formulations with proportions of CNTs varying from 0.05 to 1 wt. %. **Figure 8** represents the values of electrical resistivity for ECC mixtures (red bars). It can be seen, that even the minimum concentration of nanotubes added to the formulation (0.05 wt. %) sharply decreases the electrical resistance by 7 orders of magnitude, which is no longer suitable for high insulation applications. This means that the electrical percolation threshold of the system is lower than 0.05 wt. % of CNT, under the rheological percolation. A good dispersion plays against the electrical insulation, since if the distance between the CNTs is close, the electrons can circulate by tunneling effect at a lower energy level, producing short-circuits in electronic devices. Between 0.10 and 0.25 wt. %, range of the rheological percolation, another fall of one order of magnitude is observed, and finally in the concentration range between 0.5 and 1 wt. % of CNTs the resistivity values are in the range 10^2-10^1 Ω·m. The use of partially oxidized nanotubes improves to 10^2 Ω·m the resistivity, due to the fact that the oxidation of the nanotube surfaces disturbs the electronic transmission.

In a previous work, in which expanded graphite and BN were combined as fillers in epoxy composites, we could prove that the addition of BN allowed us to increase the amount of carbon based filler in the formulation without losing electrical insulation properties.[48] Other authors also reported that the addition of electrically insulating BN considerably increases the insulation character for graphene composites.[49] Figure 8 shows that in BN containing samples, as far as the concentration of CNTs is under 0.50 wt. % the electrical resistivity is kept just one order of magnitude lower than the neat epoxy, 10^9 Ω·m, high enough to maintain good insulating characteristics. BN particles act as a barrier that prevent the circulation and tunneling effect of electrons between the conductive particles. At 0.50 wt. % of CNT in the sample with 40 wt. % of BN the resistivity falls down 5 orders of magnitude, going down further with the increasing content of nanotubes, but with higher values than CNT/epoxy composites. The addition of 1 wt. % of oxidized CNTs to the BN formulation leads to resistivity values one order of magnitude higher than a similar formulation with non-treated CNTs. From these

results it can be summarized that formulations containing 0.25 wt. % CNTs or below and 40% BN could be the most adequate in terms of electrical insulation from all the ECC composites prepared.

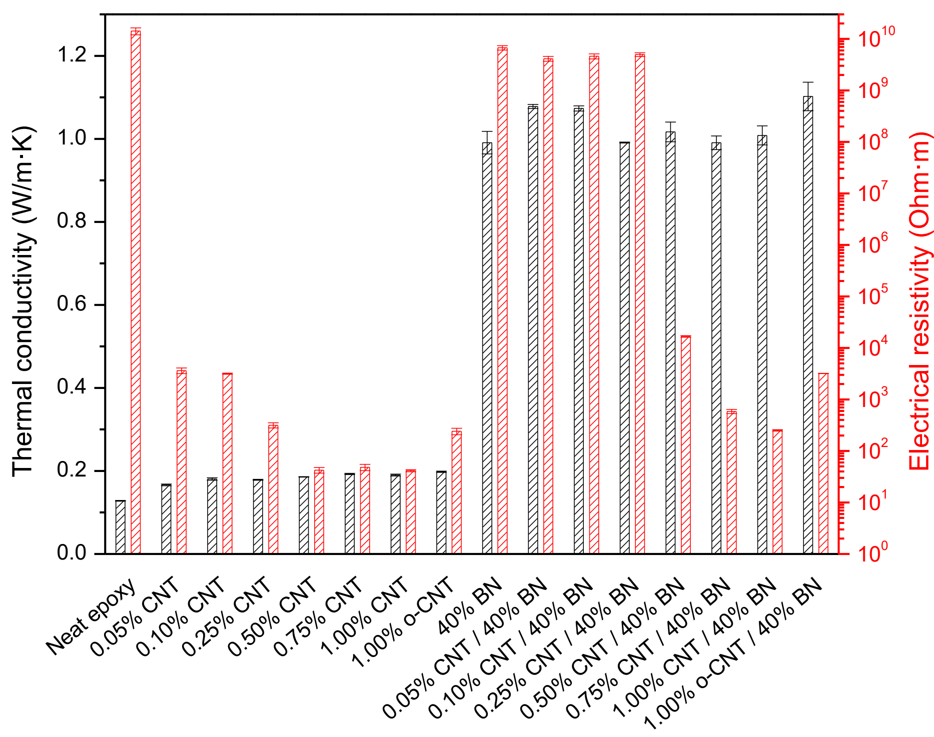

Figure 8. Thermal conductivities and electrical resistivities of ECC-CNT/BN composites.

Similar trends can be observed in **Figure 9** for DGEBA composites, although in this case less compositions were tested. While neat DGEBA epoxy resistivity is like neat ECC epoxy (10^{10} Ω·m) the addition of 1 wt. % CNT reduces drastically the resistivity 9 orders of magnitude. As in the ECC mixtures the resistivity is slightly higher when the CNTs were previously oxidized. The addition of BN, as in the previous ECC composites, acts as a barrier to the transmission of the electrical current, but its effect is less pronounced.

3.6. Thermal conductivity

The large aspect ratio of one-dimensional filler such as CNT is expected to enhance the TC of polymers at relatively low filler fractions for the high thermal conductivity they possess, which is reported to be around 6000 W/m·K.[50] Figure 8 collects the results of TC of composites with different proportions of CNTs dispersed in the ECC matrix. The presence of CNTs in the composite enhance the thermal conductivity from 0.13 W/m·K for the neat epoxy to a maximum of 0.20 W/m·K, when 1 wt. % of o-CNT was added to the formulation, which is more than a 50% of improvement in TC. The composites with non-modified CNT showed a maximum in TC

of 0.19, when 0.75 or 1 wt. % of CNT were added. The addition of 40 wt. % of BN enhanced the conductivity up to values around of 1 W/m·K, with a maximum with a 1 wt. % of o-CNT of 1.102 W/m·K. No appreciable differences were observed on increasing the amount of CNT in BN filled composites. Although a slight synergistic effect of BN and CNT of 8-11% is observed in the present study, the synergistic effect is much lower than that reported by Teng et al.[25] with values of TC about 1.91 W/m·K, using a 30 wt. % of BN and 1 vol. % of CNTs. However, they do not measure electrical resistivity characteristics of the composites and they added epoxy functionalized CNTs and amino functionalized BN particles to the epoxy resin, which enhance the interactions between the matrix and fillers, necessary to get good thermal conductivity. However, the chemical modification of fillers could not be desirable for technological applications due to the high cost and the low availability of industrial modified fillers.

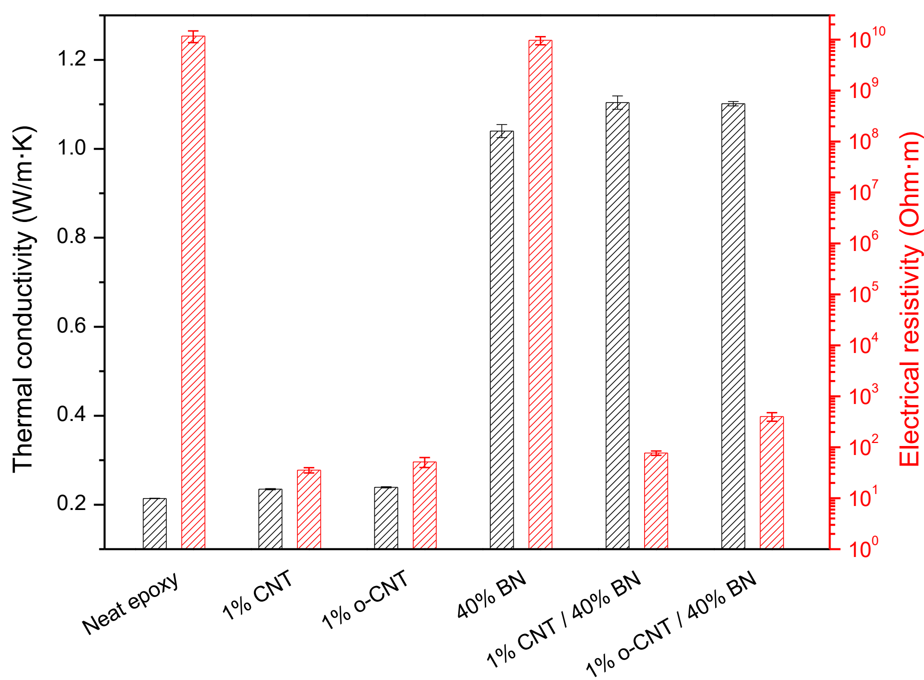

Figure 9. Thermal conductivities and electrical resistivities of DGEBA samples at room temperature.

If we consider both thermal and electrical conductivities, the samples containing between 0.05 and 0.1 wt. % of CNTs and 40 wt. % of BN are the best ones that fulfill the performance requirements for the applications desired. It should be noted that CNTs higher increase the viscosity, which is a drawback for their application. Thus, taking all of this into account, the best formulation is the one with 0.05 wt. % of CNTs and 40 % of BN. The composites obtained shows an improvement in thermal conductivity of around 750 %, keeping a good electrical insulating characteristic.

In case of using DGEBA as the epoxy matrix, we can see in Figure 9 that the addition of CNT scarcely affects the TC value, just about 10% of improvement. No

significant differences were observed with the oxidation of the nanotubes. The addition of BN alone leads to a TC of 1.04 W/m·K and the further addition of CNTs improves this property to approximately up to 1.10 W/m·K, which means an improvement higher than 400% in reference to the neat formulation. However, the synergistic effect of BN and CNTs is of only 6 %, which is even less than in case of ECC formulations. Although we hypothesized the existence of π-π interaction between phenylene units in DGEBA and CNTs to improve filler-matrix interactions, finally these effects have not been noticed in the results obtained with this resin.

4. Conclusions

In the present study, the combined addition of CNTs and BN particles to ECC and DGEBA epoxy matrices have been studied with the aim to improve their thermal conductivity without deteriorating other properties of the thermoset systems such as their electrical insulating character or their mechanical and thermal properties.

A low amount of 0.05 wt. % of CNTs well dispersed within epoxy matrix makes this material electrically conductive. However, on adding a 40 % of BN to the system, it is possible to increase up to a 0.25 wt. % the amount of CNTs to the system to improve significantly its thermal conductivity while keeping its electrical insulating character. More precisely, the most promising combinations of CNTs and BN achieved in this work lead to a synergistic effect of 11% in ECC matrix and of 6% in DGEBA. They are composed of 0.05 or 0.10 wt. % of CNTs and 40 wt.% of BN in ECC matrix, with a value of 1.07 W/m·K, which means an improvement of 750 % in reference to the unfilled material. The replacement of pristine CNTs by oxidized nanotubes further improves the thermal conductivity of the formulation to 1.10 W/m·K. In the case of DGEBA matrix, the best thermal conductivity achieved is 1.10 W/m.K, which represents an improvement higher than 400% in reference to the corresponding unfilled system.

Regarding the mechanical properties of the composites, the stiffness of cured ECC-CNT composites is found to be enhanced with both individual or joint addition of fillers but the highest improvement of Young’s modulus is achieved for the systems containing a combination of CNTs and BN particles.

In addition, pristine CNTs seem to have a slightly higher influence on the improvement of mechanical characteristics in ECC composites whereas o-CNTs are found to have a higher influence in the mechanical properties of DGEBA systems. This result suggests that reactive groups generated on the surface of o-CNTs could be involved in covalent bonding in the case of DGEBA matrix.

Interestingly, the thermal expansion coefficient of the composites is found to be positively reduced with the addition of BN and CNTs. DGEBA materials show a synergic effect of both fillers in the improvement of this parameter.

Finally, regarding the thermal stability of the composites, the presence of CNTs leads to a dual and antagonist contribution. More precisely, the CNTs are found to promote the formation of carbonaceous residues (the char yield under pyrolysis conditions is significantly increased) but at the same time, they are found to also deteriorate the initial temperature of decomposition of the composites proportionally to their amount in the composites. In addition, o-CNTs are found to accelerate even more the degradation of the composites. Anyway, the presence of BN particles allows to delay and attenuate this last effect in the composites containing both CNT and BN particles.

All these results clearly highlight that CNT and BN make a valuable combination of particles to enhance the thermal conductivity of thermoset materials without sacrificing other properties of such systems.

Acknowledgments

The authors would like to thank MCIU (Ministerio de Ciencia, Innovación y Universidades) and FEDER (Fondo Europeo de Desarrollo Regional) (MAT2017-82849-C2-1-R and MAT2017-82849-C2-2-R) and Generalitat de Catalunya (2017-SGR-77) for the financial support. The author of Materia Nova wishes to thank the ''Région Wallonne'' and the European Community for general support in the framework of the Interreg V program ("BIOCOMPAL" and "ATHENS" projects) and the FEDER 2014–2020 program ("HYBRITIMESURF" and "MACOBIO" projects).

References

[1] Burger N, Laachachi A, Ferriol M, Lutz M, Toniazzo V, Ruch D. Thermal conductivity of polymer-based composites: Fundamentals and applications. Progress in Polymer Science 59 (2016) 41-85.

[2] Aradhana R, Mohanty S, Nayak SK. High performance epoxy nanocomposite adhesive: Effect of nanofillers on adhesive strength, curing and degradation kinetics. International Journal of Adhesion and Adhesives 80 (2018) 238-249.

[3] Badenhorst H. A review of the application of carbon materials in solar thermal energy storage. Sol. Energy (2019) https://doi.org/10.1016/j.solener.2018.01.062 In press.

[4] Singh AK, Panda BP, Mohanty S, Nayak SK, Gupta MK. Recent developments on epoxy based thermally conductive adhesives (TCA): A review. Polymer-Plastics Technology and Engineering 57 (2018)

[5] Cha J, Jun GH, Park JK, Kim JC, Ryu HJ, Hong SH. Improvement of modulus, strength and fracture toughness of CNT/Epoxy nanocomposites through the functionalization of carbon nanotubes. Composites Part B 129 (2017) 169-179.

[6] Mittal G, Dhand V, Rhee KY, Park SJ, Lee WR. A review on carbon nanotubes and graphene as fillers in reinforced polymer nanocomposites. J Ind Eng Chem 21 (2015) 11-25.

[7] Polymer Nanocomposites: Electrical and Thermal Properties. Xingyi Huang, Chunyi Zhi (editors). Springer International Publishing AG, Switzerland, 2016.

[8] Joy A, Varughese S, Shanmugam S, Haridoss P. Multiwalled Carbon Nanotube Reinforced Epoxy Nanocomposites for Vibration Damping. ACS Appl Nano Mater. 2 (2019) 736-743.

[9] Kaiyan H, Weifeng Y, Shuying T, Haidong L. A fabrication process to make CNT/EP composite strain sensors. High Performance Polymers 30 (2018) 224-229.

[10] Kugler S, Kowalczyk K, Spychaj T. Transparent epoxy coatings with improved electrical, barrier and thermal features made of mechanically dispersed carbon nanotubes. Progress in Organic Coatings 111 (2017) 196-201.

[11] Goyat MS, Jaglan V, Tomar V, Louchaert G, Kumar A, Kumar K, Singla A, Gupta R, Bhan U, Rai SK, Sharma S. Superior thermomechanical and wetting properties of ultrasonic dual mode mixing assisted epoxy-CNT nanocomposites. High Performance Polymers 31 (2019) 32-42.

[12] Lau AKT, Hui D. The revolutionary creation of new advanced materials-carbon nanotube composites. Compos Part B: Engineer. 33 (2002) 263–277.

[13] Rahimian-Koloor SM, Hashemianzadeh SM, Shokrieh MM. Effect of CNT structural defects on the mechanical properties of CNT/Epoxy nanocomposite Physica B: Physics of Condensed Matter 540 (2018) 16.

[14] Silvestri C, Riccio M, Poelma RH, Jovic A, Morana B, Vollebregt S, Irace A, Zhang GQ, Sarro PM. Effects of Conformal Nanoscale Coatings on Thermal Performance of Vertically Aligned Carbon Nanotubes. Small 14 (2018) 1800614.

[15] Hong J-H, Park D-W, Shim S-E. A Review on Thermal Conductivity of Polymer Composites Using Carbon-Based Fillers: Carbon Nanotubes and Carbon Fibers. Carbon Letters Vol. 11 (2010) 347-356.

[16] Biercuk MJ, Llaguno MC, Radosavljevic M, Hyun JK, Johnson AT, Fischer JE. Carbon nanotube composites for thermal management. APPLIED PHYSICS LETTERS VOLUME 80 (2002) 2767-2769.

[17] Xiao W, Luo X, Ma P, Zhai X, Fan T, Li X. Structure factors of carbon nanotubes on the thermal conductivity of carbon nanotube/epoxy composites. AIP Advances 8 (2018) 035107.

[18] Liu JQ, Xiao T, Liao K, Wu P. Interfacial design of carbon nanotube polymer composites: a hybrid system of noncovalent and covalent functionalizations. Nanotechnology 18 (2007) 165701.

[19] Sandler JKW, Kirk JE, Kinloch IA, Shaffer MSP, Windle AH. Ultra-low electrical percolation
threshold in carbon-nanotube-epoxy composites. Polymer 44 (2003) 5893–5899.

[20] Roy S, Petrova RS, Mitra S. Effect of carbon nanotube (CNT) functionalization in epoxy-CNT composites. Nanotechnol Rev 7 (2018) 475-485.

[21] Choi JH, Song HJ, Jung J, Yu JW, You N-H, Goh M. Effect of crosslink density on thermal conductivity of epoxy/carbon nanotube nanocomposites. J. APPL. POLYM. SCI. 134 (2017) 44253.

[22] Huxtable ST, Cahill DG, Shenogin S, Xue L, Ozisik R, Barone P, Usrey M, Strano MS, Siddons G, Shim M, Keblinski P. Interfacial heat flow in carbon nanotube suspensions. Nature Materials 2 (2003) 731-734.

[23] Yang K, Gu M. Enhanced thermal conductivity of epoxy nanocomposites filled with hybrid filler system of triethylenetetramine-functionalized multi-walled carbon nanotube/silane-modified nano-sized silicon carbide. Composites: Part A 41 (2010) 215-221.

[24] Pak SY, Kim HM, Kim SY, Youn JR. Synergistic improvement of thermal conductivity of thermoplastic composites with mixed boron nitride and multi-walled carbon nanotube fillers. Carbon 50(2012) 4830-4838.

[25] Teng C-C, Ma C-CM, Chiou K-C, Lee T-M, Shih Y-F. Synergetic effect of hybrid boron nitride and multi-walled carbon nanotubes on the thermal conductivity of epoxy composites. Materials Chemistry and Physics 126 (2011) 722–728.

[26] Li Y, Tian X, Yang W, Li Q, Hou L, Zhu Z, Tang Y, Wang M, Zhang B, Pan T, Li Y. Dielectric Composite Reinforced by In-situ Growth of Carbon Nanotubes on Boron Nitride Nanosheets with High Thermal Conductivity and Mechanical Strength. Chemical Engineering Journal 358 (2019) 718-724.

[27] Su Z, Wang H, He J, Guo Y, Qu Q, Tian X. Fabrication of Thermal Conductivity Enhanced Polymer Composites by Constructing an Oriented Three-dimensional Staggered Interconnected Network of Boron Nitride Platelets and Carbon Nanotubes. ACS Appl. Mater. Interfaces 10 (2018) 36342–3635.

[28] Su Z, Wang H, Ye X, Tian K, Huang W, He J, Guo Y, Tian X. Anisotropic Thermally Conductive Flexible Polymer Composites Filled with Hexagonal Born Nitride (h-BN) Platelets and Ammine Carbon Nanotubes (CNT-NH2): Effects of the Filler Distribution and Orientation. Composites Part A 109 (2018) 402–412.

[29] Isarn I, Gamardella F, Massagués Ll, Fernàndez-Francos X, Serra À, Ferrando F. New epoxy composite thermosets with enhanced termal conductivity and high Tg obtained by cationic homopolymerization. Polym Comp 39 (2018) 1760-1769.

[30] Isarn I, Gamardella F, Fernàndez-Francos X, Serra À, Ferrando F. Enhancement of thermal conductivity by the addition of several conductive fillers to thermal cationic curing of cycloaliphatic epoxy resins. Polymers 11 (2019) 138-151.

[31] Isarn I, Massagués Ll, Ramis X, Serra À, Ferrando F. New BN-epoxy composites obtained by thermal latent cationic curing with enhanced thermal conductivity. Composites: Part A 103 (2017) 35-47.

[32] Lu K, Lago R, Chen Y, Green M, Harris P, Tsang S. Mechanical damage of carbon nanotubes by ultrasound. Carbon 1996, 34, 814-816.

[33] Cividanes LS, Franceschi W, Ferreira FV, Menezes BRC, Sales RCM, Thim GP. How Do CNT Affect the Branch and Crosslink Reactions in CNT-Epoxy 2017 Mater. Res. Express 4 (2017) 105101.
[34] Lu L, Xia L, Zengheng H, Xingyue S, Yi Z, Pan L. Investigation on cure kinetics of epoxy resin containing carbon nanotubes modified with hyperbranched polyester. RSC Adv. 8 (2018) 29830-29839.
[35] Abdalla M, Dean D, Robinson P, Nyairo E. Effect of carboxyl functionalized MWCNTs on the cure behavior of epoxy resin. Polymer 49 (2008) 3310-3317.
[36] Cui L–J, Wang Y-B, Xiu W-J, Wang W-Y, Xu LH, Xu X-B, Meng Y, Li L-Y, Gao J, Chen L-T, Geng H-Z., Mater. Design 49 (2013) 279-284.
[37] Abbasi S, Derdouri A, Carreau P, Moan M. Rheological properties and percolation in suspensions of multiwalled carbon nanotubes in polycarbonate. Rheol Acta 48 (2009) 943–959.
[38] Wilkinson A, Liu Y. Rheological percolation behaviour and fracture properties of nanocomposites of MWCNTs and a highly crosslinked aerospace-grade epoxy resin system. Composites: Part A 105 (2018) 97–107.
[39] Isarn I, Ramis X, Ferrando F, Serra À. Thermoconductive thermosetting composites based on boron nitride fillers and thiol-epoxy matrices. Polymers 10 (2018) 277-292.
[40] Wang AJ, Liao K-S, Maharjan S, Zhu Z, McElhenny B, Bao J, Curran SA. Percolating conductive networks in multiwall carbon nanotube-filled polymeric nanocomposites: towards scalable high-conductivity applications of disordered systems. Nanoscale 11 (2019) 8565–8578.
[41] Kim JA, Seong DG, Kang TJ, Youn JR. Effects of surface modification on rheological and mechanical properties of CNT/epoxy composites. Carbon 44 (2006) 1898-1905.
[42] Ulus H, Üstün T, Sahin ÖS, Karabulut SE, Eskizeybek V, Avci A. Low-velocity impact behavior of carbon fiber/epoxy multiscale hybrid nanocomposites reinforced with multiwalled carbon nanotubes and boron nitride nanoplates. Journal of Composite Materials 50 (2015) 761-770.
[43] Ekrem M, Sahin ÖS, Karabulut SE, Avci A. Thermal stability and adhesive strength of boron nitride nano platelets and carbon nano tube modified adhesives. Journal of Composite Materials 52 (2018) 1557–1565.
[44] Fan B, He D, Liu Y, Bai J. Influence of Thermal Treatments on Evolution of Conductive Paths in Carbon Nanotubes-Al_2O_3 Hybrids Reinforced Epoxy Composites. Langmuir 33 (2017) 9680-9686.
[45] Bikiaris D, Vassiliou A, Chrissafi s K, Paraskevopoulos KM, Jannakoudakis A, Docoslis A. Effect of acid treated multi-walled carbon nanotubes on the n the mechanical permeability, thermal properties and thermo-oxidative stability of isolatic polypropylene. Polym Degrad Stab 93 (2008) 952–967.

[46] Marosfői BB, Szabó A, Marosi G, Tabuani D, Camino G, Pagliari S. Complex activity of clay and CNT particles in flame retarded EVA nanotube composites. J Therm Anal Calorim 86 (2006) 669–673.
[47] Sarno M, Gorrasi G, Sannino D, Sorrentino A, Ciambelli P, Vittoria V. Polymorphism and thermal behaviour of syndiotactic poly(propylene)/carbon nanotube composites. Macromol Rapid Commun 25 (2004) 1963–1967.
[48] Isarn I, Bonnaud L, Massagués L, Serra À, Ferrando F. Enhancement of thermal conductivity in epoxy coatings through the combined addition of expanded graphite and boron nitride fillers. Prog Org Coat 133 (2019) 299-308.
[49] Shtein M, Nadiv R, Buzaglo M, Kahil K, Regev O. Thermally Conductive Graphene-Polymer Composites: Size, Percolation, and Synergy Effects. Chem. Mater. 27 (2015) 2100−2106.
[50] Berber S, Kwon Y-K, Tomanek D. Unusually high thermal conductivity of carbon nanotubes. Phys Rev Lett 84 (2000) 4613.

UNIVERSITAT ROVIRA I VIRGILI
NEW EPOXY COMPOSITES WITH ENHANCED THERMAL CONDUCTIVITY KEEPING ELECTRICAL INSULATION.
Isaac Isarn Garcia

Chapter 8

Enhancement of thermal conductivity in epoxy coatings through the combined addition of expanded graphite and boron nitride fillers

UNIVERSITAT ROVIRA I VIRGILI
NEW EPOXY COMPOSITES WITH ENHANCED THERMAL CONDUCTIVITY KEEPING ELECTRICAL INSULATION.
Isaac Isarn Garcia

Progress in Organic Coatings ***2019****, 133, 299-308*

Enhancement of thermal conductivity in epoxy coatings through the combined addition of expanded graphite and boron nitride fillers

Isaac Isarn[a], Leïla Bonnaud[b], Lluís Massagués[c], Àngels Serra[d], Francesc Ferrando[a]

a. Department of Mechanical Engineering, Universitat Rovira i Virgili, C/Av. Països Catalans, 26, 43007 Tarragona, Spain.
b. Laboratory of Polymeric and Composite Materials, Center of Innovation and Research in Materials and Polymers (CIRMAP), Materia Nova Research Center & University of Mons, 23 Place du Parc, B-7000, Mons, Belgium.
c. Department of Electronic, Electric and Automatic Engineering, Universitat Rovira i Virgili, C/Av. Països Catalans, 26, 43007 Tarragona, Spain.
d. Department of Analytical and Organic Chemistry, Universitat Rovira i Virgili, C/ Marcel·lí Domingo s/n, 43007 Tarragona, Spain.

Abstract

Expanded graphite (EG) and boron nitride (BN) were used as fillers to impart thermal conductivity (TC) while maintaining electrical insulation of a homopolymerized cycloaliphatic epoxy matrix. Even though EG leads to a higher increase of TC than BN (550% of enhancement with only a 7.5 wt.% of EG), EG is also electroconductive and its ratio in the formulation must be lower than the percolation threshold. Formulations with proportions between 2.5-7.5 wt.% of EG as the filler and mixtures with EG and a 40 wt.% of BN were thermally polymerized and composites with 70 wt.% of BN and 2.5/5.0 wt.% of EG were also prepared under pressure and then cured in the oven. Over 2 W/m·K was achieved (i.e. more than 1,500% of enhancement in reference to the neat epoxy). The composites containing a 40 wt. % of BN and 2.5 wt % of EG or 70% wt. % of BN and 5 wt % of EG were found to keep the insulation character. Mechanical and thermal characteristics of the prepared materials were also evaluated.

Keywords

Thermosetting resin, Layered structures, Polymer-matrix composites (PMCs), Thermal properties.

1. Introduction

Recently, the preparation and study of new nanocomposite materials has become a very important issue in different fields of science. Most of these composites are based on polymers.[1-4] Indeed, their low density makes these materials the most promising candidates to replace metals or ceramics when weight is a restrictive parameter.[5-7] Their good corrosion resistance, low production costs and easy processing, also make them more attractive than metals.[1,6,8,9] In the sector of energy, in

production and storage systems such as solar cells, fuel cells, rechargeable batteries and supercapacitors, there is also a great interest in thermally conductive coatings and adhesives.[10] Thermal conducting composites are used in electric and electronic industries as packaging and coating, heat dissipation structures of light emitting diodes and heat sinks.[1,8,9] Unfortunately, most polymers exhibit insulating characteristics, both electrical and thermal. To tackle this lack of conductivity, usually thermally or electro conductive nanofillers are added to polymer matrices.[11] While the electrical conductivity of polymer composites can drastically increase at a given electrical conductive particle concentration, in accordance with the percolation theory,[9,12] the dependence of thermal conductivity and filler loading are in most cases practically linear and does not exhibit large changes until high filler loadings.[13]

Following the previous studies carried out by our group,[14-17] the current work is focused on increasing the thermal conductivity of an epoxy resin while maintaining its electrical insulation. The prepared materials could be used as adhesives, coatings or packaging materials for electronic industry, usually called thermal interface materials (TIMs),[18] thermally conductive adhesive (TCA),[19] or electrical insulating layers of prepreg in a multilayer printed circuit boards (PCB). The selection of an epoxy resin as the matrix relies on the versatility of such systems in terms of curing agent and curing conditions and its good adhesion properties to a huge range of different surfaces, low shrinkage, good behaviour at elevated temperatures and high modulus and strength. All these characteristics make epoxy resins ideal matrices in composite material industries.[20-23] However, it is well known that epoxy resins have low thermal conductivity and considerable brittleness, which limit their use but the addition of inorganic particles can help to reduce both drawbacks.[22] The introduction of particles in the epoxy matrix is still today the most economical and simplest method from the point of view of the application to increase thermal conductivity[24] than the costly alignment of polymer structures.[25]

In the present study, a thermal latent epoxy system, which proceeds through a cationically initiated mechanism, was selected to crosslink a cycloaliphatic epoxy resin (ECC). This system consists in a benzylanilinium salt, which is the cationic initiator and triethanolamine (TEA) as inhibitor of low temperature curing, which provides the latency. The system is distinguished for having a long pot life, fast curing once initiated and glass transition temperatures (T_g) of the cured material above 200 °C, which is considerable high in epoxy themosets.[15,17]

The main goal of this work is the preparation of new hybrid nanocomposites, by combination of a carbonaceous filler with an inorganic material, all of them dispersed in the epoxy matrix. By the application of pressure, a higher filler loading could be added to the composite. The mechanical properties and thermal conductivity of these materials have been evaluated together with the insulating electrical characteristics.

Small proportions of carbon-based material (below the percolation threshold) were expected to improve some of these characteristics maintaining the electrical insulation.

Considering different studies already reported in the scientific literature,[9,26-28] we selected expanded graphite (EG) and boron nitride (BN) as the fillers, to determine potential synergic effects when added together to the formulation. EG is one of the most studied fillers in thermal energy storage systems.[29] Some authors[26,29] state that this filler enhances the thermal conductivity much better than other carbon-based materials such as carbon nanotubes, carbon black or carbon fibres. Other fillers like graphene or graphene oxide result much more expensive, thus limiting their use in technological applications. Corcione and Maffezzoli[26] reported a good dispersion of the EG particles in the epoxy matrix and strong polar interactions of the filler with the matrix, attributable to the partially oxidized surfaces of the expanded graphite. The manufacturing process causes this partial oxidation since graphite, which is constituted by stacked layers of graphene, is converted in expanded graphite through chemical oxidation.[8,26] When graphite is exposed to heat (thermal shock) it expands generating free space by evaporating the acid entrapped between the graphite layers.[23] This space could be filled with the epoxy resin, which could homopolymerize, increasing in this way the filler-matrix interaction that is highly convenient to reach a good heat transfer.

Among all the inorganic particles commonly used to increase thermal conductivity, hexagonal boron nitride (BN) provides the best combination of properties and therefore this material has been selected for the present study. BN platelets present high thermal conductivity, low dielectric constant, high electrical resistivity, low coefficient of thermal expansion (CTE), low density, high mechanical strength and chemical and thermal stabilities.[14,24]

2. Experimental

2.1. Materials

As the epoxy resin, 3,4-epoxy cyclohexylmethyl 3,4-epoxy cyclohexane carboxylate (EEW = 126.15 g/eq, from Sigma Aldrich, ECC) has been used. N-(4-methoxybenzyl)-N,N-dimethylanilinium hexafluoroantimonate, commercialized as CXC1612 from King Industries Inc., was mixed with 50 wt. % of propylene carbonate until dissolution. Propylene carbonate and triethanolamine (TEA) were provided by Sigma-Aldrich and purified by distillation before use. Platelets of hexagonal BN of 180 µm of average, PCTP30D, were supplied by Saint Gobain Ceramic Materials. The particles were sifted with a sieve of 250 µm due to the high difference in particle size (manufacturer specifications state that product granulometry could include particle sizes of 1600 µm). Expanded graphite particles, BNB90, with an average of particle size of 85 µm and specific surface area (SSA) of 28.4 m^2/g were provided by Songhan Plastic Technology Co., Ltd.

2.2. Sample preparation

The epoxy neat formulation was prepared as described previously,[15,17] by mixing 1 phr (parts of initiator per hundred parts of resin) of CXC1612 and 0.1 phr of TEA. Proportions of 2.5, 5.0 and 7.5 wt. % of expanded graphite were added to the epoxy system. Graphite particles were dispersed by sonication (NextGen Inside 500 from Sinaptec Ultrasonic Technology), using 35% of amplitude during 20 s, divided in batches of 5 s (leaving 10 s between each batch). After sonication, vacuum at room temperature was applied to the mixtures during 1 h to remove the bubbles formed. The epoxy-graphite mixtures were used to prepare new formulations by mixing 60 wt. % of these mixtures and 40 wt. % of BN particles. In this case, manual stirring until homogeneity was performed and then the samples were cured in a ventilated oven. Cylindrical samples with a BN content of 70 wt. % and 30 wt. % of epoxy mixture containing 2.5 or 5 wt. % of EG were also prepared and a pressure of about 74 MPa to compact and shape the sample was applied prior curing in the oven.

The curing of samples was carried out onto teflonated metallic moulds and following a multi-step temperature schedule at 100, 120, 150, 180 and 200 °C, leaving them 1 h at each temperature.

2.3. Characterization techniques

A modulated differential scanning calorimeter 2920 (MDSC) from TA Instruments was used to analyse the epoxy reaction system. Samples of ca. 3-5 mg were tested in aluminium pans in a nitrogen atmosphere. The dynamic studies were performed in the range of 30-250 °C with a heating rate of 10 K/min. Enthalpy released on curing the samples (Δh) was calculated integrating the calorimetric signal (dh/dt) using a straight baseline, with the help of TA Universal Analysis software.

Rheologic experiments were carried out to the epoxy-EG mixtures in parallel aluminium plates of 25 mm diameter in oscillatory mode with an AR G2 rheometer from TA Instruments. The aim of the rheometric measurements were to determine the percolation threshold of the EG in the epoxy system. Linear viscoelastic ranges (LVR), when there is a constant value of shear elastic modulus (G'), were determined at 1 Hz and 30 °C, varying the applied strain. Viscoelastic properties, G' and shear viscous modulus (G''), were then determined in the LVR in frequency sweep experiments at 30 °C.

Dynamic mechanical thermal analyses (DMTA) were performed with a TA Instruments DMA Q800 analyzer. The prismatic rectangular samples (20 x 4.5 x 2.2 mm^3) were analyzed by 3-point bending clamp at a heating rate of 3 K/min from 30 to 300 °C, using a frequency of 1 Hz and an oscillation of 0.1% of sample deformation. The Young modulus (E) was determined at 30 °C by means of a force ramp at a constant rate, 1 N/min, never exceeding 0.25 % of deformation to be sure that only elasticity was

evaluated. E was calculated taken the slope between 0.1 and 0.2 % of the deformation curve in accordance with the equation:

$$E = \frac{L^3 m}{4bt^3} \qquad (1)$$

where E is the elastic modulus of composite sample (MPa), L is the support span (mm), b and t are the width and the thickness of test sample (mm) and m is the gradient of the slope (N/mm). A minimum of 4 experiments were made for each sample.

Thermomechanical analyses (TMA) were carried out on a Mettler TMA40 thermomechanical analyzer. Square cured samples (9 x 9 x 2.3 mm^3) were supported by the clamp and a silica disc to distribute the force uniformly and heated at 5 K/min from 35 to 100 °C. A minimum force of 0.01 N was applied to avoid results distortion. The coefficients of thermal expansion (*CTEs*) in the glassy state of the material were calculated as follows:

$$CTE = \frac{1}{L_0} \cdot \frac{dL}{dT} = \frac{1}{L_0} \cdot \frac{dL/_{dt}}{dT/_{dt}} \qquad (2)$$

where L is the thickness of sample, L_0 the initial length, t the time, T the temperature and dT/dt the heating rate.

Thermal stability of the composites prepared were evaluated by a thermogravimetric analyser (TGA) Q50 from TA Instruments under N_2 atmosphere. Samples of ca. 6-9 mg were thermally decomposed on a platinum pan within the device. Global N_2 flow (100 mL/min) was divided between balance flow (40 mL/min) and sample flow (60 mL/min). A heating rate of 10 K/min was used between room temperature and 600 °C.

Surface hardness was evaluated through Knoop microindentation analysis being consistent with ASTM D1474-13. A minimum of 18 valid determinations were considered with a confidence level of 95% for each material. Knoop microindentation hardness (KHN) was calculated as follows:

$$KHN = \frac{L}{A_p} = \frac{L}{l^2 C_p} \qquad (3)$$

where L is the load applied by the indenter (0.010 Kg), A_p is the area of indentation in mm^2 and C_p the indenter constant relating l^2 with A_p.

Measurements of X-ray diffraction (XRD) were performed with a Siemens D5000 diffractometer (Bragg-Brentano parafocusing geometry and vertical ϴ-ϴ goniometer) fitted with a curved graphite diffracted-beam monochromator, using incident and diffracted beam Soller slits, a 0.06° receiving slit and scintillation counter as detector. The angular 2ϴ diffraction range was between 5 and 70°. The data were collected with an angular step of 0.05° at 3 seconds per step and sample rotation. $Cu_{k\alpha}$ radiation was obtained from a copper X-ray tube operated at 40 kV and 30 mA.

Environmental scanning electron microscopy (ESEM) was used to examine the fillers morphologies and dispersions and the breaking surfaces of the materials prepared. A Quanta 600 environmental scanning electron microscopy (FEI Company) allows collecting micrographs at 10-20 kV and low vacuum mode without the need to coat the samples with poor electrical conductivity.

Electrical resistance of materials was tested using a multimeter 34410A 6½ Digit from Agilent Technologies at room temperature and based on ASTM D257-14 standard. The samples with higher electrical resistance (>10^8 Ω·m) were evaluated with a Megohmmeter Resistomat 24508 at room temperature and the same standard. Samples of 9 x 9 x 2.3 mm^3 were tested between two stainless steel electrodes with a surface area of 19.635 mm^2. A voltage of 500 V during 5 min was applied to thermoset composites. Electrical resistivity (ρ) was determined as follows:

$$\rho = R\frac{A}{l} \qquad (4)$$

where *R* is the electrical resistance measured by the device, *A* the electrode area and *l* the sample thickness.

Thermal conductivity was measured using the Transient Hot Bridge method by a THB 100 device from Linseis Messgeräte GmbH. A HTP G 9161 sensor was used with a 3 x 3 mm^2 of area calibrated with poly(methyl methacrylate) (PMMA), borosilicate crown glass, marble, Ti-Al alloy and titanium. Two equal polished rectangular samples (9 x 9 x 2.3 mm^3) were placed in each one of the faces of the sensor. Due to the small size of sensor, side effects can be neglected. A measuring time of 100 s applying a current of 10 mA to each sample. Five measures were done for each formulation.

3. Results and discussion

3.1. Calorimetric analysis of the curing of the prepared formulations

In a previous study,[15] the curing of the cycloaliphatic epoxy system (ECC) was performed. An optimal combination of 1 phr of benzylanilinium hexafluoroantimoniate (CXC 1612) and 0.1 phr of triethanolamine (TEA) as initiating system ensured a complete epoxy group conversion with thermal latent characteristics. The benzylanilinium salt leads to a cationic homopolymerization of the epoxy monomers with high reactivity. In fact, the real catalytic groups, which initiate the attack to the oxiranic oxygen, are the benzyl cations released on heating the ammonium salt.[30-32] A high reactivity and an elevated degree of crosslinking were obtained because of the low nucleophilicity of the hexafluoroantimonate counter anion, which avoids the termination step in the epoxy homopolymerization. TEA was added as the thermal latent additive, since it converts the system in non-reactive until reaching temperatures in the range of 110-120 °C.[33] The fact that the curing temperature is much higher than room temperature allows the reactive mixture to be stored for long periods, which is highly desirable for industrial applications.

Different proportions of EG were dispersed in the epoxy resin using a tip sonicator. Short sonication times were applied to the mixtures to avoid mechanical damage to the graphitic particles and to maintain the system unreacted, since the heat produced by the dispersion can lead to an undesired reaction if the temperature is highly increased. This technique results more efficient than the use of ultrasonic bath. To these mixtures, a 40 wt. % proportion of BN was added. Dynamic DSC scans of the different formulations are represented in **Figure 1**. If there is a great interaction between particles and matrix, some variations in the curing evolution must be expected. There are different facts that can affect this interaction: a) Both EG and BN have a similar crystalline structure, the surfaces are not reactive but the reactive groups at the particle edges could be bonded covalently with the resin and possibly participate in the curing process. b) The low viscosity and small size of the cycloaliphatic epoxy compound could allow its penetration into the EG interlayer spaces, which will lead to good interactions through partial oxidised surfaces. On the other hand, the absence of aromatic moieties in the epoxy resin prevents in the present case π-π interactions between particles and matrix.

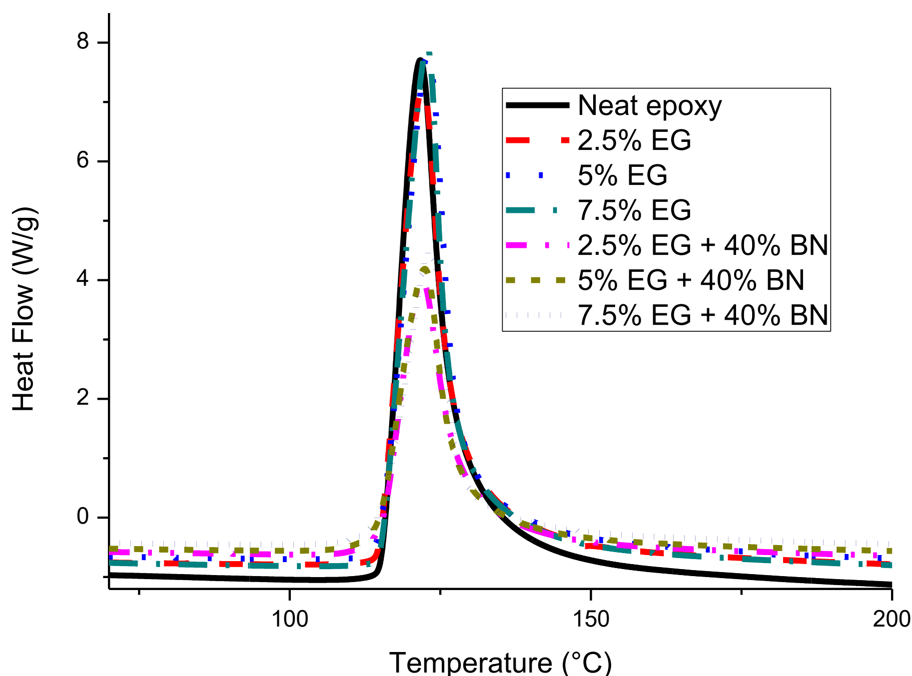

Figure 1. DSC exotherms of the epoxy mixtures containing EG or EG and BN.

As it can be seen in the figure, neither the addition of EG nor the addition of BN affects the curing process, and the exotherm appears at the same temperature range, in contrast to what was observed in earlier studies with different fillers in ECC mixtures.[15,17] **Table 1** collects the most important data extracted from the DSC experiments. It is clear that the temperature of the maximum of the peak does not

change on changing the formulation. Enthalpy per epoxy equivalent evolved during the polymerization also remains similar, although the enthalpy released by gram is reduced on increasing the proportion of filler, as expected. These results also confirm that sonication does not produce any effect on the curing of the reactive mixture, confirming the stability of the formulation. The high crosslinking density of the network formed did not allow detecting, in a second dynamic DSC scan, the T_g of the final composites.

Table 1. Most important data extracted from DSC experiments.

Sample	Composition (ECC/EG/BN) wt. %	T_{peak} [a] (°C)	Δh [b] (J/g)	Δh [b] (kJ/ee)
Neat epoxy	100/0/0	122	641	81
2.5% EG	97.5/2.5/0	122	615	80
5% EG	95/5/0	123	609	81
7.5% EG	92.5/7.5/0	122	600	82
2.5% EG + 40% BN	58.5/1.5/40	122	379	82
5% EG + 40% BN	57/3/40	122	370	82
7.5% EG + 40% BN	55.5/4.5/40	123	357	81

[a] Temperature of the maximum of the exotherm determined by TA Universal Analysis software.

[b] Enthalpy evolved by the reaction per gram of mixture or epoxy equivalent determined by the same software using a straight base line.

3.2. Rheological behaviour of epoxy-EG mixtures

The use of electrical semiconductors as carbon-based fillers leads to lose the electrical insulation character of the composites at a given filler loading. Moreover, to reach a high thermal conductivity, percolation of the particles should be reached. For this reason, it is of great importance to know at which proportion of filler the percolation occurs. Rheological percolation threshold is usually slightly higher than electrical conduction percolation.[34,35] Electrical percolation is reached at lower conductive particles content because of tunnelling effect can occur. However, in some cases they could be similar or even identical.[36] In the present study, both EG and BN particles are added to the formulation but only EG particles can negatively affect electrical insulation. It should be said that the 40% of the BN particles used in the present study have surely exceeded the percolation threshold, since in a previous study with BN particles of average size of 6 µm, it occurred at a 14.4 wt. % of loading.[15] Because the addition of BN does not increase the electrical conductivity of the composite, we have selected a 40% of BN content that allows us to easily prepare by hand mixing the formulation and obtain homogeneous samples without the inclusion of bubbles. Therefore, only the rheological study of epoxy-EG mixtures was performed to determine the concentration needed to reach rheological percolation of EG particles in the formulation to know the maximum content of EG to keep electrical insulation.

To determine the viscoelastic properties of the formulation, the linear viscoelastic region (LVR) must be considered. This means to determine the deformation to be applied where the mixture present a Newtonian behaviour. One of the simplest

Progress in Organic Coatings ***2019***, *133, 299-308*

methods to determine this region is performing experiments keeping a constant frequency (1 Hz) varying the sample strain applied. **Figure 2** represents the elastic modulus (*G'*) in front of strain, because of it is more sensitive than *G''*. The less filled formulation exhibits a practically constant modulus in all the range of strain tested, typical of dilute solutions with Newtonian behaviour. When the concentration of EG is 5 wt. %, its curve shows a complex shape with a decrease of modulus, because the structure of the mixture breaks down. An increase of *G'* with a shoulder shape when the amplitude achieved certain value can also be observed. This behaviour has been explained as a particle structure reordering because of the deformation applied according to Laun's work.[37] As expected for this type of mixtures, the LVR is shifted to lower strains when particle concentration increases, as it can be clearly seen in the sample with a 7.5 wt. % of EG.

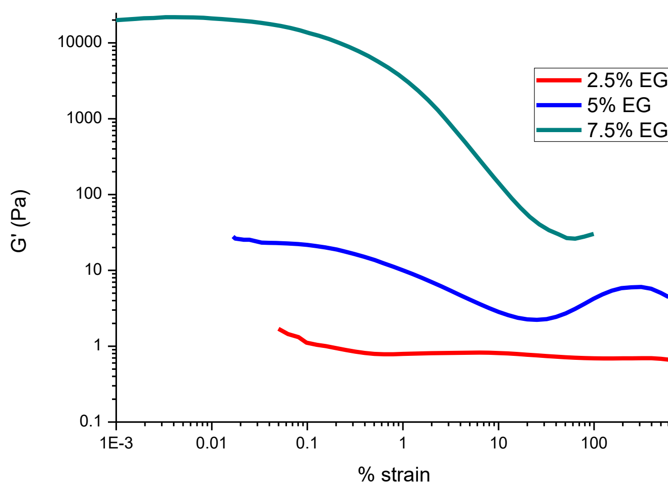

Figure 2. Elastic shear modulus (G') against amplitude applied (%) from strain sweep experiments.

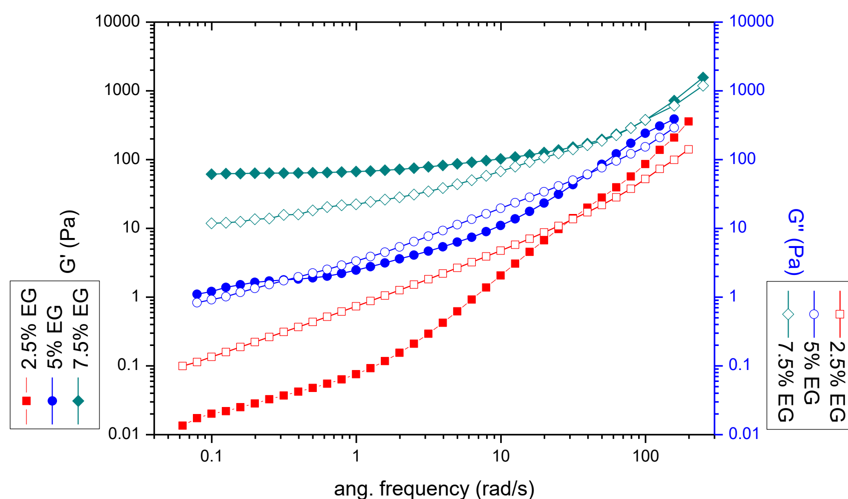

Figure 3. Elastic (G') and viscous (G'') moduli against angular frequency (ω) of epoxy-EG mixtures.

Once selected the appropriate amplitude for each mixture, frequency sweep experiments were carried out. In **Figure 3** both elastic and viscous modulus are represented. Following the scientific literature, it is usually accepted that percolation threshold of a filled mixture is achieved when *G'* reached the same value as *G''* at low frequencies.[16,38] On increasing the filler proportion in a formulation it can be seen how the transition from liquid-like (*G''>G'*) to solid-like behaviour (*G'>G''*) occurs. At low frequencies, this transition occurs between the formulations of 2.5 and 5 wt. % of EG, which means that the electrical percolation occurs at a filler loading of about 5% of EG.

3.3. Thermal and mechanical behaviour

Once finished the study of the curing of the formulations, the samples were thermally cured in the oven in a multistep temperature program, selected according to the results obtained by DSC and taking into account the results of the tests performed by DMTA analysis, aiming to reach the maximum $T_{\tan\delta}$ value. The curing schedule that starts at 100 °C and ends at 200 °C has different steps with small temperature increases to avoid the generation of internal stresses within the materials. Although, because of the latency, the reaction is very fast, to reach the complete curing of the material requires temperatures about 200 °C. T_gs of the neat material and BN filled composites were determined in a previous study and resulted to be over 200 °C.[15]

Figure 4 presents the storage modulus (*E'*), related with the elastic response of materials (Figure 4A), and the loss factor *tan δ* (Figure 4B), associated to the T_g, obtained by DMTA and the main data are collected in **Table 2**.

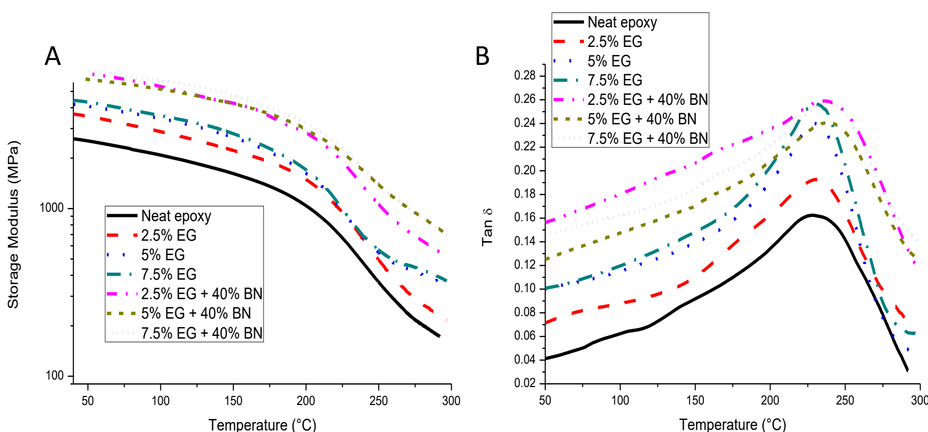

Figure 4. Storage modulus (*E'*) (A) and tan δ peak curves (B) against temperature.

Figure 4A shows the increase of the stiffness and the mechanical response of the composites when the proportion of filler increases. Once reached the mechanical percolation (at about 5 wt. % EG) the effect of increasing the proportion of EG on the storage modulus evolution is not noticeable. Similarly, when a 40 wt. % BN is in the formulation, the increase of EG content does not influence the mechanical performance.

Moreover, the storage modulus is maintained up to 200 °C. These results demonstrated that the materials can be used in a long range of temperature without loss on their mechanical response. It should be noted the change in the slope of *E'* in composites with 5 and 7.5 wt% of EG since 250 °C, which differs from the curve of the materials with lower EG content, in both series of materials with or without BN. This mechanical difference could be related to the percolation phenomenon, sensitive to the particle interactions within the matrix. In Figure 4B the relaxation process of materials lengthens over a large temperature range, but the experiments, which were stopped at about 300 °C to avoid degradation, showed that the materials were not yet completely relaxed, accordingly to their high crosslinked character. The most important difference observed among these materials is the increase of $T_{tan\delta}$ when BN particles are in the composite. However, the addition of EG does not lead to changes in the temperature of relaxation. As observed in previous studies[15,17] the *tan δ* peak is broad and low, indicating a slow relaxation process and low homogeneity of the polymer network, as a result of the homopolymerization by ring-opening mechanism in the curing process, which is inherently inhomogeneous.[39] The fact that the thermomechanical characteristics improve with the addition of fillers seems to demonstrate that there is a good interfacial interaction between particles and matrix.[40]

Table 2. Data obtained from DMTA, TGA, TMA and microindentation tests.

Sample	$T_{tan\,\delta}$[a] (°C)	Young Modulus[b] (MPa)	$T_{5\%}$[c] (°C)	Char yield[c] (%)	CTE_{glass}[d] ($10^{-6}\cdot K^{-1}$)	*KHN*[e]
Neat epoxy	229	2416 ± 20	296	1.9	115	12.3 ± 0.7
2.5% EG	231	3097 ± 20	306	4.9	110	17.6 ± 0.8
5% EG	230	3364 ± 60	342	7.8	78	20.2 ± 1.1
7.5% EG	231	3388 ± 90	339	11.0	77	20.2 ± 1.4
2.5% EG + 40% BN	240	4731 ± 150	350	46.0	64	16.7 ± 0.8
5% EG + 40% BN	239	4876 ± 230	356	46.5	64	16.5 ± 0.6
7.5% EG + 40% BN	239	5081 ± 350	355	46.9	64	17.3 ± 0.7

[a] Temperature of tan δ peak determined at 1 Hz in an oscillatory experiment by DMA.
[b] Rigidity of samples determined at 30 °C in DMA apparatus with a controlled force experiment.
[c] Temperature of 5 wt % loss and final residue in TGA test at 10 °C/min in nitrogen atmosphere.
[d] Coefficient of thermal expansion in the vitreous state determined by TMA, between 50 and 70 °C.
[e] Microindentation Knoop hardness.

By DMTA, in static controlled force test at 30°C, the Young's moduli of the composites were determined. As can be seen from the values in the table, fillers play a reinforcing role into the matrix. There are clearly two sets of moduli, the first one in samples with only EG as filler, where about a 40%. of enhancement is reached. In this case, once percolation is overpassed the EG particles seem not to increase rigidity. The

second set is formed by the composites with both EG and BN. In these materials, rigidity more than doubles the value of pure material. (from 2.4 GPa till 5.1 GPa) and the addition of EG seems not to enhance much the Young modulus. The maximum value achieved is below the previously reported with the 40 wt. % of BN (6.5 GPa).[15] This lower value is due to the change of BN particles used, larger in the present study. As seen before, bigger filler particles worse the rigidity of the composites.[16] Anyway, the rigidity is increased, and materials can be useful in some structural applications.

The thermal stability of the composites was analysed by TGA experiments under inert atmosphere. **Figure 5** shows the degradation curves and the main data extracted are collected in Table 2. The degradation seems to occur in an only process, independently of the composition of the formulation and the main differences are observed in the char residue, due to the different proportion of filler added. There is a pronounced increase in the thermal stability of epoxy-EG when percolation threshold is surpassed of about 30°C, a sign of a good particle interaction. All the char residues correlate with the proportion of filler added except for the samples including 40 wt. % of BN, where the residue is practically constant, because of the low relative variation of filler content among the samples. The increase of the initial temperature of decomposition is related with the decrease of the resin content that can be decomposed.

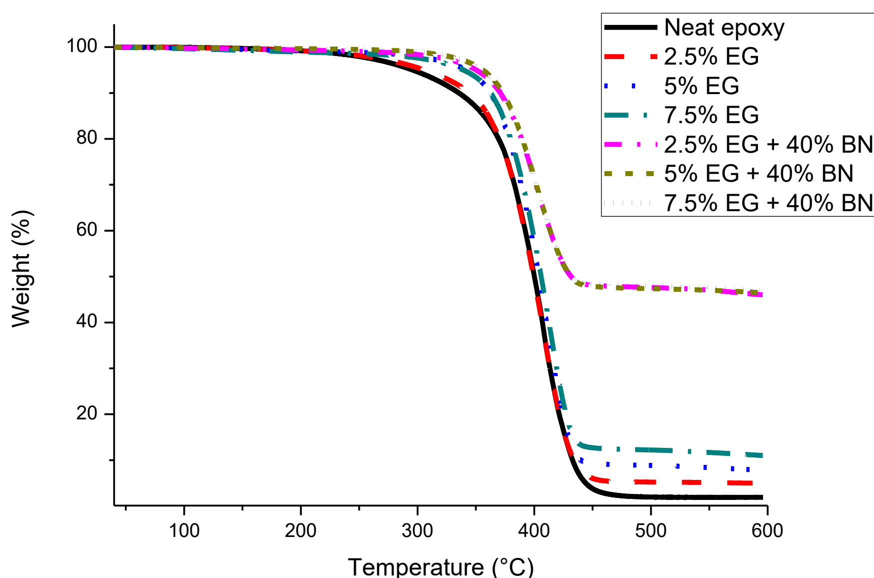

Figure 5. Decomposition curves of the neat thermoset and the composites prepared performed by TGA experiments in N_2 atmosphere.

The dimensional stability of materials on changing the temperature is an important characteristic when they are used in devices where the temperature can change and are assembled with metals, such as occurs in electronic devices. To evaluate the effect of the incorporation of fillers to the matrix on the coefficient of thermal

expansion (*CTE*), TMA analysis was performed. Generally, *CTE*s of polymers are larger than metals, and higher than ceramics. As it can be seen in Table 2, the inorganic fillers incorporated to the matrix, as expected, reduce the *CTE*s of composites approaching them to substrates they can coat. There is a sharp reduction of *CTE* on reaching EG percolation threshold, but a further addition of this filler does not produce any improvement. There is also a reduction of *CTE*s in samples with 40% of BN, but the further addition of EG does not produce any change, since the percolation has been reached by the BN particles.

From the mechanical characteristics, the hardness of materials was evaluated since it is an important property for coatings, since it confers them durability. In addition, this property is used to correlate with ultimate tensile strength (or breaking strength). In Table 2 the Knoop values are collected. Also, in this parameter, the addition of EG particles shows a high dependence on the filler loading until the percolation threshold is exceeded, and the addition of 7.5% of EG does not produce any improvement. The addition of BN particles led to a reduction of the surface hardness in comparison with materials filled with only EG. This result might be due to the decrease of cohesion of the material with such amount of filler, which is translated in an increase in the capacity to be deformed against penetration and a lower interaction epoxy-BN than epoxy-EG.

3.4. XRD characterization and microscopy inspection

X-Ray diffraction is a very powerful technique to characterize crystalline or semi-crystalline materials and to determine unit cell dimensions and sample purities. The fillers used in this work and two different composites were analysed by this technique and the registered diffractograms are represented in **Figure 6**. Figure 6A presents the diffractogram of the BN used with the characteristic peaks of hexagonal structure pattern of the BN in the ICDD database (card number 01-073-2095) in red colour. All the peaks fit well with the pattern as it was expected. However, it can also be observed small signals, the more visible ones in the range of 28-40° of 2Θ, related to the presence of calcium borate ($Ca_2(B_2O_5)$). The pattern of this impurity (card number 01-089-6630) fits well with these signals and a rough semiquantitative analysis (Reference Intensity Ratio method) determine a ~6% of concentration.

The X-Ray diffractogram of EG (Figure 6B) is represented together with the graphite pattern (03-065-6212), in blue colour, because both have the same crystalline structure. Nevertheless, some differences are shown. Peaks at approximately 42° (crystallographic plane 100) and especially 44.5° (101) are broader than the others are. Such broadening could be related with the distortion in the structure due to the expanded graphite used. In addition, the peak at 54.6° (004) has a lower intensity than the one of the graphite pattern. No impurities were detected in this diffractogram.

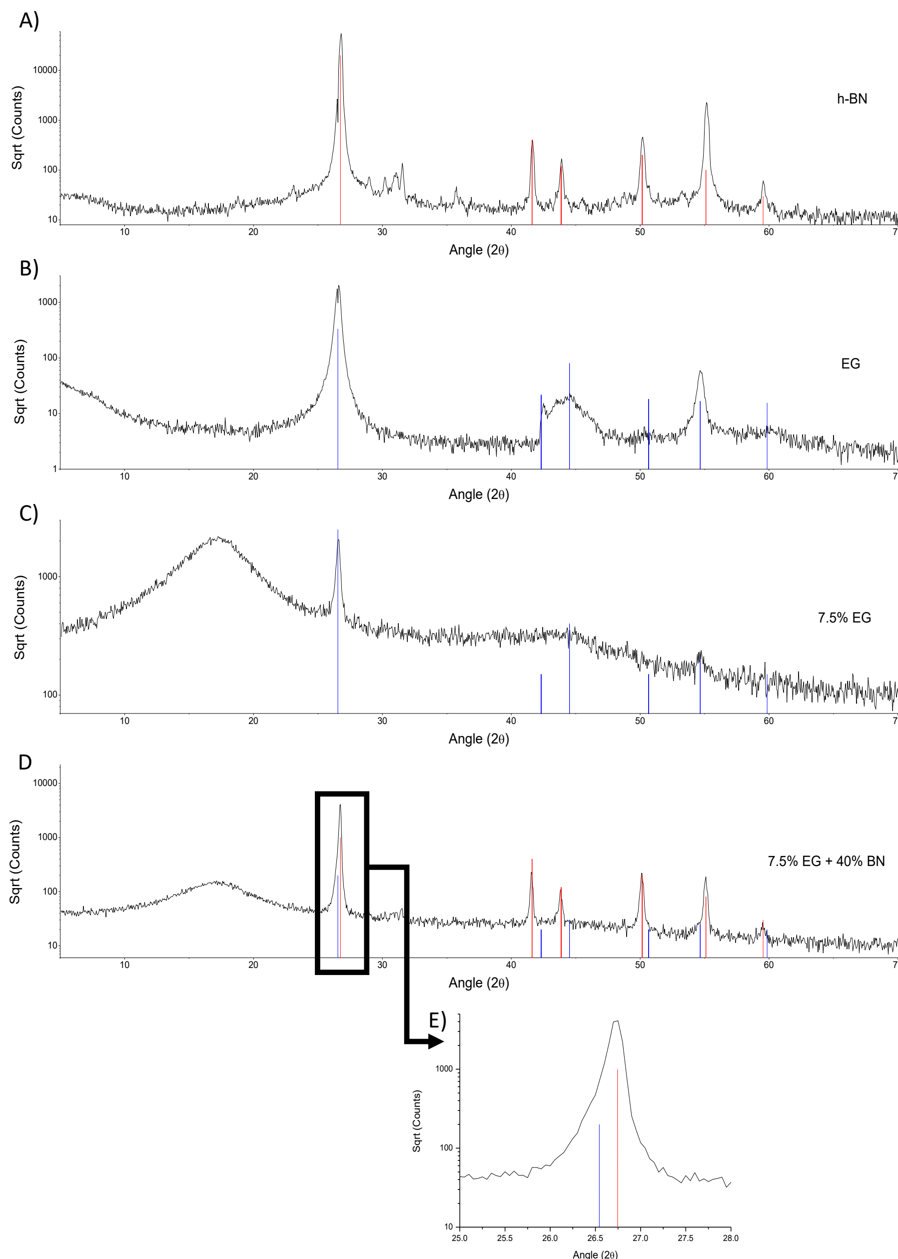

Figure 6. XRD diffractograms of the fillers: h-BN (A) and EG (B) and of the composites: 7.5 wt. % EG (C) and 7.5 wt. % EG + 40 wt. % BN (D)

Figures 6C and 6D correspond to the composites with 7.5 wt. % of EG and 7.5 wt. % + 40 wt. % of BN respectively. In both cases, they presented a broad peak at about 17°, representative of the amorphous structure of the matrix. The peaks of the fillers are kept at the same diffraction angles, although partially covered by the epoxy resin. This confirms that the dispersion procedure did not affect filler crystal lattice. It should

be noted, that the characteristic peaks of the two fillers appear at similar diffraction angles, since the two types of particles have the same crystalline structure, only differentiated by the cell size due to the different atoms in the structure. However, the peaks corresponding to expanded graphite have low intensity, because of its low proportion in the composites, but BN peaks can be easily distinguished. The first and most intense peak at about 26°, corresponding to the 002 plane of BN, is partially overlapped by the 002 plane of graphite. Despite this, in the Figure 6E, it can be observed how the peak has a shoulder at low angles because the BN and graphite peaks do not have the same position because the obvious differences in cell sizes.

ESEM inspection can be used to determine the filler dispersion and the type of fracture by examining the surfaces of the fractured samples of the composites. We firstly examined the fillers used. **Figure 7** presents a general view of the particles and a single particle (at higher magnifications) of BN and EG. BN particles exhibit a large dispersion of sizes, which might be appropriate to better fill the spaces within the matrix. In the micrograph of the single particles, we can observe the laminar shape of BN. EG particles present an amorphous shape as consequence of the thermal shock after chemical oxidation.

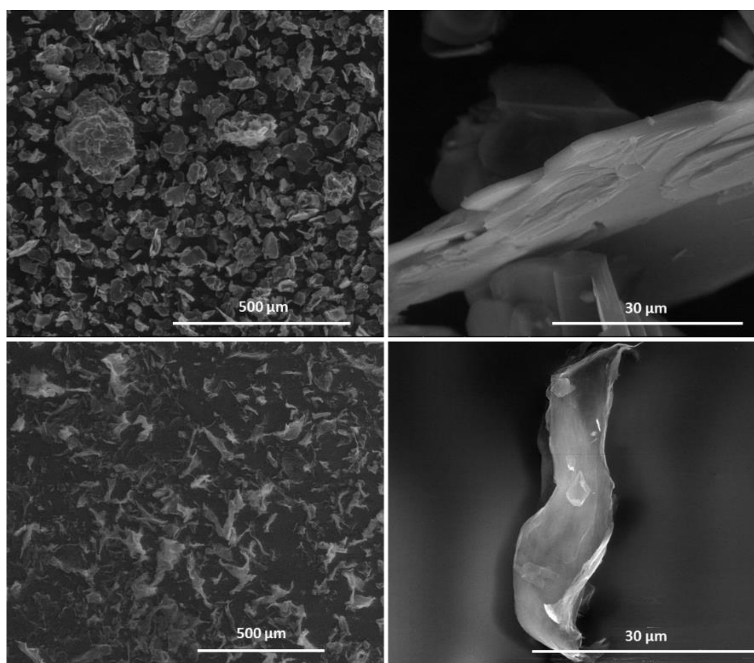

Figure 7. ESEM micrograph of fillers used in the study. BN in row above and EG in row below.

In **Figure 8** fracture surfaces of different composites are presented. The figures above correspond to the composites filled with EG at the three different proportions. In the first one (2.5 wt. % of EG), it can be seen how most of the EG particles are isolated within the matrix whilst in the figure in the middle of the row (5 wt. % of EG) the particles

are closer to each other leading to the appearance of interconnected ways, which confirm that the percolation has been reached. A similar image is observed in the micrograph of the right, corresponding to the composite with the highest proportion of EG (7.5 wt. %) that presents more interconnected EG particles and few parts of pure matrix. The particles in all the samples appear homogeneously distributed. From the left to the right it can be seen that the fracture roughness increases, indicating that the addition of EG enhances the toughness of the materials. In the line below, the first micrograph belongs to the neat epoxy breaking surface. It must be noted how cracks are straight meaning a fragile rupture typical of fragile thermosetting polymers. In the other samples containing BN+EG fillers, the fracture lines are more tortuous, changing their direction on finding a particle, which produces a great increase of the energy absorbed by the impact, increasing their toughness. The higher magnifications of the micrograph in the right below allow distinguishing some EG particles in the matrix.

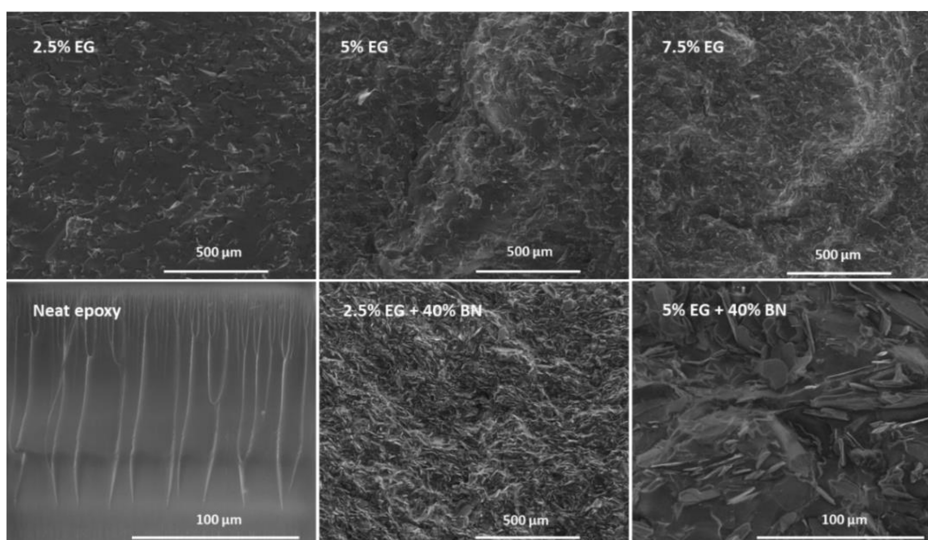

Figure 8. Fracture surfaces of the neat material and the different prepared composites at different magnifications (100 and 800).

3.5. Thermal conductivity and electrical resistivity

Since keeping electrical insulation of this type of composites is crucial for their use in electronic devices, we firstly determined the electrical resistivity of the composites to know the highest proportion of the semiconducting EG filler able to keep the insulating characteristics. It should be commented that although 40 wt. % of BN is the proportion studied until now, samples with a proportion of 70 wt.% of BN have also been prepared, including proportions of 2.5 and 5 wt. % of EG to maintain good electrical insulation character, in order to increase even further the thermal conductivity. When adding a 70 wt. % of BN to the formulation the viscosity is highly increased and pressure moulding is needed to prepare homogeneous samples without bubbles. These samples could not be characterized by rheometry or DSC, because of their low content in resin.

As a comparison mode, a sample with 40 wt. % of BN without EG was also prepared. Electrical resistivity and thermal conductivity are represented together in **Figure 9**.

In spite of the percolation threshold is found between the proportion of 2.5 and 5 wt. % of EG, the measurement of electrical resistivity indicates a progressive reduction of this value on increasing the EG content till 7.5 wt. %. However, the value of 4.5 x 10^2 Ω·m for the composite with a 5 wt. % of EG is too low to be considered as electrical insulator, which means that the electrical percolation has been overpassed.[41] The addition of a higher proportion of EG, up to 7.5 wt. % leads to a further reduction in resistivity, with a value of 2.2 x 10^1 Ω·m. Thus, the proportion of EG in the epoxy matrix is limited to 2.5 wt. % to keep electrical insulation. As in a previous study,[15] the addition of BN particles to the epoxy formulation keeps the electrical resistivity in the same value range of the neat epoxy (7.9 x 10^9 Ω·m for 40 wt. % of BN and 1.6 x 10^{10} Ω·m for the neat material). When 40% of BN is added to epoxy/EG samples, electrical resistivity increases in reference to the samples containing only EG as the filler. Since BN particles are electrical insulators, they act as walls that hinder the EG particle to interact each other, avoiding tunnelling effect and increasing the distance between electrically conductive particles. In case of materials with both BN and EG, the sample with a 7.5 wt. % (2.2 x 10^1 Ω·m) cannot be considered as electrically insulating. On increasing the proportion of BN in the composite the resistivity is enhanced and the sample with a 70 wt. % of BN and 5 wt. % of EG has a resistivity of 2.4 x 10^6 Ω·m, which are typical values for insulating adhesives for electronic applications.

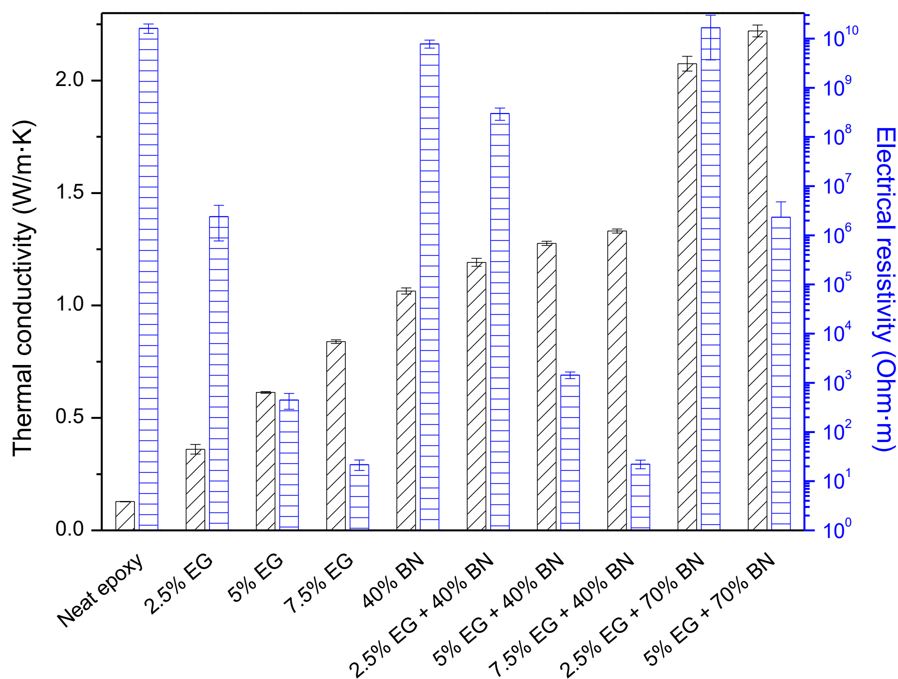

Figure 9. Thermal conductivities and bulk electrical resistance (log scale) of the materials prepared, both measured at room temperature.

Thermal conductivities (TC) were determined at room temperature by the transient hot method. The results are also represented in Figure 9. It can be noticed the great impact on TC with the addition of low proportions of EG particles as reported by previous authors,[1,26,29,42] with a much higher relative increase than in case of adding BN as the filler.[15] The conductivity is almost tripled with the addition of 2.5 wt. % of EG (from 0.128 to 0.36 W/m·K) and almost doubled with the other two higher proportions (from 0.36 to 0.61 with a 5 wt. % and 0.84 W/m·K with a 7.5 wt. %). These values are higher than other reported using graphite nanoflakes[20] (0.43 W/m·K at 8 wt. % of GN), probably due to aggregation phenomena of nanoparticles and the increased number of interfaces that results by the smaller size of the particles on comparison with ours.

The values of TC in BN filled composites revealed that a higher proportion of filler is required to equal EG composites, since in a previous study[15] a content of BN between 30 and 40 wt. % was needed to reach conductivities comparable to composites with a 7.5 wt. % of EG. In composites with a 40 wt.% of BN, the increase of EG proportion leads to an increase in TC, although the enhancement in conductivity is less pronounced and no synergic effect can be observed. This is due to the fact that the particles of EG, with a higher conductivity, are isolated each other by the presence of BN platelets, less conductive, acting as walls, similarly to what happens in the electrical conductivity behaviour. The two samples with 70 wt. % of BN, prepared under pressure, achieved TC over 2 W/m·K (2.08 with 2.5% and 2.22 with 5% of EG). These good results, with enhancements over 1600 % in reference to the neat epoxy, seem to confirm that not only the amount of BN and EG but the pressure applied plays a main role on increasing the thermal conductivity, avoiding the appearance of bubbles inside the material.

Taking into account electrical resistivity and thermal conductivity values, we can state that the composite with a 70 % of BN and 2.5 % of EG is the best one to keep the electrical insulation of the neat epoxide with a high thermal conductivity. However, material with 70 % of BN and 5% of EG, with an even larger TC, still retains high insulation characteristics.

4. Conclusions

In this article, it has been proved that the addition of BN and EG to the epoxy formulations does not affect the evolution of the curing progress. The thermomechanical performance of the prepared composites is well preserved up to temperatures as high as 200 °C, thanks to their high T_gs and the thermal stability of the network formed. Thermal expansion coefficients are highly reduced and the microindentation hardness enhanced on increasing the proportion of fillers.

ESEM images of fractured samples confirmed the good dispersion of the particle fillers in the epoxy matrix and the enhancement in toughness.

Progress in Organic Coatings ***2019***, *133, 299-308*

The addition of EG results proportionally much more effective to enhance the thermal conductivity than the addition of BN. For large filler loadings, the use of pressure is highly recommended to further increase the thermal conductivity in composites.

In EG composites, the proportion of this filler in the epoxy matrix is limited to 2.5 wt. % to keep electrical insulation. However, when 40% of BN is added to epoxy/EG samples, electrical resistivity increases in reference to the samples containing only EG as filler.

The best compromise of properties was found for the composites containing 70 wt. % of BN and 2.5 wt. % of EG and 70 wt. % of BN and 5 wt. % of EG. More precisely, the composite obtained from the formulation with 70 wt. % of BN and 2.5 wt. % of EG shows the highest electrical resistivity, similar to the neat epoxy thermoset (about 10^{10} Ω·m), with a high thermal conductivity (increase of 1500 % in reference to the neat epoxy) whereas the material with 70 % of BN and 5% of EG, exhibits the highest thermal conductivity (1640 %) keeping good insulating characteristics (about 10^{6} Ω·m).

5. Acknowledgments

The authors of URV would like to thank Ministerio de Economía y Competitividad and Fondo Europeo de Desarrollo Regional (MAT2017-82849-C2-1-R, MCIU/FEDER) and Generalitat de Catalunya (2017-SGR-77) for the financial support. The author of Materia Nova wishes to thank the ‘‘Région Wallonne’’ and the European Community for general support in the framework of the Interreg V program (“BIOCOMPAL” and “ATHENS” projects) and the FEDER 2014–2020 program (“HYBRITIMESURF” and “MACOBIO” projects).

6. References

[1] Chen X, Su Y, Reay D, Riffat S. Recent research developments in polymer heat exchangers - A review. Renew Sust Energ Rev 2016; 60: 1367-1386
[2] Huang X, Jiang P. A review of dielectric polymer composites with high thermal conductivity. IEEE Electr Insul Mag 2011; 27: 8–16.
[3] Epoxy Polymers: New Materials and Innovations. Pascault JP, Williams RJJ, editors. Weinheim: Wiley-VCH, 2010.
[4] Hong J, Park DW, Shim SE. A review on thermal conductivity of polymer composites using carbon-based fillers: carbon nanotubes and carbon fibers. Carbon Lett. 2010; 11: 347-356.
[5] Cevallos JG, Bergles AE, Bar-Cohen A, Rodgers P, Gupta SK. Polymer heat exchangers - History, opportunities, and challenges. Heat Transfer Eng. 2012; 33 1075-1093.
[6] Viana ST, Scariot VK, Provensi A, Barra GMO, Barbosa Jr JR. Fabrication and thermal analysis of epoxy resin-carbon fiber fabric composite plate-coil heat exchangers. Appl Therm Eng 2017; 127: 1451-1460.

[7] Im H, Kim J. Thermal conductivity of a graphene oxide-carbon nanotube hybrid/epoxy composite. Carbon 2012; 50: 5429-5440.
[8] Li A, Zhang C, Zhang YF. Thermal conductivity of graphene-polymer composites: mechanisms, properties and applications. Polymers 2017; 9: 437-452.
[9] Noh YJ, Kim HS, Ku B, Khil M, Kim SY. Thermal conductivity of polymer composites with geometric characteristics of carbon allotropes. Adv Eng Mater 2016; 18: 1127-1132.
[10] Ahmed MMM and Imae T. Electrochemical properties of thermally expanded magnetic Graphene composite with conductive polymer. Phys Chem Phys 2016; 18: 10400-10410.
[11] Zhang Y, Heo YJ, Son YR, In I, An KH, Kim BJ, Park SJ. Recent advanced thermal interfacial materials: A review of conducting mechanisms and parameters of carbon materials, Carbon 2019; 142: 445-460.
[12] Noh YJ, Pak SY, Hwang SH, Hwang JY, Kim SY, Youn JR. Enhanced dispersion for electrical percolation behavior of multi-walled carbon nanotubes in polymer nanocomposites using simple powder mixing and in situ polymerization with surface treatment of the fillers. Compos Sci Technol 2013; 89: 29-37.
[13] Chen H, Ginzburg VV, Yang J, Yang Y, Liu W, Huang Y, Du L, Chen B. Thermal conductivity of polymer-based composites: Fundamentals and applications. Prog Polym Sci 2016; 59: 41-85.
[14] Isarn I, Massagués Ll, Ramis X, Serra À, Ferrando F. New BN-epoxy composites obtained by thermal latent cationic curing with enhanced thermal conductivity. Composites: Part A 2017; 103: 35-47.
[15] Isarn I, Gamardella F, Massagués Ll, Fernàndez-Francos X, Serra À, Ferrando F. New epoxy composite thermosets with enhanced thermal conductivity and high Tg obtained by cationic homopolymerization. Polym Comp 2018; 39: 1760-1769.
[16] Isarn I, Ramis X, Ferrando F, Serra À. Thermoconductive thermosetting composites based on boron nitride fillers and thiol-epoxy matrices. Polymers 2018; 10: 277-292.
[17] Isarn I, Gamardella F, Fernàndez-Francos X, Serra À, Ferrando F. Enhancement of thermal conductivity by the addition of several conductive fillers to thermal cationic curing of cycloaliphatic epoxy resins. Polymers 2019; 11: 138-151.
[18] Loeblein M, Tsang SH, Pawlik M, Phua EJR, Yong H, Zhang XW, Gan CL, Teo EHT. High-density 3D-boron nitride and 3D-graphene for high-performance nano-thermal interface material. ACS Nano 2017; 11: 2033-2044.
[19] Singh AK, Panda BP, Mohanty S, Kumar S, Gupta NK, Gupta MK. Recent developments on epoxy based thermally conductive adhesives (TCA): a review. Polym Plast Technol Eng 2018; 57(9): 903-934.
[20] Luo F, Wu K, Huang X, Hu X, Lu M. Encapsulation of graphite nanoflakes for improving thermal conductivity of mesogenic epoxy composites. Ind Eng Chem Res 2017; 56: 489-494.
[21] Asante J, Modiba F, Mwakikunga B. Thermal measurements on polymeric epoxy-expandable graphite material. J Polym Sci A, vol. 2016, Article ID 1792502, 12 pages.
[22] Chatterjee S, Wang JW, Kuo WS, Tai NH, Salzmann C, Li WL, Hollertz R, Nüesch FA, Chu BTT. Mechanical reinforcement and thermal conductivity in expanded graphene nanoplatelets reinforced epoxy composites. Chem Phys Lett 2012; 531: 6-10.

[23] Xie F, Qi SH, Wu D. Thermal conductive composites based on silver-plating graphite nanosheet and epoxy polymer. Polym Composite 2017; 38: 2822-2828.
[24] Rybak A, Gaska K. Functional composites with core-shell fillers: I. Particle synthesis and thermal conductivity measurements. J Mat Sci 2015; 50: 7779–7789.
[25] Chen H, Ginzburg VV, Yang J, Yang Y, Liu W, Huang Y, Du L, Chen B. Thermal conductivity of polymer-based composites: Fundamentals and applications. Prog Polym Sci 2016; 59: 41-85.
[26] Corcione CE, Maffezzoli A. Transport properties of graphite/epoxy composites: Thermal, permeability and dielectric characterization. Polym Test 2013; 32: 880-888.
[27] Kim HS, Kim JH, Kim WY, Lee HS, Kim SY, Khil M-S. Volume control of expanded graphite based on inductively coupled plasma and enhanced thermal conductivity of epoxy composite by formation of the filler network. Carbon 2017; 119: 40-46.
[28] Wang Z, Qi R, Wang J, Qi S. Thermal conductivity improvement of epoxy composite filled with expanded graphite. Ceram Int 2015; 41: 13541-13546.
[29] Badenhorst H. A review of the application of carbon materials in solar thermal energy storage. Sol Energy. In press. https://doi.org/10.1016/j.solener.2018.01.062
[30] Nakano S, Endo T. Cationic polymerization of glycidyl phenyl ether by benzylammonium salts. J Polym Sci: Part A Polym Chem 1995; 33: 505-512.
[31] Nakano S, Endo T. Thermal cationic curing by benzylpyridinium salts. Prog Org Coat 1994; 23: 379-385.
[32] Nakano S, Endo T. Thermal cationic curing with benzylammonium salts. Prog Org Coat 1993; 22: 287-300.
[33] Tejkl M, Valis J, Kaplanová M, Jasúrek B, Syrový T. Inhibition of premature polymerization of cationically polymerizable low viscosity systems. Prog Org Coat 2012; 74: 215-220.
[34] McClory C, Chin SJ, McNally T. Polymer/Carbon nanotube composites. Aust J Chem 2009; 62: 762-785.
[35] McCrossan K, McClory C, Mayoral B, Thompson D, McConnell D, McNally T, Murphy M, Nicholson T, Martin D, Halley P. Composites of poly(ethylene terephthalate) and multi-walled carbon nanotubes. Book: Polymer-carbon nanotube composites: Preparation, properties and applications. Editors: Tony McNally and Petra Pötschke. Oxford: Woodhead Publishing Limited, 2011, p. 545-586.
[36] McNally T, Pötschke P, Halley P, Murphy M, Martin D, Bell SEJ, Brennan GP, Bien D, Lemoine P, Quinn JP. Polyethylene multiwalled carbon nanotube composites. Polymer 2005; 46(19): 8222-8232.
[37] Laun H.M. Rheological properties of aqueous polymer dispersion. Angew Makromol Chem 1984; 123/124: 335-359.
[38] Jouault N, Vallat P, Dalmas F, Said S, Jestin J, Boué F. Well-dispersed fractal aggregates as filler in polymer-silica nanocomposites: Long-range effects in rheology. Macromolecules 2009; 42: 2031-2040.
[39] Thermosetting Polymers. Pascault JP, Sautereau H, Verdu J, Williams RJJ. New York: Marcel Dekker AG, 2002.
[40] Zhang Y, Park S-J. Enhanced Interfacial Interaction by Grafting Carboxylated-Macromolecular

Chains on Nanodiamond Surfaces for Epoxy-Based Thermosets. J Polym Sci Part B: Polym Phys 2017; 55(24): 1890-1898.

[41] Sancaktar E, Bai L. Electrically Conductive Epoxy Adhesives. Polymers 2011; 3: 427-466.

[42] Ramakrishnan S, Wang X, Sanjayan J, Wilson J. Heat transfer performance enhancement of paraffin/expanded perlite phase change composites with graphene nano-platelets. Energy Procedia 2017; 105: 4866-4871.

UNIVERSITAT ROVIRA I VIRGILI
NEW EPOXY COMPOSITES WITH ENHANCED THERMAL CONDUCTIVITY KEEPING ELECTRICAL INSULATION.
Isaac Isarn Garcia

Chapter 9. General conclusions

9. General conclusions

The most important conclusions extracted from the different chapters are:

1. The use of N-(4-methoxybenzyl)-N,N-dimethylanilinium hexafluoroantimoniate (CXC1612) as cationic initiator constitutes a latent curing agent for the homopolymerization of DGEBA formulations, while the addition of a little amount (0.1 phr) of triethanolamine is required to reach a good latency for cycloaliphatic epoxy resins (ECC). The addition of small proportions of glycerol (2 phr) to DGEBA formulations increases the curing rate in this system. The cycloaliphatic epoxy thermosets obtained presented a $T_{\tan\delta}$ higher than 200 °C while DGEBA leads to a $T_{\tan\delta}$ around 140 °C.

2. The addition of BN nanoplatelets to the homopolymerized epoxies gradually increases the thermal conductivity of the composites obtained, reaching thermal conductivities in the range 0.99 to 1.06 W/mK (with a 40 wt.% of BN) in case of cycloaliphatic epoxy thermosets and 0.61 W/mK (with a 20 wt.% of BN) for DGEBA materials.

3. On comparing the kinetic effect of the addition of Al_2O_3, AlN and SiC as the fillers in ECC formulations, we can see that Al_2O_3 delays the curing process, while AlN leads to an acceleration and SiC does not produce any kinetic effect. This behaviour could be attributed to the acid-base characteristics of the fillers interacting with the cations formed in the polymerization of cycloaliphatic epoxy resins.

4. At the same loading, among AlN, Al_2O_3 and SiC fillers, the last one leads to the highest enhancement in thermal conductivity in ECC matrices, possibly due to the bigger size of the particles (1.12 W/m·K with a 70 wt. % of SiC). However, a higher proportion of AlN was needed to overpass the percolation threshold and the addition of a 75 wt. % of AlN produced the highest TC (1.21 W/m·K).

5. The measured hardness of the ECC composite with AlN is the highest among the ceramic fillers studied, which could be attributed to a strong filler-matrix interfacial interaction.

6. The surpassing of the percolation threshold positively affects thermal conductivity and mechanical properties. Filler parameters such as particle size and shape, aspect ratio, specific surface area, particle-particle and particle-matrix interactions and dispersion state influence the percolation threshold of the filler formulations.

7. Thermal expansion coefficients decrease on increasing the amount of fillers in the formulation.

8. DGEBA-pentaerythritol tetrakis (3-mercaptopropionate) formulations were cured in the presence of 4-(N,N-dimethylamino) pyridine. The thermosets show a lower $T_{tan\delta}$, hardness and Young's modulus and thermal stability than homopolymerized epoxy matrices, due to the more open network structure.
9. BN agglomerates of 80 µm lead to a higher increase in TC than BN platelets of 6 µm from 0.97 to 1.75 W/m·K in thiol-epoxy matrices at the same loading.
10. The addition of 0.05 wt. % of CNTs to the formulation produces the loss of electrical insulation properties. However, the addition of 40 wt. % of BN, which acts as electron barriers, allows to increase the CNT ratio to 0.25 wt. %.
11. The addition of CNTs to epoxy matrices does not produces big improvements in TC, because of the small amount that can be added because lost in electrical insulating characteristics.
12. Composites with mixtures of CNTs and BN as fillers reach TC values of 1.1 W/m·K in ECC and DGEBA matrices, keeping electrical insulation. The synergic effect between both fillers in TC is rather poor.
13. The addition of small amounts (till 1 wt. %) of CNTs to the epoxy matrices enhances hardness, rigidity and reduces the thermal expansion coefficient.
14. The oxidation of CNTs results in greater improvements in mechanical properties in DGEBA than in the cycloaliphatic composites. No much effect in TC is observed on adding the oxidized CNTs as fillers.
15. Expanded graphite (EG) particles are much more efficient to enhance the TC than any other filler tested in this study. However, their inherent electrical conductivity limits their proportion in the formulation to 2.5 wt. %.
16. The addition of 70 wt. % of BN platelets to EG-ECC matrix, which involves the application of pressure in the preparation of composite samples, highly enhances the TC (2.22 W/m·K) and allows the addition of 5 wt. % of EG with a sufficient electrical insulation ($>10^6$ Ω·m).
17. The elastic modulus in the glassy state of the composites prepared is reduced as the size of the filler particles increases. A percolated network of small particles hinders the movement of the already epoxy constrained networks formed. A contrary behaviour is observed in the rubbery state. Large particles prevent the movement of the adjacent particles, while small particles can be repositioned with small displacements, resulting in a reduction in stiffness. From the ceramic fillers AlN led to the highest rigidity for these materials (14.4 GPa).